建築研究報告

REPORT OF THE BUILDING RESEARCH INSTITUTE

NO. 34 NOVEMBER, 1960

Study on the Prevention of Fire-Spread Caused by Hot Upward Current

by

Sizuo YOKOI; Research Member

建設省建築研究所

Published by

The Building Research Institute, Ministry of Construction

Study on the Prevention of Fire-Spread Caused by Hot Upward Current

by

Sizuo YOKOI

Research Member, Building Research Institute
Ministry of Construction, Japanese Government

(Received June 6, 1960)

CONTENTS

INTRODUCTION

As new problems of fire protection which were born after War, the following two can be enumerated;

a) Protection of television towers against fire,

b) Protection of spread of fire from an opening of a room to the opening of the upstairs room with large openings.

In order to consider these problems, it is first of all necessary to investigate temperature distribution of the upward current from a burning house at windless condition. Problems concerning characteristics of hot upward current belong to the field of thermohydrodynamics, and so it is of extreme difficulty to solve them in direct way. On the other hand, for financial reason, it is also impossible for us to solve them by performing a number of tests with full-scale fire experiment.

In solving these difficult problems, the author performed a number of model experiments of various scales in the laboratory, basing on these results and refering to the equations of motions in hydro-dynamics and of heat continuity, he tried to find the relations among the important factors in these phenomena and to find the approximate similarity law between the model and full-scale experimental fire. The results were compared with those of the tests performed 4 times. It was successfull in this way to establish a series of systematic theories in this field of fire-study which had been left unsolved.

The two new problems of fire-protection described at the beginning have been easily solved by applying these theories. They are reported in this paper.

The author wishes to express his hearty thanks to Dr. T. Kinbara, M. Hamada, H. Hatakeyama and K. Fujita, for their kind encouragement and guidance throughout this work.

PART I　BASIC THEORY

Chapter 1.

Upward Currents from a Point Heat Source and from an Infinite Line Heat Source

1.1 Introduction

The temperature and velocity distributions of the upward currents from a point heat source and an infinite line heat source were obtained in this research as a preliminary study for obtaining the temperature distribution of the hot currents rising from burning wooden houses under windless conditions and of the one spouting out from the windows of fireproof buildings on fire.

1.2 Method of Experiment

An ordinary alcohol lamp sold on the market was used for the point heat source, while for the infinite line source was used a long narrow tin vessel 100 cm long and 1 cm wide, containing alcohol. In order to maintain the surface of the liquid in the tin vessel at a fixed height during combustion, alcohol was constantly supplied from a alcohol-tank into the vessel through a communicating tube.

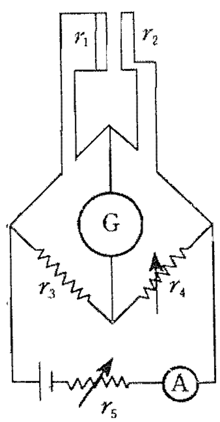

Figure 1.1 A temperature compensating type hot-wire anemometer.

For measuring the upward velocity, a temperature-compensating type hot-wire anemometer[1] (Figure 1.1) devised by Mr. Shigeo Uchida of the Scientific and Engineering Research Institute, Tokyo University, was used. This meter is not suitable for measuring the velocity of gas of very high temperature, but if the temperature of the gas is less than 100°C, it has been ascertained, as a result of the experiment made by using the low-speed air duct at the Scientific and Engineering Research Institute, that the measured velocity value has practically no connection with the temperature of the current. The temperature of the gas was measured by a copper-constantan thermocouple (diameter: 0.2 mm) connected to a simple slow-rotating oscillograph. It is a characteristic of upward current from a heat source that the upward velocity and temperature fluctuates greatly in short periods of 2 or 3 seconds. However, it was not difficult to judge mean values of temperature at every point on the self-recorded curve, and the average values for about 10 minutes was obtained by observing the record on the oscillograph with the eye, and it was considered the temperature of that point.

Concerning the temperature distribution of the upward current, we don't require the absolute values of temperature but we require the temperature difference between the inside and outside the upward current, so the cold junction of the thermocouple was not put in ice-water as usual but kept at a place of normal temperature which was thought to be beyond the limits of the upward current. It would have been best if it had been possible to measure the temperature of all the necessary points in the current simultaneously, but the automatic recording instrument could cover no more than 6 points at a time, therefore we selected 1 of the 6 points as the standard point whose position relative to the heat source were fixed.

The other 5 points were distributed at various heights on the same vertical line, and the measurements were made by successively moving the 5 points in relation to the heat source. As this method did not greatly disturb the upward current, it was considered satisfactory. However, as the temperature and velocity gradually changed with time not only in the case of the alcohol lamp but also in the case of the line heat source, adjustments were made in analysing the results of experiments according to the value of the temperature of the base point.

Slight draughts in the room markedly disturb the upward currents. In view of this fact, experiments were conducted in a dark-room for developing the photo-film (approximately 4.5m × 4.5m × 4.5m), and, moreover, they were conducted only on calm days when there was not much wind. In order to guard against draughts due to the difference in temperatures between inside and outside the room and to avoid big temperature differences in the vertical direction in the room, the duration of each experiment was limited to 2 hours.

1.3 Results of Experiment

The results of measuring the temperature and velocity of the upward current at heights ranging from about 50 cm to 140 cm above the point heat source or line heat source are given in Figure 1.2 to Figure 1.5. In the case of the point heat source, the measurements were made in an arbitrary vertical plane including the heat source, and in the case of the line heat source, in the vertical plane perpendicular to the heat source including the middle of it.

In order to represent the position of points in space, let us use circular cylindrical coordinates in the case of a point heat source, making the heat source the origin of coordinates and taking the z axis in the upward vertical direction from it and the r axis in the radial direction, and two-dimensional coordinates in the case of line heat source, making the middle point of the heat source the origin and taking the z axis on the upward vertical direction and the y axis in the direction forming a right angle to the direction of heat source. As the values of the temperature and velocity along the z axis show the maximum values for the each horizontal plane, let us express them by $\Delta\theta_m$ and w_m respectively and the values at arbitrary points by $\Delta\theta$ and w.

In ascending, the current mixes with the surrounding air because of the turbulence of the current, and the higher it rises the larger its domain becomes. By calculating the observed values of $\Delta\theta/\Delta\theta_m$ and w/w_m at various points in various levels and plotting them against r/z (point heat source) and y/z (line heat source), it was found that the values measured at various heights cluster along a single curve, as shown in Figures 1.2 to 1.5. This means that the domain of the hot current becomes larger linearly

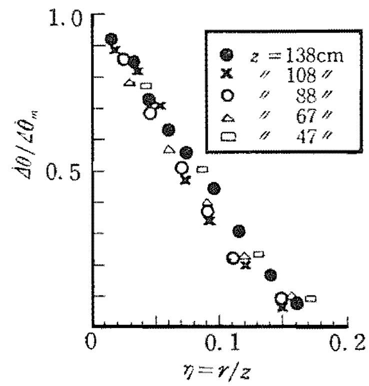

Figure 1.2

Horizontal distribution of temperature in the upward current from a point heat source.

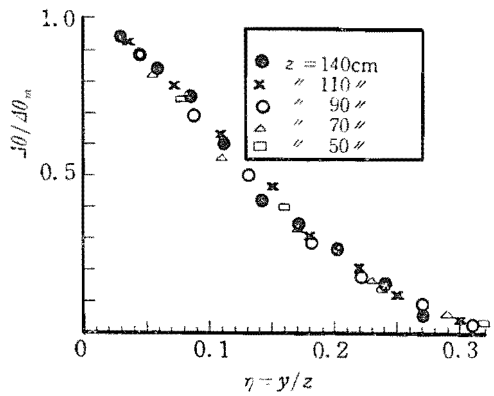

Figure 1.3

Horizontal distribution of temperature in the upward current from a line heat source.

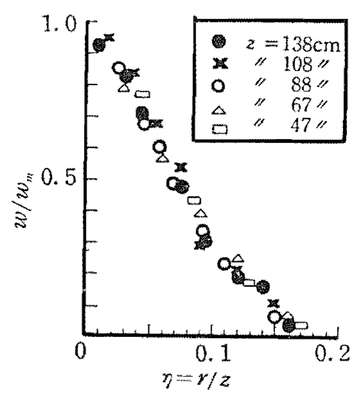

Figure 1.4

Horizontal distribution of upward velocity in the upward current from a point heat source.

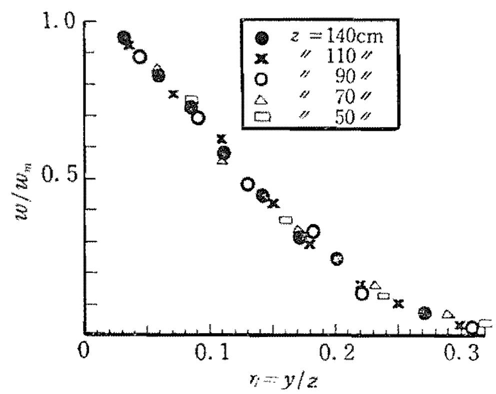

Figure 1.5

Horizontal distribution of upward velocity in the upward current from a line heat source.

as the current goes up —— in the case of point heat source, forming a conical shape whose apex is the at heat source, and in the case of a line heat source, the shape of a wedge and this also means that the horizontal temperature distributions at various levels can be represented by a single curve respectively, if they are plotted on such non-dimensional coordinates.

The fact that there is such a simple similarity law on the horizontal temperature distributions of the upward current from a point or line heat source, will be utilized in the analysis to be made in Section 1.5. Furthermore, it can be seen by comparing Figure 1.2 with Figure 1.4 and Figure 1.3 with Figure 1.5 that the horizontal distribution of temperature and that of velocity on the same horizontal surface are almost similar.

1.4 Buoyancy Acting on Heated Air Mass

If the gas in the upward current and the surrounding air are the same material as in the case of the heated air by an electric heater, the following equation is established according to the equation of state of gas:

$$p/\rho\theta = p_0/\rho_0\theta_0, \quad\cdots\cdots(1.1)$$

where the absolute temperature, pressure and density inside the current are θ, p and ρ and those outside the current are θ_0, p_0 and ρ_0, respectively.

As the upward current is in the free space, it may be assumed that $p = p_0$, therefore the Equation (1.1) reduces to ;

$$\rho_0 = \rho\theta/\theta_0. \quad\cdots\cdots(1.2)$$

Hence, the upward force acting on the unit volume of the gas mass (buoyancy minus the gravity force) is :

$$g\ (\rho_0-\rho) = g\rho\Delta\theta/\theta_0, \quad\cdots\cdots(1.3)$$

where $\Delta\theta=\theta-\theta_0$.

In the case of the hot current caused by combustion, the formula of buoyancy cannot be expressed by the Equation (1.3), strictly speaking. However, as it is usual that a considerable amount of air is mixed, Equation (1.3) may be employed to obtain an approximate value, so long as the density of the gas produced by combustion does not greatly differ from that of the air and the gas is assumed to be an ideal gas. For instance, in the author's experiments by means of alcoholic combustion, the equation of combustion reaction is :

$$2CH_3OH+3O_2=2CO_2+4H_2O. \quad\cdots\cdots(1.4)$$

The mixed gases in the right hand side of the Equation has 6 mols or 13.4 l in volume in the standard state, and according to calculation its mass is 170 gm. Therefore, its density is 1.26×10^{-3} gm/cm^3, which is practically equal to the density of air : 1.29×10^{-3} gm/cm^3.

According to Mr. Kunio Kawagoe,[2] the density of gas produced by combustion of wood in an actual fire (converted into the value in the standard state) is 1.27×10^{-3} gm/cm^3 on condition that the value of excess air factor $n=1.0$ and the rate of perfect combustion $x=0.7$ (usually in case of fire of a room of fire-proof construction); it is 1.30×10^{-3} gm/cm^3 on condition that $n=2.0$ and $x=1.0$ (an example of fire of wooden house). Generally, if the value of the rate of perfect combustion x is larger than 0.4, the density of the gas produced by combustion of wood is between 1.23×10^{-3} gm/cm^3 and 1.31×10^{-3} gm/cm^3, also approximately equal to the density of air. Therefore, the buoyancy on the gas produced by combustion of alcohol or wood can be expressed by Equation (1.3).

1.5 Equations of Motion and Heat Continuity

1.5.1 In the case of point heat source

Suppose that the heat source continuously produces a definite quantity of heat every second. The upward current is regarded to be in the stationary state because it becomes nearly stationary soon after ignition. Also the upward current is in the state of turbulent flow from the beginning. In this case, there are two possible external forces for the unit volume of the gas : buoyancy and eddy viscosity. The molecular viscosity can be neglected because it is far smaller compared with the eddy viscosity. The buoyancy can be expressed by the right hand side of Equation (1.3). As for the eddy viscosity, according to the mixture length theory in hydrodynamics, there have been the method based on the momentum transfer theory advocated by Prandtl[3] and the method based on the modified vorticity transfer theory advocated by Taylor[4]. For many years there have been discussions of the comparative merits of the two methods in connection with various problems.

Here let us make calculation by using each of these two methods.

Let us take the axes of coordinates as stated in Section 1.3 and express the components of the current velocity in the directions of z and r by w and v, respectively. Next, the density of the gas in the upward current naturally varies according to the location because the temperature varies. Although the buoyancy caused by the difference in density has a measurable value, let us assume that the difference in density is negligibly small when compared with the density itself. Then, the equation of motion, the equation of heat continuity and the equation of continuity become;

$$w\frac{\partial w}{\partial z}+v\frac{\partial w}{\partial r}=\frac{g\Delta\theta}{\theta_0}+\frac{1}{r}\frac{\partial}{\partial r}\left(Kr\frac{\partial w}{\partial r}\right), \quad \cdots\cdots (1.5)$$

$$w\frac{\partial w}{\partial z}+v\frac{\partial w}{\partial r}=\frac{g\Delta\theta}{\theta_0}+K\left(\frac{\partial^2 w}{\partial r^2}+\frac{1}{r}\frac{\partial w}{\partial r}\right), \quad \cdots\cdots (1.5_1)$$

$$w\frac{\partial \theta}{\partial z}+v\frac{\partial \theta}{\partial r}=\frac{1}{r}\frac{\partial}{\partial r}\left(K'r\frac{\partial \theta}{\partial r}\right), \quad \cdots\cdots (1.6)$$

$$\frac{1}{r}\frac{\partial}{\partial r}(rv)+\frac{\partial w}{\partial z}=0, \quad \cdots\cdots (1.7)$$

where:

$$\theta=\frac{\Delta\theta}{\theta_0}. \quad \cdots\cdots (1.8)$$

Equation (1.5) is an equation based on the momentum transfer theory, while Equation (1.5_1) is based on the modified vorticity transfer theory. K and K' are the coefficients of eddy viscosity and that of eddy diffusivity, respectively. Although the values of these are equal in the theory of mixture length, these are distinguished here. According to Prandtl[3],

$$K=-l^2\frac{\partial w}{\partial r}, \qquad K'=-l'^2\frac{\partial w}{\partial r}. \quad \cdots\cdots (1.9)$$

Here, it is assumed that l and l', called the mixture length, are in proportion to the width of the upward current and that they have a definite value on the same horizontal plane. According to the results of experiments referred to in Section 1.3, the width of heated upward current is in proportion to the height z, measured from the heat source; therefore, l and l' may be expressed as follows:

$$l=cz, \qquad l'=c'z, \quad \cdots\cdots (1.10)$$

where both c and c' are constants of proportionality. Substituting these into Equation (1.9), it reduces to:

$$K=-c^2z^2\frac{\partial w}{\partial r}, \qquad K'=-c'^2z^2\frac{\partial w}{\partial r}. \quad \cdots\cdots (1.11)$$

Accordingly, Equations (1.5) (1.5_1) and (1.6) become;

$$w\frac{\partial w}{\partial z}+v\frac{\partial w}{\partial r}=g\theta-\frac{c^2z^2}{r}\frac{\partial}{\partial r}\left(\frac{\partial w}{\partial r}\right)^2, \quad \cdots\cdots (1.12)$$

$$w\frac{\partial w}{\partial z}+v\frac{\partial w}{\partial r}=g\theta-c^2z^2\frac{\partial w}{\partial r}\left(\frac{\partial^2 w}{\partial r^2}+\frac{1}{r}\frac{\partial w}{\partial r}\right), \quad \cdots\cdots (1.12_1)$$

$$w\frac{\partial\theta}{\partial z}+v\frac{\partial\theta}{\partial r}=-\frac{c'^2z^2}{r}\frac{\partial}{\partial r}\left\{\left(\frac{\partial w}{\partial r}\right)\left(\frac{\partial\theta}{\partial r}\right)\right\}. \quad\cdots\cdots(1.13)$$

1.5.2 In the case of infinite line heat source

The equations in the case of an infinite line heat source may be obtained in the same way. The equations corresponding to (1.5), (1.5₁), (1.6) and (1.7) in the preceding Section are;

$$w\frac{\partial w}{\partial z}+v\frac{\partial w}{\partial y}=g\frac{\Delta\theta}{\theta_0}+\frac{\partial}{\partial y}\left(K\frac{\partial w}{\partial y}\right), \quad\cdots\cdots(1.14)$$

$$w\frac{\partial w}{\partial z}+v\frac{\partial w}{\partial y}=g\frac{\Delta\theta}{\theta_0}+K\frac{\partial^2 w}{\partial y^2}, \quad\cdots\cdots(1.14_1)$$

$$w\frac{\partial\theta}{\partial z}+v\frac{\partial\theta}{\partial y}=\frac{\partial}{\partial y}\left(K'\frac{\partial\theta}{\partial y}\right), \quad\cdots\cdots(1.15)$$

$$\frac{\partial w}{\partial z}+\frac{\partial v}{\partial y}=0. \quad\cdots\cdots(1.16)$$

The coefficient of eddy viscosity, K, and the coefficient of eddy diffusivity, K', become;

$$K=-l^2\frac{\partial w}{\partial y}=-c^2z^2\frac{\partial w}{\partial y}, \quad\cdots\cdots(1.17)$$

$$K'=-l'^2\frac{\partial w}{\partial y}=-c'^2z'^2\frac{\partial w}{\partial y}. \quad\cdots\cdots(1.18)$$

Substituting these into the Equations (1.14), (1.14_1) and (1.15): they reduce to;

$$w\frac{\partial w}{\partial z}+v\frac{\partial w}{\partial y}=g\theta-c^2z^2\frac{\partial}{\partial y}\left(\frac{\partial w}{\partial y}\right)^2, \quad\cdots\cdots(1.19)$$

$$w\frac{\partial w}{\partial z}+v\frac{\partial w}{\partial y}=g\theta-\frac{c^2z^2}{2}\frac{\partial}{\partial y}\left(\frac{\partial w}{\partial y}\right)^2, \quad\cdots\cdots(1.19_1)$$

$$w\frac{\partial\theta}{\partial z}+v\frac{\partial\theta}{\partial y}=-c'^2z\frac{\partial}{\partial y}\left\{\left(\frac{\partial w}{\partial y}\right)\left(\frac{\partial\theta}{\partial y}\right)\right\}. \quad\cdots\cdots(1.20)$$

1.6 Vertical Distributions of Temperature and Velocity along the Axis of Upward Current

According to the results of the experiments referred to in Section 1.3, it has been found that the pattern of the horizontal distribution of temperature, $\Delta\theta$ and that upward velocity w are similar respectively regardless of the height relative to r/z and y/z. Therefore, if r/z and y/z are expressed by

$$\left.\begin{aligned}\eta&=r/z \text{ (in the case of a point heat source),}\\ \eta&=y/z \text{ (in the case of an infinite line heat source)}\end{aligned}\right\} \quad\cdots(1.21)$$

and if it is assumed that the temperature and velocity can be expressed by a power of z, θ and w should be expressed by the following equations:

$$\theta=\frac{\Delta\theta}{\theta_0}=z^m\phi(\eta), \quad\cdots\cdots(1.22)$$

$$w=z^nf(\eta). \quad\cdots\cdots(1.23)$$

where $\phi(\eta)$ expresses the horizontal distribution of temperature shown in Figure 1.2 (point heat source) or in Figure 1.3 (infinite line heat source), and $f(\eta)$ expresses the horizontal distribution of upward velocity shown in Figure 1.4 or Figure 1.5.

By applying these to the equations of motion and heat continuity, we are going to

$$\int_0^\infty wr\frac{\partial\theta}{\partial z}dr+\int_0^\infty vr\frac{\partial\theta}{\partial r}dr=\int_0^\infty wr\frac{\partial\theta}{\partial z}dr+\Big[vr\theta\Big]_0^\infty-\int_0^\infty\theta\frac{\partial}{\partial r}(vr)dr.$$

In this case v and θ are zero at $r=\infty$; and at $r=0$, even though v and θ are finite, since $r=0$, $\Big[vr\theta\Big]_0^\infty=0$.

Also, substituting the equation of continuity, into the third term,

$$\text{Left hand side}=\int_0^\infty wr\frac{\partial\theta}{\partial z}dr+\int_0^\infty \theta r\frac{\partial w}{\partial z}dr=\int_0^\infty r\frac{\partial}{\partial z}(w\theta)dr$$

Hence, $\displaystyle\int_0^\infty r\frac{\partial}{\partial z}(w\theta)dr=0$; therefore

$$\int_0^\infty (rw\theta)dr=\text{constant.} \qquad (1.28_1)$$

This is equivalent to the following formula stating that the quantity of heat, Q, which passes through a horizontal plane at an arbitrary height in unit time is invariable regardless of the height from the heat source.

$$\int_0^\infty c_p\rho w\Delta\theta 2\pi r dr = Q. \qquad (1.30)$$

Now, let us compute the differential coefficients of w and θ:

$$\left.\begin{aligned}
\frac{\partial w}{\partial r}&=\frac{z^{n-1}}{\eta}\left(F''-\frac{F'}{\eta}\right),\\
\frac{\partial w}{\partial z}&=z^{n-1}\left\{\frac{(n+1)F'}{\eta}-F''\right\},\\
\frac{\partial^2 w}{\partial r^2}&=z^{n-2}\left(\frac{F'''}{\eta}-\frac{2F''}{\eta^2}+\frac{2F'}{\eta^3}\right),\\
\frac{\partial\theta}{\partial r}&=z^{m-1}\phi',\\
\frac{\partial\theta}{\partial z}&=z^{m-1}(m\phi-\eta\phi').
\end{aligned}\right\} \qquad (1.31)$$

By substituting these and Equations (1.28) and (1.29) into Equations (1.5) and (1.5_1), we obtain:

$$z^{2n-1}\left\{(n+2)\frac{d}{d\eta}\left(\frac{FF'}{\eta}\right)-(2n+2)\frac{F'^2}{\eta}\right\}=-z^m g\phi\eta+z^{2n-1}c^2\frac{d}{d\eta}\left\{\frac{1}{\eta}\left(F''-\frac{F'}{\eta}\right)^2\right\}, \qquad (1.32)$$

$$z^{2n-1}\left\{(n+2)\frac{d}{d\eta}\left(\frac{FF'}{\eta}\right)-(2n+2)\frac{F'^2}{\eta}\right\}=-z^m g\phi\eta+z^{2n-1}c^2\left(F''-\frac{F'}{\eta}\right)\left(\frac{F'''}{\eta}-\frac{F''}{\eta^2}+\frac{F'}{\eta^3}\right). \qquad (1.32_1)$$

In order that these expressions hold regardless of the value of z, the values of the indices of z in each term of equation should be equal. In other words, both in the expression based on the momentum transfer theory and the expression based on the modified vorticity transfer theory,

$$2n-1=m. \qquad (1.33)$$

Next, by substituting the Equations (1.21), (1.22) and (1.31) into Equations (1.28_1) we obtain:

$$\int_0^\infty z^{m+n+2}F'\phi d\eta=\text{constant.} \qquad (1.34)$$

If this is to hold regardless of the value of z, it is necessary that find the values of indices m and n.

1.6.1 In the case of point heat source

The velocity components w and v, involved in the equation of motion are not independent but are connected with each other by means of the equation of continuity, (1.7). Accordingly, let us employ the stream function, ψ used in hydrodynamics, for the purpose of expressing these by one function. As the stream function ψ is defined by the following forms:

$$w=\frac{1}{r}\frac{\partial\psi}{\partial r}, \qquad v=-\frac{1}{r}\frac{\partial\psi}{\partial z}, \quad \cdots\cdots(1.24_1)$$

it can be expressed by;

$$\psi=\int rwdr. \quad \cdots\cdots(1.24)$$

Substituting the Equations (1.21) and (1.23) into above, it reduces to:

$$\psi=z^{n+2}\int\eta f(\eta)d\eta.$$

Therefore, if we put

$$F(\eta)=\int\eta f(\eta)d\eta, \quad \cdots\cdots(1.25)$$

then it becomes to:

$$\psi=z^{n+2}F(\eta). \quad \cdots\cdots(1.26)$$

From Equations (1.26) and (1.21), w and v can be calculated as follows:

$$\left.\begin{aligned}\frac{1}{r}\frac{\partial\psi}{\partial r}&=\frac{1}{\eta z}z^{n+2}F'(\eta)\frac{\partial\eta}{\partial r}=\frac{z^n}{\eta}F'(\eta),\\ -\frac{1}{r}\frac{\partial\psi}{\partial z}&=-\frac{1}{\eta z}\left\{F'(\eta)\frac{\partial\eta}{\partial z}z^{n+2}+(n+2)z^{n+1}F(\eta)\right\}\\ &=z^n\left\{F'(\eta)-\frac{(n+2)F(\eta)}{\eta}\right\}.\end{aligned}\right\} \quad \cdots\cdots(1.27)$$

where $F'(\eta)=dF(\eta)/d\eta$, and hereafter we express F and F' briefly, instead of $F(\eta)$ and $F'(\eta)$ for simplicity.

Substituting (1.27) to Equations (1.24_1), we obtain;

$$w=z^n\frac{F'}{\eta}, \quad \cdots\cdots(1.28)$$

$$v=z^n\left\{F'-\frac{(n+2)}{\eta}F\right\}. \quad \cdots\cdots(1.29)$$

Concerning the temperature $\Delta\theta$, Equation (1.22) is employed and these are substituted into the equations of motion and heat continuity. For convenience sake, however, we employ here the equation obtained by integrating the equation of heat continuity (1.13) relative to r.

Thus, if we express Equation (1.13) as

$$wr\frac{\partial\theta}{\partial z}+vr\frac{\partial\theta}{\partial r}=-c'^2z^2\frac{\partial}{\partial r}\left\{\left(\frac{\partial w}{\partial r}\right)\left(\frac{\partial\theta}{\partial r}\right)\right\},$$

and integrate it from $r=0$ to $r=\infty$, the right hand side becomes 0 because $\frac{\partial w}{\partial r}=0$ and $\frac{\partial\theta}{\partial r}=0$ both at $r=0$ and $r=\infty$.

The left hand side is

Figure 1.6

Vertical distribution of temperature and upward velocity at the axis of upward current from a point heat source.

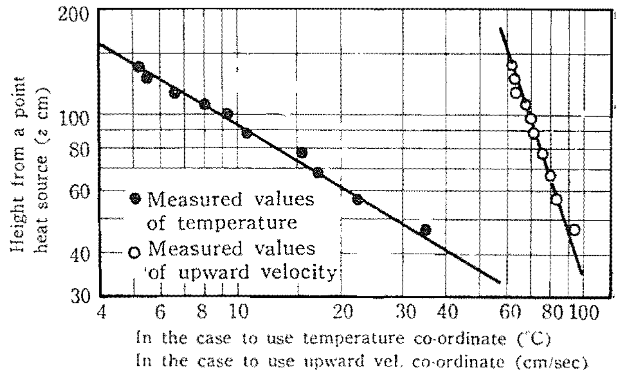

$$m+n+2=0. \qquad \cdots\cdots(1.35)$$

From simultaneous equation of (1.33) and (1.35) we obtain;

$$m=-\frac{5}{3} \text{ and } n=-\frac{1}{3}. \qquad \cdots\cdots(1.36)$$

By substituting the above results into Equations (1.22) and (1.28), we obtain;

$$\theta=\frac{\Delta\theta}{\theta_0}=z^{-5/3}\phi(\eta), \qquad \cdots\cdots(1.37)$$

$$w=z^{-1/3}\frac{F'(\eta)}{\eta}. \qquad \cdots\cdots(1.38)$$

That is, the temperature and velocity along the axis of the upward current from a point heat source decrease in inverse proportion to the 5/3 power and 1/3 power of the height measured from the heat source, respectively. Figure 1.6 is a description of the values of measurement of the temperature and velocity along the central axis of the upward current rising from a burning alcohol lamp, plotted on section paper with logarithmic scales in both directions. In this figure the slopes of the straight lines correspond to the directions of $z^{-5/3}$ and $z^{-1/3}$, respectively, and plotted points obtained by measurement, gather near these lines, so law obtained above can be said to be held.

1.6.2 In the case of infinite line heat source

As in the case of the point heat source, by use of the stream function ψ, defined by

$$w=\frac{\partial\psi}{\partial y}, \qquad v=-\frac{\partial\psi}{\partial z}, \qquad \cdots\cdots(1.39)$$

we obtain

$$\psi=\int w dy.$$

Substituting Equation (1.23) into this and we obtain,

$$z^{n+1}\int f(\eta)d\eta. \qquad \cdots\cdots(1.40)$$

As in the preceding case, by putting

$$F(\eta)=\int f(\eta)d\eta,$$

we obtain

$$\psi=z^{n+1}F(\eta). \qquad \cdots\cdots(1.41)$$

Substituting this into Equation (1.39), we obtain,

$$w=z^nF', \qquad (1.42)$$
$$v=z^n\{F'\eta-(n+1)F\}. \qquad (1.43)$$

Next, if the equation of heat continuity (1.20) is integrated from 0 to ∞, the right hand side of the equation becomes zero, and the left hand side, by virtue of the equation of continuity (1.16), becomes;

$$\int_0^\infty\left(w\frac{\partial\theta}{\partial z}+v\frac{\partial\theta}{\partial y}\right)dy=\int_0^\infty w\frac{\partial\theta}{\partial z}dy+\Big[v\theta\Big]_0^\infty-\int_0^\infty\theta\frac{\partial v}{\partial y}dy$$
$$=\int_0^\infty w\frac{\partial\theta}{\partial z}dy+\int_0^\infty\theta\frac{\partial w}{\partial y}dy=\int_0^\infty\frac{\partial}{\partial z}(w\theta)dy.$$

Thus we obtain

$$\int_0^\infty w\theta dy=\text{constant}. \qquad (1.44)$$

As in the case of the point heat source, this is equivalent to the following formula which states that if a long belt with a width of 1 cm stretching in the direction perpendicular to the direction of the line heat source is supposed to be on the horizontal section at an arbitrary height, the quantity of heat that passes through this belt in time, Q_0, is invariable:

$$2\int_0^\infty c_p\rho w\Delta\theta dy=Q_0.$$

Now, from Equations (1.22), (1.23), the differential coefficients of w and θ can be calculated as follows:

$$\left.\begin{aligned}\frac{\partial w}{\partial y}&=z^{n-1}F'',\\ \frac{\partial w}{\partial z}&=z^{n-1}(nF'-\eta F''),\\ \frac{\partial\theta}{\partial y}&=z^{m-1}\phi',\\ \frac{\partial\theta}{\partial z}&=z^{m-1}(m\phi-n\phi').\end{aligned}\right\} \qquad (1.45)$$

Substituting these into Equation (1.19) and (1.19$_1$), we obtain;

$$z^{2n-1}\{nF'^2-(n+1)FF''\}=z^mg\phi-c^2z^{2n-1}\frac{dF''^2}{d\eta}, \qquad (1.46)$$
$$z^{2n-1}\{nF'^2-(n+1)FF''\}=z^mg\phi-\frac{c^2z^{2n-1}}{2}\frac{dF''^2}{d\eta}. \qquad (1.46_1)$$

In order that the Equations (1.46) and (1.46$_1$) hold regardless of the value of z, the values of indices of z in each term of the equations must be equal, that is,

$$2n-1=m \qquad (1.47)$$

Substituting Equations (1.22) and (1.42) into (1.44), we obtain,

$$\int_0^\infty z^{m+n+1}F'\phi d\eta=\text{constant}. \qquad (1.48)$$

The condition on which these expressions hold regardless of the value of z, is

$$m+n+1=0. \qquad (1.49)$$

From Equations (1.47) and (1.49), we obtain

$$m=-1, \qquad n=0. \qquad (1.50)$$

Substituting these results into Equations, (1.22) and (1.42), we obtain,

$$\theta=\frac{\Delta\theta}{\theta_0}=z^{-1}\phi(\eta), \qquad (1.51)$$

$$\frac{5}{3} F\phi = c'^2\phi'\left(F'' - \frac{F'}{\eta}\right). \quad \cdots\cdots (1.54_1)$$

Assume that the coefficient of eddy diffusivity, K', is ε times the coefficient of eddy conductivity K, and put

$$K' = \varepsilon K, \quad \cdots\cdots (1.55)$$

and then from Equation (1.11), it becomes,

$$c' = \sqrt{\varepsilon}\, c, \quad \cdots\cdots (1.56)$$

Therefore, Equation (1.54_1) becomes

$$\frac{5}{3} F\phi = \varepsilon c^2\phi'\left(F'' - \frac{F'}{\eta}\right). \quad \cdots\cdots (1.54)$$

It suffices, for purpose to solve Equations (1.53) and (1.54) or (1.53_1) and (1.54) as simultaneous differential equations in which ϕ and F are the unknown functions. As it is impossible to solve these directly, let us employ an approximation method as shown below. We resemble the horizontal distributions of upward velocity and temperature with the exponential functions in the domain where the value of η is large, and with the power series of η in the domain where the value of η is small. They are expressed as follows:

$$\frac{F'}{\eta} = F_0(1 + p\eta^x + q\eta^{2x} + r\eta^{3x})\exp(a\eta^x), \quad \cdots\cdots (1.57)$$

$$\phi = \phi_0(1 + \alpha'\eta^x + \beta'\eta^{2x} + \gamma'\eta^{3x})\exp(a\eta^x). \quad \cdots\cdots (1.58)$$

The boundary conditions are:

(1) On the central axis, w and θ should be finite and $\frac{\partial w}{\partial r}$ and $\frac{\partial \theta}{\partial r}$ be zero,

(2) At infinity, w, θ, $\frac{\partial w}{\partial r}$ and $\frac{\partial \theta}{\partial r}$ should be all zero, which means in the case of the coordinates in question

at $\eta = 0$:

$$\frac{F'}{\eta} \text{ and } \phi \text{ are finite, and } \frac{d}{d\eta}\left(\frac{F'}{\eta}\right) = \phi' = 0,$$

at $\eta = \infty$:

$$\frac{F'}{\eta} = \phi = \frac{d}{d\eta}\left(\frac{F'}{\eta}\right) = \phi' = 0.$$

These can be satisfied if

$x > 0$, and $a < 0$.

Next, comparison of the orders of η in both sides of Equation (1.53) or (1.53_1) when Equation (1.57) is substituted into them reveals that each term of the left hand side is a primary order of η and the right hand side an order of η^{2x-2}. In Equation (1.54_1), each term of the left hand side is an order of η^2 and the right hand side an order of η^{2x-1}. In these expressions, the orders of η on both sides must be equal. For this, it is necessary that $x = 3/2$, that is the terms in the parenthesis in Equations (1.57) and (1.58) must be the power series of $\eta^{3/2}$. Accordingly, let us put the functions F and ϕ as in the following form and find the values of coefficients; α, β, γ, α', β' γ' and a.

$$F = F_0\left(\frac{\eta^2}{2} + \alpha\eta^{7/2} + \beta\eta^5 + \gamma\eta^{13/2}\right)\exp(a\eta^{3/2}), \quad \cdots\cdots (1.59)$$

Figure 1.7
Vertical distribution of temperature and upward velocity at the axis of upward current from a line heat source.

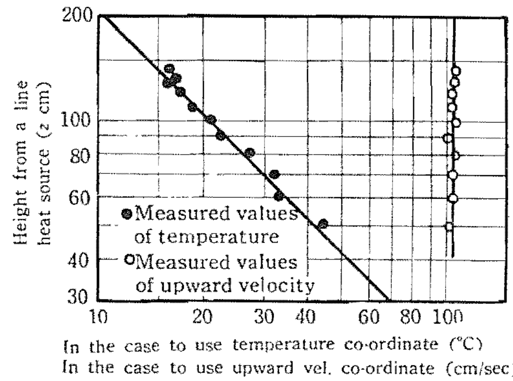

$$w=F'(\eta). \qquad \cdots\cdots(1.52)$$

which mean that the temperature along the central axis of the upward current rising from an infinite line heat source, decreases in reverse proportion to the height measured from the heat source and that the upward velocity does not vary with the height. Figure 1.7 is a description of the values of measurement of the temperature and velocity along the central axis of the upward current when alcohol is burnt in a long narrow vessel about 1 cm wide and about 1 m long, plotted on the both-logarithmic coordinates. The two straight lines in the figure are lines with a slope of z^{-1} and a slope of z^0, respectively, and we can see that the observed points gather near these lines.

1.7 Horizontal Distributions of Temperature and Velocity of Upward Current

If the horizontal distribution of temperature or velocity of an upward current, is expressed by the non-dimensional factor divided by the maximum value at the central axis of the upward current (the maximum value on the horizontal surface), and η as defined by Equation (1.21) is used as the non-dimensional coordinates of the point, then the distribution curve at any height can be expressed by one curve as is shown in Figure 1.2~Figure 1.5, or, according to Equations to (1.22), (1.28) and (1.42), by $\phi(\eta)$, $F'(\eta)/\eta$ (point heat source) and $F'(\eta)$ (line heat source). Therefore, it suffices if these functions can be obtained.

1.7.1 In the case of point heat source

By substitution of the result of Equation (1.36) into Equations (1.32) or (1.32_1), the required equation of motion expressed by the momentum transfer theory or by the modified vorticity transfer theory, as the case may be, is obtained; and by substitution of Equations (1.37) and (1.38) into Equation (1.6), the equation of heat continuity is obtained. The results of calculation of these become

$$\frac{5}{3}\frac{d}{d\eta}\left(\frac{FF'}{\eta}\right)-\frac{4}{3}\frac{F'^2}{\eta}+g\phi\eta=c^2\frac{d}{d\eta}\left\{\frac{1}{\eta}\left(F''-\frac{F'}{\eta}\right)^2\right\}, \qquad \cdots\cdots(1.53)$$

$$\frac{5}{3}\frac{d}{d\eta}\left(\frac{FF'}{\eta}\right)-\frac{4}{3}\frac{F'^2}{\eta}+g\phi\eta=c^2\left(F''-\frac{F'}{\eta}\right)\left(\frac{F'''}{\eta}-\frac{F''}{\eta^2}+\frac{F'}{\eta^3}\right), \qquad \cdots\cdots(1.53_1)$$

$$\phi=\phi_0(1+\alpha'\eta^{3/2}+\beta'\eta^3+\gamma'\eta^{9/2})\exp(a\eta^{3/2}), \quad\cdots\cdots(1.60)$$

where $a<0$. After differentiation with η, following equations are obtained;

$$\left.\begin{aligned}
\frac{F'}{\eta}&=F_0\Big\{1+\Big(\frac{7}{2}\alpha+\frac{3}{4}a\Big)\eta^{3/2}+\Big(5\beta+\frac{3}{2}a\alpha\Big)\eta^3\\
&\quad+\Big(\frac{13}{2}\gamma+\frac{3}{2}a\beta\Big)\eta^{9/2}\Big\}\exp(a\eta^{3/2}),\\
F''&=F_0\Big\{1+\Big(\frac{35}{4}\alpha+\frac{27}{8}a\Big)\eta^{3/2}+\Big(20\beta+\frac{45}{4}a\alpha\\
&\quad+\frac{9}{8}a^2\Big)\eta^3+\Big(\frac{143}{4}\gamma+\frac{63}{4}a\beta+\frac{9}{4}a^2\alpha\Big)\\
&\quad\eta^{9/2}\Big\}\exp(\eta^{3/2}),\\
F'''&=F_0\Big\{\Big(\frac{105}{8}\alpha+\frac{105}{16}a\Big)\eta^{1/2}+\Big(60\beta+\frac{375}{8}a\alpha\\
&\quad+\frac{135}{16}a^2\Big)\eta^2+\Big(\frac{1287}{8}\gamma+\frac{807}{8}a\beta+27a^2\alpha\\
&\quad+\frac{27}{16}a^3\Big)\eta^{7/2}\Big\}\exp\Big(a\eta^{3/2}\Big),\\
\phi'&=\phi_0\Big\{\Big(\frac{3}{2}\alpha'+\frac{3}{2}a\Big)\eta^{1/2}+\Big(3\beta'+\frac{3}{2}a\alpha'\Big)\eta^2\\
&\quad+\Big(\frac{9}{2}\gamma'+\frac{3}{2}a\beta'\Big)\eta^{7/2}\Big\}\exp\Big(a\eta^{7/2}\Big).
\end{aligned}\right\}\cdots\cdots(1.61)$$

Substituting above results into Equations (1.53), (1.53_1) and (1.54), placing that the coefficients of the term which has equal power of η are equal, we obtain the simultaneous equations shown below. In this case, if we substitute Equation (1.60) directly into Equation (1.53) or (1.54) the powers of the exponential in the second term of the left hand side of the equation, do not coincide with the other terms, and this is inconvenient in calculation, so we transform the exponential term in Equation (1.60) into as follows:

$$\begin{aligned}
\phi&\fallingdotseq\phi_0(1+\alpha'\eta^{3/2}+\beta'\eta^3+\gamma'\eta^{9/2})\Big(1-a\eta^{3/2}+\frac{a^2}{2}\eta^3-\frac{a^3}{6}\eta^{9/2}\Big)\exp(2a\eta^{3/2})\\
&\fallingdotseq\phi_0\Big\{1+(\alpha'-a)\eta^{3/2}+\Big(\beta'-a\alpha'+\frac{a^2}{2}\Big)\eta^3+\Big(\gamma'-a\beta'+\frac{a^2\alpha'}{2}-\frac{a^3}{6}\Big)\eta^{9/2}\Big\}\\
&\qquad\exp(2a\eta^{3/2}).
\end{aligned}$$

(a) In the case of employing momentum transfer equation

$$\frac{1}{3}F_0^2+g\phi_0=2c^2F_0^2\Big(\frac{21}{4}\alpha+\frac{21}{8}a\Big)^2, \quad\cdots\cdots(1.62)$$

$$\begin{aligned}
&\Big(\frac{161}{24}\alpha+\frac{129}{48}a\Big)F_0^2+(\alpha'-a)g\phi_0\\
&\quad=c^2F_0^2\Big(\frac{21}{4}\alpha+\frac{21}{8}a\Big)\Big(105\beta+84a\alpha+\frac{63}{4}a^2\Big), \quad\cdots\cdots(1.63)
\end{aligned}$$

$$\begin{aligned}
&\Big(\frac{95}{6}\beta+\frac{77}{6}\alpha^2+\frac{61}{4}a\alpha+\frac{13}{8}a^2\Big)F_0^2+g\phi_0\Big(\beta'-a\alpha'+\frac{a^2}{2}\Big)\\
&\quad=c^2F_0^2\Big\{\Big(15\beta+\frac{39}{4}a\alpha+\frac{9}{8}a^2\Big)\Big(75\beta+\frac{321}{4}a\alpha+\frac{171}{8}a^2\Big)\\
&\quad+10\Big(\frac{21}{4}\alpha+\frac{21}{8}a\Big)\Big(\frac{117}{4}\gamma+\frac{57}{4}a\beta+\frac{9}{4}a^2\alpha\Big), \quad\cdots\cdots(1.64)
\end{aligned}$$

$$\left(\frac{689}{24}\gamma+\frac{689}{12}\alpha\beta+\frac{79}{4}a\beta+\frac{79}{4}a\alpha^2+\frac{9}{2}a^2\alpha\right)F_0^2$$
$$+g\phi_0\left(\gamma'-a\beta'-\frac{a^2\alpha'}{2}-\frac{a^3}{6}\right)$$
$$=c^2F_0^2\left\{\left(\frac{117}{4}\gamma+\frac{57}{4}a\beta+\frac{9}{4}a^2\alpha\right)\left(195\beta+\frac{633}{4}a\alpha+\frac{243}{8}a^2\right)\right.$$
$$\left.+3a\left(15\beta+\frac{39}{4}a\alpha+\frac{9}{8}a^2\right)^2\right\}, \quad\cdots\cdots(1.65)$$

$$\frac{5}{6}=\varepsilon c^2\left(\frac{21}{4}\alpha+\frac{21}{8}a\right)\left(\frac{3}{2}\alpha'+\frac{3}{2}a\right). \quad\cdots\cdots(1.66)$$

$$\frac{5}{3}\left(\frac{\alpha'}{2}+\alpha\right)=\varepsilon c^2\left\{\left(3\beta'+\frac{3}{2}a\alpha'\right)\left(\frac{21}{4}\alpha+\frac{21}{8}a\right)\right.$$
$$\left.+\left(\frac{3}{2}\alpha'+\frac{3}{2}a\right)\left(15\beta+\frac{39}{4}a\alpha+\frac{9}{8}a^2\right)\right\}, \quad\cdots\cdots(1.67)$$

$$\frac{5}{3}\left(\beta+\alpha\alpha'+\frac{\beta'}{2}\right)=\varepsilon c^2\left\{\left(\frac{9}{2}\gamma'+\frac{3}{2}a\beta'\right)\left(\frac{21}{4}\alpha+\frac{21}{8}a\right)\right.$$
$$+\left(3\beta'+\frac{3}{2}a\alpha'\right)\left(15\beta+\frac{39}{4}a\alpha+\frac{9}{8}a^2\right)$$
$$\left.+\left(\frac{3}{2}\alpha'+\frac{3}{2}a\right)\left(\frac{117}{4}\gamma+\frac{57}{4}a\beta+\frac{9}{4}a^2\alpha\right)\right\}. \quad\cdots\cdots(1.68)$$

In this case, solution is impossible unless the relation between F_0^2 and $g\phi_0$, and the value of ε are known. Therefore, at first, basing on the results of experiments, we suppose as follows:

$$g\phi_0=\frac{2}{3}F_0^2. \quad\cdots\cdots(1.69)$$

Next, we find the value of ε which agrees with the results of experiments. As a result it was found that the assumption that

$$\varepsilon=1.56, \quad\cdots\cdots(1.70)$$

brings about a comparatively good agreement with the results of experiments. At first, from Equations (1.62) and (1.69), we obtain

$$c^2\left(\frac{21}{4}\alpha+\frac{21}{8}a\right)^2=\frac{2}{3}.$$

This is substituted into Equation (1.66), and we obtain

$$\alpha'=3.7499\alpha+0.8749a.$$

In the same way, we obtain from Equations (1.63), (1.67), (1.64) and (1.68), the follwing equations;

$$\beta=0.92085\alpha^2-0.07916a\alpha-0.019795a^2,$$
$$\beta'=5.8482\alpha^2+2.0982a\alpha+0.08706a^2,$$
$$\gamma=0.50282\alpha^3-0.16660a\alpha^2-0.043714a^2\alpha-0.00068667a^3,$$
$$\gamma'=5.2277\alpha^3+1.9935a\alpha^2-0.052284a^2\alpha-0.037729a^3.$$

All these are substituted into Equation (1.65), then we obtain

$$\alpha=-0.2974a,$$

and we obtain the equations which express the temperature and velocity distributions as follows:

$$\phi=\phi_0\left\{1+0.1597\left(\frac{\eta}{c^{2/3}}\right)^{3/2}-0.00869\left(\frac{\eta}{c^{2/3}}\right)^3-0.00490\left(\frac{\eta}{c^{2/3}}\right)^{9/2}\right\}$$

$$\exp\left\{-0.665\left(\frac{\eta}{c^{2/3}}\right)^{3/2}\right\}, \quad \cdots\cdots\cdots (1.71)$$

$$\frac{F'}{\eta}=F_0\left\{1+0.1934\left(\frac{\eta}{c^{2/3}}\right)^{3/2}-0.00888\left(\frac{\eta}{c^{2/3}}\right)^{3}-0.00766\left(\frac{\eta}{c^{2/3}}\right)^{9/2}\right\}$$

$$\exp\left\{-0.665\left(\frac{\eta}{c^{2/3}}\right)^{3/2}\right\}. \quad \cdots\cdots\cdots (1.72)$$

The curve expressing the temperature ϕ and the velocity F'/η in relation to $\eta/c^{2/3}$ $\left(=\frac{1}{c^{2/3}}\times\frac{r}{z}\right)$ is shown in Figure 1.8. The other parameter c in the equations is always combined with η in the form of $\eta/c^{2/3}$. In Figure 1.8 the curves have been drawn relative to

$$\eta'=\eta/c^{2/3}, \quad \cdots\cdots\cdots (1.73)$$

not meaning that the value of c has been obtained. As for the value of c, find a value by using which the results of the experiments expressed in Figure 1.2 and Figure 1.3 cluster along the curve in Figure 1.8. Thus, in Figure 1.8 the points of measurement were entered at $c^{2/3}=0.058$. This value of c is the parameter expressing the degree of turbulence of the upward current, and physically it expresses the degree of spreading of the domain of hot current to horizontal direction as it rises. This value of $c^{2/3}$ somewhat varies according to the season and the day. It

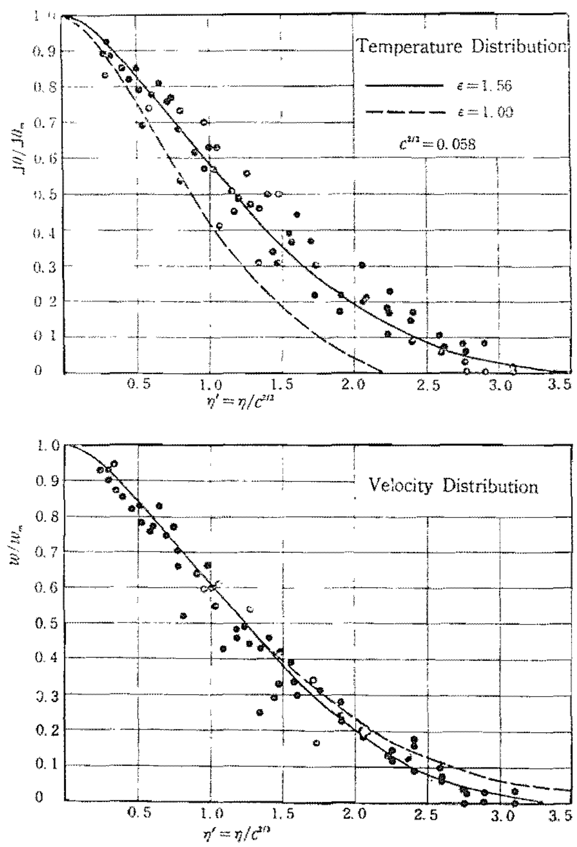

Figure 1.8

Horizontal distribution curves of temperature and upward velocity in the upward current from a point heat source, calculated basing on a momentum transfer theory

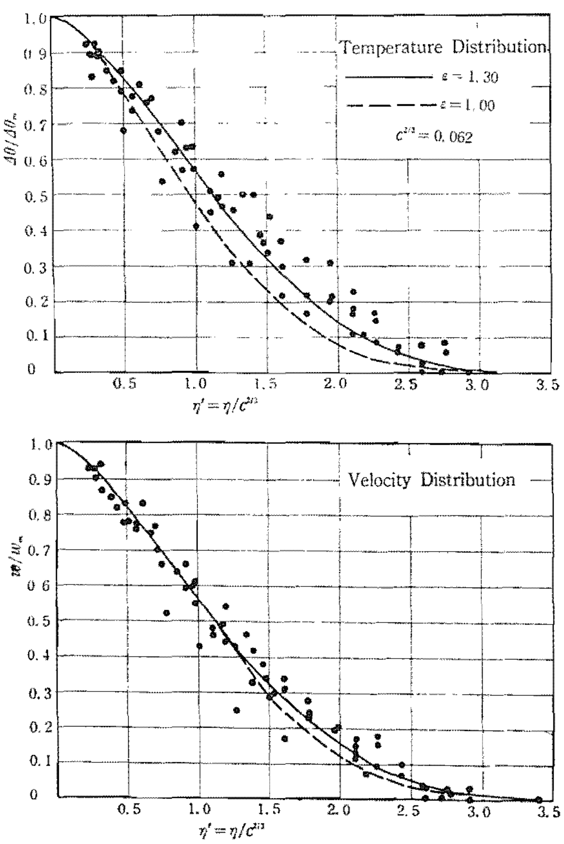

Figure 1.9

Horizontal distribution curves of temperature and upward velocity in the upward current from a point heat source, calculated basing on a modified vorticity transfer theory.

was found that the value is a little greater on fine and dry days and smaller on days of high humidity. According to the mixture length theory of turbulence, the value of the coefficient of eddy viscosity, K, and that of the coefficient of eddy diffusivity, K', should be equal. However, the broken curve expressed by broken line in Figure 1.8 which is the result of calculation on this premise ($\varepsilon=1.00$), differed from the results of experiments. The result of calculation on the assumption that $\varepsilon=1.56$ or the eddy diffusion coefficient is 1.56 times the eddy viscosity coefficient, best agreed with the results of experiments.

(b) In the case of employing modified vorticity transfer equation

In this case equations can be obtained by applying Equation (1.59) and (1.60) to Equations (1.53_1) and (1.54). The simultaneous equations corresponding to Equations (1.62)~(1.68) are as follows:

$$\frac{1}{3}F_0^2+g\phi_0=\frac{3}{2}c^2F_0^2\left(\frac{21}{4}\alpha+\frac{21}{8}a\right)^2, \quad \cdots\cdots(1.74)$$

$$\left(\frac{161}{24}\alpha+\frac{129}{48}a\right)F_0^2+(\alpha'-a)g\phi_0$$
$$=c^2F_0^2\left(\frac{21}{4}\alpha+\frac{21}{8}a\right)\left(\frac{135}{2}\beta+\frac{207}{4}a\alpha+9a^2\right), \quad \cdots\cdots(1.75)$$

$$\left(\frac{95}{4}\beta+\frac{77}{6}\alpha^2+\frac{61}{4}a\alpha+\frac{13}{8}a^2\right)F_0^2+g\phi_0\left(\beta'-a\alpha'+\frac{a^2}{2}\right)$$
$$=c^2F_0^2\left\{6\left(\frac{21}{4}\alpha+\frac{21}{8}a\right)\left(\frac{117}{4}\gamma+\frac{57}{4}a\beta+\frac{9}{4}a^2\alpha\right)\right.$$
$$+\frac{3a}{2}\left(\frac{21}{4}\alpha+\frac{21}{8}a\right)\left(15\beta+\frac{39}{4}a\alpha+\frac{9}{8}a^2\right)$$
$$\left.+\left(15\beta+\frac{39}{4}a\alpha+\frac{9}{8}a^2\right)\left(45\beta+\frac{297}{8}a\alpha+\frac{117}{16}a^2\right)\right\}, \quad \cdots(1.76)$$

$$\left(\frac{689}{24}\gamma+\frac{545}{12}\alpha\beta+\frac{79}{4}a\beta+\frac{79}{4}a\alpha^2+\frac{9}{2}a^2\alpha\right)F_0^2$$
$$+g\phi_0\left(\gamma'-a\beta'-\frac{a^2\alpha}{2}+\frac{a^2\alpha'}{2}-\frac{a^3}{6}\right)$$
$$=c^2F_0^2\left\{\left(45\beta+\frac{297}{8}a\alpha+\frac{117}{16}a^2\right)\left(\frac{117}{4}\gamma+\frac{57}{4}a\beta+\frac{9}{4}a^2\alpha\right)\right.$$
$$+\frac{9}{2}\left(15\beta+\frac{39}{4}a\alpha+\frac{9}{8}a^2\right)\left(\frac{117}{4}\gamma+\frac{57}{4}a\beta+\frac{9}{4}a^2\alpha\right)$$
$$\left.+\frac{3}{2}a\left(15\beta+\frac{39}{4}a\alpha+\frac{9}{8}a^2\right)^2\right\}. \quad \cdots\cdots(1.77)$$

The equations of heat continuity are the same with those of momentum transfer theory and are expressed by Equations (1.66), (1.67) and (1.68). The solution is obtained by use of these and Equation (1.69). This time, in order to have agreement with the results of experiments, it was necessary to put

$$\varepsilon=1.30. \quad \cdots\cdots(1.78)$$

In this case, the temperature and velocity are expressed by the following equations:

$$\phi=\phi_0\left\{1+0.938\left(\frac{\eta}{c^{2/3}}\right)^{3/2}+0.400\left(\frac{\eta}{c^{2/3}}\right)^3+0.0940\left(\frac{\eta}{c^{2/3}}\right)^{9/2}\right\}$$
$$\exp\left\{-1.462\left(\frac{\eta}{c^{2/3}}\right)^{3/2}\right\}, \quad \cdots\cdots(1.79)$$

$$\frac{F'}{\eta}=F_0\left\{1+0.917\left(\frac{\eta}{c^{2/3}}\right)^{3/2}+0.399\left(\frac{\eta}{c^{2/3}}\right)^{3}+0.1077\left(\frac{\eta}{c^{2/3}}\right)^{9/2}\right\}$$
$$\exp\left\{-1.462\left(\frac{\eta}{c^{2/3}}\right)^{3/2}\right\}. \cdots\cdots\cdots\cdots (1.80)$$

Curves corresponding to these are shown in Figure 1.9. In this case, if we put $\varepsilon=1$ according to the mixture length theory, it produces a curve like the broken line shown in Figure 1.9, making the shape of the temperature distribution dissimilar to that of the velocity distribution. Therefore it was imperative to assume $\varepsilon=1.30$ or the eddy diffusion coefficient is 1.30 times the eddy viscosity coefficient. In this case the value of a parameter c was known to be $c^{2/3}=0.062$.

1.7.2 In the case of infinite line heat source

By substitution of the results of Equation (1.50) into (1.46) and (1.46_1), the required equations of motion for the momentum transfer theory and the modified vorticity transfer theory respectively are obtained. If Equations (1.51) and (1.52) are substituted into Equation (1.20), the equation of heat continuity is obtained. The results of calculation of these are as follows:

$$FF''+g\phi=c^2\frac{d}{d\eta}(F''^2), \cdots\cdots\cdots\cdots (1.81)$$

$$FF''+g\phi=\frac{c^2}{2}\frac{d}{d\eta}(F''^2), \cdots\cdots\cdots\cdots (1.81_1)$$

$$F\phi=c'^2F''\phi'. \cdots\cdots\cdots\cdots (1.82_1)$$

Equation (1.81) and (1.81_1) are obtained basing on momentum transfer theory and modified vorticity transfer theory respectively.

If the coefficient of eddy diffusion, K', is assumed to be ε times that of eddy viscosity K and if, as in the case of the point heat source, it is put that

$$c'=c\sqrt{\varepsilon}. \cdots\cdots\cdots\cdots (1.83)$$

Equation (1.82_1) becomes

$$F\phi=c^2\varepsilon F''\phi'. \cdots\cdots\cdots\cdots (1.82)$$

As it is impossible to solve this directly as in the case of the point heat source, let us employ the method of approximation by means of the power series and the exponential function of η and put

$$F=F_0(\eta+\alpha\eta^{5/2}+\beta\eta^4+8\eta^{11/2})\exp(a\eta^{3/2}), \cdots\cdots\cdots (1.84)$$
$$\phi=\phi_0(1+\alpha'\eta^{3/2}+\beta'\eta^3+\gamma'\eta^{9/2})\exp(a\eta^{3/2}), \cdots\cdots\cdots (1.85)$$

and determine the values of coefficients α, β, γ, α', β', γ', and a as before. Of course Equations (1.84) and (1.85) satisfy the following boundary conditions meaning that along the axis of the upward current the temperature and velocity are finite and their gradients in horizontal directions are 0 and that at infinity the temperature, the velocity and their gradients are all 0:

$$\eta=0 \ : F' \text{ and } \phi \text{ are finite, and } F''=\phi'=0,$$
$$\eta=\infty \ : F'=\phi=F''=\phi'=0.$$

In preparation for substituting Equations (1.84) and (1.85) into Equations (1.81), (1.81_1) and (1.82), let us make calculation of the following quantities:

$$\left.\begin{aligned}
F'&=F_0\Big\{1+\Big(\frac{5}{2}\alpha+\frac{3}{2}a\Big)\eta^{3/2}+\Big(4\beta+\frac{3}{2}a\alpha\Big)\eta^3\\
&\quad+\Big(\frac{11}{2}\gamma+\frac{3}{2}a\beta\Big)\eta^{9/2}\Big\}\exp(a\eta^{3/2}),\\
F''&=F_0\Big\{\Big(\frac{15}{4}\alpha+\frac{15}{4}a\Big)\eta^{1/2}\\
&\quad+\Big(12\beta+\frac{33}{4}a\alpha+\frac{9}{4}a^2\Big)\eta^2\\
&\quad+\Big(\frac{99}{4}\gamma+\frac{51}{4}a\beta+\frac{9}{4}a^2\alpha\Big)\eta^{7/2}\Big\}\exp(a\eta^{3/2}),\\
\phi'&=\phi_0\Big\{\Big(\frac{3}{2}\alpha'+\frac{3}{2}a\Big)\eta^{1/2}+\Big(3\beta'+\frac{3}{2}a\alpha'\Big)\eta^2\\
&\quad+\Big(\frac{9}{2}\gamma'+\frac{3}{2}a\beta'\Big)\eta^{1/2}\Big\}\exp(a\eta^{3/2}).
\end{aligned}\right\}\quad\cdots\cdots(1.86)$$

Also Equations (1.85) and (1.86) are employed for sbustituting for ϕ and ϕ' into Equation (1.82), but, for substituting into Equations (1.81) or (1.81$_1$), only the second term involves $\exp(a\eta^{3/2})$, while other terms $\exp(2a\eta^{3/2})$, and exponential terms cannot be eliminated. So in this case Equation (1.85) must be transformed into the following equation:

$$\phi\doteqdot\phi_0(1+\alpha'\eta^{3/2}+\beta'\eta^3+\gamma'\eta^{9/2})\Big(1-a\eta^{3/2}+\frac{a^2}{2}\eta^3-\frac{a^3}{6}\eta^{9/2}\Big)\exp(2a\eta^{3/2})$$

$$\doteqdot\phi_0\Big\{1+(\alpha'-a)\eta^{3/2}+\Big(\beta'-a\alpha'+\frac{a^2}{2}\Big)\eta^3+\Big(\gamma'-a\beta'+\frac{a^2\alpha'}{2}-\frac{a^3}{6}\Big)\eta^{9/2}\Big\}$$
$$\exp(2a\eta^{3/2}).$$

The simultaneous equations concerning α, β, γ, α', β', γ', and a are as follows:

(a) In the case of employing momentum transfer equation

$$g\phi_0=c^2F_0^2\Big(\frac{15}{4}\alpha+\frac{15}{4}a\Big)^2,\quad\cdots\cdots(1.87)$$

$$\begin{aligned}
&F_0^2\Big(\frac{15}{4}\alpha+\frac{15}{4}a\Big)+g\phi_0(\alpha'-a)\\
&\quad=c^2F_0^2\Big(\frac{15}{4}\alpha+\frac{15}{4}a\Big)\Big(60\beta+\frac{105}{2}a\alpha+\frac{45}{2}a^2\Big),
\end{aligned}\quad\cdots\cdots(1.88)$$

$$\begin{aligned}
&F_0^2\Big(12\beta+\frac{15}{4}\alpha^2+12a\alpha+\frac{9}{4}a^2\Big)+g\phi_0\Big(\beta'-a\alpha'+\frac{a^2}{2}\Big)\\
&\quad=c^2F_0^2\Big\{8\Big(\frac{99}{4}\gamma+\frac{51}{4}a\beta+\frac{9}{4}a^2\alpha\Big)\Big(\frac{15}{4}\alpha+\frac{15}{4}a\Big)\\
&\quad+4\Big(12\beta+\frac{33}{4}a\alpha+\frac{9}{4}a^2\Big)^2\\
&\quad+6a\Big(\frac{15}{4}\alpha+\frac{15}{4}a\Big)\Big(12\beta+\frac{33}{4}a\alpha+\frac{9}{4}a^2\Big)\Big\},
\end{aligned}\quad\cdots\cdots(1.89)$$

$$\begin{aligned}
&F_0^2\Big(\frac{99}{4}\gamma+\frac{63}{4}\alpha\beta+\frac{33}{2}a\beta+\frac{33}{4}a\alpha^2+\frac{9}{2}a^2\alpha\Big)+g\phi_0\Big(\gamma'-a\beta'+\frac{a^2\alpha}{2}-\frac{a^3}{6}\Big)\\
&\quad=c^2F_0^2\Big\{11\Big(12\beta+\frac{33}{4}a\alpha+\frac{9}{4}a^2\Big)\Big(\frac{99}{4}\gamma+\frac{51}{4}a\beta+\frac{9}{4}a^2\Big)\\
&\quad+6a\Big(\frac{15}{4}\alpha+\frac{15}{4}a\Big)\Big(\frac{99}{4}\gamma+\frac{51}{4}a\beta+\frac{9}{4}a^2\alpha\Big)\\
&\quad+3a\Big(12\beta+\frac{33}{4}a\alpha+\frac{9}{4}a^2\Big)^2\Big\},
\end{aligned}\quad\cdots\cdots(1.90)$$

$$1=\varepsilon c^2\left(\frac{3}{2}\alpha'+\frac{3}{2}a\right)\left(\frac{15}{4}\alpha+\frac{15}{4}a\right), \quad \cdots\cdots\cdots\cdots(1.91)$$

$$\alpha+\alpha'=\varepsilon c^2\left\{\left(3\beta'+\frac{3}{2}a\alpha'\right)\left(\frac{15}{4}\alpha+\frac{15}{4}a\right)\right.$$
$$\left.+\left(\frac{3}{2}\alpha'+\frac{3}{2}a\right)\left(12\beta+\frac{33}{4}a\alpha+\frac{9}{4}a^2\right)\right\}, \quad \cdots\cdots\cdots\cdots(1.92)$$

$$\beta+\alpha\alpha'+\beta'=\varepsilon c^2\left\{\left(\frac{9}{2}\gamma'+\frac{3}{2}a\beta'\right)\left(\frac{15}{4}\alpha+\frac{15}{4}a\right)\right.$$
$$+\left(\frac{3}{2}\alpha'+\frac{3}{2}a\right)\left(\frac{99}{4}\gamma+\frac{51}{4}a\beta+\frac{9}{4}a^2\alpha\right)$$
$$\left.+\left(3\beta'+\frac{3}{2}a\alpha'\right)\left(12\beta+\frac{33}{4}a\alpha+\frac{9}{4}a^2\right)\right\}. \quad \cdots\cdots\cdots\cdots(1.93)$$

Now, solution is impossible unless the relation between F_0^2 and $g\phi_0$ and the numerical value of ε are known. Accordingly, from the results of experiments, let us find a solution by putting

$$g\phi_0=\frac{1}{2}F_0^2. \quad \cdots\cdots\cdots\cdots(1.94)$$

As for ε, let us try to apply various values and find the one which agrees best with the results of experiments. After attempts, it was found that an approximate agreement is seen if we put

$$\varepsilon=2.20, \quad \cdots\cdots\cdots\cdots(1.95)$$

and that in this case the horizontal distributions of the temperature and velocity are expressed by the following formulas:

$$\phi=\phi_0\left\{1+0.447\left(\frac{\eta}{c^{2/3}}\right)^{3/2}+0.0611\left(\frac{\eta}{c^{2/3}}\right)^3\right.$$
$$\left.-0.00967\left(\frac{\eta}{c^{2/3}}\right)^{9/2}\right\}\exp\left\{-0.875\left(\frac{\eta}{c^{2/3}}\right)^{3/2}\right\}, \quad \cdots\cdots\cdots\cdots(1.96)$$

$$F=F_0\left\{1+0.404\left(\frac{\eta}{c^{2/3}}\right)^{3/2}+0.0573\left(\frac{\eta}{c^{2/3}}\right)^3\right.$$
$$\left.+0.001383\left(\frac{\eta}{c^{2/3}}\right)^{9/2}\right\}\exp\left\{-0.875\left(\frac{\eta}{c^{2/3}}\right)^{3/2}\right\}. \quad \cdots\cdots\cdots\cdots(1.97)$$

In Figure 1.10 is shown a curve drawn by plotting the temperature, ϕ, and the velocity, F', against $\eta/c^{2/3}$. It was found that the value of c, determined in such a way that the results of experiments cluster most reasonably along the curve, is $c^{2/3}=0.107$. As in the case of the point heat source, this value of c somewhat varies according to the humidity of the day. Again, if it is assumed that the eddy diffusion coefficient and the eddy viscosity coefficient are equal, the curve is expressed by broken lines as shown in Figure 1.10, in which the horizontal distributions of the temperature and velocity are not similar in shape. Agreement is obtained only when the former is made 2.20 times the latter.

(b) In the case of employing modified vorticity transfer equation

In this case it is possible to obtain the required equations by applying Equations (1.84), (1.85) and (1.86) to Equations (1.81_1) and (1.82). The simultaneous equations corresponding to Equation (1.87) and the subsequent equations are as follows:

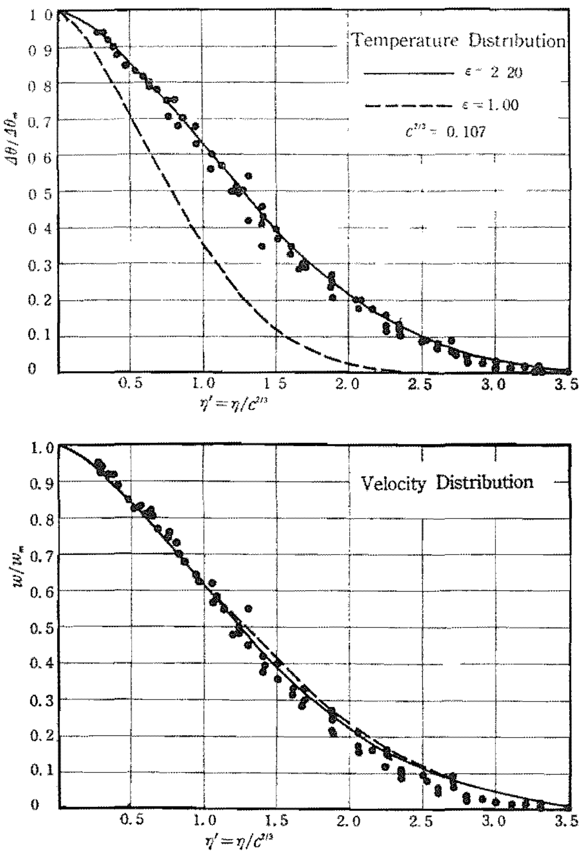

Figure 1.10
Horizontal distribution curves of temperature and upward velocity in the upward current from a line heat source, calculated basing on a momentum transfer theory.

$$g\phi_0=\frac{c^2}{2}F_0^2\left(\frac{15}{4}\alpha+\frac{15}{4}a\right)^2, \qquad \cdots\cdots(1.98)$$

$$F_0^2\left(\frac{15}{4}\alpha+\frac{15}{4}a\right)+g\phi_0(\alpha'-a)$$
$$=\frac{c^2}{2}F_0^2\left(\frac{15}{4}\alpha+\frac{15}{4}a\right)\left(60\beta+\frac{105}{2}a\alpha+\frac{45}{2}a^2\right), \qquad \cdots\cdots(1.99)$$

$$F_0^2\left(12\beta+\frac{15}{4}\alpha^2+12a\alpha+\frac{9}{4}a^2\right)+g\phi_0\left(\beta'-a\alpha'+\frac{a^2}{2}\right)$$
$$=\frac{c^2}{2}F_0^2\left\{8\left(\frac{99}{4}\gamma+\frac{51}{4}a\beta+\frac{9}{4}a^2\alpha\right)\left(\frac{15}{4}\alpha+\frac{15}{4}a\right)\right.$$
$$\left.+4\left(12\beta+\frac{33}{4}a\alpha+\frac{9}{4}a^2\right)^2+6a\left(\frac{15}{4}\alpha+\frac{15}{4}a\right)\left(12\beta+\frac{33}{4}a\alpha+\frac{9}{4}a^2\right)\right\},$$
$$\cdots\cdots(1.100)$$

$$F_0^2\left(\frac{99}{4}\gamma+\frac{63}{4}\alpha\beta+\frac{33}{2}a\beta+\frac{33}{4}a\alpha^2+\frac{9}{2}a^2\alpha\right)$$
$$+g\phi_0\left\{(\gamma'-a\beta')+\frac{a^2\alpha'}{2}-\frac{a^3}{6}\right\}$$
$$=\frac{c^2}{2}F_0^2\left\{11\left(12\beta+\frac{33}{4}a\alpha+\frac{9}{4}a^2\right)\left(\frac{99}{4}\gamma+\frac{51}{4}a\beta+\frac{9}{4}a^2\right)\right.$$
$$+6a\left(\frac{15}{4}\alpha+\frac{15}{4}a\right)\left(\frac{99}{4}\gamma+\frac{51}{4}a\beta+\frac{9}{4}a^2\alpha\right)$$
$$\left.+3a\left(12\beta+\frac{33}{4}a\alpha+\frac{9}{4}a^2\right)\right\}. \qquad \cdots\cdots(1.101)$$

The equations of heat continuity are expressed by Equation (1.91), (1.92) and (1.93) as in the case of those of momentum transfer equation. The solution is;

Figure 1.11

Horizontal distribution curves of temperature and upward velocity in the upward current from a line heat source, calculated basing on a modified vorticity transfer theory.

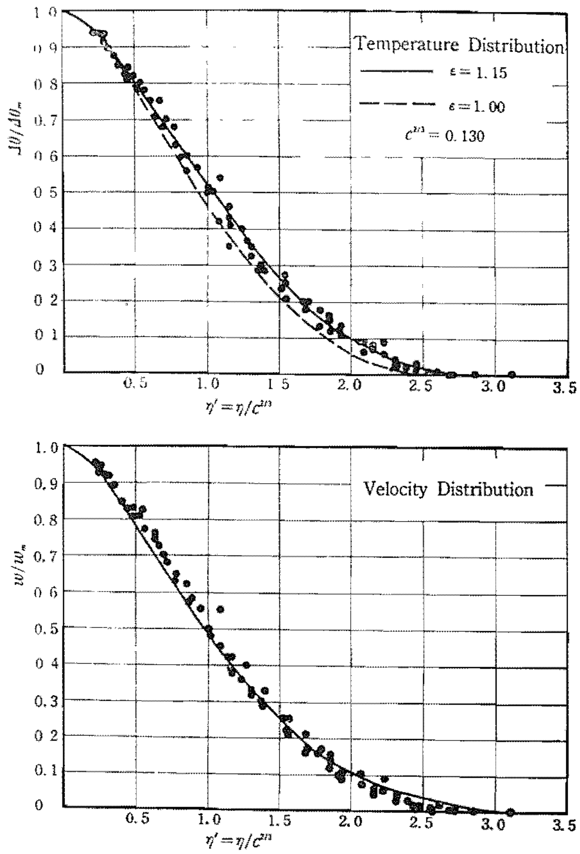

obtained by use of these and Equation (1.94). As for ε, it was found that the results of calculation agree comparatively well with the results of experiments if we put

$$\varepsilon=1.15. \quad\cdots\cdots(1.102)$$

The results of calculation revealed that the horizontal distributions of the temperature and velocity can be expressed by the following equations:

$$\phi=\phi_0\left\{1+0.529\left(\frac{\eta}{c^{2/3}}\right)^{3/2}+0.0676\left(\frac{\eta}{c^{2/3}}\right)^3 -0.0323\left(\frac{\eta}{c^{2/3}}\right)^{9/2}\right\}\exp\left\{-1.109\left(\frac{\eta}{c^{2/3}}\right)^{3/2}\right\}, \quad\cdots\cdots(1.103)$$

$$F'=F_0\left\{1+0.442\left(\frac{\eta}{c^{2/3}}\right)^{3/2}+0.0474\left(\frac{\eta}{c^{2/3}}\right)^3 -0.00850\left(\frac{\eta}{c^{2/3}}\right)^{9/2}\right\}\exp\left\{-1.109\left(\frac{\eta}{c^{2/3}}\right)^{3/2}\right\}. \quad\cdots\cdots(1.104)$$

In Figure 1.11, is shown a curve drawn by plotting the temperature ϕ and the velocity F', against $\eta/c^{2/3}$.

In this case the value of c was $c^{2/3}=0.130$. In the case of using the modified vorticity transfer theory it can be judged from the fact that the broken line fairly approaches the continuous line that the results of calculation are about the same as the results of experiments even when we put $\varepsilon=1$ or assume that the eddy viscosity coefficient and the eddy diffusion coefficient are equal.

1.8 General Formulas to Obtain the Values of Temperature and Velocity of Upward Current

Whether the momentum transfer theory or the modified vorticity transfer theory was used, the distributions of temperature and velocity of upward currents did not agree with the results of experiments when the formula was used as it was but did agree when it was assumed that the coefficient of the eddy diffusivity is several times that of the eddy conductivity. Either of the transfer theories may be used, but let us use the modified vorticity transfer theory here-after in this paper. Here let us try and find a formula for calculating the temperature and velocity at any point in the upward current rising from a heat source having given the strength of the source or the quantity of heat which it gives to the air in unit time.

1.8.1 In the case of point heat source

The following is obtained as the momentum equation of the upward current:

$$\frac{d}{dz}\int_0^\infty \rho w^2 2\pi r dr = g\int_0^\infty \rho \frac{\Delta\theta}{\theta_0} 2\pi r dr. \quad \cdots\cdots(1.105)$$

Different points in the current have different densities as they have different temperatures. However, by using the average density for the purpose of obtaining an approximate value, let us assume that the density is invariable and put ρ in Equation (1.105) to outside the sign of integration. Substituting Equations (1.21), (1.37) and (1.38) into Equation (1.105) for r, w and $\Delta\theta/\theta_0$, we obtain,

$$\frac{4}{3}\int_0^\infty \frac{F'^2}{\eta} d\eta = \int_0^\infty g\phi\eta d\eta.. \quad \cdots\cdots(1.106)$$

If equations(1.79) and (1.80) are substituted into above equation, after calculation we obtain:

$$\frac{2}{3}c^{4/3}F_0^2 \frac{\Gamma(4/3)}{2.923^{4/3}} \times 4.228, \qquad \text{from the left hand side and}$$

$$\frac{2}{3}c^{4/3}g\phi_0 \frac{\Gamma(4/3)}{2.923^{4/3}} \times 6.931, \qquad \text{from the right hand side.}$$

By equalizing the two, we obtain

$$g\phi_0 = 0.610 F_0^2. \quad \cdots\cdots(1.107)$$

This result is a little different from the assumption (1.69), used in calculating the temperature and velocity distributions in the upward current. So strictly speaking, we must recalculate them again, basing on Equation (1.107). But the equations which represent the velocity and temperature distribution coincide well with the results of experiment, as can be seen in Figures 1.9 and 1.11, we omit the re-calculation here. Equation (1.107) must be transformed into the equation expressed by $\Delta\theta$ and w. In the Equations (1.37) and (1.38), if we put the values of temperature and velocity at the central axis of upward current $\Delta\theta_m$ and w_m respectively, Equations (1.37), (1.38) hold also at the axis of the current and can be expressd by

$$\frac{\Delta\theta_m}{\theta_0} = z^{-5/3}\phi_0, \qquad w_m = z^{-1/3}F_0. \quad \cdots\cdots(1.108)$$

If above equations are substituted into Equation (1.107), the following equation can be obtained:

Table 1.1 Comparison of the calculated values with the measured values of the temperature at the central axis of the upward current. (in the case of a point heat source)

Height from a heat source, z	Measured values of ascending velocity, w_m	Absolute temperature of the ambient air, θ_0	Values of temperature at the axis of stream $\Delta\theta_m$	
			calculated	measured
47 cm	94 cm/sec	290 °K	33.9 °C	34.6 °C
57 〃	83 〃	〃	21.8 〃	22.2 〃
67 〃	80 〃	〃	17.2 〃	17.0 〃
77 〃	76 〃	〃	13.5 〃	15.1 〃
88 〃	71 〃	〃	10.4 〃	10.3 〃
98 〃	70 〃	〃	9.0 〃	9.2 〃
108 〃	68 〃	〃	7.7 〃	8.0 〃
118 〃	63 〃	〃	6.1 〃	6.5 〃
128 〃	63 〃	〃	5.6 〃	5.4 〃
138 〃	62 〃	〃	5.0 〃	5.2 〃

$$\Delta\theta_m = \frac{0.610\theta_0}{gz} w_m^2. \qquad \cdots\cdots (1.109)$$

Thus, temperature and velocity of the upward current along the central axis are not independent of each other but are connected in a relation as shown by Equation (1.109). We can calculate the values of temperature $\Delta\theta_m$ at the axis of the upward current from the measured values of the upward velocity w_m at the same point. In Table 1.1, the measured and calculated (in such way) values of the temperature at various height of the current are compared. A fair coincidence between the two can be seen. Now, if the quantity of heat to be lost by radiation etc. is ignored, the amount of heat Q that passes through the horizontal section at an arbitrary height in unit time, is expressed by Equation (1.30), and if independent variable is changed to η, using the Equations (1.34) and (1.35), following equation can be obtained:

$$Q = 2\pi c_p \rho \theta_0 \int_0^\infty F' \phi d\eta. \qquad \cdots\cdots (1.110)$$

If Equations (1.79) and (1.80) are substituted into above, it reduces after calculation;

$$Q = \frac{4}{3}\pi c_p \rho \theta_0 F_0 \phi_0 c^{4/3} \frac{\Gamma(4/3)}{2.923^{4/3}} \times 3.1701 = 2.838 c^{4/3} c_p \rho \theta_0 F_0 \phi_0.$$

Using the Equations (1.108), this can be reduced to

$$Q = 2.838 c^{4/3} c_p \rho z^2 w_m \Delta\theta_m. \qquad \cdots\cdots (1.111)$$

From this and Equation (1.109), we obtain

$$\Delta\theta_m = 0.423 \sqrt[3]{\frac{\theta_0 Q^2}{c_p^2 \rho^2 g}}\, c^{-8/9} z^{-5/3}, \qquad \cdots\cdots (1.112)$$

$$w_m = 0.833 \sqrt[3]{\frac{Qg}{\theta_0 c_p \rho}}\, c^{-4/9} z^{-1/3}. \qquad \cdots\cdots (1.113)$$

Thus it was found that the temperature and velocity of the upward current along the central axis increase in proportion to the 2/3rds power and 1/3rd power, respectively, of the quantity of heat which the heat source gives to the air per unit time. It is

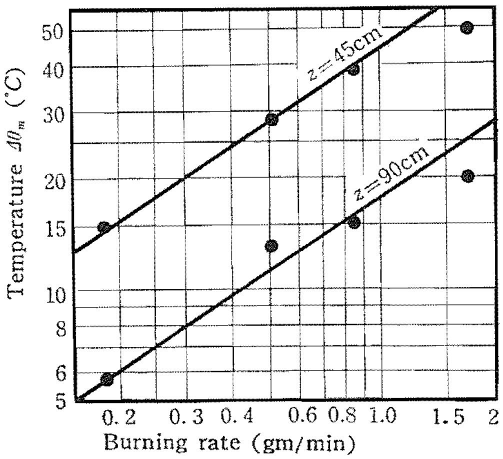

Figure 1.12

Relation between temperature at the axis of upward current and burning rate of alcohol.

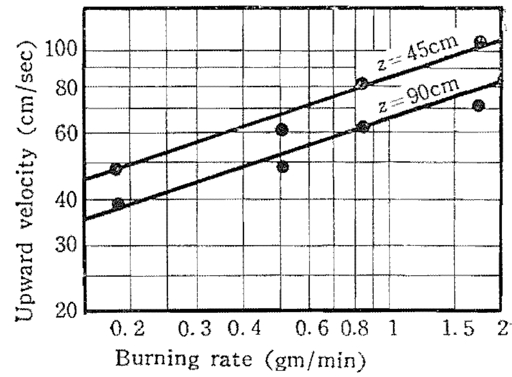

Figure 1.13

Relation between upward velocity at the axis of upward current and burning rate of alcohol.

rather troublesome to measure the value of Q directly, but it is easy to measure the quantity of alcohol consumed in burning. So we suppose that Q is proportional to the value of burning rate V_0 of alcohol, and investigate the relations between temperature, upward velocity and the burning rate. Figures 1.12 and 1.13 express the relations between the burning rate of alcohol and temperature or upward velocity at the central axis and at the height of 45 cm or 90 cm above the heat source. The burning rate was regulated by changing the number of wicks used in the alcohol lamp. Observed values are plotted in both-logarithmic graphs and straight line in graphs are drawn inclined at $\tan^{-1}(2/3)$ and $\tan^{-1}(1/3)$ to the abscissa. As the observed points cluster near these lines, the relations between $\Delta\theta_m$ and Q or w_m and Q expressed in Equations (1.112) and (1.113) has been corraborated.

The temperature and velocity at any point (r, z) above a heat source can be expressed by the following formulas according to Equations (1.79) and (1.80), and (1.112) and (1.43), respectively:

$$\Delta\theta = 0.423\sqrt[3]{\frac{\theta_0 Q^2}{c_p^2\rho^2 g}}\,c^{-8/9}z^{-5/3}\left\{1+0.938\left(\frac{r}{zc^{2/3}}\right)^{3/2}+0.400\left(\frac{r}{zc^{2/3}}\right)^{3}\right.$$
$$\left.+0.0940\left(\frac{r}{zc^{2/3}}\right)^{9/2}\right\}\exp\left\{-1.462\left(\frac{r}{zc^{2/3}}\right)^{3/2}\right\}, \quad \cdots\cdots\cdots(1.114)$$

$$w = 0.833\sqrt[3]{\frac{Qg}{\theta_0 c_p\rho}}\,c^{-4/9}z^{-1/3}\left\{1+0.917\left(\frac{r}{zc^{2/3}}\right)^{3/2}+0.399\left(\frac{r}{zc^{2/3}}\right)^{3}\right.$$
$$\left.+0.1077\left(\frac{r}{zc^{2/3}}\right)^{9/2}\right\}\exp\left\{-1.462\left(\frac{r}{zc^{2/3}}\right)^{3/2}\right\}. \quad \cdots\cdots\cdots(1.115)$$

1.8.2 In the case of infinite line heat source

In this case, the quantity of heat Q, produced per unit time, is infinite because the length of line is infinite. Therefore instead of Q, let us consider the quantity of heat which unit length of the heat source gives to the air, Q_0, and find the relation between Q_0, and the temperature $\Delta\theta_m$ or velocity w_m of the upward current.

The momentum equation of the heated current is

$$\frac{d}{dz}\int_0^\infty \rho w^2 dy = g\int_0^\infty \rho \frac{\Delta\theta}{\theta_m} dy. \quad \cdots\cdots (1.116)$$

Expressing this by the non-dimensional coordinates of η by use of Equations (1.51) and (1.52), we obtain;

$$\int_0^\infty F^2 d\eta = g\int_0^\infty \phi d\eta. \quad \cdots\cdots (1.117)$$

Substituting Equations (1.103) and (1.104) into this and integrating the result, we obtain,

$$\frac{2}{3}c^{2/3}F_0^2 \frac{\Gamma(5/3)}{2.217^{5/3}} \times 4.441 = \frac{2}{3}c^{2/3}g\phi_0 \frac{\Gamma(5/3)}{2.217^{5/3}} \times 7.243,$$

or $$g\phi_0 = 0.613F_0^2. \quad \cdots\cdots (1.118)$$

Though above result, Equation (1.118) differs a little from Equation (1.94), the relation assumed from the results of experiment, we shall not repeat the calculation in Section 1.7.2 on the same reason as in the case of a point heat source (Section 1.8.1).

In order to return the expression in Equation (1.118) to original one, we use the relation derived from Equations (1.51) and (1.52),

$$\frac{\Delta\theta_m}{\theta_0} = z^{-1}\phi_0, \qquad w_m = F_0, \quad \cdots\cdots (1.119)$$

where $\Delta\theta_m$ and w_m are temperature and upward velocity at the axis, respectively. Substituting this into Equation (1.118), we obtain the relation

$$\Delta\theta_m = \frac{0.613\theta_0}{gz} w_m^2. \quad \cdots\cdots (1.120)$$

The temperature and velocity of the upward current along the central axis are not independent of each other but are connected by the condition expressed by Equation (1.120). Table 1.2 indicates a comparison of the values of $\Delta\theta_m$ calculated following Equation (1.120) from the values of w_m measured in our experiments with the

Table 1.2 Comparison of the calculated values with the measured values of the temperature at the central axis of the upward current. (in the case of an infininte line heat source)

Height from a heat source, z	Measured values of ascending velocity, w_m	Absolute temperature of the ambient air, θ_0	Values of temperature at the axis of stream, $\Delta\theta_m$	
			calculated	measured
50 cm	103 cm/sec	290 °K	41 °C	44 °C
60 〃	105 〃	〃	34 〃	33 〃
70 〃	105 〃	〃	29 〃	32 〃
80 〃	108 〃	〃	26 〃	27 〃
90 〃	102 〃	〃	23 〃	22 〃
100 〃	107 〃	〃	20 〃	21 〃
110 〃	103 〃	〃	18.6 〃	18.5 〃
120 〃	104 〃	〃	17.1 〃	17 〃
130 〃	106 〃	〃	15.8 〃	16.5 〃
140 〃	108 〃	〃	14.6 〃	16 〃

measurement values. In this case, as the velocity should be invariable for all heights, we employed the average of mesurement values for all heights (105cm/sec) and calculated the temperature on the basis of this value.

Next, the quantity, Q_0 of heat which in unit time passes through such part of the horizontal section at an arbitrary height as constitutes unit width in the direction perpendicular to the heat source is

$$Q_0 = 2c_p\rho\theta_0\int_0^\infty w\Delta\theta dy.$$

Substituting the coordinates of η,

$$Q_0 = 2c_p\rho\theta_0\int_0^\infty F'\phi d\eta. \quad\cdots\cdots(1.121)$$

Substituting the results of Equations (1.103) and (1.104) into this,

$$Q_0 = \frac{4}{3}c^{2/3}c_p\rho\theta_0F_0\phi_0\frac{\Gamma(5/3)}{2.217^{5/3}}\times 4.543 = 1.451c^{2/3}c_p\rho\theta_0F_0\phi_0.$$

Returning to original variables, w_m and $\Delta\theta_m$, it reduces to

$$Q_0 = 1.451c^{2/3}c_p\rho z w_m\Delta\theta_m. \quad\cdots\cdots(1.122)$$

From this and Equation (1.109), we obtain,

$$\Delta\theta_m = 0.663\sqrt[3]{\frac{\theta_0 Q_0^2}{c_p^2\rho^2 g}}c^{-4/9}z^{-1}, \quad\cdots\cdots(1.123)$$

$$w_m = 1.040\sqrt[3]{\frac{gQ_0}{c_p\rho\theta_0}}c^{-4/9}. \quad\cdots\cdots(1.124)$$

The temperature and velocity of the upward current along the central axis, increase in proportion to the 2/3rds power and 1/3rd power, respectively, of the quantity of heat which the unit length of the heat source gives the air per minute, as in the case of the point heat source. The temperature and velocity at an arbitrary point (y, z) may be expressed from Equations (1.123), (1.124) and (1.103), (1.104) as

$$\Delta\theta = 0.663\sqrt[3]{\frac{\theta_0 Q_0^2}{c_p^2\rho^2 g}}c^{-4/9}z^{-1}\left\{1 + 0.529\left(\frac{y}{zc^{2/3}}\right)^{3/2} + 0.0676\left(\frac{y}{zc^{2/3}}\right)^3 - 0.0323\left(\frac{y}{zc^{2/3}}\right)^{9/2}\right\}\exp\left\{-1.109\left(\frac{y}{zc^{2/3}}\right)^{3/2}\right\},$$

$$\cdots\cdots(1.125)$$

$$w = 1.040\sqrt[3]{\frac{gQ_0}{c_p\rho\theta_0}}c^{-2/9}\left\{1 + 0.442\left(\frac{y}{zc^{2/3}}\right)^{3/2} + 0.0474\left(\frac{y}{zc^{2/3}}\right)^3 - 0.00850\left(\frac{y}{zc^{2/3}}\right)^{9/2}\right\}\exp\left\{-1.109\left(\frac{y}{zc^{2/3}}\right)^{3/2}\right\}.$$

$$\cdots\cdots(1.126)$$

1.9 Conclusion

We have derived the formulas to obtain the temperature and upward velocity at any point in the upward current from a point or infinite line heat source, when the heat quantity transfered per unit time from the heat source to the air is given.

Part Ⅱ. CONVECTION CURRENT FROM A BURNING WOODEN HOUSE IN A CALM CONDITION

Chapter 2.

Wind Velocity Distribution along Axis of Jets

2.1 Introduction

The velocity distribution of air current at atmospheric temperature spurting horizontally from a circular and a rectangular orifices has been studied with many laboratory experiments. It is considered that results of this study may be applied in analysing the behaviour of the hot current from a circular or a rectangular heat source and of the one ejected from a window of a fire resistive construction on fire.

2.2 Test Method

Using a Sirocco-fan at one opening of a horizontal duct whose section is 36.2cm× 30cm, wind was blown into it to make the air eject from a circular or a rectangular orifice attached to another opening of the duct. Fifteen kinds of orifices were used in the experiment; the circular orifices (1.5, 3.5, 5.0 and 7.5cm in radii), the square ones (7×7, 12×12cm) and the rectangular ones (5×10, 8×16, 3.5×14, 7.5×30, 3×18, 4×24, 5×30, 2×24 and 2.4×30cm).

The wind velocity was measured with a Pitot-tube connected to a Göttingen-type manometer or an inclined manometer. It was moved from one point to another on the axis of the jet, and wind velocity on those points were measured successively. Four steps of the initial outflowing velocity (about 22, 17, 12 and 7 m/sec) at the orifices were given by changing the opened area of a damper. So, 60 kinds of

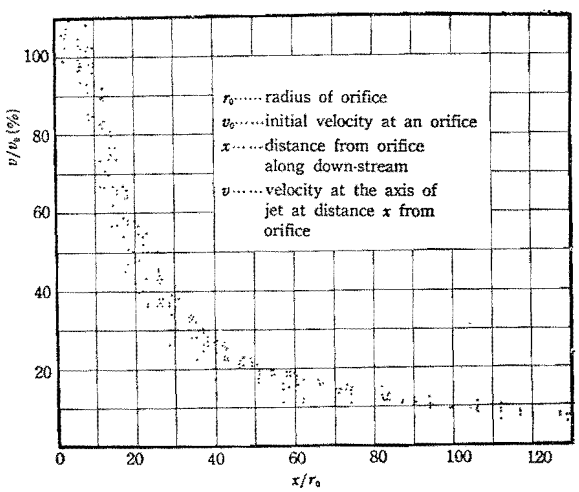

Figure 2.1

Velocity distribution along the axis of jet, discharged from a circular orifice.

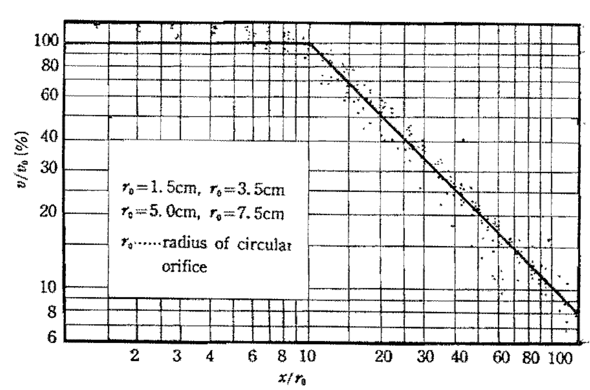

Figure 2.2

Velocity distribution along the axis of jet, discharged from a circular orifice. (plotted in both- logarithmic coordinates.)

experiments were made in all.

2.3 Test Results and Analysis

2.3.1 In the case of a circular orifices

If we assume that the dimension of the duct changes similarly with that of the orifice, the velocity v on any point of the axis is expressed as a function of the distance x from the orifice to the point, the radius r_0 of the orifice and the outflowing velocity v_0 of jet at the orifice. In this case, the dimension of the duct does not change, when the dimension of the orifice changes, so the above-mentioned relation does not hold exactly. But the section-area of the duct is large compared with that of the orifice, and so we ignore the effect of the direct influence of the duct upon the jet. Then, the non-dimensional equation which exists between those four variables (v, x, v_0, r_0) is expressed as follows:

$$\frac{v}{v_0}=f\left(\frac{x}{r_0}\right). \qquad \cdots\cdots(2.1)$$

The function f is to be obtained from the results of experiment.

The experimentally observed velocity distributions are shown in Figure 2.1 by points of measured v/v_0 plotted against x/r_0. In this figure, the results of above-mentioned 60 kinds of experiments were plotted and we see plotted points gathered near a curve. This curve corresponds to the function f in Equation (2.1). Tollmien[5] resolved the equations of motion as to the turbulent spreading of jet, discharged from a point and an infinite line orifices and derived the following results;

in the case of a point source: $v \propto 1/x$,

in the case of an infinite line source: $v \propto 1/\sqrt{x}$.

As we can see the approximate relation $v \propto 1/x$ in Figure 2.1, we replot Figure 2.1 on both-logarithmic co-ordinates as shown in Figure 2.2. It is obvious from Figure 2.2, that wind velocity along the axis of the jet is nearly constant up to the distance 10 times of the radius r_0 of the orifice, and after that, it decreases hyperbolically with distance (in Figure 2.2 the inclination of a straight line is 45°).

Let us consider the reason why the velocity distribution on the axis of a jet appears as shown in Figure 2.2. Figure 2.3 shows a diagrammatical velocity distribution at three cross sections I, II, III of a jet. At sections I and II, velocity distributions show trape-zoid types with flat distributions near the central axis. At section III, this flat distribution disappears and the velocity distribution becomes like

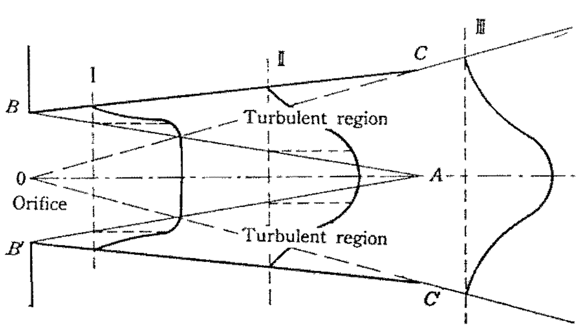

Figure 2.3
Velocity distribution at cross sections I, II, III of a jet, discharged from a circular orifice.

one of Gauss' error curve. Near the orifice, velocity is nearly equal at whole cross section, but at a border of the jet, velocity gradient is very large and strong turbulent shearing stress is generated there. On account of this shearing stress, retard action works to jet, and velocity-decrease begins at the border and penetrate toward the central axis of the jet. When this region attains to the central axis (at a point A in Figure 2.3), the whole region of the cross section is covered with turbulent region, and velocity distribution becomes as if there were a point orifice at the center of the circular one. Investigating the behaviour of a jet from a circular nozzle, Kuethe[6] found that BAB' in Figure 2.3, is a laminar region, where the velocity is almost constant and turbulent flow gradually penetrates from BC or $B'C'$ into the central region and finally whole region becomes the turbulent one. In Figure 2.2, the region where the velocity along the jet is constant, seems to correspond to the said laminar region.

The velocity distribution of the jet from a circular orifice of radius r_0 is expressed as follows:

$$\text{in the case } x \leqq 10r_0: \ \frac{v}{v_0} = 1 \ \text{(constant)}, \quad \cdots\cdots (2.2)$$

$$\text{in the case } x \geqq 10r_0: \ \frac{v}{v_0} = \frac{10r_0}{x}. \quad \cdots\cdots (2.3)$$

From the result of experiment, there has been found that the function f in Equation (2.1) is expressed by the right hand sides of above two equations.

2.3.2 In the case of a rectangular orifice

Concerning various shapes of rectangular orifices, relations between velocity on the axis of the jet and distance from the mouth of it were investigated. Figure 2.4 shows one of the results gained in the case of a rectangular orifice whose size is 24 cm×4 cm. According to this result, at first there exists the region where the velocity v changes little with the distance x from the mouth (we call this "the 1st region") in this paper. Next, comes the "2nd region" where the velocity v decreases inversely proportional to the square root of a distance x.

$$v \propto \frac{1}{\sqrt{x}}. \quad \cdots\cdots (2.4)$$

This is just as in the case of an infinite line source. Finally there comes the "3rd region" where the velocity v decreases inversely proportional to the distance x, just

Figure 2.4
An example of velocity distributions along the axis of jets, discharged from a rectangular orifice.

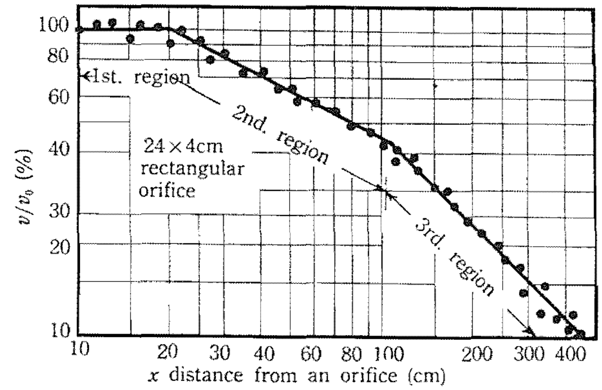

like in the case of a point source.

$$v \propto \frac{1}{x}. \qquad \cdots\cdots (2.5)$$

Since the velocity distribution in the case of a point source is the most stable one, the distribution may finally come to this state.

If velocity distribution in the 3rd region of a jet from a rectangular orifice comes finally to the same state as that of a point or a circular orifice, there must exist a circular orifice whose velocity distribution in the region of $x \geqq 10r_0$ in Equation (2.3), coincides with that of the rectangular one in the 3rd region. We call the radius of this circular orifice "an equivalent radius" of a rectangular one. Let us find the relation between two side-lengths na_1 a_1 $(n \geqq 1)$ of the rectangle and this equivalent radius r_0. The relation seems to be the one which shows that both areas are equal, that is:

$$\pi r_0^2 = na^2. \qquad \cdots\cdots (2.6_1)$$

But according to the results of experiments performed on various sizes of orifices, above relation does not hold exactly but a modification factor α^2 $(\leqq 1)$ must be multiplied to the right hand side of it:

$$\pi r_0^2 = \alpha^2 na^2. \qquad \cdots\cdots (2.6)$$

The value of a factor α^2 has been found to become smaller as the value of n grows larger; that is the shape of the rectangle becomes slenderer. This is due to the fact that air is not discharged with uniform velocity in the whole section of the orifice-mouth but the velocity decreases near the border of it, on account of friction. If the area is equal, the slenderer the shape of a rectangular becomes, the longer the length of its border is, and the smaller the value of n becomes. In Table 2.1, values of α^2 obtained by experiments are given. Of course its value will change with the thickness, roughness or any other factors of an orifice, and is not decided uniquely even if the size and the shape of the orifice are given. Above-mentioned values correspond to the orifice, made by an iron-plate whose thickness is 4 mm, and in this case values of α^2 are nearly equal if the shapes of the orifices are similar.

Calculating values of r_0 for various shapes of rectangles by Equation (2.6) and Table 2.1, we plot velocity distributions of the jets from rectangular orifices in non-dimensional co-ordinates as represented in Figures 2.5, 2.6 and 2.7. In these figures, straight lines in the 1st and the 3rd regions coincide with those in Figure 2.2.

Next, we shall find the co-ordinate of boundary between the 1st and the 2nd

Table 2.1 Modification factor (α^2)

Ratio of lengths of two sides of rectangles	α^2	α
1 : 1	0.98	0.995
2 : 1	0.95	0.975
4 : 1	0.90	0.949
6 : 1	0.85	0.921
12 : 1	0.80	0.894

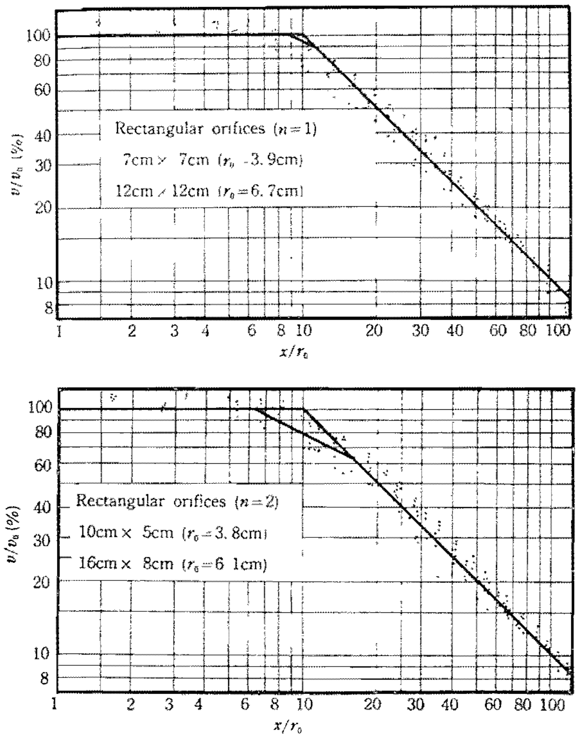

Figure 2.5

Velocity distributions along the axes of jets, discharged from rectangular orifices. (in the cases of $n=1$ and $n=2$)

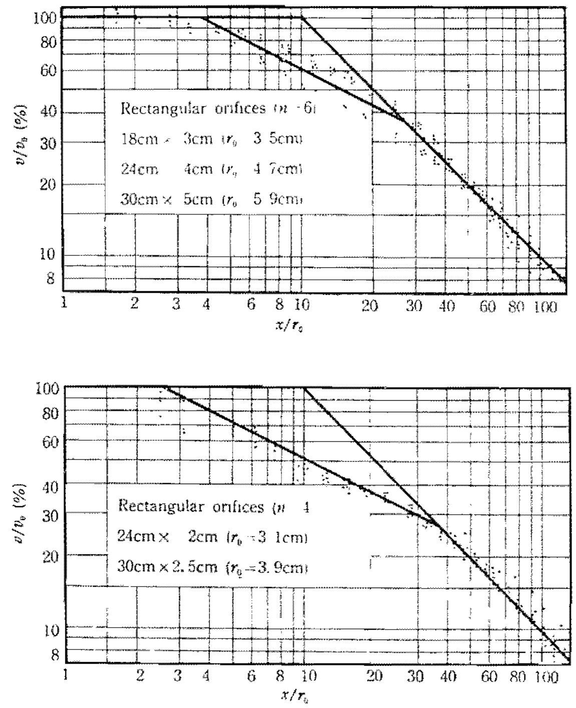

Figure 2.7

Velocity distributions along the axes of jets, discharged from rectangular orifices. (in the cases of $n=4$ and $n=6$).

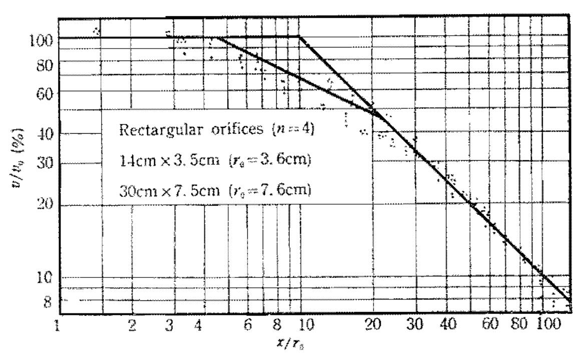

Figure 2.6

Velocity distributions along the axes of jets discharged from rectangular orifices. (in the case of $n=4$)

regions. To do this, we must consider the mechanism by which the 2nd region is produced. The state of the jet near the mouth of rectangular orifice is almost equal to the one of circular orifice, but the line AB in Figure 2.3 exists not axial-symmetrically but separately from one another with respect to the directions parallel to longer and shorter sides of rectangles. They are represented by A_1 B_1 (for shorter side of rectangle) and A_2 B_2 (for longer side) in Figure 2.8. As the state of turbulence outside AB are equal in the cases of circular and rectangular orifices, the gradient of lines A_1 B_1 and A_2 B_2 in Figure 2.8 must be equal. Then A_1 B_1 crosses with the axis of the jet at nearer point (A_1) from the mouth of orifice than A_2 B_2 does at (A_2). Between A_1 and A_2, there exists the velocity gradient in the direction parallel to the shorter side of the rectangle near the axis but it shows trape-zoid types in the direction parallel to the longer side. This state of flow near

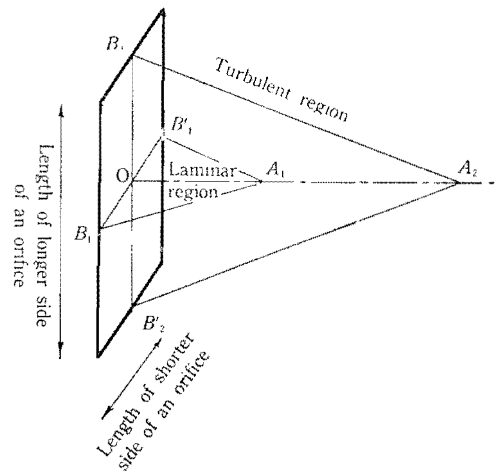

Figure 2.8
Two kinds of boundary lines near the mouth of a rectangular orifice.

the axis of A_1 A_2 makes two-dimensional flow. This is the reason why the velocity distribution in the 2nd region of the jet from a rectangular orifice is similar to that of the one from an infinite line orifice.

If we draw Figure 2.3 and Figure 2.8 with their axis OA and OA_1 overlapped one another, B_1 A_1 must be parallel to BA in that figure, so ΔB_1A_1O is similar to ΔBAO. Now, as $OA=10r_0$, $OB=r_0$ and $OB_1=\alpha a/2$, we obtain the following proportional expression:

$$x_1 : 10r_0 = \frac{\alpha a}{2} : r_0,$$

$$\text{or} \quad \frac{x_1}{r_0} = \frac{5\alpha a}{r_0}, \qquad \cdots\cdots(2.7_1)$$

where x is the length of OA_1, α is a square root of α^2 expressed in Table 2.1. Using the Equation (2.6), we eliminate α from above equation and obtain

$$\frac{x_1}{r_0} = 5\sqrt{\frac{\pi}{n}} = \frac{8.85}{\sqrt{n}}, \qquad \cdots\cdots(2.7)$$

where n is the ratio of two side lengths of the rectangle. This is the co-ordinate of the boundary between the lst and the 2nd regions. We calculate the numerical values of x_1/r_0 for rectangular orifices used in experiment and obtain the following results:

$$n=2 : x_1/r_0=6.26,$$
$$n=4 : x_1/r_0=4.43,$$
$$n=6 : x_1/r_0=3.62,$$
$$n=12 : x_1/r_0=2.56.$$

We drew straight lines in the 2nd regions, so as to pass the above co-ordinates and to have the inclination $tan^{-1}(1/\sqrt{2})$ to abscissa in Figures 2.5, 2.6 and 2.7. Points plotted by result of experiment, gathered arround them in those figures, so the above-mentioned view on the co-ordinate of the boundary between the lst and the 2nd regions may be correct.

Lastly we must obtain the formula which represent the velocity distribution in the 2nd region. We transform the Equation (2.4) into the following non-dimensional form, putting the constant of proportionality K.

$$\frac{v}{v_0}=K\sqrt{\frac{r_0}{x}}.$$

Boundary condition is,

$$\text{at} \quad \frac{x}{r_0}=\frac{8.85}{\sqrt{n}} \quad : \quad \frac{v}{v_0}=1,$$

so,

$$K=\frac{2.98}{\sqrt[4]{n}},$$

and the equation of velocity distribution is

$$\frac{v}{v_0}=\frac{2.98}{\sqrt[4]{n}}\sqrt{\frac{r_0}{x}}. \qquad \cdots\cdots\cdots(2.8)$$

The co-ordinate of the boundary between the 2nd and the 3rd regions can be obtained as an intersection point of straight lines, represented by Equations (2.8) and (2.3):

$$\frac{x}{r_0}=20\sqrt{\frac{n}{\pi}}=11.3\sqrt{n}. \qquad \cdots\cdots\cdots(2.9)$$

Results of experiments expressed in Figures 2.5, 2.6 and 2.7, follow above equation.

Summarizing the above-mentioned results, velocity distributions of the jet from rectangular orifices can be expressed as follows:

$$\left.\begin{array}{lll} x\leqq\dfrac{8.85r_0}{\sqrt{n}} & : & v=v_0, \\ \dfrac{8.85r_0}{\sqrt{n}}\leqq x\leqq 11.3\sqrt{n}\,r_0 & : & v=\dfrac{2.98v_0}{\sqrt[4]{n}}\sqrt{\dfrac{r_0}{x}}, \\ x\geqq 11.3\sqrt{n}\,r_0 & : & v=\dfrac{10v_0r_0}{x}, \end{array}\right\} \qquad \cdots\cdots\cdots(2.10)$$

where n is a ratio of the two lengths of rectangles.

2.4 Conclusion

1) We investigated the velocity distributions along the axes of jets, discharged from circular and rectangular orifices.

2) In the case of a circular orifice, velocity is nearly constant up to the distance 10 times of the radius of the orifice, and after that, it decreases in inversely proportional to the distance from the oifice.

3) In the case of a rectangular orifice, velocity is nearly constant at first, then decreases in the same state as in the case of the jet from an infinite line orifice, and lastly decreases just like in the case of a point orifice. Boundary points between those three regions vary according to the ratio of the two side lengths of the rectangle.

Chapter 3

Temperature Distribution of Upward Current from a Circular Heat Source

3.1 Introduction

In Chapter 1, the temperature distributions in the upward currents from a point heat source and from an infinite line heat source were obtained. In this Chapter, basing on the results obtained there and the way of thinking stated in Chapter 2, it is intended to find out the temperature distribution of the upward currents from a circular heat source with a finite radius (radius$=r_0$). This was done to obtain a basic datum for finding the temperature distribution of the upward currents from a rectangular heat source to be referred in the next chapter.

3.2 Dimensional Analysis

Let us take the origin of coordinates at the center of the heat source, the z-axis in the upward vertical direction, and the r-axis in the radial direction. As the momentum equation (cf. Equation 1.105, Section 1.8.1) and the equation of heat continuity (Equations 1.30, Section 1.6.1) hold in the case of an upward current even when the heat source is not a point or a line, they are given again below, where the respective letters express the same things as those in Chapter 1 do.

$$\frac{d}{dz}\int_0^\infty \rho w^2\, 2\pi r dr = g\int_0^\infty \rho \frac{\Delta\theta}{\theta_0}\, 2\pi r dr, \quad \cdots\cdots (3.1)$$

$$\int_0^\infty c_p \rho w \Delta\theta\, 2\pi r dr \equiv Q. \quad \cdots\cdots (3.2)$$

Although it is impossible to solve these equations directly, it is possible to know in what dimensional relation the temperature $\Delta\theta$ and the upward velocity w at an arbitrary point (r, z) in the upward current are related with r, z and Q (strength of the heat source). Therefore, if we replace the coordinates r and z with the non-dimensional ones r/r_0 and z/r_0 which are obtained by dividing them by the radius of the heat source r_0, the Equations (3.1) and (3.2) are changed as follows:

$$\frac{d}{d(z/r_0)}\int_0^\infty \left(\frac{w}{r_0^{1/3}}\right)^2\left(\frac{r}{r_0}\right) d\left(\frac{r}{r_0}\right) = \int_0^\infty \left(\frac{\Delta\theta g r_0^{1/3}}{\theta_0}\right)\left(\frac{r}{r_0}\right) d\left(\frac{r}{r_0}\right), \quad \cdots\cdots (3.3)$$

$$\int_0^\infty \left(\frac{w}{r_0^{1/3}}\right)\left(\frac{\Delta\theta g r_0^{1/3}}{\theta_0}\right) 2\pi\left(\frac{r}{r_0}\right) d\left(\frac{r}{r_0}\right) = \frac{Qg}{c_p \rho \theta_0 r_0^2}. \quad \cdots\cdots (3.4)$$

In the Equations (3.3) and (3.4), the quantities expressed in the forms of $w/r_0^{1/3}$ and $\Delta\theta g r_0^{1/3}/\theta_0$ can be thought to be the functions of $Qg/(c_p\rho\theta_0 r_0^2)$ and the non-dimensional coordinates r/r_0 and z/r_0. So the solution of above equations are supposed to have the following forms:

$$\frac{w}{r_0^{1/3}} = A^x f_1(r/r_0,\ z/r_0), \quad \cdots\cdots (3.5_1)$$

$$\frac{\Delta\theta g r_0^{1/3}}{\theta_0} = A^y f_2(r/r_0,\ z/r_0). \quad \cdots\cdots (3.6_1)$$

where f_1 and f_2 are certain functions which represent the velocity and temperature distributions in the upward current, and A is

$$A = \frac{Qg}{c_p \rho \theta_0 r_0^2} \quad \cdots\cdots (3.7)$$

x and y are exponents to be determined later.

In Equations (3.5_1) and (3.6_1), the following two points are supposed:

a) Velocity or temperature at any point in the upward current can be expressed by the product of two functions which express the heat-strength and velocity or temperature distribution.

b) f_1 and f_2 which are functions of velocity and temperature respectively, are independent of heat strength.

These two points will be examined by experiment later. If Equations (3.5_1) and (3.6_1) are substituted into Equations (3.3) and (3.4), the values of exponents of A in both sides of equations are compared, then the following equations are derived:

$$2x = y, \qquad x + y = 1.$$

In other words, $x = 1/3$, and $y = 2/3$.

Therefore, Equations (3.5_1) and (3.6_1) reduce to:

$$\frac{w}{r_0^{1/3}} = A^{1/3} f_1\left(\frac{r}{r_0}, \frac{z}{r_0}\right), \quad \cdots\cdots (3.5)$$

$$\frac{\Delta\theta g r_0^{1/3}}{\theta_0} = A^{2/3} f_2\left(\frac{r}{r_0}, \frac{z}{r_0}\right). \quad \cdots\cdots (3.6)$$

According to these results, it can be seen that if the raidus of heat source r_0 is fixed and the strength of heat source Q changes, the upward velocity w and the temperature $\Delta\theta$ at any point change in proportion to $Q^{1/3}$ and $Q^{2/3}$ respectively. This relation is similar to the one derived in the cases of a point heat source (cf. Equations 1.114 and 1.115, Section 1.8.1) and an infinite line heat suorce (Equations 1.125 and 1.126, Section 1.8.2). Also, in the case of two circular heat sources the values of whose radii r_0 are not equal, but if the strengths of the heat sources per unit area $Q/\pi r_0^2$ are equal, then, according to the Equations (3.5) and (3.6) the values of the upward velocity w at two different points where the values of r/r_0 and z/r_0 are equal, are in proportion to $r_0^{1/3}$ and the temperature $\Delta\theta$ is in inverse proportion to $r_0^{1/3}$. Such similarity laws must hold in the case of upward currents from circular heat sources. In order to change Equations (3.5) and (3.6) to non-dimensional ones, let us use the following substitutions:

$$W = \frac{w r_0^{1/3}}{\sqrt[3]{\dfrac{Qg}{c_p \rho \theta_0}}}, \quad \cdots\cdots (3.8)$$

$$\Theta = \frac{\Delta\theta r_0^{5/3}}{\sqrt[3]{\dfrac{Q^2 \theta_0}{c_p^2 \rho^2 g}}}. \quad \cdots\cdots (3.9)$$

Let us call these two, the non-dimensional upward velocity and non-dimensional excess temperature, and use them hereafter in expressing the results of experiments. From Equations (3.5), (3.6), (3.8) and (3.9), we obtain

$$W = f_1(r/r_0,\ z/r_0), \quad \cdots\cdots (3.10)$$

$$\Theta = f_2(r/r_0,\ z/r_0). \quad \cdots\cdots (3.11)$$

These are the equations which express the space distributions of the upward velocity and the temperature. The forms of the functions of f_1 and f_2 should be determined according to the results of experiments.

3.3 Experimental Method and Results

Two types of heat sources were employed. In the case of the first type, alcohol was put and burnt in seven circular vessels with radii of 3.3 cm, 6 cm, 9.9 cm, 14.3 cm, 18.75 cm, and 37.5 cm. In this case, a communicating tube connecting the vessel and the alcohol tank was employed so as to keep the surface of the burning alcohol at a definite height. This type of heat source is provisionally called "continuous heat source" here. In the case of the second type, a great many little wicks of alcohol lamps were placed within a circle of a certain radius as shown in Figure 3.1. This is provisionally called "discontinuous heat source".

The method of using a solid heat source such as an electric heater was also considered. However, this kind of the heat source was not employed here because it has following defects; according to this source, the greater part of the heat produced, is lost by radiation, only a small amount of heat is given to the upward current, and so the upward current is weak and is liable to be disturbed by a faint accidental breeze in the room. Also, the thermocouple, under direct influence of the radiation of heat source, may indicate a temperature considerably different from that of the gas in the upward current. The continuous heat source employed here had a defect that it shoots out the flame to a considerable height bringing an undesirable result of making the temperature of the outer part of the flame higher than that of its center. It was intended to cover this defect by means of the discontinuous heat source. However, even the discontinuous heat source had the defect that in the part directly above the heat source the temperature differs greatly according to whether the point is directly above one of the constituent heat sources or not.

We took the gas temperature with the bare chromel-alumel or copper-constantan thermocouples connected with a slow-moving oscillograph. The average value for about 10 minutes was obtained by observing the record on the oscillograph with the eye, and it was considered the temperature of that point.

Figure 3.2 indicates the horizontal distributions of temperature of the upward current from a continuous heat source of 9.9 cm in radius and a discontinuous heat

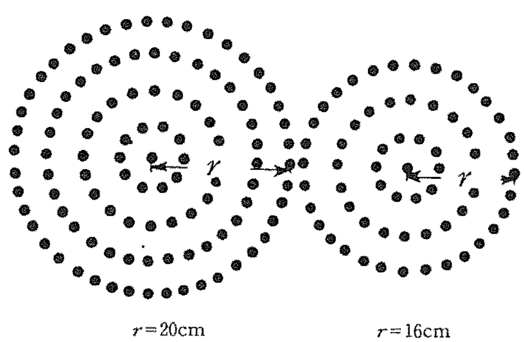

Figure 3.1
Distribution of little wicks of alcohol lamps in discontinuous heat sources.

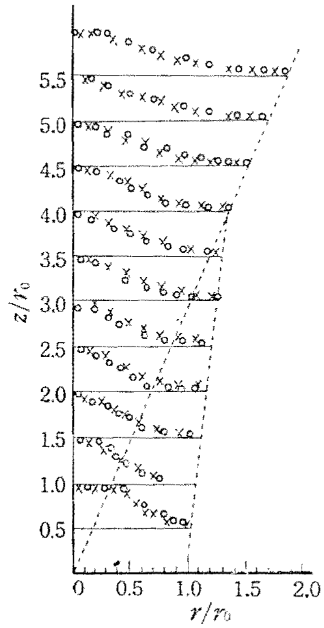

Figure 3.2

Horizontal distributions of temperature above circular heat source.

$\times r_0 = 9.9$	Continuous heat source
$\bigcirc r_0 = 20$	Discontinuous heat source

Figure 3.3

Diagrammatical temperature distributions near a circular heat source.

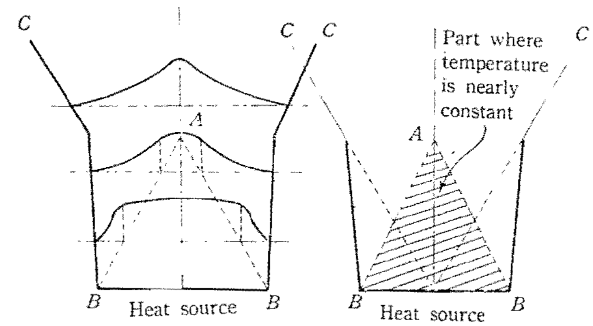

source of 20 cm in radius. They are expressed on the non-dimensional coordinate system. From this figure, we can recognize the following two facts:

1) The horizontal temperature distributions at any height in the upward current from the circular heat sources of various radii can be represented by one curve in these non-dimensional coordinates.

2) There are two kinds of domains as to the horizontal temperature distribution: In the domain near the heat source ($z/r_0 < 2.5$), horizontal distribution of the temperature takes the shape of a plateau and hot current does not spread so widely in the horizontal direction as it rises, whereas in the domain far from the heat source ($z/r_0 > 2.5$), horizontal temperature distribution is like the one of the upward current from a point heat source and hot current spreads widely as if it started from a point heat source placed at the center of the circular one.

Figure 3.6 indicates the vertical distributions of temperature of the upward current from the circular heat sources of various radii. In this figure, coordinates are represented by non-dimensional ones; instead of height z from the origin, z/r_0, and instead of excess temperature $\Delta\theta$, the non-dimensional temperature Θ represented in the Equation (3.11) are used. We can divide the distribution into two domains as to the vertical temperature distribution, too. In this figure, all the vertical temprature distributions in the current from the source of various radii, can be represented by one curve, although there are some exceptions in the cases of sources whose radii are $r_0=3.3$ cm and 6 cm. This shows that there also exists the similarity law as to the vertical temperature distributions of the currents from circular heat sources. Figure 3.3 shows the diagrammatical temperature distribution near a heat source. The similar way of thinking as in the case of jets from a circular and rectangular orifices (Chapter 2) can be applied in this case: Near the heat source, hot gas and surrounding air mix at the boundary of the upward current, and temperature drops there. The higher the gas rises upwards, the deeper the air penetrates from the surroundings into the hot gas and at last the boundary between the mixed and unmixed gases disappear at point A in Figure 3.3. In the domain BAB, the temperature of the gas is nearly constant, but above A, the central temperature decreases with height because the mixing is performed even on the central axis. This is why there are two different parts in this upward current.

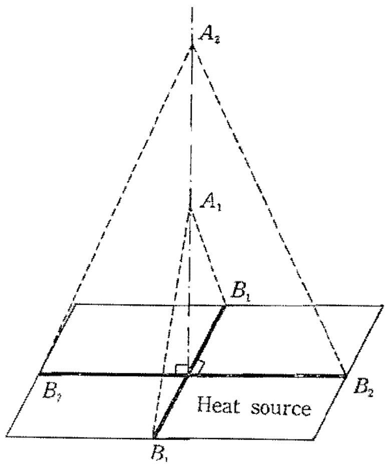

Figure 3.4
Two kinds of boundary lines between the mixed and unmixed hot gas with the surrounding air. (In the case of a rectangular heat source)

In the case of rectangular heat source, we can imagine two kinds of boundary lines: A_1 B_1 and A_2 B_2 which mean the boundaries due to the shorter side of the rectangle and to that of the longer one respectively. Figure 3.4 shows the diagrammatical picture of these boundaries. At point A_1 the boundary line due to the shorter side disappears while the one to the longer side still remains. So in the domain between A_1 and A_2 the temperature remains constant in the direction of B_2 B_2 and the temperature distribution is similar to the one produced by a line heat source. In the domain, above a point A_2, hot gas and surrounding air mix in all directions, and so the temperature distribution must show the similar distribution to the one when a point heat source exists at the center of the rectangle.

3.4 Temperature Distribution in the Domain far from the Heat Source

In the case of the point heat source, upward current spreads upward in the shape of an inverted cone with its vertex at the heat source. So if instead of the horizontal distance r measured from the central axis in the radial direction, the non-dimensional quantity r/z is employed as the axis of abscissa, and the non-dimensional quantity obtained by dividing the temperature $\Delta\theta$ at an arbitrary horizontal distance r, by the temperature $\Delta\theta_m$ at the central axis in the same level. is employed as the axis on ordinate, the similarity law that the horizontal distribution of temperature at any height may be expressed by a single curve (Figure 1.2). In Chapter 1, the expression was further more generalized, and instead of r/z, the quatient $r/zc^{2/3}$ was employed, where c was a parameter expressing the strength of turbulence in the current.

Judging from the result of experiment, it can be presumed that the temperature distribution of the upward current from a circular heat source, in the domain far from the heat source, is similar to that of the upward current from a point heat source. In Figure 3.5, results of the experiments as to the horizontal temperature distribution of various circular sources and at various heights are plotted and the temperature distribution curve corresponding to a point heat source is also drawn. We can see that this curve passes near the center of plotted points. This shows that horizontal temperature distribution of the upward current from a circular heat

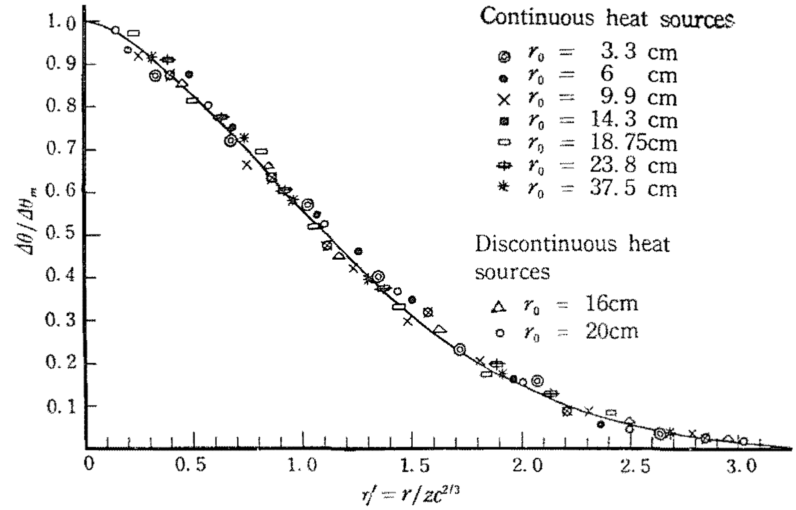

Figure 3.5
Horizontal temperature distribution of the upward currents from circular heat sources, in the domain far from the sources.

source, in the domain far from the heat source is similar to that of the current from a point source.

Next, let us proceed to the temperature distribution along its central axis. Figure 3.6 shows the result of experiment and is expressed in non-dimensional and both-logarithmic coordinates. As we can see, the inclination of the temperature-distribution line is nearly $\pi - tan^{-1}$ (3/5), on this graph, we can say that vertical temperature distribution in this domain, is the same as that of the current from a point heat source. The vertical temperature distribution in the case of a point heat source could be expressed by the Equation (1.112).

$$\Delta\theta_m = 0.423\sqrt[3]{\frac{\theta_0 Q^2}{c_p{}^2\rho^2 g}}\,c^{-8/9}z^{-5/3}. \quad \cdots\cdots(1.112)$$

In the mean time, by the Equation (3.9), the temperature distribution along the axis of the current can be expressed in non-dimensional form as follows:

$$\Theta = \frac{\Delta\theta_m r_0{}^{5/3}}{\sqrt[3]{\dfrac{\theta_0 Q^2}{c_p{}^2\rho^2 g}}} \quad \cdots\cdots(3.12)$$

Eliminating $\Delta\theta_m$ from both equations, we obtain

$$\Theta = \frac{0.423}{c^{8/9}}\left(\frac{z}{r_0}\right)^{-5/3}. \quad \cdots\cdots(3.13)$$

If we give the numerical value of $c^{2/3}=0.1$, derived from the laboratory experiment, we obtain

$$\Theta = 9.115\left(\frac{z}{r_0}\right)^{-5/3}. \quad \cdots\cdots(3.13_1)$$

This is the non-dimensional equation for the vertical temperature distribution of the upward current from a circular heat source, in the domain from far the source.

The non-dimensional equation which expresses the upward velocity along the central axis of the upward current in this domain can also be obtained in the same way. The equation expressing the upward velocity in the case of a point heat source was obtained in Chapter 1 (Equation 1.113). By substituting the value of w_m in place of w in the Equation (3.10), we obtain the following non-dimensional expression of the upward velocity,

$$W=\frac{0.833}{c^{4/9}}\left(\frac{z}{r_0}\right)^{-1/3} \qquad (3.14)$$

This is the non-dimensional equation which expresses the upward velocity distribution along the central axis of the upward current in the domain far from the heat source. In the special case where the value of parameter which expresses the strength of disturbance c is $c^{2/3}=0.10$ as in the case of the experiments performed here, the above equation reduces to;

$$W=3.87\left(\frac{z}{r_0}\right)^{-1/3} \qquad (3.14_1)$$

The upward velocity was not measured this time. But we believe that if it is measured, the results will satisfy the above Eqution (3.14) or (3.14_1).

3.5 Relation between the Radius of the Heat Source and the Strength of It.

In the dimensional analysis concerning the temperature of the upward current from the circular heat source in Section 3.2, it was stated that, on the assumption that the patterns of the temperature distribution in the upward current are independent to the strength of the heat source Q, certain similarity law may be introduced from the dimensional analysis, if the values of $Q/\pi r_0^2$ (the strength per area of the heat source) are equal irrespective of the radius. In order to verify this experimentally, it is necessary first to check whether the values of $Q/\pi r_0^2$ or of Q/r_0^2 are equal for all circular heat sources with different radii used in the experiment.

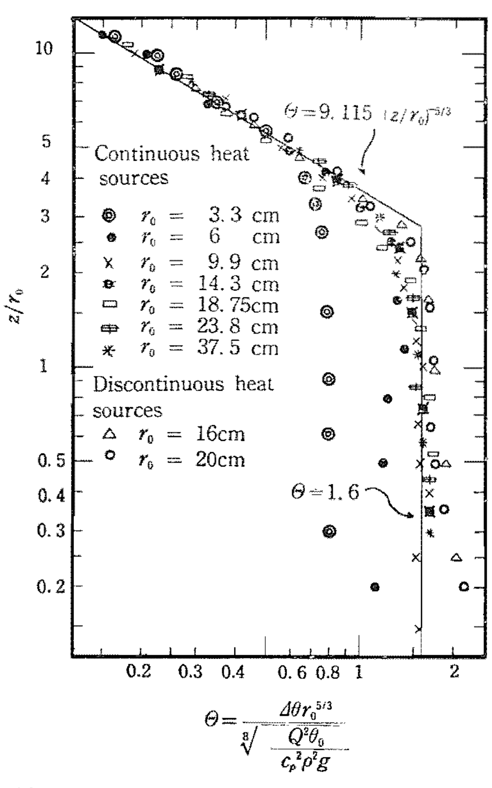

Figure 3.6

Temperature distributions along the central axes of upward currents from circular heat sources, expressed on the non-dimensional coordinate system.

To attain this, the value of the heat source strength Q must be found. Q is the quantity of heat given per unit time from the heat source to the upward current. In order to determine this quantity directly, the quantity of heat which a unit quantity of the burning alcohol used gives out, must be known. Generally speaking, the burning heat of methyl alcohol is 5,365 cal/g, and that of ethyl alcohol is 7,140 cal/g. But the value varies according to the components of the alcohol and so the components of the alcohol used must be closely analyzed. This requires much trouble, and even when the value of the combustion heat is found, the amount of heat that escapes through the vessel and the amount of heat that radiates must be subtracted from the value. Therefore, it is difficult to find the heat source strength Q accurately. Accordingly, the value of Q is determined indirectly in the following way.

In the preceding Section 3.4, it was found that the temperature distribution on the horizontal section of the upward current is, within the limits of $z/r_0>2.5$, similar to the temperature distribution in the case of the point heat source, irrespective of the radius. By substituting the measurement values of the height z and the temperature $\Delta\theta_m$ along the central axis obtained here into the Equation (1.112), the value of Q is obtained indirectly. The values of Q/r_0^2 obtained by averaging the values at various heights within the limits of $z/r_0>4$ for each heat source are shown in Table 3.1. Even when alcohol of the same quality is used in the same vessel, the burning rate varies more or less according to the weather condition of the day (it seems that the humidity is an important factor). As all the experiments were not conducted on the same day, there were some irregularities in the results. However, judging from the results shown in Table 3.1, there is a tendency that the value of Q/r_0^2 increases somewhat with the increase in the radius of the vessel, except in cases the radius is smaller than 6.0 cm, where the relation is inverted. A similar tendency is seen in the results of experiments on the relation between the burning rate of alcohol and the radius of the vessel conducted in 1947 in the laboratory of Prof. Minoru Hamada, Engineering Faculty, Tokyo University as well[7].

In the cases of heat sources with a radius larger than $r_0=9.9$ cm, however, the increase in the value of Q/r_0^2 corresponding to the increase in the radius r_0 is very small. Therefore, for the purpose of the experimental confirmation of the said law of similarity we may safely assume that the value of Q/r_0^2 is independent to the size of the radius r_0. However, the situation is a little different in case of the heat sources whose radii are smaller than 6.0 cm. In such cases, there is a distinct tendency that the value of Q/r_0^2 increases with the decrease of the radius. So it is obvious that no results of experiments using such small heat sources can be employed for checking the said law of similarity.

The fact that in the case of a circular heat source with a radius larger than 9.9 cm, the value of Q/r_0^2 does not greatly vary with the size of the radius leads us to consider that in the case of such heat sources alcohol burns nearly on the whole surface of sources, whereas in the case of small heat sources, alcohol burns chiefly on the boundary of the container. When the heat source is large, under the influence

Table 3.1 Relation between the radius of heat source and the strength of it.

Radius of heat source (r_0 cm)	Strength of heat source (Q cal/sec)	$\frac{Q}{r_0^2}$
3.3	90.72	8.33
6.0	191.38	5.32
9.9	441.7	4.51
14.3	1173	5.73
18.75	2064	5.38
23.75	3469	6.15
37.50	9141	6.50

of the rising in temperature the reaction speed is accelerated and this causes some systematic irregularities.

It has been experimentally confirmed by many researchers that generally speaking the burning rate is approximately proportional to the radius of the heat source in the case of small radius and to the area of combustion in the case of large radius. It may be said that the experiments performed here have proved the fact from another viewpoint.

In actual fires, for instance in the fire test of an full-scale wooden house conducted in Tokyo University in 1933 and in another test conducted later at Mito, it was confirmed that the duration of fire, especially the duration of high temperature, is not greatly influenced by the scale of the houses so long as they are of the same material.[8] It is supposed that they burn in the same way as in the case of a circular heat source of a big radius. Therefore, it is considered that, of the results of the experiments performed here, those obtained from the cases of $r_0=3.3$ cm and $r_0=6.0$ cm cannot be connected with the phenomena of full-scale fires. Incidentally, as it has been found that the discontinuous heat sources of $r_0=16$ cm and $r_0=20$ cm have a nature similar to continuous heat sources of big radii (the experimental proof omitted here), they will be employed in subsequent investigations.

3.6 Similarity Law with Respect to the Temperature Distribution

In the dimensional analysis in Section 3.2, it was assumed that the patterns of the upward velocity and of the temperature in upward currents are independent to the strengths of the heat sources. Let us first check the adequacy of this assumption. The fact that, as shown in Figure 3.2, the continuous heat source with a radius of $r_0=9.9$ cm and the discontinuous heat source with a radius of $r_0=20$ cm have such horizontal temperature distributions as, in spite of the different strengths of heat sources, are nearly similar if only the correction for the strength of turbulence (c) in the upward current is made, and the fact that, in Figure 3.6, the temperature distributions along the vertical axis are similar for almost all heat sources, may be said to be experimental results, contributing to affirming the above-mentioned assumption.

Now the adequacy of the Equation (3.6) will be further examined on the basis of experiments. On assumption that Equation (3.6) holds, if it is assumed further that the values of Q/r_0^2 do not vary according to the radius of the heat source as stated in Section 3.2, the values of $\Delta\theta r_0^{1/3}$ for all heat sources at the points where the values of z/r_0 and r/r_0 are equal must be equal. Let us check this fact in relation to the results of experiments performed here. In the cases of the heat sources of $r_0=3.3$ cm and $r_0=6.0$ cm in the experiments, the values of Q/r_0^2 are considerably different from those of the other heat sources, as stated in the preceding Section. Therefore, such data are omitted here and the results obtained relative to the other five sizes of heat sources from $r_0=9.9$ cm to $r_0=37.5$ cm are used.

First we check whether the values of $\Delta\theta/r_0^{1/3}$ are all equal at various points where the values of z/r_0 and r/r_0 are equal, even if the radii r_0 of the heat sources are different. With regard to the value of z/r_0, the value corresponding to the point

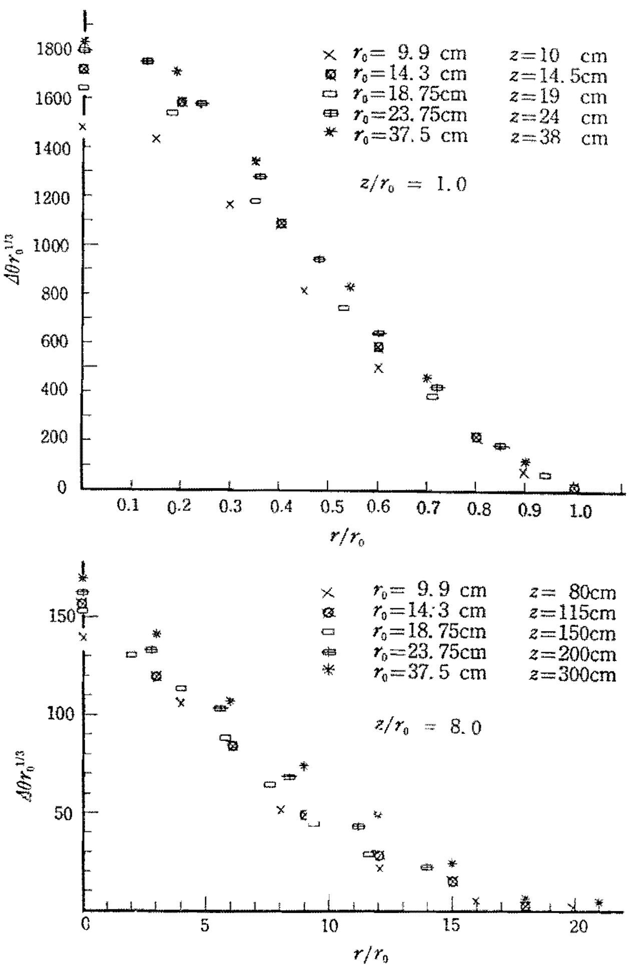

Figure 3.7
Similarity of the horizontal temperature distributions of the upward currents from circular heat sources of various radii.

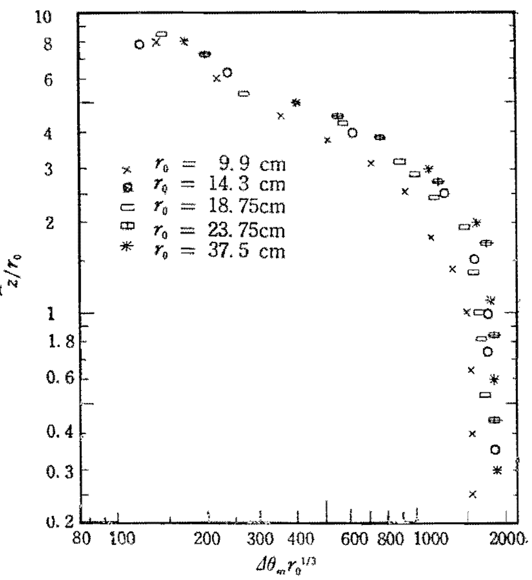

Figure 3.8
Similarity in the temperature distributions along the central axes of the upward currents.

z/r_0= 1.0 which is near the heat source and the value corresponding to the point z/r_0=8.0 which is far from the heat source are checked. To attain this purpose, by taking $\Delta\theta/r_0^{1/3}$ as the axis of ordinates and r/r_0 as the axis of abscissas, we plot the values gained by experiment using the heat sources of various radii in Figure 3.7. In this figure, the results at the heights of z/r_0=1.0 and 8.0 are shown. As stated in the preceding Section, the value or Q/r_0^2 tends to a slight increase with the increase of the radius r_0. Accordingly, the results of the experiments relative to the five heat sources do not quite agree: it is explicit that the greater the radius r_0, the greater the value of $\Delta\theta r_0^{1/3}$ tend to be. As in Figure 3.5, if the temperature distribution is expressed by taking $\Delta\theta/\Delta\theta_m$, as the axis of ordinates, the points indicating the temperature distribution in the horizontal direction cluster very accurately along a curve. This may be given as a proof of the fact that the divergence in the value of Q/r_0^2 is caused by the systematic divergence mentioned above.

Next, let us examine if all the values of $\Delta\theta r_0^{1/3}$ are equal at the various points where the values of z/r_0 are equal. Here let us confine the examination to the special case where r/r_0=0, that is to the central axis of the upward current. For this purpose let us compare the temperature distributions along the central axes of the upward currents from the heat sources of various radii. The results of experiments made here relative to the heat sources of various radii were plotted on the both-logarithmic scale coordinate system whose axis of ordinates is z/r_0 and whose that of abscissas is $\Delta\theta_m r_0^{1/3}$, as is shown in Figure 3.8. In this case also, the results of experiments relative to the various heat sources substantially clustered along one curve. However, the systematic divergence —— the greater the radius of the heat source, the greater the value of $\Delta\theta_m r_0^{1/3}$ —— is also seen here. This divergence is also due to the systematic divergence of the values of Q/r_0^2 relative to those of the radii r_0 of heat sources. We may find a proof of this in the fact that, when the temperature distributions along the central axes of upward currents are expressed by means of a non-dimensional quantity Θ including $\Delta\theta_m$ and Q instead of $\Delta\theta_m r_0^{1/3}$, as in Figure 3.6, they can be represented by one curve except in the cases of the heat sources of $r_0=3.3$ cm and $r_0=6.0$ cm.

It has been found that the Equation (3.6) holds with respect to the temperature distribution. Similarly, we can believe that the Equation (3.5) holds with respect to the upward velocity, although no experiments for the latter were performed here.

3.7 Temperature Distribution in the Domain near the Heat Source

In Figure 3.6 are plotted on the non-dimensional coordinate system, the temperature distribution along the axis of upward currents, basing on the result of experiment. We find that in the domain near the heat source ($z/r_0<2.5$), observed points, except in the cases of the small continuous heat sources of $r_0=3.3$ cm and $r_0=6$ cm, cluster along a straight line roughly expressed by

$$\Theta \doteqdot 1.6 \qquad \cdots\cdots (3.15)$$

In other words, we find that in this domain, the similarity law expressed by the Equation (3.15) holds, concerning the vertical distribution of temperature.

In this case too, regarding to the heat sources or $r_0=3.3$ cm and 6.0 cm, no similarity law holds as is shown in this figure. This may be due to the following facts; the flames rising from heat sources of $r_0=9.9$ cm and more are turbulent flames and alcohol burns nearly on the whole surface of sources, whereas the flames and alcohol burns nearly on the whole surface of sources, whereas the flames from heat sources of $r_0=3.3$ cm and 6.0 cm may be roughly considered laminar flames in which alcohol burns chiefly on the boundaries of containers.

Examples of temperature distribution measurement for the horizontal section in this domain were already given in Figure 3.2. Figure 3.9 shows some examples of the results of measurement only in the part near the heat source. In the left of the Figure is shown the temperature distribution of the turbulent flame in the case of $r_0=9.9$ cm, and in the right of the laminar flame in the case of $r_0=3.3$ cm. In both cases, the temperature distributions at each horizontal section are expressed by the values relative to the maximum values in the same horizontal section. That in the case of a laminar flame, alcohol burns chiefly on the boundaries of the source, can be seen from the fact that just above the heat source, the temperature near the boundary of the current is obviously higher than in the central part. Of course it is the same with a turbulent flame, but in this case the difference in temperature between the outer and central parts is very small and we can assume that the pattern

Figure 3.9
Horizontal temperature distributions of the upward currents from circular heat source, in the part near the heat source.

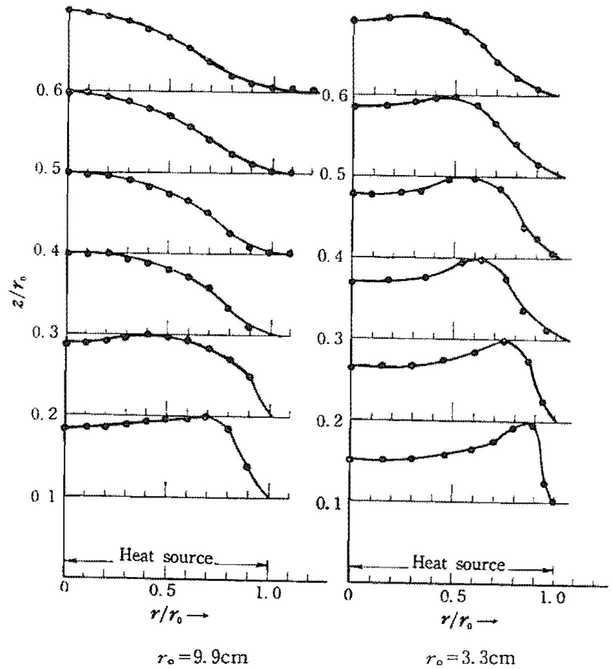

of the horizontal temperature distribution is a plateau-type. This distribution collapses from the outer parts with the increase of height. At the height of $z/r_0=0.5$ or so, the plateau almost disappears and, as stated before, we find that there the transition to the upper domain is already beginning.

The temperature distributions corresponding to the four heat sources whose radii are larger than 9.9 cm, though not included in the Figure, have nearly the same pattern as in the case of $r_0=9.9$ cm when they are expressed in the same way. Thus we can confirm that the similarity concerning the horizontal temperature distributions holds in this domain.

3.8 Summarization

1) We have seen the temperature distributions of upward currents from heat sources with finite radii.

2) There are two different domains in these upward currents: the upper and the lower domains. The temperature distribution in the upper domain is similar to that of the upward current from a point heat source of the same strength placed at the center of the circular heat source. In the lower domain, the temperatures along the central axis do not change greatly with the height from the heat source, and the horizontal temperature distribution has a pattern of a plateau shape.

3) The transition from the lower to the upper domain occurs in a considerably wide range of height. However if we come to divide the range into two parts, it should be divided at a height from the heat source about 2.5 times its radius.

4) In the case of a discontinuous heat source or a continuous heat source whose radius is 9.9 cm or larger, a similarity law holds between the strength of the heat source Q and the temperature of the upward current $\Delta\theta$, and if the effect of radiation is disregarded this similarity law may be extended to the scale of actual fires.

As for the continuous heat sources with a smaller radius than about 6 cm, as the flames from them may be roughly considered laminar flames and their characteristics are different from those of actual fires, they are excluded from our investigations.

Chapter 4

Temperature Distribution above a Burning Wooden House

4.1 Introduction

In the preceding Chapter, the temperature distribution in the upward current from a circular heat source was discussed, but the shape of the plan of a house is generally a rectangle and not a circle. Therefore, the conclusion reached in the preceding Chapter cannot be applied directly to actual fires. In this Chapter, by use of the conclusion of Chapter 2 on the air current spurting from a rectangular orifice and the conclusion of the preceding Chapter on the temperature distribution of the upward current from a circular heat source, the temperature distribution in the upward current from a rectangular heat souce was obtained. Then the similarity law was confirmed, and the results were applied to full-scale fires. The distribution of temperature above a burning wooden house was calculated with respect to two or three examples.

4.2 Experimental Method on the Upward Current from a Rectangular Heat Source and the Results

For the rectangular heat sources were used a square 29×29 cm and rectangles 33×23 cm, 47.5×17.5 cm and 66.5×12 cm within which alcohol-lamp wicks were made to stand close together and burn. They constituted discontinuous heat sources. Also, in order to confirm the similarity law, a continuous heat source, consisting of a rectangular vessel 27×10 cm in which alcohol was burnt was used. The method of measuring the temperature was the same as in the cases of the point heat source and the circular heat source.

If we follow the thinking, as described in the Section 3.3, the distribution of temperature of the upward current from a rectangular heat source will be as follows: with regard to the temperature distribution along the central axis in the vertical direction, there are three domains —— the first domain directly above the heat source where the temperature does not vary with the height; above this, the second domain where the vertical distribution of temperature is the same as in the case of the upward current from a line heat source; and at the top, the third domain where the distribution of temperature is the same as in the case of the upward current from a point heat source. As anticipated, the results of the experiments turned out to be as above.

If the temperature distribution of the upward current in the third domain, becomes, the same as in the case of a circular heat source, there must exist a circular heat source which gives the same strength and temperature distribution as the rectangular heat source in the third domain. Here, the radius of this corresponding circular heat source (r_0) will be called the "equivalent radius" of the original rectangular heat source.

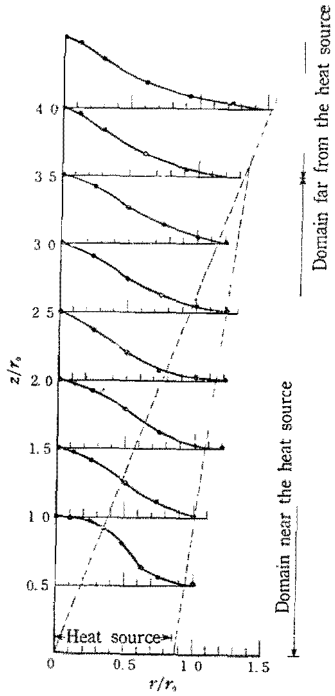

Figure 4.1

Horizontal temperature distribution above a square heat source.

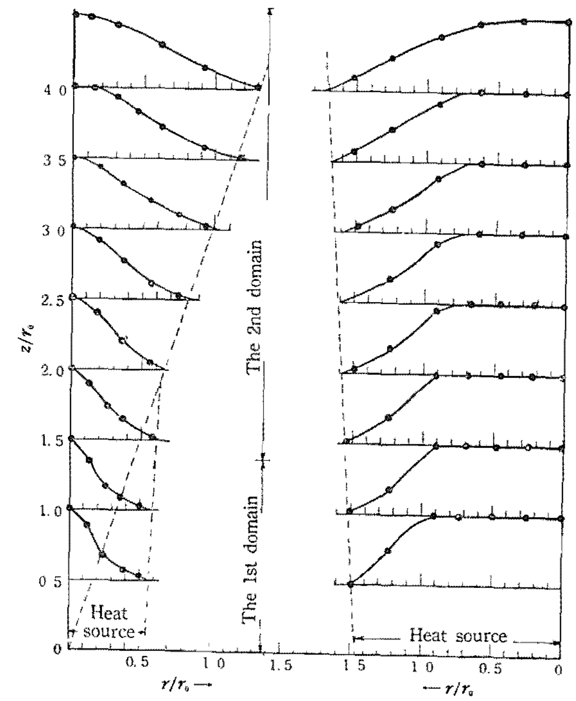

Direction parallel to a shorter side of the rectangle.

Direction parallel to a longer side of the rectangle.

Figure 4.2

Horizontal temperature distribution above a rectangular heat source (47.5cm×17.5cm)

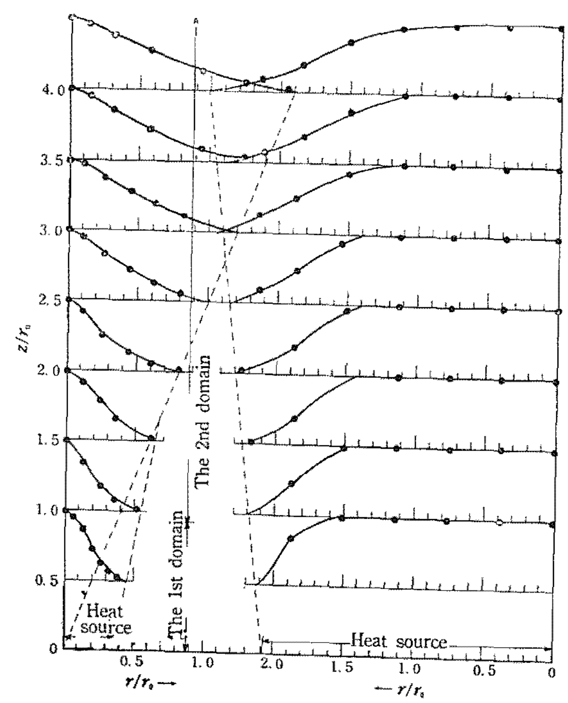

Direction parallel to a shorter side of the rectangle.

Direction parallel to a longer side of the rectangle.

Figure 4.3

Horizontal temperature distribution above a rectangular heat source (66.5cm×12cm)

In the case of the orifice, owing to the contraction of flow and the effect of friction at the opening, the equivalent radius r_0 did not perfectly equal the radius of the circle having an area equal to that of the rectangle, but in this case, there being no effect of the opening, it was expected and was confirmed by the results of the experiments that the value of the equivalent radius r_0 is equal to the value of the radius of a circule having the same area as the original rectangle. That is to say, if we make the lengths of the adjoining sides of the rectangular heat source, a and na respectively (making $n \geqq 1$) the equivalent radius r_0 of this heat source satisfies the following equation:

$$\pi r_0^2 = na^2. \qquad (4.1)$$

If we plot the results of the experiments on the temperature distribution of the upward current from a rectangular heat source, by using this r_0, on the non-dimensional coordinates as in the case of the circular heat source, the results will be as shown in Figures 4.1, 4.2, 4.3 and 4.6.

4.3 Horizotal Spreading of the Upward Current from a Rectangular Heat Source as It Goes Up

In Figures 4.1 to 4.4 showing the horizontal temperature distribution plotted on the non-dimensional coordinate system, we can see how the domain of the upward current from a rectangular heat source spreads horizontally as it goes up.

There is some difference, as for the way of the horizotal spreading of the upward current from a rectangular heat source as it goes up between the direction parallel to the longer side and to the shorter side of the rectangle. As can be seen in Figures 4.2 and 4.3, in the first domain nearest the heat source, the upward current does not spread so widely as it rises in both directions; parallel to the longer and shorter sides. Soon after the upward current ascends to the second domain, the spreading of the current in the direction of the shorter side becomes conspicuous as in the case of a line heat source, but with regard to the spreading in the direction of the longer side, it is still very small as in the case of the first domain. In the second domain, after ascending a little, there exists a height at which, the scale of the spreading of the current in the direction of the shorter side becomes approximately equal to that of the spreading in the direction

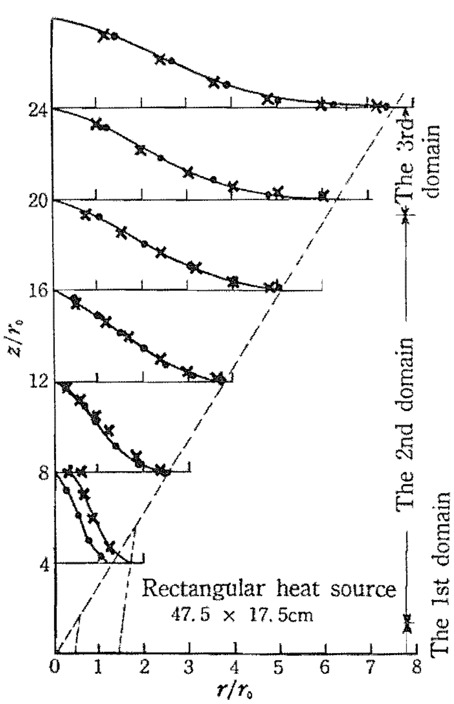

● Temperature distribution parallel to the shorter side of rectangle
× Temperature distribution parallel to the longer side of rectangle.

Figure 4.4

Horizontal temperature distribution in the upward current from a rectangular heat source (47.5cm×17.5 cm) in the wide range of heights.

of the longer side, as can be seen in Figure 4.4 ($z/r_0=8$ in this figure). Above this height, the upward current spreads widely in direction parallel to the longer side, too, and the horizontal spreading in both directions is neatly equal when the current ascends to the third domain.

4.4 Temperature Distribution in the First Domain

This is the domain in which the temperature along the central axis of the upward current does not change very much with the height. The results of the experiments show that the temperature drops somewhat as the current goes up (Figure 4.6), as in the case of the circular heat source. Also in this domain the horizontal distribution of temperature of the upward current takes the shape of a plateau, and the plateau part is broken from the outside as the current goes up. In the case of a rectangular heat source, there is a difference in the height at which the plateau-shape distribution is completely broken for the direction of the shorter side (length a) and the direction of the longer side (length na). It takes at a lower height for the direction of the shorter side, than the longer one. It is at this height that the transition to the second domain is supposed to take place; therefore, theoretically the temperature along the central axis should not change with the height in the first domain. This notwithstanding, as stated above, the results of the experiments showed that the temperature dropped, though only a little, with the increasing height. The reason for this is as follows: as in the case of a circular heat source and as can be seen in Figure 4.5, which shows the results of measuring the temperature distribution at heights very near the heat source, the plateau-shape distribution of temperature is hardly noticeable above the height $z/r_0=0.5$; from this it may be said that the transition to the second domain takes place very slowly over a wide range of height starting from $z/r_0=0.5$ or a lower height, and the greater part of what was thought to be the first domain is really a range of transition to the second domain. Another and less important reason is that since the temperature is high in this domain, even in the case of alcohol flame, there is gas radiation through the vapour and carbon dioxide, and this causes the temperature to fall. The slenderer the rectangular heat source, the lower is the height for transition to the second domain and the wider the transition range, so that it is only in the case of a square heat source that we see in the first domain a temperature distribution which, as in the case of a circular heat source, practically satisfies the equation

$$\Theta=1.6. \quad \cdots\cdots (4.2)$$

In Figure 4.6, the slenderer the shape is, the more the distribution line shifts to the side of lower temperature.

In Figure 4.6, if we define the height at which the line of vertical distribution of temperature seems to be the boundary between the first domain and the second domain, the height of that boundary should comply with the following rule: In the case of the circular heat source with a radius r_0, the height of the boundary was about $2.5\ r_0$ according to Section 3.3. If it is considered that in the case of a rectangular heat source too, the breaking of the plateau-shape distribution of

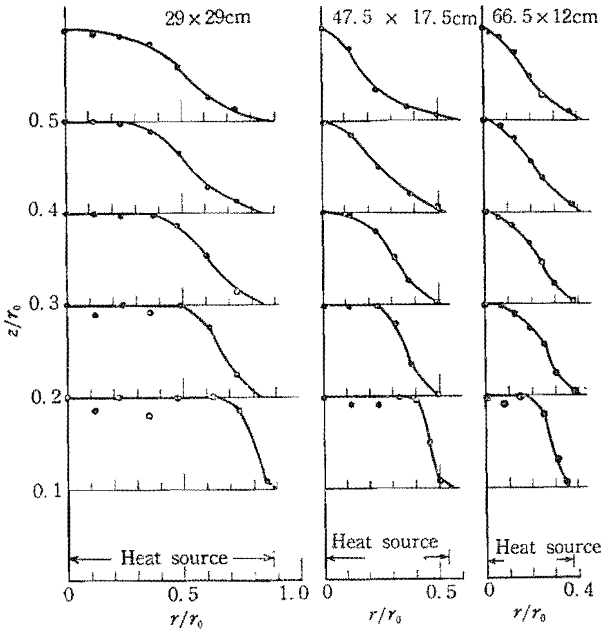

Figure 4.5

Horizontal temperature distribution in the direction parallel to the shorter side of a rectangle (the heat source) in the domain nearest to the heat source.

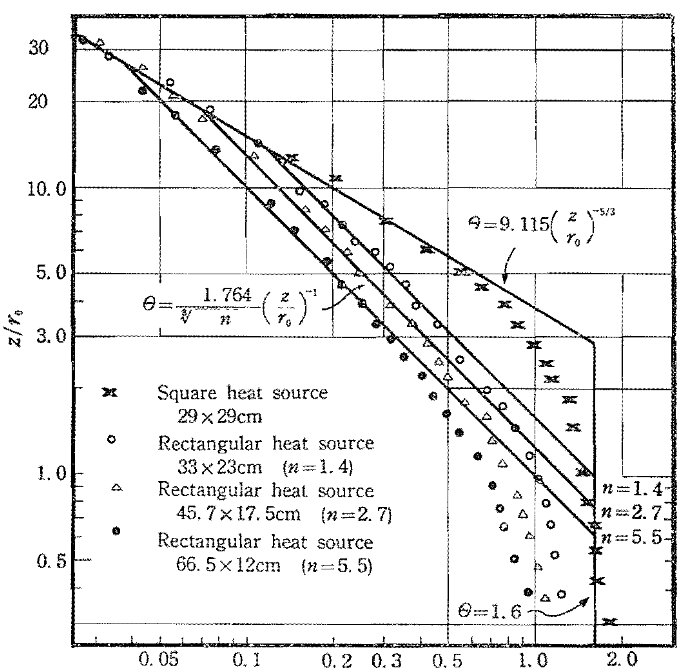

$$\Theta = \frac{\Delta\theta r_0^{5/3}}{\sqrt[3]{\dfrac{Q^2\theta_0}{c_p^2\rho^2 g}}}$$

Figure 4.6

Temperature distributions along the central axes of the upward currents from rectangular heat sources.

temperature goes on at the same rate as in the case of a circular heat source, then the height where the first domain ends should be the position $(a/2)\times 2.5$. Accordingly, if we express this by the equivalent radius r_0 and n according to the Equation (4.1), a point somewhere near

$$\frac{z}{r_0} = \frac{2.5}{2}\sqrt{\frac{\pi}{n}} \doteqdot \frac{2.251}{\sqrt{n}}, \qquad \cdots\cdots(4.3)$$

becomes the upper limit of the first domain. If we apply this to the three kinds of rectangular heat source used in experiment, the upper limit of the respective first domain can be calculated as follows:

For heat source of $39 \cdot \times 23$ cm ($n=1.4$), $z/r_0=1.85$,
〃 47.5×17.5cm ($n=2.7$), $z/r_0=1.35$,
〃 66.5×12 cm ($n=5.5$), $z/r_0=0.94$.

According to the results of the experiments, since the transition from the first domain to the second takes place slowly as stated earlier, it is not possible to distinctly indicate the boundary points, but roughly speaking, the above-shown points can be said to be boundary points.

In the case of a square heat source, the point where the first domain ends is somewhere near $z/r_0=2.2$, according to the Equation (4.3) at $n=1$. In this case, as in the case of a circular heat source, the current moves to the third domain directly without going through the second domain, so that the above-mentioned height is not the center of transition, a point somewhere around $z/r_0=2.5$ being the center. This transition takes place over a wider range of heights than in the case of a circular heat source. The reason for this is: for the direction parallel to the one of the sides of a square, on a account of the relation, $a/2<r_0$, the first domain ends at a height lower than in the case of the circular heat source with an equivalent radius, but since the length of the diagonal is longer than the equivalent radius r_0, for that direction the plateau-shape horizontal distribution of temperature still remains, and the complete transition into the third domain takes place at a height higher than in the case of the circular heat source; the space between these two heights constitutes the transition range.

We have thus shown the distristrion of the temperature of the upward current from the rectangular heat source by means of non-dimensional co-ordinates, but have not yet undertaken experimental verification of the similarity law. As in the case of the circular heat source, the similarity law should of course hold, and we do not think it necessary to check by means of experiments. However, to make sure, we burned alcohol in a rectangular vessel 27×10 cm, continuous heat source ($r_0=9.3$ cm, $n=2.7$) and measured the distribution of temperature above it. We plotted the results on the non-dimensional co-ordinate system, and it was confirmed that they agreed well with the horizontal and vertical distributions of temperature of the rectangular discontinuous heat source (47.5×17.5 cm, $r_0=16.3$ cm. $n=2.7$) used in the previous experiment whose result is shown in Figures 4.2 and 4.6. This is only one example, but we think it is sufficient to confirm the validity of the above-mentioned similarity law.

4.5 Temperature Distribution in the Second Domain

Here, with regard to the direction parallel to the shorter side of the rectangular heat source, the plateau-shape distribution of temperature is almost completely broken, but with regard to the direction parallel to the longer side, the horizontal distribution of temperature shows still the shape of a plateau, so that the distribution of temperature of the upward current along the central axis is the same as in the case of the line heat source or $\Delta\theta\propto z^{-1}$. That is to say, on the both-logarithmic scale coordinate system in Figure 4.6, the vertical distribution line of temperature inclines 135°

to the direction of abscissa. We shall introduce here the equation for this distribution line. As hitherto, the definition of Θ which expresses the temperature in terms of non-dimensional quantity will be in accordance with the Equation (3.9). This time however, instead of using the heat quantity Q given to the upward current per unit time from the whole heat source, we use the heat quantity Q_0 which, as in the case of the infinite line heat source, is given to the upward current per unit time from the part constituting a unit length in the direction of the longer side of the rectangular heat source. That is:

$$Q=anQ_0. \qquad\cdots\cdots(4.4)$$

Also, since the distribution of the temperature $\Delta\theta_m$ along the central axis of the upward current from the line heat source was, according to the Equation (1.123)

$$\Delta\theta_m=0.663c'^{4/9}z^{-1}\sqrt[3]{\frac{\theta_0 Q_0^2}{c_p^2\rho^2 g}}\ . \qquad\cdots\cdots(4.5)$$

If we substitute the Equation (4.4) for Q of the Equation (3.9) and $\Delta\theta_m$ of the Equation (4.5) for $\Delta\theta$ of the Equation (3.9), we obtain

$$\Theta=\frac{0.663}{c'^{4/9}}(n\pi)^{-1/3}\left(\frac{z}{r_0}\right)^{-1}, \qquad\cdots\cdots(4.6)$$

as the equation for the line which expresses the vertical distribution of temperature in this domain. The reason why in this equation we wrote c' instead of c for parameter expressing the intensity of turbulence is to distinguish it from parameter c in the third domain. Since the intensity of the turbulence in the upward current, is the same for the upper half of the second domain and for the third domain, as can be seen in Figure 4.4, the value of the intensity of turbulence is equal for both, but the equations expressing the horizontal distributions of temperature (Equation 1.79 and Equation 1.103) are different for the point heat source and the line heat source, so the value of c becomes different.

Since the right hand side of the Equation (4.6) includes n which expresses the ratio of the lengths of the adjacent two sides of the rectangular heat source, the position of the temperature distribution line varies according to the degree of slenderness of the rectangle, and even if the strengths of the heat sources are equal, the slenderer the heat source is, the lower the temperature is at the points of equal height from heat sources. If in the Equation (4.6) the numerical value 3.1416 is given to π and, as in the indoor experiments performed this time, the value of the parameter for the intensity of disturbance is $c'^{2/3}=0.13$ the Equation (4.6) becomes

$$\Theta=\frac{1.764}{\sqrt[3]{n}}\left(\frac{z}{r_0}\right)^{-1}. \qquad\cdots\cdots(4.6_1)$$

The three straight lines inclined 135 degrees to the horizontal axis in Figure 4.6 represent the three equations (given below) obtained by substituting in the Equation (4.6_1) the numerical values of n, corresponding to the three kinds of rectangular heat sources used in the experiments performed this time, and the results of the experiments on the vertical distribution of temperature along the central axis cluster around the lines corresponding to the respective heat sources:

$$\Theta=1.565\left(\frac{z}{r_0}\right)^{-1}, \qquad\cdots\cdots 33\ \times 23\ \ \text{cm},\ n=1.4,$$

$$\Theta = 1.265\left(\frac{z}{r_0}\right)^{-1}, \quad \cdots\cdots 47.5 \times 17.5\ \text{cm},\ n = 2.7,$$

$$\Theta = 0.997\left(\frac{z}{r_0}\right)^{-1}, \quad \cdots\cdots 66.5 \times 12\ \ \text{cm},\ n = 5.5.$$

The height of the boundary point between the second domain and the third domain can be obtained on Figure 4.6 as the point of intersection of the two straight lines of the Equations (3.13) and (4.6). The reason is that in the third domain, regardless of the slenderness of the heat source, the distribution of temperature along the central axis of the upward current can be given by the Equation (3.13). If we calculate and express the height of the boundary point non-dimensionally, we obtain

$$\frac{z}{r_0} = 0.510 \frac{c'^{2/3}}{c^{4/3}} \sqrt{n\pi}\,. \quad \cdots\cdots (4.7)$$

Substituting in the above equation the values of $c'^{2/3} = 0.13$ and $c^{2/3} = 0.10$ obtained by the laboratory experiments and the value of π, we obtain

$$\frac{z}{r_0} = 11.75\sqrt{n}\,. \quad \cdots\cdots (4.7_1)$$

In the experiments performed this time, it was not possible to measure the temperature up to the height of the boundary point in the case of the rectangular heat source 66.5×12 cm because of the insufficient height of the ceiling of the laboratory room, but in the cases of the two other rectangular heat sources, it was observed that the third domain had been reached at heights which satisfy the Equation (4.7_1) —— namely, at the height $z/r_0 = 14.1$ in the case of the heat source 33×23 cm and $z/r_0 = 19.3$ in the case of the heat source 47.5×17.5 cm.

As anticipated, the results of measuring the temperature distribution of the continuous heat source 27×10 cm in this domain turned out to be similar to those of the discontinuous heat source 47.5×17.5 cm in Figures 4.2 and 4.6. Table 4.1 shows the equations of the temperature distributions in the second domain calculated from Equation (4.6_1) for rectangular heat sources of representative n values in the case that the value the parameter expressing the intensity of turbulence is $c'^{2/3} = 0.13$.

We did not measure the vertical distribution of velocity along the central axis of the upward current in this domain, but it can be obtained in the following manner, as in the case of the temperature distribution. As the velocity shows in this domain the same distribution as in the case of the upward current from an infinite line heat source, its equation can be expressed by the Equation (1.124). Since the velocity

Teble 4.1 Equations of temperature distributions in the second domain for some representative rectangular heat sources

n	Equations	n	Equations
1.25	$\Theta = 1.637\ (z/r_0)^{-1}$	5	$\Theta = 1.032\ (z/r_0)^{-1}$
1.5	$\Theta = 1.541\ (z/r_0)^{-1}$	10	$\Theta = 0.819\ (z/r_0)^{-1}$
2	$\Theta = 1.401\ (z/r_0)^{-1}$	20	$\Theta = 0.650\ (z/r_0)^{-1}$
2.5	$\Theta = 1.300\ (z/r_0)^{-1}$	40	$\Theta = 0.516\ (z/r_0)^{-1}$
3	$\Theta = 1.223\ (z/r_0)^{-1}$	80	$\Theta = 0.409\ (z/r_0)^{-1}$

expressed non-dimensionally was the Equation (3.8), substituting w_m of the Equation (1.124) for w of this equation and the Equation (4.4) for Q of the Equation (3.8), we obtain

$$W = \frac{1.040}{c'^{2/9}} (n\pi)^{-1/6}, \qquad \cdots\cdots (4.8)$$

This is the velocity distribution along the central axis in this domain expressed non-dimensionally, and it has a constant value regardless of the height from the heat source, as in the case of an infinite line heat source. If the numerical value $c'^{2/3}=$ 0.13, is given in the Equation (4.8), it reduces to

$$W = \frac{1.696}{\sqrt[6]{n}} \qquad \cdots\cdots (4.8_1)$$

That is to say, the value of velocity depends only on the value of n, that is, on the degree of the slenderness of the rectangular heat source and the bigger the n, in other words, the slenderer the shape of a rectangular heat source, the smaller the upward velocity at the central axis is.

4.6 Temperature Distribution in the Third Domain

In this last domain the temperature and velocity distributions are the most stable, and the temperature distribution is similar to that in the case of a point heat source of equal strength placed at the intersecting point of the diagonals of the rectangle. Also, it accords with the temperature distribution in the upper domain of the circular heat source with a radius equal to the equivalent radius of the rectangle. In other words, the temperature along the central axis of the upward current decreases in inverse proportion to the 5/3 power of the height from the heat source. We can express this vertical distribution of temperature in non-dimensional form as follows:

$$\Theta = \frac{0.423}{c^{8/9}}\left(\frac{z}{r_0}\right)^{-5/3}, \qquad \cdots\cdots (4.9)$$

which is the same as the Equation (3.14), the formula for the distribution of temperature along the central axis in the domain far from the circular heat source. If we give the numerical value of $c^{2/3}=0.10$, in the above equation we obtain

$$\Theta = 9.115\left(\frac{z}{r_0}\right)^{-5/3}, \qquad \cdots\cdots (4.9_1)$$

which is the same as the Equation (3.13_1). That is to say, regardless of the slenderness and of the rectangle, the vertical temperature distribution in this domain, can be represented by one curve. In Figure 4.6 the results of the experiments using a square heat source of 29×29 cm and rectangular heat sources of 33×23 cm and 47.5×17.5 cm fall near the line of the Equation (4.9_1). With regard to the rectangular heat source 66.5×12 cm, we were not able to measure the temperature up to the height corresponding to the third domain, as stated earlier. As regards the horizontal distribution of temperature in this domain, we merely show that of the heat source 47.5×17.5 cm in the upper part of Fignre 4.4, omitting those of the other heat sources, but we wish to report here that the results of experiments for all the heat sources satisfy the Equation (1.79), which is the formula for horizontal distribution of temperature in the case of the point heat source.

The velocity distribution along the central axis of the upward current is equal to the case of a circular heat source and when expressed in terms of non-dimensional quantity W, it becomes

$$W=\frac{0.833}{c^{4/9}}\left(\frac{z}{r_0}\right)^{-1/3} \quad \cdots\cdots(4.10)$$

which is the same as the Equation (3.14), and if the numerical value of $c^{2/3}=0.10$ is given, it reduces to the Equation (3.14_1) or

$$W=3.87\left(\frac{z}{r_0}\right)^{-1/3} \quad \cdots\cdots(4.10_1)$$

This distribution shows that the velocity decreases in inverse proportion to the 1/3 power of the height from the heat source. The value of velocity is independent to the value of n, that is, to the degree of the slenderness of the heat source.

4.7 Summary of the Upward Current from a Rectangular Heat Source

The temperature distribution along the central axis of the upward current from a square heat source is almost similar to that of a circular heat source, and if we have r_0 for its equivalent radius, at heights lower than $z/r_0 <1$, the temperature does not vary very much according to height, but decreases a little. At the height of $z/r_0 >5$, the temperature decreases in inverse proportion to the 5/3 power of the height from the heat source. The intermediate heights comprise the transition range where the temperature distribution shifts from the former condition to the latter. By combining Figure 4.6 which shows the vertical distribution of temperature above a square heat source with Figures 4.1 and 4.5 which show the horizontal distributions of temperature at various heights, we can express the temperature distribution above a square heat source by means of non-dimensional quantity Θ. Figure 4.7 shows isothermal lines expressed in non-dimensional form and should hold if the strength and size of the heat source are changed to the scale of the actual wooden house fire.

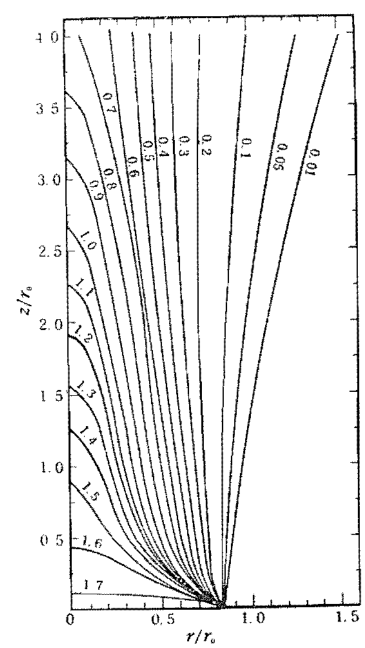

The numerical values indicated on the curves represent the values of non-dimensional temperature Θ

Figure 4.7

Isothermal lines above a square heat source.

In the case of a rectangular heat source, if we suppose the ratio of the longer side to the shorter one, n : 1 and the equivalent radius r_0, the temperature drop with height is generally small in the range of the height of $z/r_0 < 2.215/\sqrt{n}$, but the slenderer the shape of a rectangle is, the greater the drop of temperature. Above this and in the range of the height of $z/r_0 < 0.510(c'^{2/3}/c^{4/3})\sqrt{n\pi}$, the temperature along the central axis is in inverse proportion to the height from the heat source, and its distribution can be expressed by the Equation (4.6). Farther up, the temperature decreases in inverse proportion to the 5/3 power of the height from the heat source, and its distribution can be expressed by the Equation (4.9). The temperature

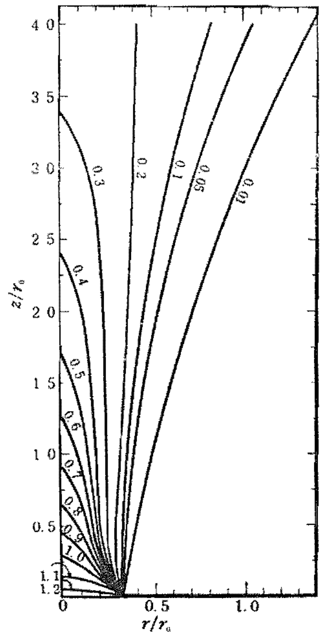

The numerical values indicated on the curves represent the values of non-dimensional temperature Θ

Figure 4.8

Isothermal lines above a rectangular heat source in the direction parallel to the shorter side of the rectangle whose value of n is 5.

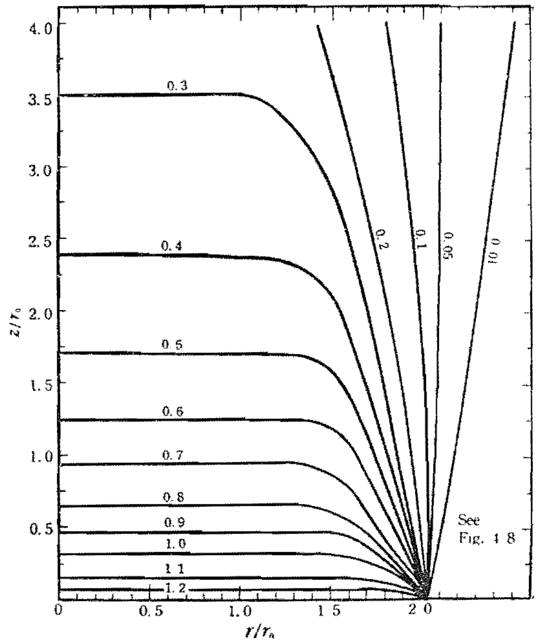

Figure 4.9

Isothermal lines above a rectangular heat source, in the direction parallel to the longer side of the rectangle whose value of n is 5.

distribution in this domain is independent to the value of n, the ratio between the lengths of the two adjacent sides of a rectangle.

Thus the heights of the boundaries between these three domains are determined only by the equivalent radius r_0 of rectangle and the ratio n between the lengths of two adjacent sides, and they do not depend on the strength of the heat source. If the size of the rectangle increases keeping the similar shape, the heights of transition change with corresponding magnifications. Figures 4.8 and 4.9 were prepared in the same way as in the case of the square heat source, basing on Figures 4.3, 4.5 and 4.6. They show the temperature distributions in the directions parallel to the shorter side and to the longer side of a rectaugular heat source whose radio of the lengths of the adjacent two sides are 5 : 1.

4.8 Rate of Heat Generation in a Burning Wooden House During the Period of its Maximum Intensity.

We will first obtain the quantity of heat produced from a burning wooden house, during 10 minutes of its maximum intensity. Assuming the plan of the house on fire to be reclangular, we suppose the lengths of the two sides of the house 'a' meters and 'b' meters respectively, and the height of ridge and the height of eaves h_1 meters and h_2 meters respectively, as shown in Figure 4.10. Let us suppose the quantity of combustibles contained in the house w Kg/m². The value of w is generally considered to be 165 Kg/m² for a dwelling and 135 Kg/m² for other buildings.[9] The

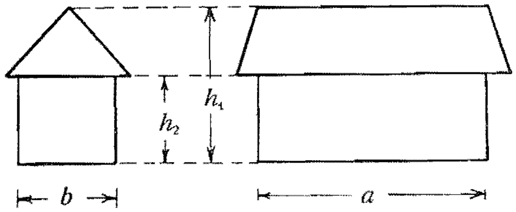

Figure 4.10 Dimensions of a wooden house on fire

total quantity of combustibles in this house is *wab* kg. Assuming that the house burns completely and that the amount of generated heat per Kg of lumber is 3560 Kcal, the total quantity of heat generated from the house during the period of fire is 3560 *wab* Kcal. In order to find the approximate ratio of the generated heat quantity during the above-mentioned 10 minutes, to the total heat quantity, we take the standard temperature-time curve of the first grade for the wooden house (J.I.S. A. 1301) which was obtained by averaging the results of a large number of fire tests of full-scale wooden houses. In this, the indoor temperature θ corresponding to time t (unit: hour) is approximately expressed by the following equation:[12]

$$\Theta = 6200(e^{-10t} - e^{-15t}) + 200. \qquad \cdots\cdots(4.11)$$

Here, $t=0$ does not mean the time of the start of the fire, but indicates the time when the indoor temperature attains to 200°C. That is to say, it is not until about four minutes after the start of fire (on the J. I. S. curve) that the above formula holds. The percentage of heat, generated during the period from 6 to 16 minutes after fire-start, (we regard this period as the one at maximum intensity of fire) to the total heat quantity is calcuated by use of this formula. For this purpose, the calculation is made on the assumption that the amount of heat generated is approximately proportional to the temperture: that is to say, we neglect the decrease of gas density caused by the rise of temperature. This is not correct, strictly, but this will do for the approximate calculation. As the 16th minute after the fire-start approximately corresponds to $t=1/40$ hr and the 16th minute to $t=1/5$ hr of this curve, let us integrate the Equation (4.11) from $t=1/40$ to $t=1/5$ This calculation reduces as follows:

$$\int_{1/40}^{1/5} \left\{6200(e^{-10t} - e^{-15t}) + 200\right\} dt = 170.$$

For the value corresponding to the amount of heat generated in the course of one hour from the fire start, we integrate the Equation (4.11) from $t=0$ to $t=1$. Although the time corresponding to $t=1$ in the Equation (4.11) differs from the first one hour after the outbreak of the fire, we assume that the amount of heat produced during the period from the outbreak to the time corresponding to $t=0$ in the Equation (4.11) is equal to the amount of heat produced in the period of time from the first one hour after the outbreak of the fire to the time corresponding to $t=1$. After integration, we obtain

$$\int_0^1 \left\{6200(e^{-10t} - e^{-15t}) + 200\right\} dt = 407.$$

Accordingly, we may conclude that during the 10 minutes of the maximum intensity of fire, about $170/407 \doteqdot 42\%$ of the amount of heat, produced in the course of one hour after the start of fire, is produced. Now, as it is known that about 80% of the total amount of heat produced, is produced in the course of one hour of the fire,[11] the amount of heat produced during the 10 minutes when the fire is at its height is 3560 $w.a.b.\times 0.8\times 0.42=1196.2\ w.a.b.$ Kcal. Accordingly, the average amount of heat Q_1 produced per second is

$$Q_1=1993.6\ w.a.b.\ \text{cal/sec}, \qquad (4.12)$$

where, as before:

w············amount of combustibles (Kg/m^2),

a, b·········length and width of the plan of the building (m).

4.9 Calculation of Temperature Distribution above a Wooden House on Fire

The results obtained on the temperature distributions of upward currents from the rectangular heat sources as stated in the Sections up to 4.7 may apply to the cases of fires of full-scale wooden houses according to the similarity law, when there is no wind. However, Figure 4.6 gives only the results of experiments, and it is inconvenient for finding the temperatures along the central axis of the upward currents from very narrow oblong heat sources. Accordingly, the author exterpolated the results of experiments, calculated the temperature distributions corresponding to the respective heat sources of $n=1$ (square), $n=1.25$, 2.5, 5, 10, 20 and 40 (oblong), and prepared Figure 4.11.

The distribution curves corresponding to the values of n not shown in the Figure, can be obtained by interpolation on the basis of Figure 4.11.

Next, the flames in an actual fire, not like the flames from alcohol, obtained in the laboratory experiment, contain a large amount of carbon particles and the amount of radiation from these is considerably large. Therefore, a proper correction is necessary. Whether it is in the case of a circular heat source or in the case of a rectangular heat source, Q in the Equation (3.9) which expresses the temperature in

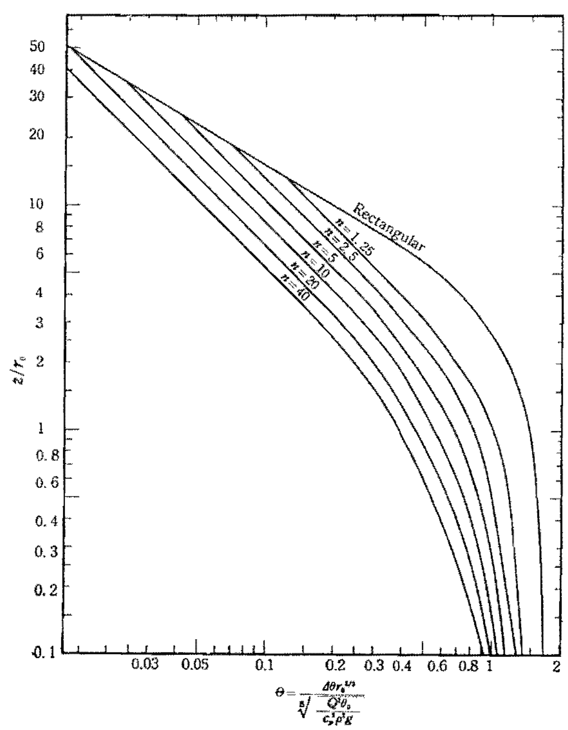

Figure 4.11

Curves expressing the vertical temperature distributions along the central axes of upward currents from various rectangular heat sources.

non-dimensional quantity Θ:

$$\Theta = \frac{\Delta\theta r_0^{5/3}}{\sqrt[3]{\frac{Q^2\theta_0}{c_p^2\rho^2 g}}} \quad \cdots\cdots (4.13)$$

expresses, as defined in the Equation (1.30) in the case of the point heat source in Chapter 1, the amount of heat that passes the horizontal section at an arbitrary height in unit time, and if the radiation heat is disregarded as has been in the above, the value of Q is independent to the height from the heat source and at the same time it expresses the strength of the heat source. When heat is lost by radiation as in an actual fire, the value of Q is different for each horizontal section. Accordingly, in case we try to find the temperature distribution above a house on fire, by using for instance, Figure 4.6, 4.7, 4.8 or 4.9, we must give a different value of Q contained in Θ for each height according to the amount of heat lost by radiation. An explanation of the method is given below.

Now let us suppose that the plan of a wooden house on fire be a rectangle, whose adjacent two sides being 'a' meters and 'b' meters long ($a \geqq b$) and whose height of ridge and height of eaves being h_1 meters and h_2 meters, respectively. With regard to the amount of heat radiated by the flames rising from the burning house during the period of its maximum intensity, we have the study by Dr. Kin-ichiro Fujita,[12] according to which the area of flames is approximately equal to the side-area of the house and the emissivity of the flames is approximately 114×10^3 Kcal/m^2. h. Accordingly, as the side building area of the house of which calculation was made this time are $2(a+b)\ h$ sq. m., and this is approximately equal to the areas of the flames, the heat Q_2 lost per second from the flames during the period of its maximum intensity of fire is,

$$Q_2 = 63330\ (a+b)\ h \text{ cal/sec.} \quad \cdots\cdots (4.14)$$

The heat Q_1 produced from the burning house per second at its maximum stage of fire can be calculated from the Equation (4.12) in the preceding Section. As the radiation from the flames in fire occurs mainly when the flame-temperature is higher than 500°C, the radiation may practically be over when the flame rises up farther and the its temperature drops lower than 500°C. Therefore, the heat Q which passes the horizontal section in unit time at any height above the point where the temperature of upward current drops to 500°C, can be approximately expressed by the difference between the heat Q_1 produced from the burning house and the heat Q_2 radiated, or

$$Q = Q_1 - Q_2. \quad \cdots\cdots (4.15)$$

At the height where the temperature on the central axis of the upward current is 500°C we can substitute the following numerical values into the Equation (4.13).

$\Delta\theta = 500$°C, $\quad \Theta_0 = 290$°K $\quad c_p = 0.24$ cal/g. deg,

$g = 980$ cm/sec^2, and $\rho = 0.000456$ g/cm^3,

and we obtain

$$Q_{500} = \frac{1.717 r_0^{5/3}}{Q^{2/3}}. \quad \cdots\cdots (4.16)$$

As the equivalent radius r_0 is the radius of a circle with a horizontal area equal to that of the house, it can be expressed as follows:

$$r_0=\sqrt{\frac{ab}{\pi}}=\sqrt{\frac{ab}{3.1416}} \quad \cdots\cdots\cdots\cdots(4.17)$$

By substituting Q in the Equation (4.15) and r_0 in the Equation (4.17) into the Equation (4.16), we obtain the value of the non-dimensional temperature Θ corresponding to the temperature $\Delta\theta=500°C$ in the upward current. Next, by finding the ratio between the lengths of the two adjacent sides of the house from the equation,

$$n=a/b, \quad \cdots\cdots\cdots\cdots(4.18)$$

and by finding by use of Figure 4.11 the value of $(z/r_0)_{500}$ corresponding to the values of n and Θ_{500} now obtained, we can find the value of z_{500}, the height where the temperature on the central axis is 500°C. In this case, it seems reasonable to take the origin of the z axis at the height of the eaves of the house, so the values of z express the height from this level, hereafter.

The temperature at a lower height than this can be obtained in the following way: Supposing that the total amount of radiation increases proportional to the height from the eaves of the house, the total radiant heat loss Q_2 from the eaves of the house to the height z can be expressed as follows:

$$Q'_2=Q_2z/z_{500} \quad \cdots\cdots\cdots\cdots(4.19)$$

The heat quantity which passes the height z per unit time, is expressed by Q_1-Q_2' and this value is substituted for Q into the Equaton (4.13), then the temperature at that height is obtained. As for the temperature at a height beyond z_{500}, it can be obtained by substituting the value of Q obtained from the Equation (4.15) for Q into the Equation (4.13).

Now, as an example of calculation, let us take four wooden houses, all having a ridge height of $h_1=4$ m and eaves height of 3 m, whose two adjoining sides of the plan are 12 m × 12 m, 24 m × 6 m, 48 m × 3 m and 12 m × 3 m respectively and which invariably contain combustibles of $w=165$ Kg per 1 m² of the floor (average value for dwelling houses), and suppose that a fire has broken out when there is no wind. Under such conditions, let us calculate the temperatures at the heights of 2.5 m, 5 m, 10 m, 15 m, 20 m, and 25 m from the eaves of the house during the period of the maximum intensity of fire.

Example of Calculation

No. of building	No. 1	No. 2	No. 3	No. 4
a	12m	24m	48m	12m
b	12m	6m	3m	3m
r_0	677cm	677cm	677cm	338cm
$n=a/b$	1	4	16	4
Heat lost in radiation (Q_2) (10cal/sec)	6080	7600	12919	3800
Total amount of wab (Kg)	23706	23760	23760	4940
Combustibles Q_1 (10 cal/sec)	47368	47368	47368	11842
$Q^{2/3}$	119460	116510	105870	40140
$r_0^{5/3}$	52197	52197	52197	16401

No. of building	No. 1	No. 2	No. 3	No. 4
$r_0^{5/3}/Q^{2/3}$	0.4309	0.4480	0.4903	0.4086
Θ_{500}	0.750	0.769	0.846	0.700
$(z/r_0)_{500}$	3.96	0.86	0.28	0.10
z_{500}	2681cm	575cm	190cm	372cm

It is indicated that, though the houses No. 1 to No. 3 have equal floor area, the narrower the building, the lower the height where the temperature on the central axis of the upward current is as low as 500°C. On the basis of these results, we further calculate the temperatures at the various heights:

No. of building	No. 1	No. 2	No. 3	No. 4
Q ($=Q_1$) at $z=0$m (10 cal/sec)	47368	47368	47368	11842
$Q^{2/3}$	130920	130920	130920	51954
$r_0^{2/3}/Q^{2/3}$	0.3987	0.3987	0.4987	0.3157
Θ	1.70	1.20	1.03	1.20
$\Delta\theta$	1354°C	1354°C	1354°C	1207°C
Q at $z=2.5$m (10 cal/sec)	46760	44064	34449	9228
$Q^{2/3}$	129790	124760	105870	43995
$r_0^{5/3}/Q^{2/3}$	0.402	0.416	0.493	0.373
z/r_0	0.37	0.37	0.37	0.74
Θ	1.62	0.99	0.76	0.76
$\Delta\theta$	1347°C	926°C	415°C	687°C
Q at $z=5$m (10 cal/sec)	46152	40759	3449	8042
$Q^{2/3}$	128670	119100	105870	40140
$r_0^{5/3}/Q^{2/3}$	0.406	0.438	0.493	0.409
z/r_0	0.74	0.74	0.74	1.48
Θ	1.33	0.59	0.41	0.36
$\Delta\theta$	1284°C	324°C	141°C	180°C

No. of building	No. 1	No. 2	No. 3	No. 4
Q at $z=15$m (10 cal/sec)	47320	39768	34449	8042
$Q^{2/3}$	124100	116510	105870	40140
$r_0^{5/3}/Q$	0.421	0.448	0.493	0.409
z/r_0	2.22	2.22	2.22	4.44
Θ	1.10	0.42	0.31	0.26
$\Delta\theta$	1132°C	197°C	116°C	119°C

No. of building	No. 1	No. 2	No. 3	No. 4
Q at z=20m (10 cal/sec)	42504	37768	34449	8042
$Q^{2/3}$	12179	116510	105870	40140
$r_0^{5/3}/Q^{2/3}$	0.429	0.448	0.493	0.409
z/r_0	2.95	2.95	2.95	5.92
Θ	0.94	0.35	0.24	0.162
$\Delta\theta$	687°C	153°C	85°C	67°C
Q at z=25m (10 cal/sec)	41698	39768	34449	8042
$Q^{2/3}$	120230	115610	105870	10140
$r_0^{5/3}/Q^{2/3}$	0.434	0.448	0.493	0.409
z/r_0	3.69	3.69	3.69	7.40
Θ	0.79	0.29	0.195	0.154
$\Delta\theta$	555°C	118°C	67°C	63°C

With regard to the houses No. 1 to No. 3 whose floor areas are equal to one another, the decreasing of the temperature with the height is the most acute in the case of the narrowest house No. 3, and a conspicuous difference is seen between this and the square house at equal height. It is also noteworthy that, while the plans of No. 2 and No. 4 are similar in the shape, the temperature of the one at a height is not twice as high as that the other at the same height.

4.10 Summarization

1) By utilizing the results obtained on the velocity distribution of the air currents spurting out of the rectangular orifice stated in Chapter 2, the law of similarity on the temperature distribution of the upward current from the rectangular heat source has been introduced.

2) In order to apply the obtained law to actual-size house fires, it is necessary to make correction of radiation through the flames. The author has worked out a method to make the revision by approximation.

3) Supposing that the plan of the house is rectangular, and that its size and the ratio between the two adjoining sides are given, the author has introduced a method of calculating the temperature distribution above the house in case of a fire.

4) The temperatures above two houses may differ greatly according to the ratio between the two adjoining sides even if the plan areas and the quantities of combustibles contained, are equal. Namely, the lowering of the temperature as the point of measurement goes up is not very acute in case the plan is more or less square; the narrower the building, the more acute the lowering becomes.

Chapter 5

Fire-Protection of Television Towers

5.1 Introduction

Burning of a wooden house caused by spreading of fire usually occurs either when it is directly subjected to flames or heated gas or when it is exposed to many small blocks of fire flying towards it, and in most cases it occurs when there is some atmospheric wind, though it may not always be strong. Accordingly, the results obtained in the preceding Chapters on the temperature distsibutions of upward currents from wooden houses burning when there is no wind, can seldom be put to practical use. However, there is an important application thereof which we should not neglect. It is connected with the problem of fire protection of television towers and other tower-shaped structures.

The television towers that are built one after another in cities are designed to resist strong winds and earthquakes, but it is surprising that measures against the possible decrease in strength which may be caused by heating of the members of such a tower when there occurs a fire in the vicinity are often neglected. There are some actual cases where the vicinity of the television tower is crowded with wooden houses or there are big wooden houses there. It is terrifying to think that if a fire breaks out among them the tower may collapse owing to the heat of fire.

In the following are given an explanation about the fire load which the tower receives from a fire in the windless and windy conditions, and one of the plans of protection of the tower from fire-damage.

5.2 Boundary of Danger Temperature of Members of a Tower

Here is discussed what is the critical temperature (in terms of ℃) of the hot gas current which endangers the tower as to its strength when it is exposed to the hot gas. Suppose that, a tower is designed to have a safety factor twice as large as the dead load strength. If the tower is so designed, therefore, it is not dangerous when there is no wind for the tower to be exposed to a hot gas whose temperature is not beyond the temperature which decreases the strength to 1/2. As an another case, we suppose that, a tower is designed to resist a strong wind of $20\sqrt{h}$ m/sec, where h indicates the metric measurement of the height above the ground. In winter and spring when conflagrations in strong winds are liable to occur, the wind is rarely stronger than $15\sqrt{h}$ m/sec. So let us assume a conflagration in a strong wind of $15\sqrt{h}$ m/sec. As the wind pressure is proportional to the square of the wind velocity, the safety allowance of strength decreases to 1/2 when wind velocity is $1/\sqrt{2}$ of the design wind velocity. Therefore, in this case too, the tower can stand a hot gas up to the temperature where the strength is reduced to 1/2. Althcugh the percentage decrease of strength-under-heat of steel to its strength at the normal temperature, somewhat varies according to the kind of steel, it reduces to about 1/2 at 550°C.[13] Accordingly, here, the discussion is limited only to the case where the critical temperature is 550°C.

First, let us suppose that there is a wooden house under the tower or on the adjoining site, that a fire breaks out when no wind or a low wind is blowing and that the members of the tower are exposed to the hot gas currents ascending from the fire. Our problem is to what height above the ground the tower members are exposed to a hot gas of 550°C or higher temperature. This is the problem discussed in Section 4.9 (the preceding Chapter). Let us suppose, as we did in that Section, that the ridge and the eaves heights of the house are h_1 meters and h_2 meters respectively, that the lengths of the two sides of the plan of the house are 'a' meters and 'b' meters respectively ($a \geqq b$) and that the amount of combustibles is w Kg/m². Then the quantity of heat produced by combustion of the building at the maximum stage of fire, is expressed by Equation (4.12), and the quantity of radiation heat of flames from the house, Q_2, by Equation (4.14). As it is after the radiation from flames has nearly finished that the temperature of the upward current lowers to 550°C, the quantity of heat that passes the horizontal section of the current per second, Q, is approximately expressed by Equation (4.15). Therefore, on the assumption that $c_p=0.24$ cal/g.deg. $\rho=0.000428$ g/cm³, $g=980$ cm/sec², $\Delta\theta=550$°C and $\theta_0=290$°K (absolute temperature of the surrounding air), the value of the non-dimensional temperature Θ corresponding to 550°C is, from Equation (4.13):

$$\Theta_{550}=\frac{1.812\ r_0^{5/3}}{Q^{2/3}}. \quad \cdots\cdots(5.1)$$

Here r_0 expresses the equivalent radius of the wooden houses and is calculated according to Equation (4.17). Next, the value of n of the house is obtained from Equation (4.18); the value of $(z/r_0)_{550}$ corresponding to this value of n and to Θ_{550} is obtained referring to Figure 4.11; and from these the value of z_{550} can be obtained.

The last problem is: at what height of the house the heat source or the origin of height (point where $z=0$) should be placed. As the house burns not two-dimensionally but three-dimensionally, it was considered difficult to indicate the origin of height. The author burnt firewood piled up in the form of a rectangular parallelipiped and observed the temperature distribution along the central axis of the upward current rising from it. He found that when the origin is placed at a height a little lower than the highest surface of the piled-up firewood the distribution of temperature coincides with that in the case of a flat heat source with an equal horizontal section. Accordingly, in order to simplify the calculation, let us regard the eaves height of the house as the position of the heat source or the origin of height. Then, the value of z_{550} calculated previously is the height from the eaves of the house, and so the members of the tower up to the height $z_{550}+h_2$ from the ground are exposed to heat of 550°C or more.

What was said above concerns cases of fires which occur when there is no wind. Let us find out what the situation is when there is a strong wind. According to Dr. Kin-ichiro Fujita's calculation of the spreading distance of fire stream in conflagration, if such fire breaks out in a district where the total floor space ratio of the houses (ratio of the total floor area to the land area) is 1, when the velocity of wind is 15 m/sec, the area where the air temperature rises to 550°C or higher as a result of the flow of the heat due to the fire, extends to a distance of about 60 meters leeward from the burning house, and in this area the height up to which the temperature rises to 550°C or higher is about 10 meters from the ground. If the velocity of wind is 8 m/sec, the area extends to a distance of about 50 meters leeward from the burning house and the height up to which the temperature rises to 550°C or higher is 12 meters.[14] It is true that in the case where the velocity of wind is 8 m/sec, the strength allowance of the tower is a little larger than in the case where the velocity is 15 m/sec and there would be no harm even if the tower were exposed to hot currents of temperature a little higher than 550°C, but to simplify matters, the boundary of the danger temperature was set at 550°C here, taking the safer side. In short, if there is an area crowed with wooden houses where the total floor space ratio of the houses is 1 or greater, within a distance of about 60 meters from the foot of the tower, there is a danger that the tower will be exposed to hot currents of temperature over 550°C up to the height of 10 or 12 meters from the ground, if a conflagration occurs in strong wind.

In the above were discussed cases of both extremes — the case where there is no or hardly any wind the case where there is a strong wind, but also in the case of moderate strength, we can consider in the same way. At any rate, when there are dangerous wooden houses near the tower, it is necessary to give appropriate fire-protection treatment to the tower according to the size and density of the houses.

5.3 Necessary Measures for Fire-Protection of the Members of a Tower

For preventing the lowering of the strength of a television tower caused by the heating of the members, it is desirable that there be no wooden houses within 60 meters around tower. In case it is impossible to satisfy this condition, some other step, say covering the steel frame members with a fire-retardant material, must be taken.

Here let us consider the prevention of the rising in temperature of the steel members of a television tower by covering them with concrete in cylinders. First, the value of the necessary radius of each cylinder is calculated. In this calculation, let us consider that the member is a line and that it is to be placed along the central axis of the cylinder cover. What we have to do is to find the value of the radius of the cylinder large enough to prevent the temperature in the center from rising beyond 550°C under the severe condition that the surface of the concrete pillar in the shape of a cylinder be exposed for 20 minutes in a hot current of 1000°C.

It takes much time to solve a problem of non-stationary heat transfer or heat conduction even when the diagram solution or the simplified calculation method is employed. For the engineering purpose in this case, it is convenient to use Gurney-Lurie's Chart.[15] This Diagram expresses the relations between the time and the temperature at any place of the cylinder under certain initial and boundary conditions. The different curves are drawn according to the values of heat conductivity and heat

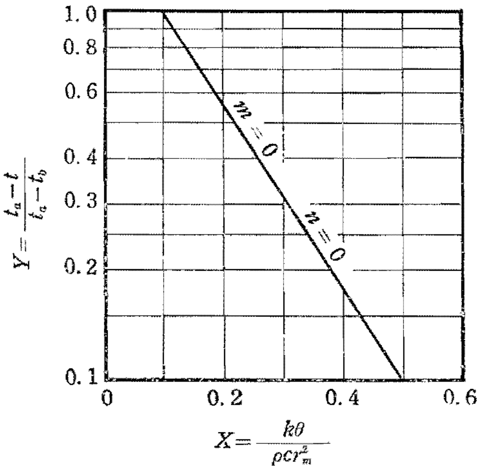

Figure 5.1
A part of Gurney-Lurie Chart to be applied to long cylinder.

transfer coefficient of the substance which forms the cylinder. In this Diagram non-dimensional factors m and n defined by the Equations (5.4) and (5.5) are used instead of above mentioned two factors. Figure 5.1 shows a part of the Chart, in which,

$$X=\frac{k\theta}{\rho c r_m^2}, \quad \cdots\cdots (5.2)$$

$$Y=\frac{t_a-t}{t_a-t_b}, \quad \cdots\cdots (5.3)$$

where

t_a ············ temperature of hot current to which the outer surface of a cylinder is exposed;

t_b ············ initial temperature of a cylinder as a whole;

t ············ temperature of the point in question, θ hours after cylinder is exposed to hot current;

k ············ heat conductivity of the substance of the cylinder;

ρ ············ density of the cylinder-substance;

c ············ specific heat of the cylinder-substance;

r_m ············ radius of cylinder;

θ ············ time elapsed after cylinder is first exposed to hot current (unit: hour).

Again, m and n are non-dimensional quantities as defined below:

$$m=\frac{k}{\alpha\ r_m}, \quad \cdots\cdots (5.4)$$

$$n=\frac{r}{r_m}, \quad \cdots\cdots (5.5)$$

where:

α ············ heat transfer coefficient of the surface of the cylinder;

r ············ radial distance of the point whose temperature is to be sought from the center of cylinder.

What we try here is to find the radius r_m of the concrete cylinder large enough to keep the temperature at the center of the concrete cylinder lower than 550°C when it has been exposed to a hot current of 1000°C for 20 minutes. At 800°C or so, the values of the thermal conductivity of concrete $(k/c\rho)$ and the ratio between heat conductivity and heat transfer coefficient are given, respectively:

$$k/c\rho = 0.0013\text{m}^2/\text{h},^{16)} \quad \cdots\cdots (5.6)$$

$$k/\alpha = 0.0025\text{m}.^{17)} \quad \cdots\cdots (5.7)$$

Also, so far as the temperature at the center of the cylinder is concerned, we can put here; and according to the Equation (5.5),

$$n = 0. \quad \cdots\cdots (5.8)$$

In concrete, the value of k/α is very small (Equation (5.7)), so from Equation (5.4), we may suppose

$$m \fallingdotseq 0 \quad \cdots\cdots (5.9)$$

Accordingly, we may only use the curve corresponding to $m=0$, $n=0$ in Gurney-Lurie Chart. By substituting $t_a=1000$°C, $t=550$°C and $t_b=20$°C, we obtain from Equation (5.3)

$$Y = 0.46. \quad \cdots\cdots (5.10)$$

The value of X corresponding to that value of Y on the line of $m=0$, $n=0$ in Figure 5.1 becomes

$$X = 0.234. \quad \cdots\cdots (5.11)$$

Substituting $X=0.234$, $k/c\rho=0.0013$ m²/hr and $\theta=1/3$ hr in Equation (5.2), we obtain

$$r_m = 0.043 \text{ m}. \quad \cdots\cdots (5.12)$$

Therefore, we may conclude that the necessary dimension of the radius of the concrete cylinder as the coat is approximately 4.3 cm. In practice, however, a cylinder with a radius of 4.3 cm will not do, because the steel member is not a line but has a considerable thickness. What we should do is to cover it so that the steel is placed at least 4.3 cm deep from the surface of concrete.

The above depth corresponds to the height where the member is exposed to heat of 1000°C for 20 minutes. This corresponds to the height of the eaves. What about the height where it is exposed to heat of 700°C for 20 minutes? In this case, $Y=0.22$ in Equation (5.3), and the value of X corresponding to $Y=0.22$ on the line of $m=0$, $n=0$ in Figure 5.1 is $X=0.36$. Calculation according to Equation (5.2) reveals that $r_m=0.035$ m, which means 3.5 cm will be enough for the thickness of the coat. Thus the higher the part of the tower, the thinner the concrete coat may be made.

Now let us check some of the existing television towers. As the Tokyo Tower and the television tower in Nagoya are intended for sight seeing as well, it may be natural that the owners of the tower should be unwilling to have them covered because it may spoil the beauty of their appearance. In the case of the Tokyo Tower, as there are no big wooden houses nor group of crowded wooden houses within 60 m around, it is not necessary at present to take any fire-protection measure. As for the television tower in Nagoya, standing in the middle of a street, it is more than 60 m away from most of the wooden houses blocks in the vicinity, and there are no big wooden houses at all under the tower. However, there is an area crowded with wooden houses within 40 m to the east and north-east direction of the tower.

In this connection, the author called the attention of the owner, but, regret to say, no fire-protection measure has been taken for the tower. If it is undesirable to cover the steel with concrete for the purpose of fire protection, there is another method. That is to install a drencher at about 20 m above the ground in order to protect the four pillars of the tower with water screens from the flame of fire. In case of a conflagration, however, a great quantity of water is needed for fire-fighting and the hydraulic pressure in the vicinity will naturally lower. Generally speaking, therefore, I hesitate to affirm that the drencher can always defend the tower against fire. Success depends on the water supply at that time.

5.4 Examples of Calculation on the Height up to Which Fire-Protection is Necessary

It was stated in Section 5.2 that the part of a tower for which some fire-protection treatment is necessary for securing the safety of the tower at the time of a conflagration in a strong wind is the part up to the height of 10~20 meters above the ground. Here, we calculate the height to which fire-protection coating is necessary in the case of a fire which occurs in a wooden house standing just under the tower or on an adjoining lot when there is no or little wind. In the calculation examples in Section 4.9 (the preceding Chapter), made relative to four kinds of wooden houses with a building area of 12×12 m, 24×6 m, 48×3 m, 12×3 m, the heights where the temperature of the upward currents at the time of a fire in case the amount of combustibles is 165 Kg/m² is 500°C were approximately 27 m, 6 m, 2 m, and 4 m respectively. The heights where the temperature of the upward current is 550°C do not differ greatly from these figures, and therefore, in case such a building is just under the tower or on the adjoining lot, the part of the tower needing the fire-protection treatment is calculated to be 30 m, 9 m, 5 m and 7 m according to the case, which figures are obtained by adding 3 m, the eaves height, to the above. We made similar calculations following the method stated in Section 5.2 relative to four kinds of wooden buildings with a building area of 15×15 m, 6×6 m, 24×12 m and 8×4 m somewhat different in size from the above examples. Although this may seem to be a repetition of the same thing, it was conducted in order to make calculations for the various cases. The results were as shown below. In the calculation, the ridge height of the building, its eaves height, and the amount of combustibles were considered to be the same as those in the previous case.

$h_1 = 4$ m, $h_2 = 3$ m, and $w = 165$ Kg/m², respectively.

No. of bldg.		No. 1	No. 2	No. 3	No. 4
Size of building	a	15m	6m	24m	8m
	b	15m	6m	12m	4m
Equivalent radius r_0		846cm	338cm	957cm	319cm
$n = a/b$		1	1	1	1
$(a+b)h_1$		120m²	48m²	144m²	48m²
Heat lost in radiation Q_2		7600×10³ cal/sec	3040×10³ cal/sec	9120×10³ cal/sec	3040×10³ cal/sec

No. of bldg.	No. 1	No. 2	No. 3	No. 4
Heat produced at the maximum stage of fire Q_1	74012×10^3 cal/sec	11842×10^3 cal/sec	94736×10^3 cal/sec	10526×10^3 cal/sec
$Q=Q_1-Q_2$	66412×10^3 cal/sec	8802×10^3 cal/sec	85616×10^3 cal/sec	7486×10^3 cal/sec
$Q^{2/3}$	164000	42631	194250	38268
$r_0^{5/3}$	75675	16401	92937	14893
$r_0^{5/3}/Q^{2/3}$	0.4614	0.3847	0.4784	0.3892
Θ_{550}	0.836	0.697	0.867	0.705
$(z/r_0)_{550}$	3.43	4.20	1.15	1.65
z_{550}	2902cm	1420cm	1101cm	526cm
$z_{550}+h_2$	32m	17m	14m	8m

Thus the heights up to which the fire-protection treatment is necessary have been found to be 32 m, 17 m, and 8 m, respectively. From the eight calculation examples (including the examples in the preceding Chapter), we can make rough estimation of the value of the height up to which the fire-protection treatment is necessary when the size and shape of the wooden house are given.

5.5 Concluding Remarks

In the above have been discussed the several conditions of repelling the danger concerning to the strength when a television tower is exposed to a hot current in a fire.

These studies were originally made, in response to the request of the Housing Bureau, Ministry of Construction, under the direction of Dr. Kin-ichiro Fujita while he was the Director of the Building Research Institute. However, as the author's study on the temperature distribution of the upward current from a rectangular heat source had not made much progress at that time, the conclusion relative to such part was made on a mere assumption. As the study was completed subsequently, the author re-checked such part in preparing the present paper.

PART Ⅲ LENGTH OF SPANDREL NECESSARY FOR PROTECTING THE FIRE-SPREAD TO UPSTAIRS

Chapter 6

Fire Test with a Full-Scale Fire Resistive Construction

6.1 Introduction

The modern concrete buildings with large window area have much possibility of fire-spread to upstairs in case of a fire. For, when a fire occurs in one of the rooms, long flame will eject from the window and the flame heat will break the upstairs window-panes, which will make the fire spread to the room upstairs. For preventing such fire-spread, it is, first of all, necessary to investigate the trajectory and the temperature distribution of the ejecting gas from the window in such a case. These factors have been studied on the results of several full-scale experimental fires, and they are reported here.

6.2 Outline of Experiments

The following four fire-tests were made:

No. 1. …… Test with a vacant fire resistive concrete building in front of Shibuya Station, Tokyo which belonged to Yamaichi Company. Performed on Jan. 30, 1956.

No. 2. …… Test with a concrete block house in the Building Research Institute, Shinjuku-ku, Tokyo, Performed on Nov. 21, 1956.

No. 3. …… Test with a concrete house in the Building Research Institute. Performed on Oct. 10, 1958.

Table 6.1 Conditions of the rooms used in tests

	No. of tests	No. 1	No. 2	No. 3 and No. 4
Room volume	Frontage	13.35m	4.30m	5 m
	Depth	9.70m	3.48m	2.5 m
	Height of ceilings	3.50m	2.47m	1.67m
	Floor area	105 m²	14.96m²	12.50m²
Window	Horizontal length	91cm	82cm	300cm
	Vertical length	167cm	155cm	100cm
	Remarks	One of the 5 windows was used.	One of the 2 windows was used.	The room has only one window.
Fuel (Timber)	Total weight	4400kg	800kg	500kg
	Weight per 1 m²	42kg	53kg	40kg
	Water Content	20%	15%	13%
Meteorological condition	Weather	Fine	Cloudy	Fine (in both cases)
	Wind direction	SW	NNW	E (in both cases)
	Wind speed	1.5m/sec.	1m/sec.	1m/sec. (in both cases)

No. 4. …… Test with the same house as in the Test No. 3. Performed on Oct. 26, 1958.

In the Test No. 3, no combustible linings were used, but in the Test No. 4, plywood internal linings were used for both wall and ceiling. The details of the test room used in each experiment are shown in Table 6.1.

6.3 Measured Factors and Method of Measurements

6.3.1 Room temperature

Test No. 1. …… Chromel-alumel thermo-couples were used for measuring the room temperature. They were set at plane position as shown in Figure 6.1, and at each position they were set at 3 levels; near the ceiling, near the floor and middle of the room.

Test No. 2. …… 4 chromel-alumel thermo-couples were placed at the middle of the room in vertical direction; 20 cm, 26 cm, 108 cm and 198 cm under the ceiling respectively.

Test No. 3 and No. 4. …… 6 chromel-alumel thermo-couples were placed as shown in Figure 6.2. They were set 30 cm under ceiling.

6.3.2 Temperature of flame ejecting from window

Test No. 1. …… Temperature of flame ejecting from the window W_2 as shown in Figure 6.1 was measured. A pole of a steel angle was set up in front of the window, and thermo-couples were set on its branches. Temperature of flame was measured at 19 points shown in Figure 6.8.

Test No. 2. …… Temperature of flame was measured at 20 points in front of the window shown in Figure 6.9.

Test No. 3 and No. 4. …… Temperature of flame was taken 32 points in the former test and 30 points in the latter as shown in Figure 6.10. In the test No. 3, a steel sash, half of which was of plane glass and the rest was wired-glass, was placed along the wall 50 cm above the window, and another wooden sash with plane

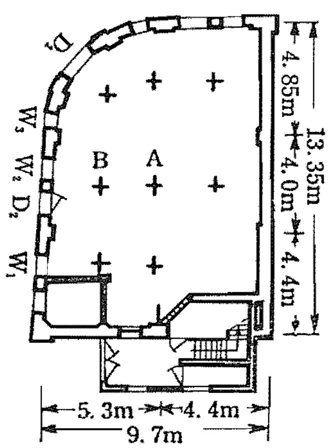

+……Point at where temperature was measured
W……Window D……Door

Figure 6.1
Positions of measurement points for room-temperature in Test No. 1.

Figure 6.2
Positions of measurement points for room-temperature in Test No. 3 and No. 4.

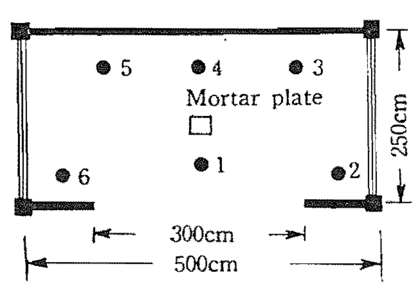

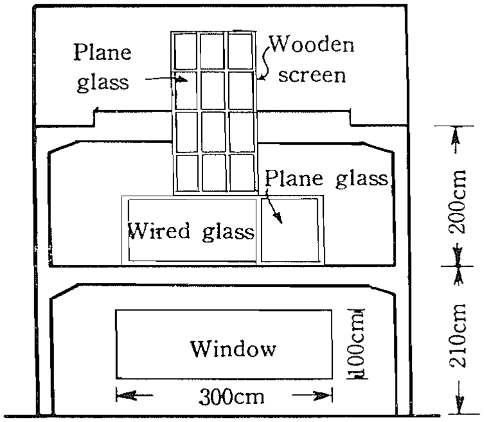

Figure 6.3
Glass, set above window from which flame is ejected.

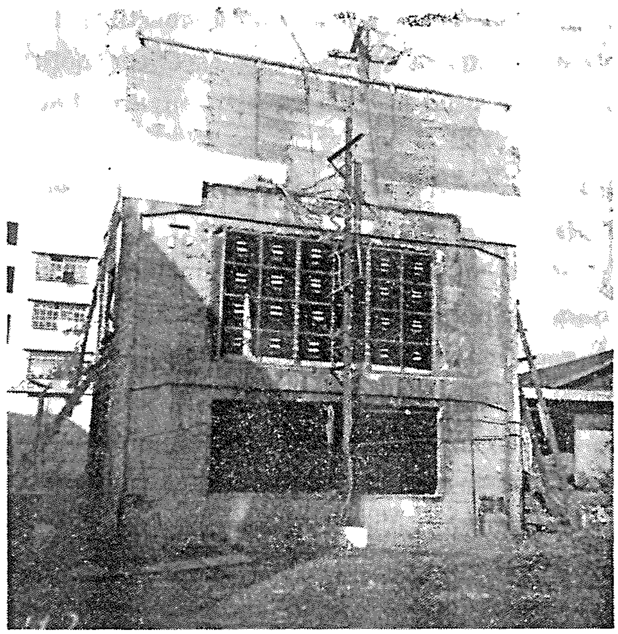

Photo. 6.1
Window glass, set above the window of a test room (Test No. 4)

glass in it was also placed along the external wall 150 cm above the upper edge of the window (Figure 6.3). In the Test No. 4, an opening was made upstairs and a steel sash with plane glass was fitted to it (Photo. 6.1). The length of the spandrel between these two windows is about 50 cm.

6.3.3 Outflow velocity of flame from window

Pitot-tube was placed at the middle of the window to measure the outflow velocity of flame, but in the Tests No. 3 and No. 4 it was placed 24 cm under the upper edge of the window. The measured values were converted into the velocity values by calculation.

6.4 Test Results

6.4.1 Room temperature

Test No. 1. …… A sheet of curtain hung on the window, caught flame soon after the ignition and the window-panes were broken down one after another and then flame began to eject from the window. But it took pretty long time for the fire to gain headway in the room, because the room was too big. At about 17 min. after the ignition, the fire came to be active. The time-temperature curves at the points A and B (Figure 6.1) are given in Figure 6.4: the solid line indicates the average temperature of A and B, while the dotted line represents the standard time-temperature curve (JIS A1302) with its initial time displaced to the time at 17 min. after ignition in this fire. The rate of temperature rise is similar to that of the standard curve. The average room temperature during the most active combustion (from 51 to 60 min. after ignition) was 851°C. As the temperature of the surrounding air marked about 0°C, the excess temperature $\Delta\theta$ was also 851°C.

Test No. 2. …… In this case there were no window-panes in the openings and

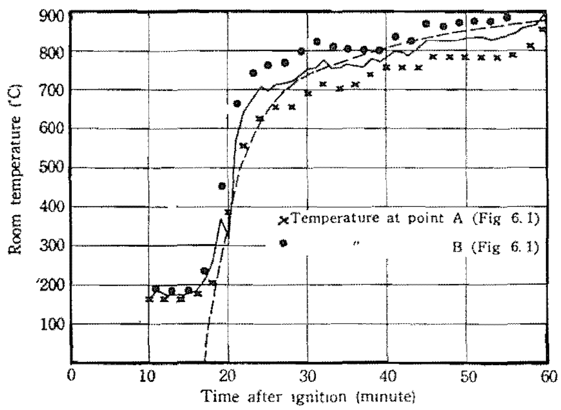

Figure 6.4

Time-temperature curve in Test No. 1.

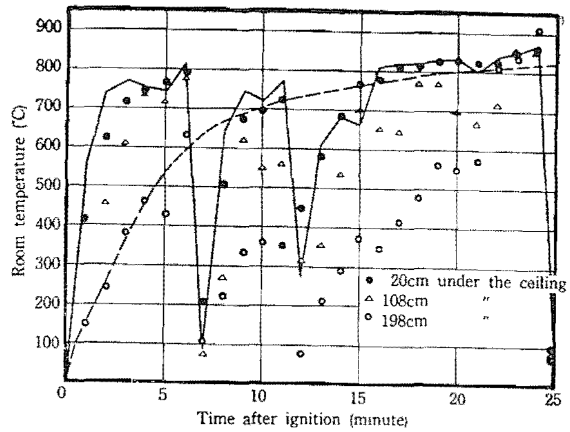

Figure 6.5

Time-temperature curve in Test No. 2.

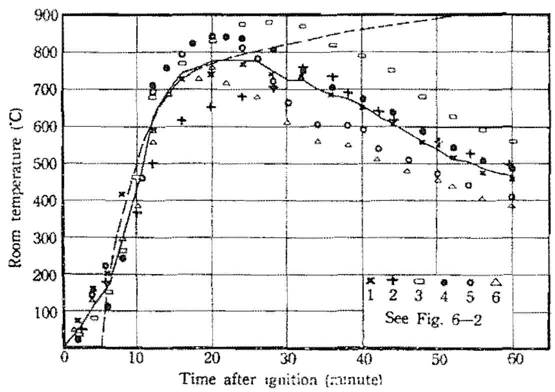

Figure 6.6

Time-temperature curve in Test No. 3.

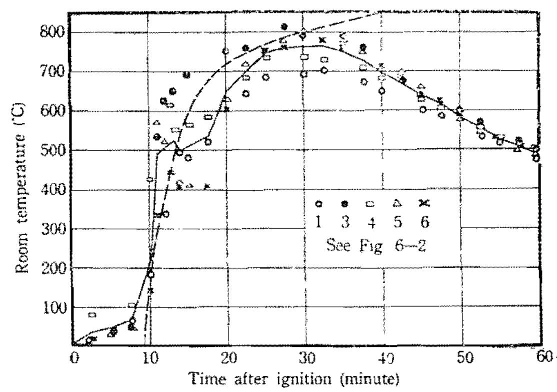

Figure 6.7

Time-temperature curve in Test No. 4.

the fire became active soon after ignition and the rate of temperature-rise was higher than that of the standard curve as shown by the dotted line in Figure 6.5. In this test, water test was performed with spray three times during the fire. At each time the room temperature dropped suddenly on account of it. The mean temperature during the most active combustion (from 16 to 24 min. after ignition) was 830°C, and the excess temperature $\Delta\theta$ was 810°C.

Test No. 3. ······ Ignited the fuel with gasoline. It took about 8 min. for the flame to spread over the floor. The rate of temperature rise in the room was almost the same as that of the standard curve indicated by the dotted line in Figure 6.6. The average temperature during the most active combustion (from 20 to 38 min. after ignition) was 735°C and the excess temperature $\Delta\theta$ was 715°C.

Test No. 4. ······ The fire-wood used in this test was harder than that used in the test No. 3. No sooner the plywood boards of the ceiling caught flame (about 12 min. after ignition) than the room reached the flash-over point explosively, and the ejected flame from the opening reached higher than 5 meters along the external wall and broke the most of the upstairs window-panes. Such condition continued for about 2 min. and then room-temperature dropped a little. But it soon began to

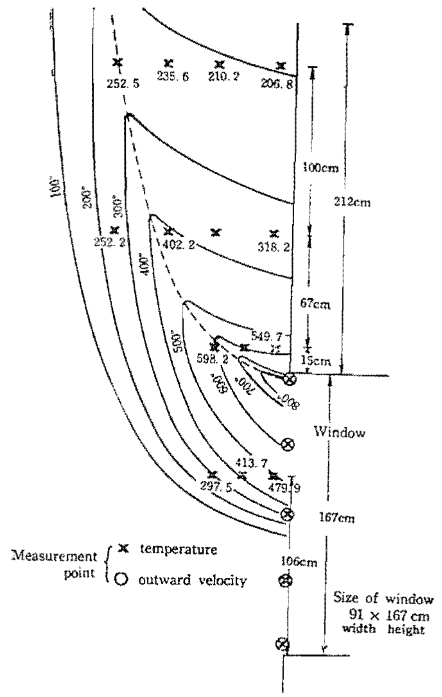

Numbers written under × mean mean-temperature during maximum intensity

Figure 6.8

Isothermal lines near the window from which fire-flame is flowing out. (Test No. 1)

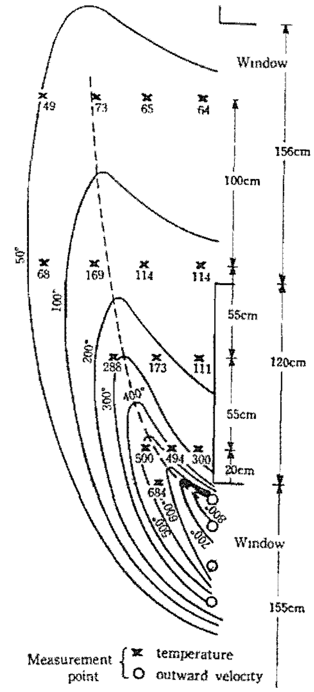

Numbers written under × mean mean-temperature during maximum intensity.

Figure 6.9

Isothermal lines near the window from which fire-flame is flowing out. (Test No. 2)

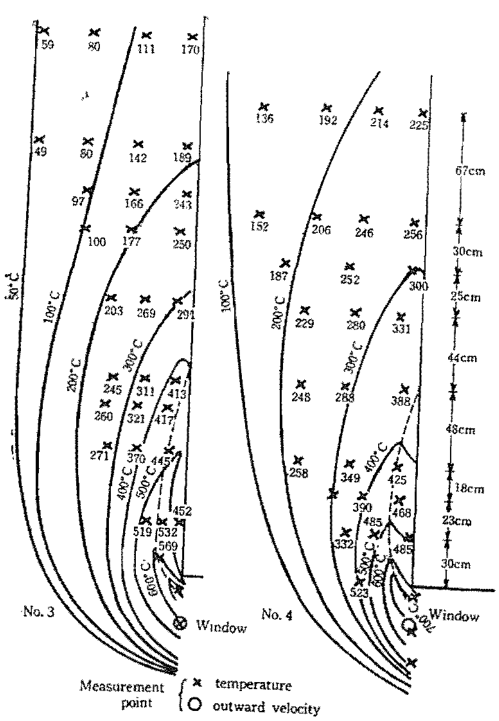

Numbers written under × mean mean-temperature during maximum intensity.

Figure 6.10

Isothermal line near the window from which fire-flame is flowing out. (Tests No. 3 and No. 4)

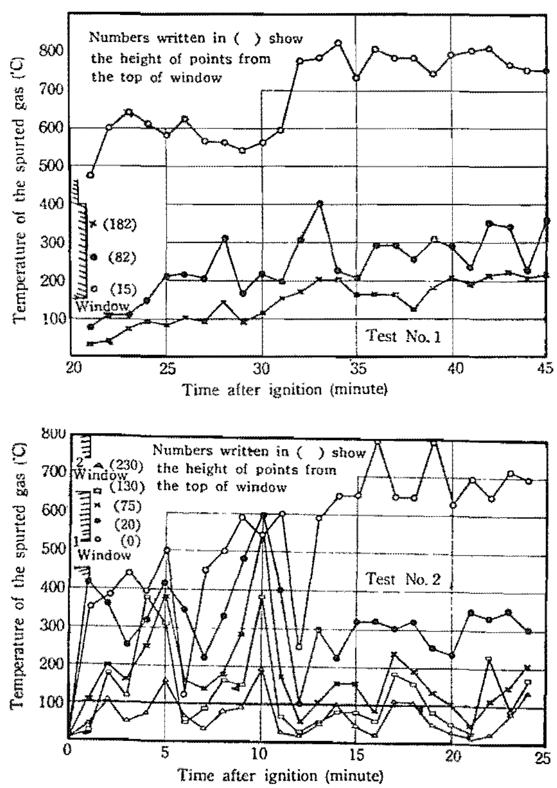

Figure 6.11 Time-temperature curve at the points near the wall above window. (Tests No. 1 and No. 2)

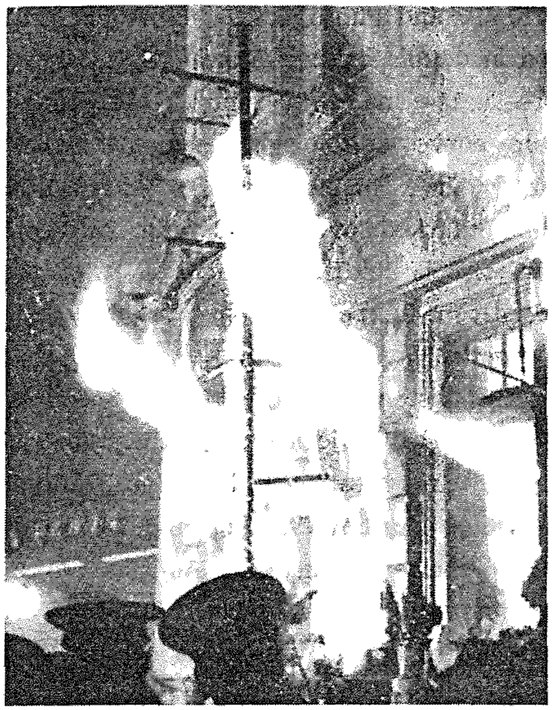

Photo 6.3

Flame ejecting from a window whose horizontal length is longer than the vertical one (Test No. 4)

Photo 6.2

Flame ejecting from a window whose horizontal length is shorter than the vertical one. (Test No. 1)

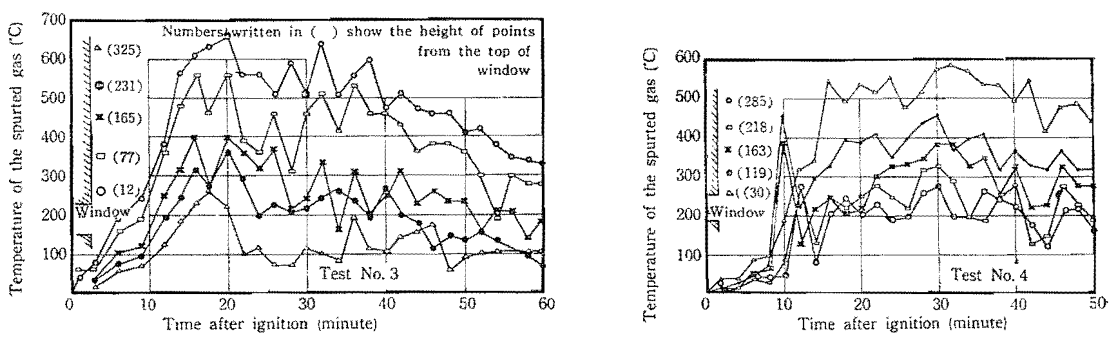

Figure 6.12 Time-temperature curve at the points near the wall above window. (Tests No. 3 and No. 4)

rise because the fuel in the room was burning furiously at this time. The average temperature during the most active combustion (from 22 to 40 min. after ignition) was 750°C, and the excess temperature $\Delta\theta$ was 736°C.

6.4.2 Temperature of ejected flame from opening

The average temperature of the ejecting flame at the various points during the most active combustion in each test is indicated by the isothermal line in Figure 6.8, 6.9 and 6.10.

It is noticed that there is apparent difference between the figures of the flames ejected from two different rectangular openings; one is that its horizontal length is longer than the vertical one and the other has the contrary shape to the former. In other words, the hot gas current ejecting from the former opening rises more closely to the wall than the latter as shown in Figure 6.10 and Photo. 6.3, but the hot gas current from the latter opening rises more ahead of the wall as shown in

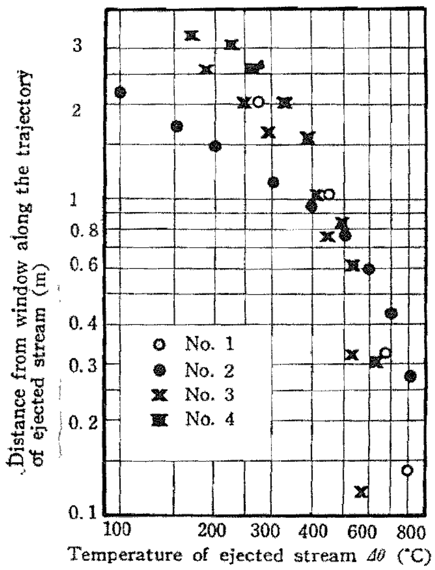

Figure 6.13

Temperature-decrease along the trajectory of the hot gas, ejected from the window of a burning room.

Figure 6.8, 6.9 and Photo. 6.2. This fact will be studied in details in the following Chapter.

Figure 6.11 and 6.12 show the time-temperature curves at the points near the wall above the opening. At the points where the temperature marked over 500°C, the rate of temperature-rise is almost the same as that of the standard time-temperature curve of the third class for wooden house.

Then, the distance of the point from the opening along the trajectory of the ejected flame and its temperature are indicated by the both-logarithmic coordinates. Figure 6.13 shows the result of the experiment. As this figure shows, temperature decrease with increase of distance from the opening is not so conspicuous to some extent, but it decreases remarkably afterwards. This tendency can also be found in the behaviour of the upward current from the heat source of the finite dimension described in Chapter 3 and 4. The relation between these two will be discussed in Chapter 8.

6.4.3 Out flow velocity of flame at the opening

The time-velocity curves of the flame at several points of the opening are shown in Figures 6.14 and 6.15. These curves are similar to those of the time-temperature curve of the flame.

The average out-flow velocity at several points of the opening during the most active combustion is given in Figure 6.16. From this figure, height of the neutral zone at the opening can be calculated. In the test No. 1, it is 126 cm and 80 cm under the upper edge of the opening in the test No. 2.

When room temperature is given, height of the neutral zone can be calculated (Table 7.1 in the following chapter). Compared them with the results of calculation, height of the neutral zone obtained from the test is too low in the test No. 1 and too high in No. 2. This may be due to the fact that the theoretical height of the neutral zone is calculated without regard to wind but in the tests No. 1 and No. 2 the air flew all the time from one opening to the other on account of the outdoor wind, which affected height of the neutral zone in these cases. As the flow-velocity was measured at only one point in the tests No. 3 and No. 4, it is not certain that height of the neutral zone obtained from the calculation is correct. But in these cases there were no other openings, and therefore height of the neutral zone obtained from the experiment would be the same as the theoretical one.

6.4.4 Behaviour of ejected flame

During the most active combustion the temperature of the flame ejected from the opening on the first floor marked below 130°C at the opening on the second floor in

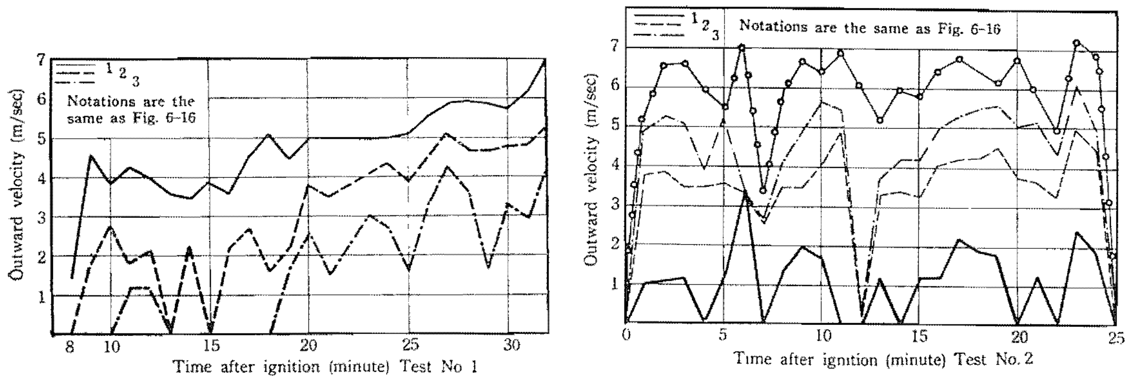

Figure 6.14 Time-outflow velocity curves of the gas at the window.

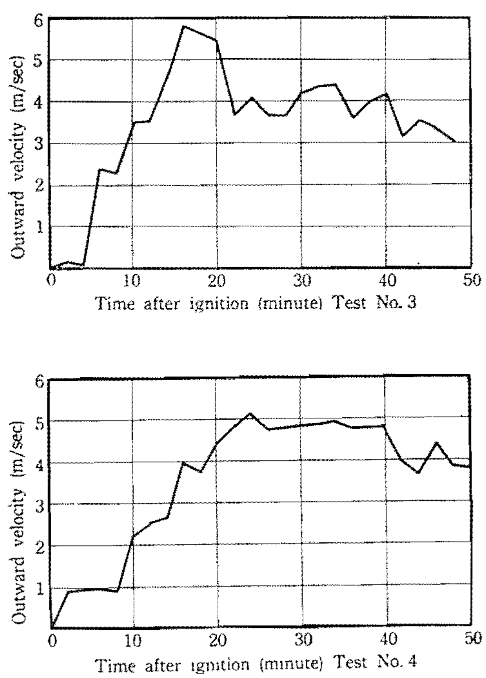

Figure 6.15

Time-outflow velocity curves of the gas at the window.

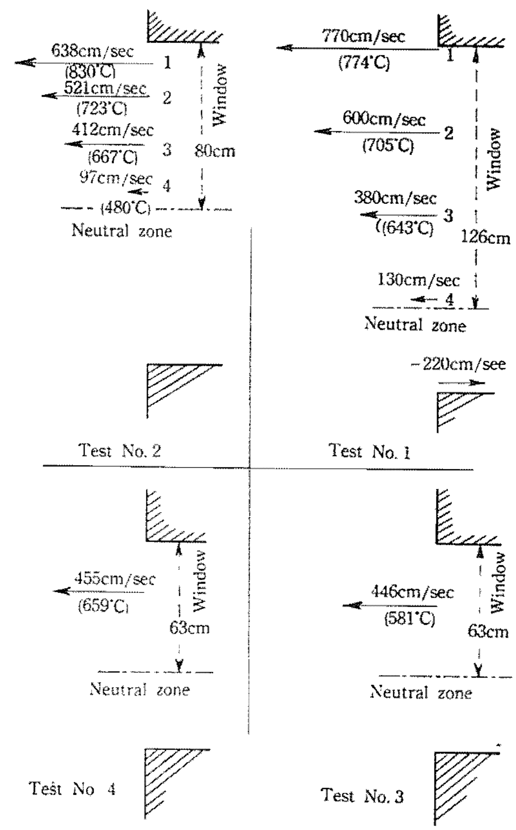

Figure 6.16

Mean outflow velocity of the flame at the window during the period of maximum intensity.

the tests No. 1 and No. 2. No cracks were observed in the window-panes upstairs. Though wired-glass and plane glass, placed on the wall 50 cm above the upper edge of the opening on the first floor, were exposed to the hot gas, the temperature of which was about 500°C, for about 10 min. in the test No. 3, no cracks were observed on the former (wired-glass), but on the latter cracks were observed. Plane glass placed 150 cm above the upper edge of the opening on the first floor was involved in the hot gas of about 350°C for 14 min. to be cracked, but was not broken down. In the test No. 4, plane glass placed 175 cm above the upper edge of the opening on the first floor was completely broken at the flash-over point. At this time temperature of the ejected flame marked 400°C~600°C at the second-storey and the rate of temperature-rise exceeded that of the second class standard time-temperature curve for wooden house.

6.5 Conclusion

Full-scale fire-tests were made by using concrete houses with two different rectangular openings; in the first case the width of the opening is longer than its legnth and in the other case the length of the opening is longer than its width. The following results were obtained:

1) The main stream of the flame ejecting from the former opening (the width of which is longer than its length) may rise more closely to the external wall than the latter case (the length is longer than the width).

2) Consequently, in the case where the width of the opening is longer than the length), the wall above the openig may be exposed to the hot gas current over longer range than in the latter case, even if the opening area and temperature of the ejected gas at the opening are equal.

3) The temperature distribution along the central axis of the hot gas ejected from an openig is similar to that of the upward current from the heat source having a finite dimension.

4) Plane-glass window-panes of 3 mm in thickness, fitted to the sash may be cracked when they are exposed to the hot gas current at 400°C ejected from the opening on the first floor, and when it is 500°C they may be broken down, which makes the fire spread easily to upstairs, while the wired-glass window-panes may not be cracked by the hot gas current even at 600°C.

Chapter 7

Trajectory of Hot Gas Ejected from a Window of a Burning Concrete Building

7.1 Introduction

When a fire breaks out in one of the rooms in a concrete building, the horizontal component of the velocity of the hot air current ejected from a window of the room decreases gradually because of its turbulent stress, and at the same time, direction of the current varies gradually upward on account of voyancy produced by higher temperature of the gas than surrounding air. This is the similar phenomenon as motion of a projectile in gravity field though vertical direction is quite contrary each other in these two cases. As already mentioned in Chapter 6, the position of the central axis of hot gas varies according to the shape of window from which it is ejected. The range of diffusion of the ejected current varies according to whether it rises closely to the wall or apart from it. Consequently, it results in difference of temperature of the current in these two cases, even if the discharged heat quantity per unit time is equal. In other words, if ejected current rises closely to the wall, its range of diffusion would not be so wide as in the other case. Accordingly, temperature of the ejected current would be lower than in the other case. Then the trajectory of the hot gas discharged from a window becomes an important factor to consider fire-spread hazard to upstairs by means of ejected hot gas from window. In this chapter, relation between the trajectory of hot gas and shape of windows from which it is ejected is discussed.

7.2 Outflow velocity of flame at windows

During the period of maximum intensity of fire, temperature of the air at any points of the room is almost equal, as reported by Kunio Kawagoe.[18] It is, therefore assumed, that temperature is constant eveywhere in the room. Temperature-rise in the room (temperature difference between the room and outdoor air) is expressed as $\Delta\theta$. Then, neutral zone, where difference of indoor pressure and outdoor one is zero is observed at certain point of the window; below the neutral zone the outdoor air flows into the room and above it indoor air flows out of the room. Outflow velocity at h'' above the neutral zone can be expressed as follows[19];

$$v_0=\sqrt{\frac{2gh''(\rho_0-\rho)}{\rho}}, \qquad \cdots\cdots(7.1)$$

where ρ_0 and ρ represent density of outdoor air and indoor gas respectively. ρ is nearly equal to the density of air at the same temperature if the gas is produced by combustion of wood or alcohol (see Section 1.4. Chapter 1). g is the acceleration due to gravity. If expansion coefficient of gas is represented as α,

$$\rho_0=\rho(1+\alpha\Delta\theta), \qquad \cdots\cdots(7.2)$$

then, Equation (7.1) reduces to

$$v_0=\sqrt{2gh''\alpha\Delta\theta} \doteqdot 2.678\sqrt{h''\Delta\theta}. \qquad \cdots\cdots(7.3)$$

If the change of value of h'' by change of room temperature $\Delta\theta$ is ignored, it can be said that outflow velocity at the window is proportional to the square root of room-temperature. It will be seen if the Equation (7.3) holds in full-scale fire tests performed four times (see Chapter 6). If the value of v_0 at the window is calculated basing on the observed values of temperature in the room during the period of the maximum intensity, and is compared with the observed value of v_0 in each experiment, the following results can be obtained.

No. of test		No. 1	No. 2	No. 3	No. 4
Temperature-rise in a room $\Delta\theta$ (°C)		851	810	715	735.7
Height of observed point from neutral zone h'' (cm)		124	70	35	40
Outward velocity v_0 (cm/sec)	Calculated	870	637	432	461
	Observed	770	638	446	455

As the calculated values agree with the observed ones considerably well in each experiment, Equation (7.3) may be applied to many cases.

It must be noted that the Equation (7.3) holds only near the upper edge of the window, because the temperature of outflow gas does not coincide with that of the room; temperature of the former is generally lower than that of the latter owing to its slow outflow velocity, especially near the neutral zone. If the density, temperature and outflow velocity at any point of the window are expressed in (ρ', θ', v_0') respectively and those at point near the upper edge of the window are represented as (ρ, θ, v_0) respectively, equations of momentum conservation and gas law are;

$$\rho' v'^2_0 = \rho v_0^2,$$

$$\rho'(273+\theta') = \rho(273+\theta).$$

From the above, it follows that:

$$v'_0 = \sqrt{\frac{\rho}{\rho'}}\, v_0 = \sqrt{\frac{273+\theta'}{273+\theta}}\, v_0 .$$

Substituting the Equation (7.3) into the above, the following equation may be obtained.

$$v'_0 = 2.673\sqrt{h''\Delta\theta}\sqrt{\frac{273+\theta'}{273+\theta}} \; . \qquad \cdots\cdots (7.3_1)$$

Figure 7.1 shows the relation of the observed velocity and temperature of outflow gas at four points at the window in the test No. 2, reported in Chapter 6. Four kinds of point-groups are plotted basing on the results of the experiment, and the four curves in this figure are obtained from the Equation (7.3$_1$), by giving the values of h'', 70 cm, 54 cm, 31 cm and 8 cm, $\Delta\theta$=810°C, θ=830°C and θ'=830°C, 723°C 667°C and 480°C (values of θ' are derived by thermo-couple observation). h'' is the distance from the neutral zone to the obsererved point.

The value of h'' in the Equations (7.3) and (7.3$_1$) cannot be obtained unless the position of neutral zone at the window is given. Mr. Kunio Kawagoe found the equation for the position of the neutral zone.[19] It is;

$$\frac{H''}{H'} = \left\{\left(\frac{\rho}{\rho_0}\right)^{1/2} \frac{G}{L}\right\}^{2/3}, \qquad \cdots\cdots (7.4)$$

where H'' and H' are the distance from the neutral zone to the upper and lower edges of the window respectively. G represents the volume of exhausted gas

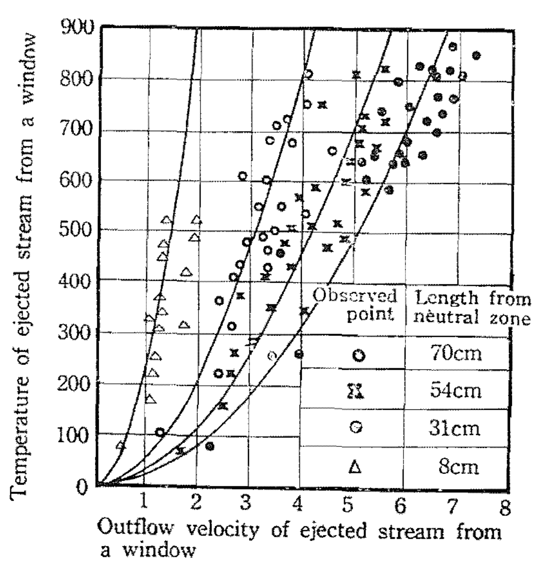

Figure 7.1

Relation of temperature and velocity of outflowing gas at window of a burning room.

Table 7.1 Locations of the neutral zone at various room temperature.

Fuel……Wood, Excess air factor……1.0 Rate of perfect combustion……0.6 Outdoor temperature……17°C.

θ……Room temperature. H''……Length from neutral zone to the upper edge of the window.

H……Vertical length of window

θ°C	1,200	1,000	800	600	400	200	100	50
H''/H	0.67	0.66	0.64	0.63	0.61	0.58	0.56	0.55

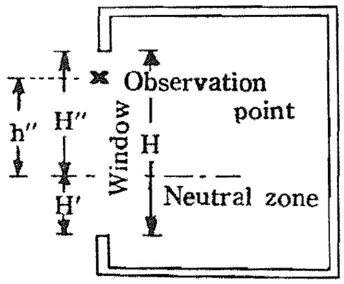

Figure 7.2
Vertical section of a model of windows used in experiments.

produced in combustion of wood of 1 kg, L shows the volume of air necessary for combustion of wood of 1 kg. ρ and ρ_0 represent density of indoor gas and outdoor air respectively, having the following relation;

$$\rho_0 \doteqdot \rho(1+\alpha\Delta\theta),$$

where α is the expansion-coefficient of gas. If the value of G at 0°C is expressed as G_0, then

$$G \doteqdot G_0(1+\alpha\Delta\theta),$$

and Equation (7.4) reduces to

$$\frac{H''}{H'} = \left(\frac{G_0}{L}\right)^{2/3}(1+\alpha\Delta\theta)^{1/3} \quad \cdots\cdots\cdots\cdots\cdots\cdots(7.4_1)$$

As in a fire in a concrete building, values of excess air factor n and rate of perfect combustion x are,[19]

$$n \doteqdot 1.0 \qquad x \doteqdot 0.6,$$

And also values of G_0 and L become:

$$n = 3.975\ \mathrm{m^3/kg}, \qquad G_0 = 4.859\ \mathrm{m^3/kg}.$$

Substituting those into Equation (7.4_1), the following equation is obtained,

$$\frac{H''}{H'} = 1.143\ (1+\alpha\Delta\theta)^{1/3} = 0.1762\ (273.2+\Delta\theta)^{1/3} \quad \cdots\cdots(7.4_2)$$

If alcohol is used for fuel instead of wood, values L and G_0 become $5.226\ \mathrm{m^3/kg}$ and $6.218\ \mathrm{m^3/kg}$ respectively, provided that its water content is zero, $x=1.0$ and $n=1.0$. Then:

$$\frac{H''}{H'} = 1.123\ (1+\alpha\Delta\theta)^{1/3} = 0.1731\ (273.2+\Delta\theta)^{1/3} \quad \cdots\cdots(7.4_3)$$

The above equation is nearly equal to the Equation (7.4_2), when wood is used for fuel. Accordingly, the Equation (7.4_2) is used hereafter even when alcohol is used for fuel in laboratory experiments. Table 7.1 shows the positions of neutral zone at various room temperature, and in this case outdoor air temperature is assumed to be 17°C. In this table H is used instead of H', where H shows the vertical length of the window (see Figure 7. 2)

$$H=H'+H''.$$

If room temperature θ is given, position of the neutral zone are found from Table 7. 1, and outflow velocity v_0 at the window is also obtained from the Equation (7. 3) or (7. 3$_1$).

7.3 Trajectory of Ejected Gas

Distribution of outflow velocity of the ejected gas at the opening shows that the velocity marks the maximum near the upper edge of the opening, and it decreases parabollically downwards. This is like the semi-velocity distribution of the stream at some distance from the mouth of a line-jet. Then, a line source of a jet is assumed at x_0 inside the window. Origin of coordinates is taken at the point where outflow velocity marks the maximum at the opening plane (this is almost the same level of the upper edge of opening), and x and z axes are taken to outward and vertical directions respectively. As already reported in Chapter 2, the velocity along axis of jet issued from a line source decreases inversely proportional to the square root of the distance from the mouth, and the horizontal velocity at the point x forward from the opening is,

$$\frac{dx}{dt}=v_0\sqrt{\frac{x_0}{x+x_0}}, \qquad \cdots\cdots(7.5)$$

where v_0 is velocity at opening ($x=x_0$). Intergrating the above equation under the intial condition of $t=0$: $x=0$

$$t=\frac{1}{v_0\sqrt{x_0}}\int_0^x\sqrt{x+x_0}\,dx=\frac{2\{(x+x_0)^{3/2}-x_0^{3/2}\}}{3\,v_0\sqrt{x_0}}. \qquad \cdots\cdots(7.6)$$

Vertical acceleration of the gas due to voyancy is,

$$\frac{d^2z}{dt^2}=\frac{\Delta\theta g}{\theta_0}. \qquad \cdots\cdots(7.7)$$

where $\Delta\theta$ is excess temperature of gas, and θ_0 represents absolute temperature of surrounding air. Integrating it under the intial conditions of $t=0$; $dz/dt=0$ and $z=0$,

$$z=\frac{\Delta\theta g}{2\theta_0}t^2. \qquad \cdots\cdots(7.8)$$

Eliminating t from Equations (7. 7) and (7. 8),

$$z=\frac{2\Delta\theta g\{(x+x_0)^{3/2}-x_0^{3/2}\}^2}{9\,v_0^2\theta_0 x_0}. \qquad \cdots\cdots(7.9)$$

Substituting Equation (7. 3) into the above,

$$z=\frac{\{(x+x_0)^{3/2}-x_0^{3/2}\}^2}{9\,\theta_0 x_0 h''\alpha}. \qquad \cdots\cdots(7.10)$$

In this eqation, there is no factor giving temperature of gas except that h'' varies a little with it. So it can be said that the trajectory of gas ejected from the opening is almost independent of its temperature. If it is assumed that outdoor temperature is 17°C or $\theta_0=290$°K, and value of $\alpha=1/273.2$ is substituted into the Equation (7. 10), the following equation is obtained,

$$z=\frac{0.1047\{(x+x_0)^{3/2}-x_0^{3/2}\}^2}{x_0 h''} \quad \cdots\cdots\cdots(7.10_1)$$

Here, h'', distance from the neutral zone to the point where outflow velocity marks the maximum at the opening is nearly equal to H'', distance from the neutral zone to the upper edge of the opening. Therefore H'' may be used instead of h'' in the above equation, and it is represented in non-dimensional form:

$$\frac{z}{H''}=\frac{0.1047\left\{\left(\frac{x}{H''}+\frac{x_0}{H''}\right)^{3/2}-\left(\frac{x_0}{H''}\right)^{3/2}\right\}^2}{\frac{x_0}{H''}} \quad \cdots\cdots\cdots(7.11)$$

Value of H''/H (H is the vertical length of the window), as seen in Table 7.1, varies little with the room temperature so far as room fire is concerned, H'' can be considered as a representative term which represent the vertical length of the opening. The trajectory of the ejected gas depends chiefly on the vertical length of the opening. In the Equation (7.11), x_0 is unknown parameter and if it varies in proportional to H'' or H, that is, if x_0/H'' is independent of size of opening, trajectory will be similar in regard to the vertical length of the opening. But this must be proved in experiments.

7.4 Results of Model Experiment

According to the Equation (7.11), trajectory of gas ejected from opening of a burning building is determined according to the vertical length of opening. The trajectory of hot gas ejected from openings having the same vertical length will be the same even if width of openings are different. It is supposed that value of non-dimensional factor x/H'' in the Equation (7.11) is constant and independent of the size of openings, the Equation (7.11) can be applied to almost all sizes of openings. These two points will be proved in model experiments.

Rectangular parallelopiped model room made of steel-plate, having an opening on one vertical plane was used. This model room is 40×40 cm in square ground plane area, and 20 cm in height. Dimensions of openings were various as follows:

Width (cm)	7, 10.5, 14, 17.5, 21, 24	32	9.2
Vertical length (cm)	14	10	20

Alcohol was used for fuel in this model room and temperature of gas ejected from openings was measured with thermo-couples arranged in front of the opening (See, Figure 7.3). The curve produced by connecting the points of maximum temperature in various levels, is regarded as the trajectory of gas. The results of experiments showed that the trajectory was not similar in the following two cases even if the same model room having the same opening was used. The case where the space above the opening is free and the case where the vertical wall is above it. The Equation (7.11) is induced supposing that the space above the opening is free, accordingly, experiments regarding the former case must be made in order to check the Equation (7.11). On the other hand there are many such cases as the latter in practise and the latter case also must be considered. Experiments of the former

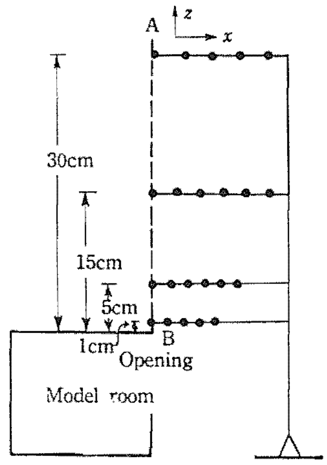

● shows thermo-couples.

Figure 7.3

Positions of thermo-couples.

case are performed at first, and then those of the latter case. Thus, relation between those two cases are studied, and effect of wall on trajectory is considered.

7.4.1 In the case where the space above the opening is free

Origin of the coordinates is taken at the middle of the upper edge of the opening, x and z axes, to outward horizontal and upward vertical directions, respectively.

The result of experiments is shown in Table 7.2. In this table, it is shown that the values of x, the positions at the maximum temperature at every level, may not vary width of the opening if its vertical length is constant; that is to say, the trajectory of the hot gas ejected from openings can be determined according to the vertical length of openings. If positions (horizontal forward length from the openings, x) where the temperature marks the maximum at levels $z=1$ cm, 5 cm, 15 cm and 40 cm, are compared, the two cases where openings are 14 cm and 10 cm, in vertical length may show such results as given in Table 7.3.

As the room temperature marked 730°C in both cases, the distance between the

Table 7 2 Positions where temperature is the maximum at various heights from the upper edge of the window. (in the case where the space above openning is free.)

The breadth and vertical length of the window.	7×14 cm		10.5×14 cm		14×14 cm		17.5×14 cm		21×14 cm		24×14 cm		32×10 cm	
Horizontal distance from the opening (x) and temperature ($\Delta\theta$)	x (cm)	$\Delta\theta$ (°C)	x (cm)	$\Delta\theta$ (C)	x (cm)	$\Delta\theta$ (°C)	x (cm)	$\Delta\theta$ (°C)	x (cm)	$\Delta\theta$ (°C)	x (cm)	$\Delta\theta$ (°C)	x (cm)	$\Delta\theta$ (°C)
The distance from the upper edge of the opening (z): 1cm	1	400	1	410	1	403	1	402	1	405	1	411	1.5	395
	2	580	2	585	2	575	2	574	2	591	2	588	2	387
	3	**600**	3	**590**	3	**600**	3	**596**	3	**595**	3	**598**	2.5	**596**
	4	480	4	478	4	511	4	499	4	457	4	476	3	481
	5	310	5	300	5	295	5	332	5	291	5	294	3.5	321
5cm	4	400	4	440	4	375	4	240	4	325	4	364	3	325
	5	550	5	535	5	400	5	330	5	375	5	395	4	501
	6	**720**	6	**540**	6	**410**	6	**410**	6	**441**	6	**460**	5	**560**
	7	415	7	465	7	352	7	370	7	436	7	454	6	556
	8	400	8	335	8	309	8	230	8	223	8	315	7	326
15cm	6	217	6	345	6	183	6	145	6	185	6	174	4	195
	7	304	7	353	7	201	7	166	7	222	7	204	5	250
	8	**375**	8	**428**	8	**202**	8	**190**	8	**279**	8	**227**	6	**265**
	9	364	9	332	9	197	9	175	9	265	9	220	7	262
	10	331	10	275	10	167	10	160	10	245	10	201	8	253
20cm	6	105	6	140	6	93	6	77	6	101	6	90	6	100
	8	121	8	164	8	106	8	101	8	127	8	104	7	121
	10	**133**	10	**179**	10	**120**	10	**106**	10	**135**	10	**111**	8	**126**
	12	125	12	172	12	100	12	104	12	129	12	103	9	119
	14	92	14	110	14	80	14	94	14	115	14	98	10	104

Notice : The Gothic letters indicate the maximum temperature.

neutral zone and the upper edge of the opening is calculated to be 8.96 cm and 6.4 cm respectively in the cases where the openings are 14 cm and 10 cm in vertical length. Substituting values of z/H'' and x/H'' shown in Table 7.3 into the Equations (7.11), obtaining the mean value of x_0/H'' it was found with probable error of 2 % that

$$x_0/H''=0.0558. \qquad (7.12)$$

The same experiment was made with model room openings of which are 20 cm in vertical length and 9.2 cm in horizontal breadth. In this case the value of x_0/H''

Table 7.3 Comparison of positions at the maximum temperature in two cases where openings are 14cm and 10cm in length.

	Vertical length of openings					
	14cm			10cm		
z cm	x cm	z/H''	x/H''	x cm	z/H''	x/H''
1	3	0.112	0.34	2.5	0.156	0.39
5	6	0.56	0.67	5	0.78	0.78
15	8	1.67	0.89	6	2.34	0.94
30	10	3.35	1.12	8	4.69	1.25
	$H''=8.96$cm			$H''=6.40$cm		

Table 7.4 Positions where the temperature is maximum at various heights from the upper edge of the widow. (in the case where the wall exists above the opening.)

The breadth and vertical length of the window.	7×14 cm		10.5×14 cm		14×14 cm		17.5×14 cm		21×14 cm		24×14 cm		32×10 cm	
Horizontal distance from the opening (z) and temperure ($\Delta\theta$).	x (cm)	$\Delta\theta$ (°C)	x (cm)	$\Delta\theta$ (C)	x (cm)	$\Delta\theta$ (C)	x (cm)	$\Delta\theta$ (°C)	x (cm)	$\Delta\theta$ (°C)	x (cm)	$\Delta\theta$ (°C)	x (cm)	$\Delta\theta$ (°C)
The Distance from the upper edge of the opening. (z) 1cm	2.0	340	2.0	364	1.5	400	1.0	431	0.5	451	0.5	376	0	504
	2.5	500	2.5	504	2.0	584	1.5	604	1.0	546	1.0	544	0.5	574
	3.0	**604**	3.0	**606**	2.5	**615**	2.0	**624**	1.5	**631**	1.5	**641**	1.0	**600**
	3.5	584	3.5	580	3.0	600	2.5	581	2.0	630	2.0	600	1.5	517
	4.0	400	4.0	404	3.5	411	3.0	416	2.5	423	2.5	471	2.0	415
5cm	3	220	3	123	3	250	2	255	2	275	2	271	0	491
	4	358	4	365	4	367	3	440	3	403	3	404	1	504
	5	**424**	5	**428**	5	**446**	4	**464**	4	**480**	4	**500**	1.5	**560**
	6	401	6	404	6	363	5	355	5	384	5	472	2	403
	7	240	7	258	7	276	6	265	6	305	6	316	2.5	256
15cm	5	146	5	104	4	151	3	181	2	223	2	216	0	**480**
	6	201	6	202	5	206	4	226	3	260	3	258	1	472
	7	**224**	7	**230**	6	**240**	5	**260**	4	**281**	4	**317**	2	432
	8	198	8	204	7	211	6	241	5	275	5	300	3	311
	9	154	9	175	8	175	7	195	6	203	6	217	4	252
30cm	7	75	6	72	5	102	3	104	2	140	1	141	0	**415**
	8	92	7	99	6	120	4	121	3	161	2	170	1	400
	9	**110**	8	**112**	7	**125**	5	**143**	4	**165**	3	**183**	2	387
	10	101	9	105	8	116	6	131	5	161	4	166	3	305
	11	88	10	91	9	101	7	115	6	159	5	143	4	272

Notice : The Gothic letters indicates the maximum temperature.

was also 0.0558.

From the results of the above model experiments, it may be said that value of x_0/H'' is invarient with the size of openings. If this value is substituted into the Equation (7.11), the non-dimensional equation of trajectory of hot gas ejected from the rectangular opening is obtained, as follows:

$$z/H''=1.876\left(\frac{x}{H''}+0.0558\right)^3-0.04946\left(\frac{x}{H''}+0.0558\right)^{3/2}+0.000326 \qquad \cdots\cdots(7.13)$$

This equation is independent of size of openings. The curve a in Figure 7.4 is obtained from this equation.

7.4.2 In the case where wall is above opening

Model experiments were performed in the same way as described in the preceding Section 7.4.1, except that the asbestos slates were placed above the opening of the model in these experiments (at the position AB in Figure 7.3). The results of experiments are shown in Table 7.4. The maximum temperature at several levels are shown by the gothic letters in this table. In this case the position where the temperature marks the maximum at each level comes nearer to the wall above the opening compared with the case where the space above the opening is free. The slenderer the shape of openings is in horizontal direction, the nearer it approaches to the wall. Distance H'' between the neutral zone and the upper edge of the opening is calculated, and coordinates (x, z) are changed into the non-dimensional ones $(x/H'', z/H'')$ and the points where the temperatures at several levels mark the maximum are plotted. They are connected and trajectory curves shown in Figure 7.4 are obtained.

Then, the reason why hot gas rises closely to the wall in this case must be considered. Generally, upward current in free convection rises mixing with the ambient air and taking it away, which makes breeze blow horizontally into the current from the surroundings. But if vertical wall exists on one side of the current, supply of air from this side is restricted and more air comes from the other side, so the upward current is inclined towards the wall. This is illustrated in Figure 7.5. In the case where shape of the openings is slender in vertical direction, air from the direction of the wall can be easily supplied by the air coming from sideways, so the hot gas may not be inclined so much to the wall, but in the case where openings are slender in horizontal direction, air supply from sidewards may be little, and the upward current may come near to the wall. It can be expected from above-mentiond phenomena that grade of inclination of the upward current towards the wall does not directly depend on the absolute value of horizontal length of openings but it depends on its relative ratio to the length of the vertical one. It is furthermore supposed that the trajectory of hot gas obtained from the results of model experiments and expressed in non-dimensional coordinates shown in Figure 7.4 can be applied even to a full-scale fire. This will be examined in the following Section.

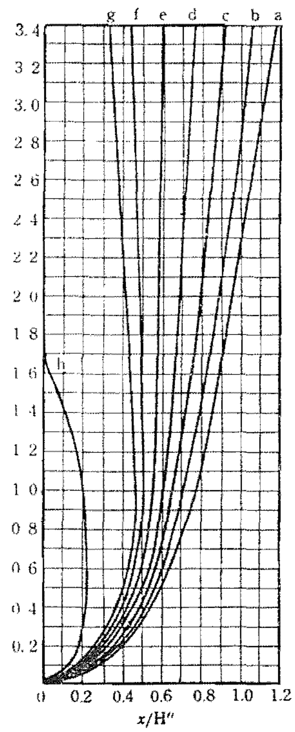

Figure 7.4

Trajectories of hot gas ejected from various rectangular windows.

a…… In the case where there is no wall above the window.

b~h…… In the case where there is the wall above the window and they are classified into as follows according to the value of the ratio (n) of the breadth to one half of the height of window.

b……n =1	f……n =3
c……n =1.5	g……n =3.4
d……n =2	h……n =6.4
e……n =2.5	

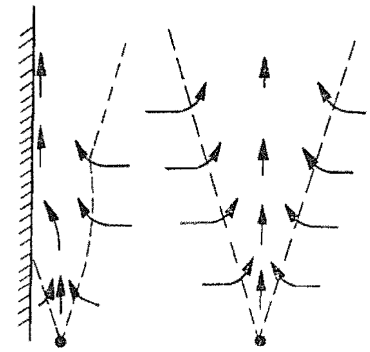

Figure 7.5

Upward currents in free space (on right side) and in the case where vertical wall exists on one side of it (on the left side).

7.5 Comparison with Results of Full-Scale Fire Test

If the curves b, c, ………… h (shown in Figure 7.4) obtained from the results of the model experiments can be determined only by ratio of horizontal length of openings to vertical one, trajectories of the ejected hot gas in a full-scale fire test described in the preceding chapter, (Chapter 6), may agree with the corresponding curves obtained in the model experiments. In this section, this will be examined. A parameter n, which defines the above-mentioned ratio, will be used here. In this case it means ratio of horizontal length of openings to the half of its vertical length.

7.5.1 Fire test No. 1

Size of the opening ………… 91 cm in horizontal length and 167 cm in vertical length.

Room temperature during the maximum intensity of fire ………… about 800°C.

Value of H'' is calculated to be ………… 167 cm×0.64=107 cm (Table 7.1)

In this case there were other openings in the test room and the real value of H'' of this opening was 126 cm. Then, the ejected gas must behave as if it were ejected from the opening of 91 cm in horizontal length and 126 cm÷0.64=196.9 cm in vertical one. The value of n is, then, 91 cm÷(196.9 cm÷2)=0.93. Accordingly, position of the trajectory of hot gas ejected from this opening, must be between the curves a and b in Figure 7.4.

7.5.2 Fire test No. 2

Size of the opening ··········· 82 cm in horizontal length and 155 cm in vertical length.

Room temperature during the maximum intensity of fire ··········· about 800°C.

Value of H'' is calculated to be: $155 \times 0.64 = 99.2$ cm.

In this test, H'' was found to be 80 cm, because there was another opening in the room.

Apparent vertical length of opening becomes:

$$80 \text{ cm} \div 0.64 = 125 \text{ cm},$$

and n is,

$$82 \text{ cm} \div (125 \text{ cm} \div 2) = 1.31.$$

Position of trajectory must be between the curves b and c in Figure 7.4.

7.5.3 Fire tests No. 3 and No. 4

Size of the opening: 300 cm in horizontal length and 100 cm in vertical length. In these cases there were only one opening in the room and the real position of the neutral zone must be the same as the calculated one. The n is $300 \text{ cm} \div (100 \text{ cm} \div 2) = 6.0$. Position of the trajectory must be very near to the curve h in Figure 7.4.

The curves of trajectories in the above-mentioned three cases can be drawn in Figure 7.4, and then, the coordinates are translated from (x/H'', z/H'') system to (x, z) one, as is shown in Table 7.5, and then the curves illustrated by dotted lines in Figure 6.8

Table 7.5 Trajectories of hot gas in full-scale fire tests obtained by calculation.

z/H''	Test No. 1 $H''=126$cm $n=0.93$			Test No. 2 $H''=80$cm $n=1.31$			Test No. 3 and No. 4 $H''=63.5$cm $n=6.0$		
	x/H''	z (cm)	x (cm)	x/H''	z (cm)	x (cm)	x/H''	z (cm)	x (cm)
0.1	0.29	12.6	36.5	0.26	8.0	20.8	0.19	6.4	12.1
0.2	0.39	25.2	49.1	0.37	16.0	29.6	0.20	12.7	12.7
0.3	0.47	37.8	59.2	0.45	24.0	36.0	0.22	19.1	14.0
0.4	0.54	50.4	68.0	0.51	32.0	40.8	0.24	25.4	15.2
0.5	0.59	63.0	74.3	0.56	40.0	44.8	0.24	31.8	15.2
0.6	0.63	75.6	79.4	0.59	48.0	47.2	0.24	38.1	15.2
0.8	0.69	101	86.9	0.65	64.0	52.0	0.24	50.8	15.2
1.0	0.74	126	93.2	0.68	80.0	54.4	0.23	63.5	14.6
1.2	0.78	151	98.3	0.73	96.0	58.4	0.19	76.2	12.1
1.6	0.86	202	108	0.79	128	63.2	0.08	102	5.1
2.0	0.92	252	116	0.85	160	68.0	0.00	127	0.0
2.5	1.00	315	126	0.90	200	72.0	0.00	159	0.0
3.0	1.07	378	135	0.95	240	76.0	0.00	191	0.0
3.4	1.12	428	141	0.98	272	78.4	0.00	216	0.0

(Test No. 1), Figure 6.9 (Test No. 2) and Figure 6.10 (Test No. 3 and No. 4) are obtained. It seems reasonable to regard those three dotted lines to be trajectories of hot gases in these Figures. That is to say, the curves in Figure 7.4 may be applied to any sizes of openings.

7.6 Conclusions

1) The equation of the trajectory of the hot gas from a rectangular opening was obtained analytically in the case where the space above the opening is free, and was checked by model experiments.
2) In this case, the trajectory depends only on the vertical length of openings and is independent of horizontal one.
3) In the case where there is a wall above the opening, the ejected hot gas rises closely to the wall and position of the above-mentioned trajectory must be corrected.
4) The slenderer the shape of the opening becomes in horizontal direction, the more the hot gas rises closely to the wall, and the larger becomes the value of correction.
5) The non-dimensional quantity obtained by dividing the value of correction by H'' is determined only by ratio n of the opening.
6) In this way the curves of trajectories of the hot gas from the rectangular openings of various sizes are obtained.

Chapter 8

Temperature Distribution of Hot Gas Spurting out of the Window of Burning Concrete Building

8.1 Introduction

It has been found from the results of the full-scale fire tests described in Chapter 6 and from the results of examining the trajectory of the spurting current referred to in Chapter 7, that the nature of hot current spurting from the window of the burning room varies according to the shape of the window even if the temperature of the gas at the window and the area of the window are the same. In this Chapter it is intended to examine how the temperature distribution differs according to the length of horizontal width and vertical length of the window, by referring to many model experiments, and to the law of similarity among the different models and to establish the formula to determine the temperature distribution of spurting hot currents when the dimensions of the window and the quantity of heat discharged in unit time are known. The ultimate object is to obtain information for the next Chapter in which the spandrel height (distance) necessary for preventing the fire-spread, will be discussed.

8.2 Method of Experiments

The experiments are roughly divided into two stages. In the first stage were examined the temperature distributions of hot currents spurting from windows different in size but similar in shape, and in the second stage was examined how the temperature

Table 8.1
Dimensions of Windows of Model Rooms Used for Experiments.

	Dimensions of Windows		
	n	Breadth (cm)	Height (cm)
No. 1	0.92	9.2	20
No. 2		6.9	15
No. 3		4.6	10
No. 4	3.2	24	15
No. 4′		16	10
No. 5		12	7.5
No. 6		8	5
No. 7	6.4	32	10
No. 8		24	7.5
No. 9		16	5

distribution changes if the vertical length of the window is constant and the horizontal breadth is changed.

8.2.1 In case of window different in size but similar in shape

The model fire compartment made of steel sheets as in the case of the preceding Chapter and windows were opened on only one of the vertical planes. Three models having windows with horizontal width and vertical length of 9.2×20 cm (frontage and depth 30 cm, height 25cm), 24×15 cm (frontage and depth 40 cm, height 20 cm), and 32×10 cm (frontage and depth 40 cm, height 20 cm), respectively, were used. The size of the window of each model was lessened by means of steel sheets to form two steps of similar figures, and experiments were executed on windows of ten different kinds. The combinations were as shown in Table 8.1. Alcohol was used as the fuel, and the temperature of the spurting hot current was registered on a slow-rotating oscillograph by use of an chromel-alumel or copper-constantan thermocouple. The average temperature for ten minutes was estimated on the record by the eye and it was adopted as the temperature of the spot. The temperature means the difference between the temperature of the hot gas current and that of the air outside.

Above the window placed a vertical screen made of asbestos, supposing there was a spandrel, and the temperature distribution in the space in front of the window and the screen was measured. Thermocouples were placed at 12 points in the vertical direction and the temperatures at those points were measured by changing the relative positions of the respective points in relation to the model room.

8.2.2 In case the ratio between the width and the vertical length is changed

The used model was the same as the one used in the case of the preceding Chapter. As for the size of the window, the vertical length of it was made invariably 14 cm and the horizontal width was changed in six stages of 7 cm, 10.5 cm, 14 cm, 17.5 cm, 21 cm and 24 cm. The temperature of the hot current spurting from the window was taken by connecting the cupper-constantan or chromel-alumel thermocouple to an self-recording oscillograph. As it had been found as a result of the experiment referred to in the preceding Chapter that the wall above the window affects the trajectory of a spurting hot current and it had been expected that it would affect the temperature distribution as well, experiments were conducted with the same model under two different conditions: in case the space above is free and in case there is a wall above.

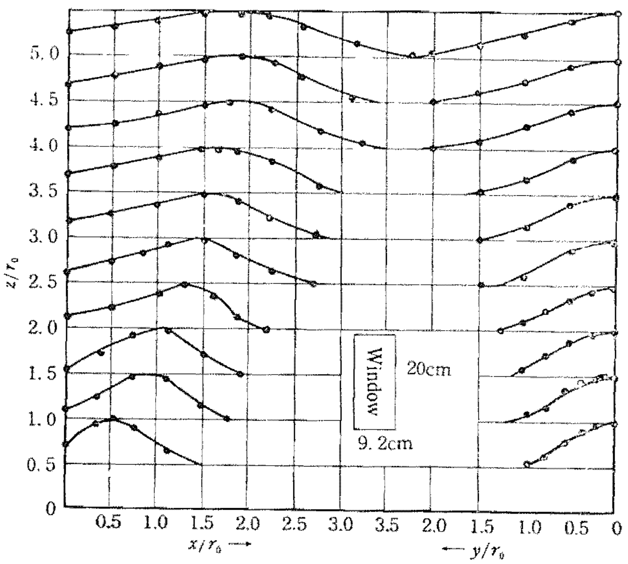

Direction perpendicular to the window face

Direction parallel to the window face

Figure 8.1
Horizontal distributions of temperature of the spurting hot gas in Test No. 1

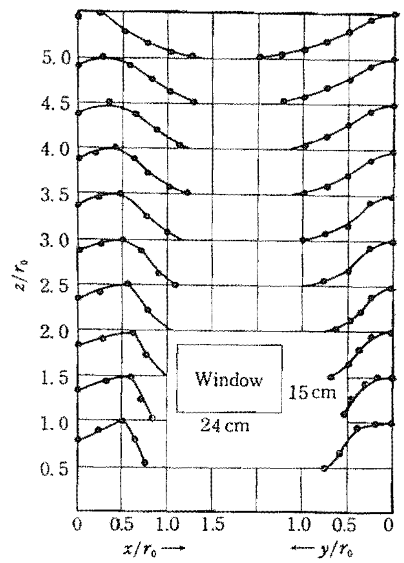

Direction perpendicular to the window face

Direction horizontal and parallel to the window face

Figure 8.2
Horizontal distributions of temperature of the spurting hot gas in Test No. 4

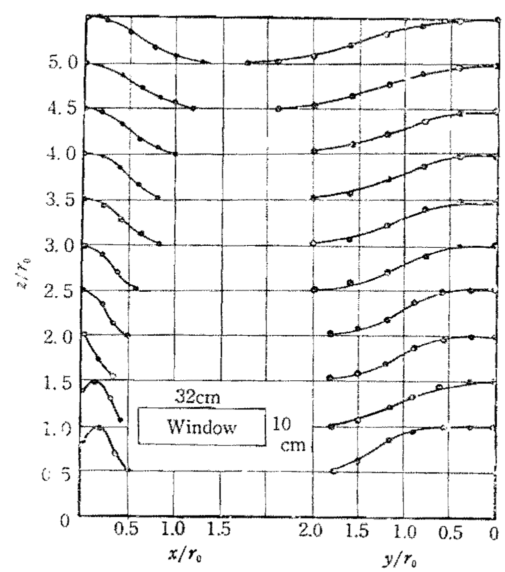

Direction perpendicular to the window face

Direction horizontal and parallel to the window face

Figure 8.3
Horizontal distributions of temprature of the spurting hot gas in Test No. 7

8.3 Results of Experiment

8.3.1 In case the window sizes are changed in similar shape

Figure 8.1, 8.2 and 8.3, show the results ot measurement concerning the horizontal distribution of temperatures of the spurting hot currents in the experiments of No. 1, No. 4 and No. 7 of Table 8.1. The left side of each figure shows the horizontal temperature distributions at the respective heights in the plane which contains the vertical line along the middle of the window and which is perpendicular to the window plane experessed by the relative value in relation to the highest temperature at each height. The length in the figures is expressed by the non-dimensional quantity obtained by dividing the actual length by the equivalent radius of the window (defined

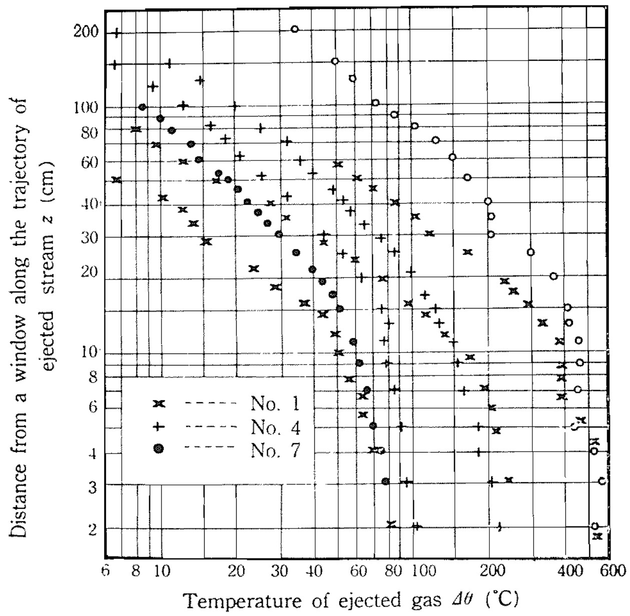

Figure 8.4

Temperature distributions of the hot gas spurting from windows No. 1, No. 4 and No. 7

in Section 8.4). The right side of each figure shows the temperature distributions in the horizontal direction in the plane which contains the points indicating the said highest temperatures on the respective horizontal lines and which is parallel to the window plane. Each curve was obtained by averaging the corresponding values in the left and right sides relative to the middle line of the window. The temperature distributions are expressed in the same manner as in the case of the figure on the left side of those figures.

The results of experiments on the other windows shown in Table 8.1 were also plotted in the same way, and it was found that in No. 2 and No. 3 the results of experiments practically coincide with those of No. 1 when they are plotted, in No. 4′, No. 5 and No. 6 with those of No. 4, and in No. 8 and No. 9 with those of No. 7. Therefore it can be said that the temperature distributions in the horizontal direction of spurting hot currents are fixed in similar shape by the ratio between the width and vertical length of the window alone.

In Figure 8.4 the temperature distributions along the main axis of the hot current spurting from the windows in the experiments of Models No. 1, No. 4 and No. 7 mentioned in Table 8.1 are plotted on the both-logarithmic coordinate system. The experiments were made by use of the same model and by changing the fire temperature in the room. When the temperature is changed, the temperature distribution curves relative to the respective models merely indicate the results of parallel movements of the same curve. In other words, the shapes of the temperature distribution curves vary according to the shape of the window, but their shapes do not change with the temperature of fire.

Another fact seen from Figure 8.4 is that, no matter what the shape of window may be, the lowering of temperature with the distance from the window is not so conspicuous in the figure for some distance after the spurting, but after passing a certain distance the temperature distribution curve makes a turn and the lowering of temperature with the distance becomes conspicuous. This closely resembles the

Figure 8.5
Temperature distributions along the main axes of hot gas, ejected from various shapes of windows

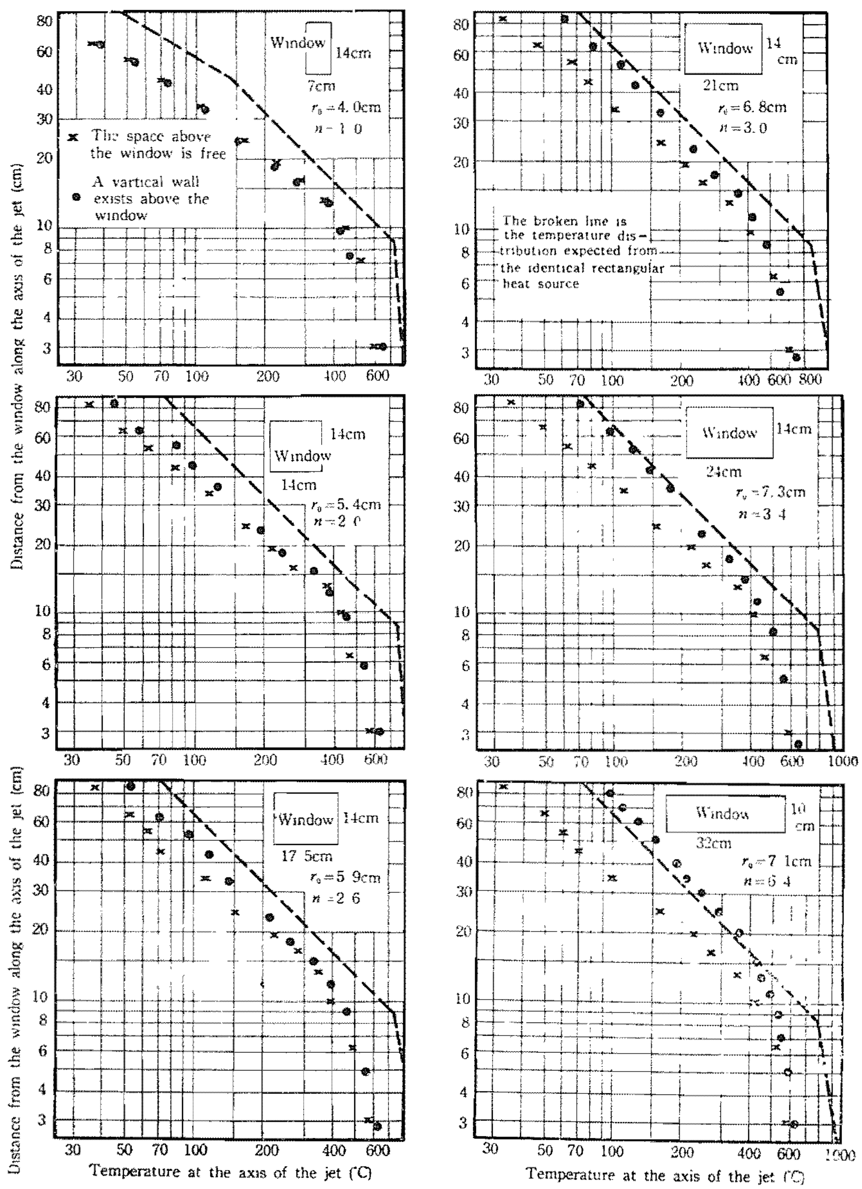

temperature distribution along the central axis of the upward currents from the circular heat source (Chapter 3) and the rectangular heat source (Chapter 4). The relation between this and the other instances stated in the respective Chapters will be examind in Section 8. 4.

8.3.2 In case the ratio between the width and vertical length of the window is changed

In this experiment it was known that the temperature distribution of the spurting hot gas in the horizontal section vary according to the ratio between the width and vertical length of the window, but according to the respective values of ratio, the distributions were similar to those of Figures 8.1 through 8.3. Next, concerning various shapes of windows, the relation between the temperature and distance along the main axis of hot currents spurting from the windows, was plotted on the both-logarithmic coordinate system. They are shown in Figure 8.5.

As was in the case of Section 8.3.1, the temperature distribution along the main axis of hot gas for any window resembles the temperature distribution along the central axis of the upward current from a rectangular heat source. Especially, in the case of the distribution for the window of 7×14 cm, the domain where the temperature distribution shows the one corresponding to the third domain in the upward current, is also seen.

Now let us proceed to the case where the space directly above the window is free (temperature distributions indicated by marks × in Figure 8.5). The temperature distribution in this case differs from that in the case where there is a wall (temperature distributions indicated by marks ● in the same figure). In other words, regardless of the size and shape of window, the temperature of the gas at any point, in the case where there is a wall, is higher than that at the same point in the case where there is no wall. It has been found that the difference in temperature is the greater when the window is the shorter and wider in shape.

8.4 Comparison with the Temperature Distribution of the Upward Current from a Rectangular Heat Source

As it has been found from the experiments referred to in the preceding paragraph that the temperature distributions of hot currents spurting from windows are very similar to those of upward currents from rectangular heat sources, here will be given a further consideration for the relation between the two.

As both are ascending currents in the form of a turbulent flow caused by buoyancy, it is natural that they are similar in the shape of temperature distribution. However, the spurting currents from the window differ from ordinary upward currents in the following points:

1) The window plane corresponding to the heat source in the case of the ordinary upward current, is in a vertical plane and the hot current spurts out of it first horizontally and then gradually turns its direction of flow upwards under the effect of buoyancy.

2) The current spurts out not with uniform velocity from the entire window plane but only from the part constituting the upper 2/3 or so. Reversely, about one-third or so constituting the lower part serves as the entrance through which outer air comes in.

3) As it is usual that there is a wall, and not free space, directly above the window, the spurting current moves in the semi-infinite space.

First, let us examine the results of experiments in the case where there is free space directly above the window with a view to investigating the effects of the wall above the window. Let us call the domain in Figure 8.5 where the decrease in temperature with the distance from the window is not very conspicuous, the domain in the figure where the decrease makes a gradient of about 45°, and the domain where the decrease makes an angle of approximately $\tan^{-1}(3/5)$, the first domain, the second domain and the third domain respectively as in the case of the upward currents from rectangular heat sources. Checking the distance where the temperature distribution of the hot current changes from the first domain to the second domain in Figure 8.5, we find that in the case of windows whose vertical length (height) is 14 cm, it is invariably a point about 9 cm from the window plane along the main flow regardless of the horizontal width, and in the case of windows whose vertical length (height) is 10 cm a point about 6 cm. While the transition point in the case of rectangular heat sources was at the height corresponding to 1.25 times the length of the shorter side (See Section 4.4), the transition point in the case of spurting hot currents may be considered to be at a distance about 1.25 times the half of vertical length (height) of the window, because $(14\ \text{cm} \div 2) \times 1.25 = 8.75$ cm, and $(10\ \text{cm} \div 2) \times 1.25 = 6.25$ cm. Thus we find that half the vertical length (height) of window may be considered to correspond to one side of the rectangular heat source. It is true that the current flows out of the upper 2/3 of the window, but the velocity in the part near the neutral zone is small and there is a vena contracta of the stream at the opening, so the upper half of the window may be considered the actual source of spurting.

Next, by making the horizontal width of window correspond to one side of the rectangular heat source and half the window height to the adjoining side of it, the equivalent radius r_0 and ratio n are defined as below, as in the case of the rectangular heat source.

$$r_0 = \sqrt{\frac{HB}{2\pi}} \doteqdot \frac{\sqrt{HB}}{2.507}, \quad \cdots\cdots (8.1)$$

$$n = \frac{B}{2H}, \quad \cdots\cdots (8.2)$$

where B and H are the window width and window height respectively and π the circular constant. The values of r_0 and n for the windows employed in the experiments are expressed by the figures shown under the respective windows in Figure 8.5. The height where the second domain changes to the third domain was $11.75\, r_0 \sqrt{n}$ (Equation 4.7_1) in the case of the rectangular heat source. By applying this formula to the window whose dimensions are 7×14 cm used this time, we find that the height is $4\ \text{cm} \times 11.75 \times 1 = 47$ cm because $n = 1$ and $r_0 = 4.0$ cm here. Although it is not very clearly shown in Figure 8.5, it is sure that the transition point may be set at the vicinity of this height. From what has been said it can be concluded that in case there is free space directly above the window the temperature distribution of a spurting hot current can be known by making it correspond to the case of a rectangular heat source whose two adjoining sides are the width of the window and half the vertical length (height) of the window respectively.

Equations (8.1) and (8.2) are applicable only when the neutral zone on the window plane is at the normal position. In case the neutral zone is away from the normal position as in fire-tests No. 1 and No. 2 in the full-scale fire experiments described in Chapter 6, it is necessary to substitute the value of the apparent vertical length of the window by making calculation for the respective cases (for example Section 7.5) of the actual vertical length for H in Equations (8.1) and (8.2).

Next, as regards the temperature distribution in the second domain, the gradient of the distribution curve is lower than 45° in Figure 8.5 for windows of any measurements. In this point the distribution is somewhat different from that in the case of the upward current from the rectangular heat source. This shows that a considerable quantity of heat goes away from the main flow after spurting, namely that after spurting, while the current has a horizontal component of velocity, a considerable quantity of heat goes away from the main flow and goes up. This is proved by the fact that in Figure 8.1 the horizontal temperature distribution in the direction vertical to the window face (figure on the left) is not symmetrical relative to the position where the temperatuıe is maximum, but the temperature is higher on the side of the window plane than on the other side, where the corresponding quantity of heat has gone away from the main flow and ascended. Even in the first domain a considerable quantity of heat must have deviated from the main flow. If the quantities of heat, Q, issuing per second from the respective windows were calculated by use Equations (8.4) and (8.5) mentioned in the following section, and, on the assumption that the quantities of heat equivalent to these issue from rectangular heat sources corresponding to the windows, the temperature distributions were sought according to the method explained in Figure 4.9, the temperature distributions from these heat sources become to those shown in broken line in Figure 8.5, indicating that the temperatures distributed are considerably higher than in the case of spurting currents.

Lastly, if there is a wall above the window, the spurting current is drawn to the wall as stated in Section 7.4.2. As a result the diffusion domain of the current is narrower than in the case of free space, and, as heat is confined in the narrower space, the temperature of the current becomes higher, although some part of the heat is conducted to the wall. It may be theoretically concluded that the shorter and wider the window is, the nearer is the current drawn to the wall and so the higher becomes the temperature. The actual results shown in Figure 8.5 prove this conclusion: the shorter and wider the window is, the higher the temperature is. In the case of the shortest and widest window with dimensions 32×10cm, the temperature distribution is even higher than the temperature distribution shown in broken line. If it is assumed that the main axis of the spurting current from a short and wide window is directly in touch with the wall surface, that the diffusion domain of the current is half of the domain in the case of free space, and that no heat is conducted to the wall, theoretically the quantity of heat contained in the current ought to be twice as much as that of the case of free space because the heat which is diffused freely in the free space is in this case diffused only in the semi-infinite space and, for the same reason as in Equations (4.4) and (4.5) in Chapter 4, if Q is twice as large and the temperature $\Delta\theta$ is $\sqrt[3]{2^2}=1.59$ times as large, the temperature ought to be 1.59 times as high as that in the free space. Actually, however, regarding the window with dimensions 32×10 cm shown in the right below in Figure 8.5, the temperature in the case where there is a wall above the window is only a little higher than in the case of the free space. The principal reason is supposed to be the fact that a considerable quantity of the heat contained is lost through conduction to the wall.

8.5 Shape of Window and Temperature Distribution

From Figure 8.5 it can be seen how the temperatures of the currents spurting from windows change according to the shape of window, or, in other words, in what degree the temperatures increase as the height of the window becomes shorter and its width becomes longer. First, in the case of a window whose width is 7 cm and whose height is 14 cm ($n=1$), the temperature distribution is nearly the same as in the case of the free space, because, according to Chapter 7, Section 7.4.2, the trajectory of the spurting current is practically the same as in case there is no wall, although in this case there is a wall above the window. As the shape of the window becomes shoter and wider, the spurting current is drawn nearer to the wall, and so the temperature becomes higher. Therefore, if the area of the window and the heat quantity issued out of it per unit time are definite, the temperature of the current spurting from a higher window is lower. This means that higher windows are safer from the view point of fire-protection and that short and wide windows which are often seen in fire-proof buildings in these days are disadvantageous.

Next, let us discuss the method of finding the general temperature distribution when the dimensions of the window and the heat quantity Q issued per second out of it are known. If there is a wall above the window, the temperature distributions of spurting currents vary according to the kind of the wall material because of the difference in the thermal property of the wall material. Here, however, let us neglect it. And the law of similarity will hold here, as in the case of upward currents from rectangular heat sources referred to in Chapter 4 Section 4.7, and it will be possible to extend the results of model tests to the case of full-scale fires.

As in the case of rectangular heat sources, let us put

$$\Theta = \frac{\Delta\theta\, r_0^{5/3}}{\sqrt[3]{\dfrac{Q^2\theta_0}{c_p^2\rho^2 g}}}, \quad \cdots\cdots\cdots (8.3)$$

as the non-dimensional quantity expressing the temperature $\Delta\theta$ of the spurting gas. In the formula, r_0 is the equivalent radius the window and is defined by Equation (8.1). θ_0 is the absolute atmospheric temperature, c_p and ρ are the specific heat at constant pressure and density of the spurting gas respectively, and g is the acceleration due to gravity. The value of Θ on the window surface is calculated first. Let us express the breadth and height of the window by B and H respectively, the coefficient of vena contracta of the window by a and the spurting velocity by v. Then the heat quantity issued out of the window per unit time, Q, is expressed by the following equation:

$$Q = a\, c_p\, \rho\, \Delta\theta\, B \int_0^{H/2} v\, dh''. \quad \cdots\cdots\cdots (8.4)$$

Although the height of the neutral zone is usually at the height of $1/3H$ from the lower edge of the window the limit of integral was limited to $H/2$ on the basis of conclusion of Section 8.4 that as a matter of fact the upper half of the window constitutes the actual heat source. As the spurting velocity on the window surface can be expressed by

$$v = \sqrt{2gh''\alpha\Delta\theta}, \quad \cdots\cdots\cdots (8.5)$$

from Equation (7.3) of Chapter 7, let us substitute it into Equation (8.4) and integrate it, and by using Equations (8.1) and (8.2), again substitute the values of B and H expressed by r_0 and n into Equation (8.3). Then r_0 is eliminated. If the

Table 8.2 Slenderness n of Window and Non-Dimensional Temperature Θ of Spurting Current on Window Surface

n	1	1.5	2	2.5	3	3.5
Θ	0.498	0.533	0.559	0.580	0.598	0.612
n	4	5	6	8	10	20
Θ	0.627	0.651	0.671	0.704	0.731	0.820

coefficient of vena contracta a, is given by

$$a = 0.7,^{20)} \qquad (8.6)$$

Equation (8.3) becomes

$$\Theta = 0.498 \sqrt[6]{n}. \qquad (8.7)$$

This means that if the value of the temperature of the spurting current on the surface of the window is expressed by the non-dimensional quantity, Θ, the value is determined only by the ratio between the breadth and the height of the window. The results of calculation of the values of non-dimensional temperature Θ corresponding to various values of n are shown in Table 8.2. These values are fatalistic magnitudes which are fixed if only the value of n is given.

If we plot the temperature distributions along the trajectories of spurting currents from various windows obtained from the experiments shown in Figure 8.5 on the both-logarithmic non-dimensional coordinates whose ordinate is graduated in the quotients obtained by dividing the distance from the window surface, z, by the equivalent radius of the window, r_0, and whose abscissa is in the above-mentioned non-dimensional temperatures, Θ, the results are as shown in Figure 8.6 in case the space above the window is free and as shown in Figure 8.7 in case there is a wall above the winbow. In both cases the results obtained are similar to the temperature distribution curves along the center axis of upward currents from rectangular heat sources (see Figure 4.6 of Chapter 4). For instance, if the space above the window is free as is the case of Figure 8.6, the wider and shorter the window is, the lower is the temperature distribution curve in the second domain, similar to the case of rectangular heat sources shown in Figure 4.6. However, the curves of spurting currents are lower in position than those of upward currents even when the value of n is equal, because in the case of spurting currents a considerable amount of heat goes away from the main stream.

In the case there is a wall above the window as shown in Figure 8.7, the temperature distribution shows a different aspect, because the shorter and wider the window is, the smaller the diffusing domain of the hot current is and the higher the absolute value of the temperature is. This and the said fact that the shorter and wider the window is, the lower temperature distribution curve is, cancel each other, and thus after all the temperature distribution curve is located in practically the same position regardless of the shape of window. Therefore, we draw a curve passing the vicinity of the centers of the scattered points in the Figure as shown in Figure 8 8, and we make it the standard curve of temperature distribution of hot

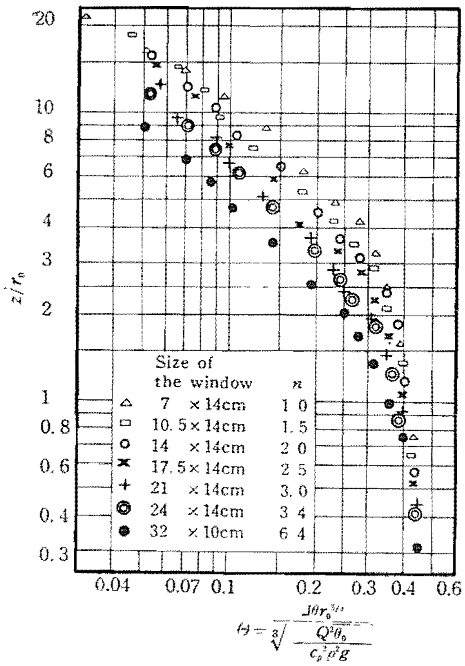

The space above the window is free.

Figure 8.6

Temperature distributions along the axes of hot streams ejected from windows of various shapes (No. 1)

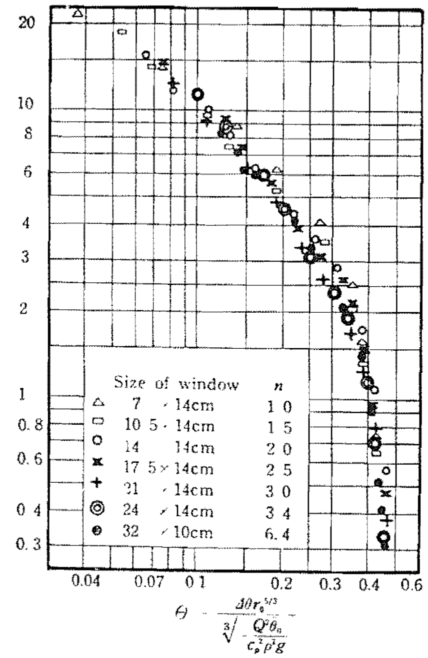

A vartical wall exists above the window

Figure 8.7

Temperature distributions along the axes of hot streams ejected from windows of various shapes (No. 2)

current spurting from the window with a wall above it. This fact in the non-dimensional coordinates the temperature distribution curves can be represented fairly well by a single curve regardless of the measurements of the window is favourable to our study because it greatly simplifies the treatment of matters in our further study.

When the quantity of heat, Q, which is issued out of the window per second and the dimensions of the window are given, the temperature at an arbitrary distance can be found by calculating first the equivalent radius, r_0, of the window from Equation (8.1), finding the necessary value of Θ corresponding to z/r_0 from Figure 8.8 in the following section, and by calculating $\Delta\theta$ from Equation (8.3).

8.6 Comparison with Experimental Full Scale Fire

As the model experiments described in Section 8.3.2 were conducted by making the room fire temperature more than 800°C, there is no great difference between them and actual fires as far as temperature concerns. However, there is a difference between the radiant emissivity of the gas produced by combustion in the case of the model experiments in which alcohol is used as fuel and that in the case of actual fire in which what is burnt is chiefly wood. Also, there is a difference in thermal property between asbestos boards used for the material of the wall above the window in the model experiments and concrete and glass blocks in actual fires, as already stated. For these reasons, it is doubtful whether or not the non-dimensional temperature distribution curves obtained in Figure 8.7 in the preceding section can be applied to actual fires as they are without any correction to actual fires. In order to examine the differences, here the temperature distributions of hot currents spurting from the window observed in the four tests stated in Chapter 6 will be applied to Figure 8.7, and the two will be compared.

First, for calculation of the non-dimensional temperature Θ in Equation (8.3), Q contained in Θ or the value of the quantity of heat issued out of the window per unit time must be known. This can be found easily if the temperature on the window surface and the distribution of current velocities have been observed. As they were observed fairly correctly in Test No. 1 and No. 2, the quantity of issued heat will be calculated directly from the results. Let us divide the window surface into several horizontal zones with the points of temperature observation and current velocity observation at the centers, calculate the quantities of heat issued for the respective zones, and total the results. Concerning the i-th zone, the quantity of heat issued Q_i is:

$$Q_i = aBc_p\rho_i v_i \Delta\theta_i \Delta H_i,$$

where:

a ············ Coefficient of vena contracta at opening

c_p ············ Specific heat at constant pressure of spurting gas

ρ_i ············ Density of spurting gas

$\Delta\theta_i$ ············ Temperature ot spurting current

v_i ············ Issuing speed

B ············ Breadth of window

ΔH_i ············ Thickness of i-th zone, devided.

Therefore, the quantity of heat issued out of the window during the unit time is:

$$Q = aBc_p \sum_i \rho_i v_i \Delta\theta_i \Delta H_i. \quad \cdots\cdots (8.8)$$

Supposing that the coefficient of vena contracta be $a=0.7$ from Equation (8.6), and $c_p=0.24$ cal/g.deg., then above equation reduces to,

		$i=1$	$i=2$	$i=3$	$i=4$
Test No. 1	ρ_i	0.000338g/cm³	0.000362g/cm³	0.000388g/cm³	0.000404g/cm³
	v_i	770cm/sec	600cm/sec	380cm/sec	130cm/sec
	$\Delta\Theta_i$	774°C	705°C	643°C	600°C
	ΔH_i	20cm	40cm	40cm	20cm
	$\rho_i v_i \Delta\theta_i \Delta H_i$	4029	6125	3792	819
	$\Sigma\rho_i v_i \Delta\theta_i \Delta H_i$	14765			
	B	91cm			
	Q	225.7×10³cal/sec			
Test No. 2	ρ_i	0.000320g/cm³	0.000351g/cm³	0.000427g/cm³	0.000465g/cm³
	v_i	638cm/sec	521cm/sec	412cm/sec	97cm/sec
	$\Delta\theta_i$	830°C	723°C	667°C	480°C
	ΔH_i	19cm	20cm	20cm	21cm
	$\rho_i v_i \Delta\theta_i \Delta H_i$	3220	2644	2347	455
	$\Sigma\rho_i v_i \Delta\theta_i \Delta H_i$	8666			
	B	82cm			
	Q	119.4×10³cal/sec			

$$Q=0.168B\sum_{i}\rho_i v_i \Delta\theta_i \Delta H_i. \quad \cdots\cdots\cdots\cdots\cdots\cdots\cdots\cdots\cdots\cdots\cdots (8.8_1)$$

As there were four points of observation for the issuing part of the window surface in Tests No. 1 and No. 2, let us make calculation for them by using the values during the period of maximum intensity of fire.

This method cannot be employed for the results of Tests No. 3 and No. 4, because in the those cases the current velocity measured at only one point on the window face. Accordingly, calculation is made by the indirect method which will be stated in Section 9.4. Leaving the principle of the method to the next Chapter, by utilizing the formula, we obtain

$$Q=25.9\ v\ \Delta\theta.$$

Here, v is the burning rate of wood in the room, and it can also be found by the method stated in Section 9.2. According to the method of Section 9.2, their values during the period of maximum intensity of fire in Tests No. 3 and No. 4 are:

	v	$\Delta\theta$	Q
No. 3	18.9kg/min	715°C	350×10^3cal/sec
No. 4	18.9kg/min	735.7°C	360×10^3cal/sec

Accordingly, the values necessary for calculation of Θ are as follows:

	No. 1	No. 2	No. 3	No. 4
r_0	53.3cm	40.4cm	69.1cm	69.1cm
$r_0^{5/3}$	754.88	475.67	1163.6	1163.6
Q	225.7×10^3cal/sec	119.4×10^3cal/sec	350×10^3cal/sec	360×10^3cal/sec
$Q^{2/3}$	3707.3	2424.4	4966.4	5061.8
$r_0^{5/3}/Q^{2/3}$	0.2036	0.1962	0.2343	0.2299

Therefore, by finding the values of density ρ corresponding to the respective values of temperature $\Delta\theta$, and by use of Equation (8.3), the values of the non-dimensional temperature Θ corresponding to the various values of the temperature, $\Delta\theta$, of the spurting gas can be calculated. Thus, the results of observation of the temperature of spurting hot currents during the maximum intensity of fire in the fire tests made four times were converted into Θ. By employing these figures for the abscissa of the both-logarithmic coordinate system and the non-dimensional quantities obtained by dividing the distances from the window along the trajectory of the spurting current by the equivalent radius of the window for the ordinate, the temperature distribution was plotted, as shown in Figure 8.8. In the Figure, the curve expressed by solid line is the curve which passes the centers of the scattering observation points in Figure 8.7 obtained by model experiments. From this, it can be seen the results of observation in full-scale tests coincide with the results of model experiments. As was already stated, for combining the two, theoretically it is necessary to make adjustment of the radiation capacity of spurting flames and the thermal property of the wall material above the window. However, whether because such factors affect little to the (results of) temperature distribution as a matter of fact or because the two factors

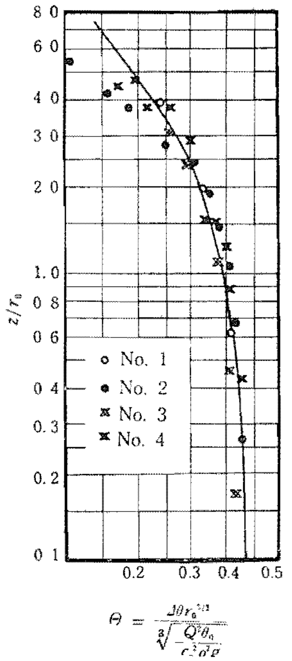

Figure 8.8

Temperature distribution along the trajectory of spurting hot current in the four full scale fire tests (Expressed by non-dimensional coordinates)

accidentally cancelled each other, the results of the model experiments in Figure 8.7 can, at least within the distance of 6 or 7 meters from the window face, be applied to the case of full scale fires.

8.7 Conclusion

A method of finding the temperature distribution of the spurting hot current from the window during the period of maximum intensity of fire of a building of fire-proof construction has been developed on the assumption that the dimensions of the window and the quantity of heat issuing out of the window in unit time are known.

1) The temperature distribution of an spurting hot current is very similar to the temperature distribution along the central axis of the upward current rising from a rectangular heat source whose one side is equal to the width of the window and whose adjoining side is equal to half the vertical length (height) of the window. However, the values of temperature are not equal in the two cases.

2) In case there is free space directly above the window, the temperatures distributed along the trajectory of the spurting current are lower than the temperatures of the upward current from the rectangular heat source.

3) In case there is a wall above the window, the shorter and wider the window is, the higher the temperature of the spurting current is.

4) If the radiative emissivity of flames spurting from the window and the thermal property of the wall material above the window are equal respectively, such law of similarity holds relating to the temperature of the spurting current as is little influenced by the degree of slenderness of the window.

5) However, it has been found that the results of the model experiments this time can be applied without any revision to the case of actual fires, which may be accidental.

6) Therefore, if the dimensions (length and width) of the window and the quantity of heat issuing from the window in unit time are given, the temperature distribution along the trajectory of the hot current spurting from the window can be found on the basis of the results stated in this Chapter.

7) It must be noted that above-mentioned facts have been discussed on the assumption that the fuel burns perfectly in the room, that is to say, it must be confined the case where the ventilation of the room is not low. If the ventilation of the room is restricted, the combustion in the room is not performed perfectly,

and the gas will continue to burn even after it is ejected from the window. In that case, temperature distribution of the gas will not obey the above-mentioned law.

Chapter 9

The Height of Spandrel Necessary to Prevent Fire from Spreading Upstairs

9.1 Introduction

With regard to reinforced concrete buildings, it was usual before the war for their windows to be small and the wall ratio large. However, after the war, very large ones have become popular as new designs; in fact, they are so large that it may be appropriate to call them glass walls rather than windows. These buildings of new design are often criticized from the standpoint of preventing disasters which may be caused by earthquakes etc. and from that of climate in a room such as the room temperature etc. In this paper, they will be criticized from the standpoint of preventing the spread of fire and countermeasures will be considered. If a fire breaks out in any room in a building like this, the windows of the burning room are broken by the flames so that large air-supply openings are made, causing the temperature in the room to rise. In case the height of the fire-proof spandrel between these windows and the windows of the story above is low, the hot flames spurting out trom the openings break the window-glass of the story above with their heat and create the danger of the fire spreading to the upper story. Therefore, the Ministry of Construction has issued a notification that the height of spandrel must be at least 90 cm as a tentative standard. This value should not be made the same for all cases; it should change according to the size of the room and window, quantity of combustible materials in the room, etc.

In this paper, the author considers the method of computing the necessary height of spandrel for preventing the spread of the fire to the upper stories principally when there is no wind for various cases where the conditions of the room vary, based on the results of the researches hitherto conducted by the author's seniors and colleagues and by himself.

9.2 Duration of Fire

The term "duration of fire" as used here means the period from the time the temperature in the fire-proof room begins to rise after the start of fire until the time it begins to drop after the combustibles in the room burn up. According to the results of the frequent fire experiments conducted hitherto, this duration time can be approximated by the value obtained as follows: assume the fire burns at a constant burning rate from the start of fire and divide the quantity of combustibles in the room by the value of the burning rate.[21]

For obtaining the burning rate in a burning room approximately and conveniently, Mr. Kunio Kawagoe's chart[22] may be used. According to his report, the burning rate varies with the size of the opening of the room, rate of excess air, coefficient of vena contracta at the opening, rate of complete combustion, fire temperature in the room, etc. He states, however, that even if the rate of complete combustion changes within the range of 0.4～1.0 or if the fire temperature in the room changes within the range of 500°～900°C, actually the burning rate changes only about 4 %, the burning rate being determined principally by the first three of the factors mentioned above. In his chart are given only the burning rate computed on the following basis: the room temperature 700°C and the rate of complete combustion 1.0. This chart will be used in this paper and, as stated in Mr. Kawagoe's report, since the results of the past experimental full scale fires show that ordinarily the values of excess air factor $n=1.0$ and the coefficient of vena contracta at the opening $a=0.7$, the author will use these values in his calculation.

Of the four fire tests mentioned in Chapter 6, in the first one (No. 1), fire extinguishing by means of water spray was carried out when the fire was still on the way to its height so that it was not possible to check its duration. Therefore, this test will be excluded, but the method described above will be applied to the other three tests. The size of the openings in accordance with Section 6.2; in Test No. 2, there are two openings, each 82×155 (cm) and in No. 3 and No. 4 one, each measuring 300×100 (cm). Accordingly, computing the burning rate in the room from Mr. Kawagoe's chart, we obtain

No. 2………18.0 kg/min. No. 3, No. 4………18.9 kg/min.

The quantity of combustibles used was as follows: 800 kg in No. 2 and 500 kg each in No. 3 and No. 4. On the assumption that the fire burns at this rate from the start, the duration of fire is computed to be

No. 2 …………………800 kg÷18.0 kg=44.4(minutes)

No. 3, No. 4…………500 kg÷18.9 kg=26.5(minutes).

In Figure 6.5 which shows the curve of the fire temperature in the room in Test No. 2, only the temperature for the period up to twenty-five minutes after the ignition is shown, but actually the room temperature began to drop forty-two minutes after the ignition. In Test No. 3, the temperature began to drop in about twenty-five minutes, but since the start of fire is considered to be really five minutes after the ignition according to Figure 6.6, the duration of fire ended about six minutes earlier than expected. The reason for this may be that the fuel consisted mostly of old materials and the force of the flames was not so persistent. In Test No. 4, although the room temperature began to drop about thirty-three minutes after the ignition according to Figure 6.7, the start of fire was really 8～9 minutes after the ignition, making the duration of fire about twenty-five minutes, or practically equal to the expected value.

9.3 Fire Temperature in the Room

Concerning the mean room temperature during the period of maximum intensity of fire, there are Dr. Kin-ichiro Fujita's formula[23] and Mr. Takashi Sekine's formula.[24] Both were derived from the equations of heat transfer in the room, and the use of either formula gives similar results. According to Mr. Sekine, in case the ceiling, floor and the surrounding walls excluding the windows are built of concrete and all the window-panes are considered to have been broken at the start of the fire, when the rate of complete combustion is 0.6 and the rate of excess air 1.0, the room temperature during the period of maximum intensity of fire can be expressed merely by the vertical length, H, of the window and the ratio between the area of window A_B and the total surface area A_T (total surface area of the window, walls, floor and ceiling). He has prepared a simple chart for obtaining the room temperature thirty minutes after the start of fire from these factors. This chart will be used here.

Depending on the quantity of combustibles and the burnig rate, the fire may end before reaching its height, or, conversely, it may reach its height much later than thirty minutes. In order to obtain the highest room temperature in such cases, it is necessary to know the changes in the fire temperature of the room in terms of time. It is very difficult to obtain the changes theoretically, and even if they are obtained, practically it is clear that the conditions of the rising of temperature vary greatly according to factors such as delay in the breaking of window-panes in the early stage of fire, arrangement of the combustibles in the room and whether or not the ceiling has an incombustible finish. Here, considering the case to be one of the most standard type, we shall use the standard curve for fireproof construction given in the Japanese Indurtrial Standard, J.I.S. A 1302 and assume that the room temperature changes at the same rate as this. According to this standard curve, the temperature after thirty minutes from the start of fire reaches 843°C, but if the temperature after thirty minutes is calculated to be 1000°C when obtained by use of the above-mentioned method devised by Mr. Sekine, the room temperature at any time after the start of fire is supposed to have the value 1000/843 times to that obtained from the standard curve. Then, if the room temperature at the end of the time which has elapsed from the start of fire corresponding to the value of the fire duration obtained in the preceding section is calculated, the temperature thus obtained is the estimated value of the highest temperature in the room.

Let us compare this with the results of experimental full scale fire described in Chapter 6. In Section 6.2 the total surface area of the room A_T, window area A_B and A_B/A_T are

No. 2…………$A_T = 2(4.3\times3.48+3.48\times2.47+2.47\times4.3)=34.18\ \mathrm{m}^2$,

$A_B = 2(0.82\times1.55)=2.542\ \mathrm{m}^2$,

$A_B/A_T=0.074$, $H=1.55\ \mathrm{m}$

No. 3, No. 4…………$A_T = 2(5\times2.5+2.5\times1.67+1.67\times5)=50.05\ \mathrm{m}^2$,

$A_B = 3\times1=3\ \mathrm{m}^2$,

$A_B/A_T=0.060$, $H=1\ \mathrm{m}$;

therefore, according to Mr. Sekine's chart, the temperatures after thirty minutes are

No. 2…………980°C

No. 3, No. 4············900°C.

These temperatures are respectively 1.163 and 1.068 times the temperature 843°C obtained from the standard curve. Since the fire durations obtained by calculation in the preceding section are 44.4 minutes for No. 2 and 26.5 minutes for No. 3 and No. 4, and the temperatures obtained from the standard curve for the said time durations are 890°C and 828°C, the expected highest temperatures in the room are

No. 2 ·····················$890°C \times 1.163 = 1035°C$,

No. 3, No. 4············$828°C \times 1.068 = 884°C$.

Actually, the temperatures are 910°C for No. 2 according to Figure 6.5, 900°C for No. 3 according to Figure 6.6 and 830°C for No. 4 according to Figure 6.7 (since all the values represent the difference between the room temperature and the outdoor temperature, the outdoor temperature 20°C must be added to them to make them the room temperatures), so that practically the above calculation is believed to be satisfactory.

9.4 Quantity of Heat Discharged from the Opening

The quantity of heat Q discharged in unit time from the opening of the room on fire is the quantity of heat which the flame or ho tgas carries out through the opening. Since it is equivalent to the heat quantity necessary to raise the temperature of the gas discharged during the combustion of the wooden materials from the outdoor temperature up to the fire temperature, it may be expressed by the following equation:

$$Q = Gc_p'v\Delta\theta. \qquad (9.1)$$

Here G is the volume of gas discharged through combustion of 1 kg of wooden material. If the values of the rate of perfect combustion and excess air factor are given, G can be obtained from Dr. Fujita's or Mr. Kawagoe's chart. c_p' is specific heat of the discharged gas at constant pressure and, according to Dr. Matake Kurokawa,[25] it has the value of approximately 0.32 kcal/Nm³. deg. v is the burning rate in the room and can be obtained by the method described in Section 9.2. Assuming that the rate of perfect combustion $x=0.6$ and the excess air factor $n=1.0$ as we did in Section 9.2, we can obtain the value of G from Mr. Kawagoe's chart[22] as follows:

$$G = 4.85 \text{ Nm}^3/\text{kg}.$$

If we substitute the value of $c_p' = 0.32$ kcal/Nm³ into Equation (9.1) and express v in terms of the unit kg/min. and calculate Q in terms of the unit cal/sec, Equation (9.1) becomes

$$Q = 25.9\ v\Delta\theta \text{ (cal/sec)}. \qquad (9.1_1)$$

$\Delta\theta$ is the difference between the room temperature and the outdoor temperature. With reference to the experimental full scale fire described in Chapter 6,

in No. 2, according to Section 9.2, $v = 18.0$ kg/min.

and according to Section 9.3,

$\Delta\theta = 1035°C - 20°C = 1015°C$;

in No. 3 and No. 4 $v = 18.9$ kg/min,

$\Delta\theta = 884°C - 20°C = 864°C$.

Therefore the heat quantity Q discharged from one window becomes

No. 2············$Q = 1/2\ (25.9 \times 18.0 \times 1015) = 236597$ cal/sec,

No. 3
No. 4 .... $Q=25.9\times18.9\times864=422937$ cal/sec.

There is some discrepancy between these values and the results of calculation described in Section 8.6 of the preceding Chapter. The reason for this is that the results in the preceding Chapter were obtained by calculation based on the average room temperature during the period of maximum intensity of fire, while here the calculation was done on the basis of the highest temperature in the room.

9.5 The Temperature Distribution of the Fire Current Spurting from the Opening and the Temperature at Which Window-Panes of the Upper Story are Broken

If the quantity of heat, Q, discharged from the opening in unit time and the dimensions of the window are given, the temperature distribution along the trajectory of the hot gas spurting from the window can be obtained from Figure 8.7 or Figure 8.8 in the preceding Chapter. The non-dimensional temperature Θ in this case is exrpessed by Equation (8.3) and the equivalent radius r_0 by Equation (8.1).

For obtaining the critical temperature at which the flames spurting from the window of the lower story break the window-panes of the upper story, it must be known under what degree of hot current window-panes are broken. Needless to say, the degree varies according not only to the condition of heating but also to various other factors including the kind of the glass, its size, and the way in which it is fixed. Here, however, let us suppose a bad condition that the glass is sheet-glass of the medium quality with a thickness of 3 mm. In the case of the experimental full scale fire discussed in Chapter 6, the puttied sheet-glass of the medium quality with a thickness of 3 mm or so placed at the position equivalent to that of the window of the upper story subjected to heating of the heating speed of J. I. S. A 1301 Outdoor Third Class Heating was only cracked at 400°C, and was broken and fell down at 600°C. When it was subjected to heating of a heating speed exceeding the curve of the Outdoor Second Class Heating, it was broken and fell down at 400°C (See Section 6.5 of Chapter 6).

According to a report[26] by Dr. Minoru Hamada and Mr. Shoji Ikeda, the results of experiments in compliance with J. I. S. A 1301 Outdoor Second Class Heating Test showed that the glass 3 mm thick and 60 sq. cm in area came off and fell down after 5.5~8.5 minutes from the start of heating when it is attached to sash by bead and after 5~12.5 minutes when it is attached to sash by putty with clips. In case of heating according to the Outdoor Second Class Heating Curve, the temperature reaches 500°C at the 6th minute. in the experiments by Dr. Hamada and Mr. Ikeda, it is supposed that the heating speed was about this grade and that the window-pane was broken at about 500°C.

With regard to the speed of heating the wall of the upper story by the fire current spurting from the window of the lower story, the wall is heated at the heating speed of the curve of Outdoor Second Class or Third Class Heating when it is exposed to a hot current of more than 500°C according to the results of the full scale fire tests referred to in Chapter 6 (See Section 6.4). Therefore, let us suppose that the wall is heated at the heating speed equivalent to the curve of Outdoor Second Class Heating, and, taking into consideration the results of the two series of experiments mentioned above, the critical temperature at which the window-pane falls down is set at 500°C.

In order to prevent the window-panes of the upper story from breaking and falling down caused by the fire current spurting out of the lower story, it is sufficient to make the temperature of the hot current fall below 500°C when it reaches the surface of the window-panes of the upper story. As in the cases stated hitherto, let us express Θ which is the non-dimensional expression of the temperature of hot current $\Delta\theta$ by the following expression:

$$\Theta = \frac{\Delta\theta r_0^{5/3}}{\sqrt[3]{\dfrac{Q^2\theta_0}{c_p^2\rho^2 g}}}, \qquad \cdots\cdots(9.2)$$

where:

r_0 ············ Equivalent radius of window,

Q ············ Quantity of heat discharged out of the window in unit time,

θ_0 ············ Absolute outdoor temperature,

ρ, c_p ············ Density and specific heat of the gas at constant pressure,

g ············ Acceleration due to gravity.

And, if $\theta_0 = 290°K$ according to the calculation explained in Section 4.9 of Chapter 4, the value of Θ corresponding to $\Delta\theta = 500°C$ is expressed by Equation (4.16):

$$\Theta_{500} = \frac{1.717 r_0^{5/3}}{Q^{2/3}}, \qquad \cdots\cdots(9.3)$$

Then, substituting in the above equation the value of Q computed from Equation (9.1_1) of the preceding section and the value of the equivalent radius of window, r_0, computed from Equation (8.1) of Chapter 8, the value of Θ_{500} can be obtained. Next, for obtaining the value of z/r_0 corresponding to Θ_{500} by use of the curve of Figure 8.8, Chapter 8, it is more convenient to utilize Table 9.1 which is tabulation of Figure 8.8 than to use Figure 8.8 itself. When the value of z/r_0 is obtained, the value of z can be obtained by multiplying it with r_0. This value of z is the distance from the window face from which the fire current has spurted to the point where the temperature of the current is 500°C, measured along the trajectory.

Now, in the case of No. 2, No. 3 and No. 4 full scale fire tests, the value of Q is as was obtained in the preceding section and the value of r_0 as was obtained in Section 8.6 of the preceding Chapter. From these, calculation is made as follows:

	No. 2	No. 3, No. 4
$r_0^{5/3}$	475.7	1163.6
$Q^{2/3}$	3825.4	5634.5
Θ_{500}	0.214	0.355
z/r_0	4.28	1.40
z	173cm	97cm

Therefore, it may be said that the point where the temperature of the spurting current

Table 9.1 Values of z/r_0 corresponding to Θ in temperature distributions along trajectories of fire currents spurting from the window.

z/r_0	Θ	z/r_0	Θ	z/r_0	Θ	z/r_0	Θ
0.20	0.46	1.00	0.39	2.40	0.30	4.10	0.22
0.25	0.45	1.10	0.38	2.60	0.29	4.40	0.21
0.30	0.445	1.20	0.37	2.75	0.28	4.70	0.20
0.40	0.44	1.30	0.36	2.90	0.27	5.00	0.19
0.50	0.43	1.50	0.35	3.10	0.26	5.40	0.18
0.60	0.425	1.70	0.34	3.30	0.255	5.80	0.17
0.70	0.42	1.90	0.33	3.50	0.245	6.30	0.16
0.80	0.41	2.05	0.32	3.70	0.235	6.80	0.15
0.90	0.40	2.20	0.31	3.90	0.23	7.40	0.14

falls to 500°C is 1.73 m in Test No. 2 and 0.97 m in Tests No. 3 and No. 4 from the window face measured along the trajectory of the spurting current.

9.6 Necessary Height of Spandrel

As the value of z obtained in the preceding section is the distance measured from the window face along the trajectory of the spurting hot current, it is a matter of course that the value of z is longer than the necessary spandrel height, that is the vertical distance z_0 from the upper edge of the window (actually the position of the main flow of the spurting hot current when it has just spurted out of the window is a little lower than the upper edge of the window, but, ignoring the difference, let us suppose that it is at the height of the upper edge of the window) to the height where the temperature of the current falls to 500°C, because the spurting current flows horizontally at first and then gradually changes its course to take the vertical direction. According to the results obtained in Chapter 7, the position of the trajectory of the spurting current varies according to the ratio of the horizontal width to the vertical length of the window. Therefore, in this case, the conversion of z into z_0 varies according to the ratio. For the conversion, we can use Figure 7.5, Chapter 7. For convenience' sake, however, the conversion at the typical values of n are obtained from Figure 7.5 by interpolation and are tabulated in Table 9.2. By use of this table, we can obtain the values of z_0 corresponding to the respective values of n (which is the ratio between the horizontal width of the window and the one half of the vertical length thereof) within the range of $0.5\sim8$. In the table, H'' is the height measured from the neutral zone of the window to the upper edge thereof as defined by Equation (7.4), Chapter 7, and its ratio to the vertical length, H, of the window varies to some extent according to the fire temperature in the room. The values are given in Table 7.1. When the value of z has been fixed, as a result of the calculations in the preceding sections, the value of H''/H is obtained from the maximum temperature of the fire in the room by use of Table 7.1, and then, and when it is multiplied by H, the value of H'' is obtained. Then, z/H'' is computed, the value of z_0/H'' corresponding to it is found by use of Table 9.2,

Table 9.2 Table to find the vertical distance, z_0/H'', of a point from the upper edge of the window when the distance, z, along the trajectory of the fire current spurting out of the window is given.

z/H'' \ z_0/H''	n = 0.5	1	1.5	2	3	4	5	6	8
0.1	0.02	0.02	0.03	0.03	0.04	0.05	0.05	0.06	0.06
0.2	0.04	0.04	0.06	0.08	0.09	0.10	0.11	0.12	0.14
0.4	0.14	0.15	0.17	0.20	0.23	0.26	0.28	0.30	0.33
0.6	0.28	0.29	0.32	0.35	0.40	0.44	0.47	0.49	0.52
0.8	0.44	0.46	0.49	0.53	0.59	0.63	0.66	0.69	0.71
1.0	0.62	0.64	0.67	0.72	0.78	0.82	0.86	0.89	0.90
1.2	0.80	0.83	0.87	0.91	0.98	1.02	1.05	1.08	1.10
1.4	0.99	1.02	1.06	1.10	1.17	1.21	1.24	1.27	1.30
1.6	1.18	1.21	1.25	1.30	1.37	1.41	1.44	1.46	1.50
1.8	1.37	1.40	1.45	1.49	1.57	1.61	1.64	1.66	1.70
2.0	1.57	1.60	1.65	1.69	1.76	1.80	1.83	1.86	1.90
2.2	1.76	1.79	1.84	1.89	1.96	2.00	2.03	2.06	2.10
2.4	1.96	1.99	2.04	2.08	2.16	2.20	2.23	2.26	2.30
2.6	2.15	2.18	2.23	2.28	2.36	2.40	2.43	2.46	2.50
2.8	2.35	2.38	2.43	2.48	2.56	2.60	2.63	2.66	2.70
3.0	2.55	2.59	2.54	2.68	2.75	2.79	2.83	2.86	2.90
3.2	2.74	2.78	2.83	2.88	2.95	2.99	3.03	3.06	3.10
3.4	2.94	2.98	3.03	3.08	3.15	3.19	3.23	3.26	3.30

Notice : H'' is the height measured from the neutral zone of the window to the upper edge thereof, and its value varies according to the fire temperature in the room. Its ratio to the vertical length, H, of the window is obtained by use of Table 7.1; n is the quotient of the horizontal width of the window divided by one half of the vertical length.

and when it is multiplied by H'', z_0 which is the necessary spandrel height, is obtained.

Now, according to experimental full scale fire,

	No. 2	No. 3 and No. 4
Maximum room temperature	1035°C	884°C ············ Section 9.3
H''/H	0.66	0.65 ············ Table 7.1
H	155cm	100cm ············ Section 6.2
H''	102cm	65cm
z	173cm	97cm ············ Section 9.5
z/H''	1.70	1.49
n	1.06	6.00 ············ Equation (8.2)
z_0/H''	1.31	1.36 ············ Table 9.2
z_0	133cm	88cm

Thus the spandrel height z_0 is 133 cm in the case of Test No. 2 and 88 cm in the case of No. 3 and No. 4. With reference to Test No. 2, since the height of spandrel was only 120 cm according to Figure 6.9, if the experiment had been conducted without spraying water, the temperature of the spurting current might have risen much more, breaking the window-pane of the above story. In Test No. 3, it was quite natural that the ordinary glass affixed 50 cm above the window was broken (Section 6.4, item

(2)). In Test No. 4, it was inevitable that the glass located higher up was broken because it was exposed to the hot current at a sudden heating speed for exceeding the Outdoor Second Class Heating Curve when the ceiling plywood burned. Accordingly, in case the ceiling consists of plywood sheathing the spandrel height does not conform to this calculation, it being an exception.

By z_0 is meant the vertical distance from the upper edge of the window to the place where the temperature of the spurting hot current drops to 500°C, as stated earlier. This does not necessarily mean that the spot on the wall surface z_0 distance above the upper edge of the window is exposed to the hot air current of 500°C, because if the position of the main flow of the spurting fire current is away from the wall above the window, the temperature of the current near the wall is in general lower than the temperature near the main flow. In this case, however, considering that the glass surface receives the radiant heat from the flame, and for simplifying the calculation procedure and by way of taking the safer value for establishing regulations, the value of z_0 has been made here the necessary spandrel height.

9.7 Cases Where a Room Has Two or More Windows

In case a room has two or more windows, some modification is necessary. In calculating the fire duration, the fire temperature in the room and the quantity of heat discharged from the opening, in place of the surface area of one window the total area of the windows should be used and in place of the horizontal width of the window the total of the widths of the individual windows should be used, and with regard to the calculation of the temperature distribution of the spurting hot current, special caution is needed. When the fire-proof wall part between the windows is sufficiently wide and the hot currents spurting from the windows do not reach the temperature of 500°C when they combine at a considerable height after spurting out, the value obtained by dividing the total quantity of heat, Q, discharged from the windows by the number of windows is made the quantity of heat discharged from each of the windows, and then the calculation described above should be done for each window. However, when the interval between the windows is very narrow, the flames coming out of the windows combine shortly after spurting out; therefore, the temperature of the hot currents after combining is higher than the temperature calculated for each window. For simplifying matters if we consider only the cases where the sizes of the windows are equal, it is safe to add up the widths of the windows and replace the windows with one window having a width equivalent to the total of the added-up widths, and then calculate as described above. It is extremely difficult to determine the value of the window-to-window interval which should be taken as the boundary between the two cases (case where the interval is wide and case where it is narrow). This is because the gathering of the flames spurting from the windows is influenced even by trivial conditions and changes. Further studies are necessary regarding this matter, but judging from the results of the full scale fire tests and model experiments conducted hitherto, it is likely the value of the interval about twice the width of one window will be the boundary between the two cases.

9.8 Examples of Calculation

Since the value of the necessary spandrel height is governed by various conditions in the room on fire, it is not possible to obtain the value easily just by preparing a simple chart; it is necessary to diligently perform calculation case by case. Two or three examples of calculation are given here to show to what extent the necessary height changes according to various conditions in the burning room.

Let us suppose there is one window in a room of fire-proof construction whose frontage is 4 m, depth 5 m and ceiling height 4 m. Then let us do calculation for various combinations of windows ranging from 1 m to 4 m in both the width and length and also various combinations involving quantities of combustibles in the room ranging from 25 kg/m² (bedroom in a hotel, meeting room. etc.) to 200 kg/m² (library, storehouse, etc.).[27)]

Table 9.3 shows the results of calculation —— n obtained by dividing the width of window by one-half of the length, the equivalent radius of window r_0 (Equation 8.1), the ratio between the window area and the total inner surface area of the room A_B/A_T, the burning rate in the room (Section 9.2) and the room temperature 30 minutes after the start of fire (Section 9.3). Then the fire duration (Section 9.2) and the maximum room temperature (Section 9.3) are calculated. The results are shown in Table 9.4. In this case, however, as it is supposed that thanks to fire service the room temperature does not rise from the 50 th minute after the outbreak of fire on, in case the maximum temperature is reached after the 50 th minute, the temperature at the 50 th minute is employed as the maximum room temperature, though, needless to say, in case the maximum temperature is reached before the 50 th minute, the value is employed as such.

Table 9.3 Given elements of the room of fire proof construction (4m×5m×4m)

Dimensions of opening (Horizontal) (Vertical)	$\frac{A_B}{A_T}$	Room temperature 30 min. after fire outbreak (℃)	Rate of combusion (kg/min)	n	r_0 (cm)	$r_0^{5/3}$
1m × 1m	0.009	420	6.3	2	39.9	466
2 × 1	0.018	580	12.6	4	56.4	829
3 × 1	0.027	680	18.9	6	69.1	1164
4 × 1	0.036	760	25.2	8	79.8	1479
1 × 2	0.018	630	15.4	1	56.4	829
2 × 2	0.036	820	30.8	2	79.8	1479
3 × 2	0.054	930	46.2	3	97.7	2073
4 × 2	0.071	1000	61.6	4	112.8	2633
1 × 3	0.027	800	28.7	0.7	69.1	1164
2 × 3	0.054	990	57.4	1.3	97.7	2073
3 × 3	0.080	1080	86.1	2	119.7	2907
4 × 3	0.107	1140	114.8	2.7	138.2	3694
1 × 4	0.036	920	44.1	0.5	79.8	1479
2 × 4	0.071	1110	88.2	1	112.8	2633
3 × 4	0.107	1190	132.3	1.5	138.2	3694
4 × 4	0.143	1250	176.4	2	159.6	4696

The results of calculation of the quantity of heat, Q, discharged out of the window in unit time (Section 9.4) at the time of the maximum temperature are shown in Table 9.5.

Then, the values of $Q^{2/3}$ are calculated from the values of Q in Table 9.5, and substituting the values obtained and the values of $r_0^{5/3}$ in Table 9.3 in Equation (9.3), we obtain the values of the non-dimensional temperature Θ_{500} corresponding to $\Delta\theta=500°C$. The results are as shown in Table 9.6.

From the values of the maximum room temperature in Table 9.4, the height measured from the neutral zone on the window face up to the upper edge of the

Table 9.4 Duration of fire (figures in the upper line of each column) and maximum room temperature (figures in the lower line).

Dimensions of opening (Horizontal) (Vertical)	Quantity of combustibles in room (kg/m²)					
	25	50	75	100	150	200
1m × 1m	79min 451°	159min 451°	238min 451°	317min 451°	476min 451°	635min 451°
2 × 1	40 604	79 623	119 623	159 623	238 623	317 623
3 × 1	26 669	53 730	79 730	106 730	159 730	212 730
4 × 1	20 717	40 792	60 816	79 816	119 816	159 816
1 × 2	32 637	65 676	97 676	130 676	195 676	260 676
2 × 2	16 744	32 828	49 875	65 880	97 880	130 880
3 × 2	11 801	22 891	33 947	43 982	65 998	87 998
4 × 2	8.1 791	16 907	24 972	32 1009	49 1068	65 1074
1 × 3	17 735	35 818	52 859	70 859	105 859	139 859
2 × 3	8.7 801	17 910	26 974	35 1012	52 1063	70 1063
3 × 3	5.8 749	12 935	17 993	23 1039	35 1104	46 1147
4 × 3	4.4 656	8.7 922	13 1007	17 1049	26 1120	35 1166
1 × 4	11 791	23 886	34 939	45 973	68 988	91 988
2 × 4	5.7 764	11 956	17 1020	23 1068	34 1132	45 1175
3 × 4	3.8 635	7.6 932	11 1023	15 1074	23 1145	30 1190
4 × 4	2.8 504	5.7 860	8.5 1008	11 1075	17 1149	23 1204

Table 9.5 Calculated values of heat discharged out of the window. (cal/sec)

Dimensions of opening (Horizontal) (Vertical)	Quantity of combustibles in room (kg/m^2)					
	25	50	75	100	150	200
1m × 1m	73590	73590	73590	73590	73590	73590
2 × 1	197109	203310	203310	203310	203310	203310
3 × 1	327482	357342	357342	357342	357342	357342
4 × 1	467972	516923	532587	532587	532587	532587
1 × 2	254074	269629	269629	269629	269629	269629
2 × 2	593504	660512	698005	701994	701994	701994
3 × 2	958461	1066153	1133161	1175042	1194187	1194187
4 × 2	1261993	1447064	1550768	1609799	1703930	1713503
1 × 3	546348	608044	638520	638520	638520	638520
2 × 3	1190815	1352861	1448007	1504500	1580320	1580320
3 × 3	1670263	2085041	2214380	2316960	2461909	2557800
4 × 3	1950498	2741401	2994133	3119013	3330118	3466891
1 × 4	903472	1011980	1072516	1111351	1128484	1128484
2 × 4	1745266	2183867	2330068	2439718	2585918	2684147
3 × 4	2175872	3193563	3505381	3680136	3923423	4077618
4 × 4	2302655	3929134	4605310	4911417	5249505	5500787

Table 9.6 Calculated values of non-dimensional temperature Θ_{500} corresponding to $\Delta\theta=500$°C

Dimensions of opening (Horizontal) (Vertical)	Quantity of combustibles in room (kg/m^2)					
	25	50	75	100	150	200
1m × 1m	0.456	0.456	0.456	0.456	0.456	0.456
2 × 1	0.420	0.411	0.411	0.411	0.411	0.411
3 × 1	0.421	0.397	0.397	0.397	0.397	0.397
4 × 1	0.421	0.394	0.386	0.386	0.386	0.386
1 × 2	0.355	0.341	0.341	0.341	0.341	0.341
2 × 2	0.360	0.335	0.323	0.321	0.321	0.321
3 × 2	0.366	0.341	0.327	0.320	0.316	0.316
4 × 2	0.387	0.353	0.337	0.329	0.317	0.316
1 × 3	0.299	0.278	0.269	0.269	0.269	0.269
2 × 3	0.317	0.291	0.278	0.271	0.262	0.262
3 × 3	0.354	0.306	0.294	0.285	0.274	0.267
4 × 3	0.406	0.324	0.305	0.297	0.286	0.278
1 × 4	0.272	0.252	0.242	0.237	0.234	0.234
2 × 4	0.312	0.269	0.257	0.248	0.240	0.234
3 × 4	0.378	0.292	0.275	0.266	0.255	0.248
4 × 4	0.462	0.324	0.291	0.279	0.267	0.259

winow is calculated by use of Table 7.1, the results being shown in Table 9.7.

Next, by use of Table 9.1 the values of z/r_0 corresponding to Θ_{500} in Table 9.6 are obtained; by multiplying the obtained values by r_0 the values of z are obtained; by use of H'' obtained from Table 9.7 the values of z/H'' are calculated; and by use of Table 9.2 the values of z_0/H'' corresponding to the respective values of n are obtained, the results being given in Table 9.8. The figures left above, right above, right below and left below in each block are in order z/r_0, z, z/H'', and z_0/H''.

If the values of z_0/H'' obtained last of all are multiplied by the values of H'' for the respective windows, the values of z_0 expressing the height of spandrel are obtained. Table 9.9 shows the results of calculation.

From this table we find that the necessary height of spandrel greatly varies according to the size of the opening even when the room size is definite. It is also conspicuous that in the case of a large window the necessary spandrel height is greatly affected by the quantity of the combustibles in the room. If the quantity of the combustibles in the room is within a certain limit and the area of the window is beyond a certain limit, the results of experiments indicate that the larger the window area, the smaller the necessary spandrel height is. This is probably because in case of a large window the burning rate is great and so the fire comes to an end before the temperature rises so high and because the quantity of heat discharged out of the window is greater and accordingly such part of the total quantity of heat used for the rising of the room temperature is smaller.

Next, while in the case of No. 3 and No. 4 full scale fire tests the necessary spandrel height was 88 cm according to the calculation in Section 9.6 if the window is

Table 9.7 Calculated values of the height, H'', measured from the neutral zone to the upper edge of the window.

Dimensions of opening	Quantity of combustibles in room (kg/m²)					
(Horizontal) (Vertical)	25	50	75	100	150	200
1 m × 1 m	61 cm	61 cm	61 cm	61 cm	61 cm	61 cm
2 × 1	63	63	63	63	63	63
3 × 1	63	64	64	64	64	64
4 × 1	64	64	64	64	64	64
1 × 2	126	126	126	126	126	126
2 × 2	128	128	128	128	128	128
3 × 2	128	130	130	132	132	132
4 × 2	128	130	131	132	132	132
1 × 3	192	192	193	193	193	193
2 × 3	192	194	196	198	199	199
3 × 3	191	195	198	199	200	200
4 × 3	190	195	198	199	200	200
1 × 4	256	260	261	263	264	264
2 × 4	253	262	264	265	266	267
3 × 4	252	261	264	265	266	268
4 × 4	248	258	264	265	266	268

3 m in width and 1 m in height and the quantity of the combusibles in the room is 40 kg/m², the calculation of this section reveals that the the necessary spandrel heght is only 57 cm on the same condition that the window is 3 m in width and 1 m in height and the quantity of the combustibles in the room 40 kg/m². This is due to the fact that while the room area in the former is $A_T=50.05\text{m}^2$ (see Section 9.3) that in the latter is $A_T=112\text{ m}^2$, and accordingly the value of A_B/A_T in the former is more than twice as large as that of the latter, which results in the higher fire temperature in the room in the former case.

Thus, the necessary spandrel height is affected by several factors. It cannot be determined by one and the same rule but must be calculated for the respective cases.

Table 9.8 Calculated values of z/r_0, z, z/H'' and z_0/H''

Dimensions of opening	Quantity of combustibles in room (kg/m²)					
(Horizontal) (Vertical)	25	50	75	100	150	200
1m × 1m	0.24, 9.6 0.06, 0.16	0.24, 9.6 0.06, 0.16	0.24, 9.6 0.06, 0.16	0.24, 9.6 0.06, 0.16	0.24, 9.6 0.06, 0.16	0.24, 9.6 0.06, 0.16
2 × 1	0.70, 39.5 0.49, 0.63	0.79, 44.6 0.55, 0.71	0.79, 44.6 0.55, 0.71	0.79, 44.6 0.55, 0.71	0.79, 44.6 0.55, 0.71	0.79, 44.6 0.55, 0.71
3 × 1	0.69, 47.7 0.65, 0.76	0.93, 64.3 0.89, 1.00	0.93, 64.3 0.89, 1.00	0.93, 64.3 0.89, 1.00	0.93, 64.3 0.89, 1.00	0.93, 64.3 0.89, 1.00
4 × 1	0.69, 55.1 0.77, 0.86	0.96, 76.6 1.10, 1.20	1.04, 83.0 1.19, 1.29	1.04, 83.0 1.19, 1.29	1.04, 83.0 1.19, 1.29	1.04, 83.0 1.19, 1.29
1 × 2	1.42, 80.1 0.33, 0.64	1.68, 94.8 0.42, 0.75	1.68, 94.8 0.42, 0.75	1.68, 94.8 0.42, 0.75	1.68, 94.8 0.42, 0.75	1.68, 94.8 0.42, 0.75
2 × 2	1.35, 108 0.75, 0.84	1.85, 148 0.87, 1.15	2.00, 160 0.95, 1.24	2.03, 162 0.98, 1.27	2.03, 162 0.98, 1.27	2.03, 162 0.98, 1.27
3 × 2	1.26, 123 0.74, 0.96	1.68, 164 1.04, 1.26	1.95, 191 1.24, 1.47	2.05, 200 1.29, 1.52	2.11, 206 1.33, 1.56	2.11, 206 1.33, 1.56
4 × 2	1.03, 116 0.74, 0.91	1.45, 164 1.08, 1.26	1.76, 199 1.32, 1.51	1.92, 217 1.45, 1.64	2.10, 237 1.60, 1.79	2.11, 248 1.69, 1.88
1 × 3	2.42, 167 0.53, 0.87	2.79, 193 0.63, 1.00	2.91, 201 0.67, 1.04	2.91, 201 0.67, 1.04	2.91, 201 0.67, 1.04	2.91, 201 0.67, 1.04
2 × 3	2.10, 205 0.72, 1.06	2.58, 252 0.95, 1.30	2.78, 272 1.03, 1.39	2.92, 285 1.08, 1.44	3.06, 299 1.13, 1.50	3.06, 299 1.13, 1.50
3 × 3	1.44, 172 0.63, 0.90	2.28, 273 1.10, 1.40	2.52, 302 1.22, 1.52	2.67, 320 1.31, 1.61	2.84, 340 1.40, 1.70	2.96, 354 1.46, 1.77
4 × 3	0.84, 116 0.39, 0.61	1.99, 275 1.16, 1.41	2.30, 318 1.36, 1.61	2.46, 340 1.46, 1.71	2.69, 372 1.61, 1.86	2.78, 385 1.67, 1.93
1 × 4	2.86, 228 0.50, 0.89	3.30, 263 0.63, 1.01	3.55, 283 0.70, 1.08	3.69, 294 0.74, 1.12	3.78, 302 0.76, 1.14	3.78, 302 0.76, 1.14
2 × 4	2.17, 245 0.61, 0.97	2.92, 329 0.88, 1.25	3.17, 358 0.97, 1.35	3.40, 384 1.08, 1.46	3.60, 406 1.14, 1.53	3.78, 426 1.20, 1.59
3 × 4	1.12, 155 0.33, 0.61	2.56, 354 1.01, 1.35	2.82, 390 1.14, 1.48	2.98, 412 1.20, 1.55	3.30, 456 1.36, 1.71	3.40, 470 1.40, 1.75
4 × 4	0.16, 25.5 0.03, 0.10	1.99, 318 0.94, 1.23	2.58, 412 1.26, 1.56	2.77, 442 1.37, 1.67	2.96, 472 1.46, 1.77	3.12, 498 1.55, 1.86

Table 9.9 Calculated values of the necessary spandrel height (cm)

Dimensions of opening (Horizontal) (Vertical)	Quantity of combustibles in room (kg/m²) 25	50	75	100	150	200
1m × 1m	4cm	4cm	4cm	4cm	4cm	4cm
2 × 1	31	35	35	35	35	35
3 × 1	41	57	57	57	57	57
4 × 1	49	70	76	76	76	76
1 × 2	42	53	53	53	53	53
2 × 2	73	111	122	125	125	125
3 × 2	95	135	161	170	176	176
4 × 2	95	140	173	191	211	223
1 × 3	102	121	129	129	129	129
2 × 3	138	184	202	214	225	225
3 × 3	120	215	242	261	280	292
4 × 3	74	226	269	291	322	334
1 × 4	128	164	183	195	201	201
2 × 4	154	231	256	286	303	320
3 × 4	83	264	301	318	362	375
4 × 4	7	243	333	363	388	415

9.9 Summarization

On the condition that the room size of the concrete building, the dimensions of the window and the quantity of the combustibles in the room are given, we have examined a method of calculating the height of spandrel (which is supposed to have sufficient fire resistivity) necessary for preventing the fire from spreading to the upper story caused by the fire current spurting out of the window when a fire breaks out in the room.

1) The burning rate of the combustibles in the room and the duration of fire were calculated chiefly on the basis of the results of studies by Mr. Kunio Kawagoe.

2) The fire temperature in the room was calculated on the basis of the results of studies by Mr. Takashi Sekine.

3) From the results of the calculation referred to in the preceding item, the quantity of heat discharged out of the window in unit time was calculated.

4) With regard to the temperature at which the window-panes of the upper story break in the fire current, the results of experiments by Dr. Hamada and others and the results of the author's full scale fire tests stated in Chapter 6 were combinedly considered, and, in the case the panes are exposed to the heating speed of approximately J. I. S. A 1301 Outdoor Second Class Heating Curve, this temperature was estimated at 500°C.

5) On the basis of the results obtained in Chapter 8, the distance from the window face to the point where temperature of the fire current spurting out of the window lowers to 500°C, measured along the trajectory of the hot gas, was obtained.

6) On the basis of the results obtained in Chapter 7, the distance referred to in

the preceding item was converted into the value of the necessary spandrel height.

7) By imagining a room of concrete construction whose frontage is 4 m, depth 5 m and ceiling height 4 m, the necessary spandrel height was calculated for various cases in which the dimensions of the window and the quantity of the combustibles in the room are changed.

As the value of the necessary spandrel height is affected by various conditions, it is impossible to prepare a chart or any other device by which the value can be determied easily. Laborious calculation is required for the respective cases.

In the discussion above, especially in the calculation of the example referred to in item 7, it was assumed that all the window-panes of the room were broken at the time of the outbreak of fire and so the window was an opening, that there was no effective fire service until the 50 th minute after the outbreak of fire, and that there was no wind outside. Therefore, in most cases the actual spandrel height may safely be made a little smaller than the value obtained by calculation. On the contrary, however, if the ceiling is finished by use of plywood or similar material the said value is far from being satisfactory.

The greater the window size is, the greater is the necessary spandrel height. To have a large window and a low spandrel height is impossible. When it is desired to have a large window from the viewpoint of design beauty, it may not be possible to make spandrel height as high as 2 m. When a large window is imperative, wire glass should be used at least for the area corresponding to the necessary spandrel height.

Chapter 10

Fire Preventive Effect of the Concrete Projection Attached above the Window

10.1 Introduction

The danger that the heat of the fire currents spurting from the lower floor window of a fire-proof building may cause the spreading of fire to the upper story was pointed out and the necessary height of the spandrel was discussed in the preceding Chapter. Among the apartment houses built in recent year, however, there are some with veranda below the windows and concrete projections above the windows. Here let us discuss how effective these projections are for diminishing the danger of the said spreading of fire and to what extent the height of spandrel treated in the preceding Chapter may be reduced when the building is provided with such a projection.

10.2 Method of Model Experiments

Out of the model rooms made of steel-sheet used in Chapter 7 and Chapter 8, those whose window has horizontal width and vertical length measurements of 9.2 × 20 cm, 24 × 14 cm, and 32 × 10 cm were adopted, and in each case a projection made of asbestos cement board was attached to the upper edge of the window in the horizontal direction. The width of the projection was made to vary in 6 grades: 10, 8, 6, 4, 2, and 0 cm for each of the windows. As substitute for the supposed upper story wall, asbestos boards were set perpendicularly above the window as in the case of Chapter 8.

The first step experiments were performed with only one projection attached to the upper edge of the window, and the temperatures of the spurting current at several points above the window were observed. Then, on the basis of the temperatures observed, the location of the main stream of the spurting current and the temperature distribution along the main stream were sought and the effect of the projection on them were examined. In the case of actual buildings, however, if the window of the lower story has a projection, it is usual that the upper story also has a projection. Therefore, in the second step experiments, another projection of the same size was added at the height 20 cm above the first projection, and the same examination was made (Figure 10.1).

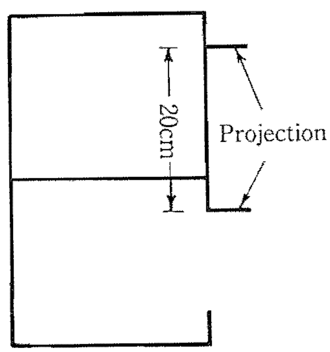

Figure 10.1
Projections attached in two steps

The temperature was taken in the same way as in Chapter 8. Twelve thermocouples were placed at equal intervals in a vertical line and the temperatures of the various points were taken by putting the whole series of thermocouples nearer to and farther from the window on the plane which contains the vertical line passing through the middle of the window. Thermocouples were connected with a electron-tube self-registering thermometer placed at twelve different points.

10.3 Relation between Projection Width and Trajectory of Spurting Hot Current

The results of tracing the position of the maximum temperature on the various horizontal sections of spurting currents in cases where projections 10 cm to 2 cm wide are fixed horizontally from the respective windows in the first step experiments and in case no projection is fixed are shown in Figures 10.2, 10.3 and 10.4. Although it is not certified that the line which connects the points where the temperature is highest coincides with the trajectory of the spurting current, it may be said that they coincide broadly speaking. It is a clear fact that if a projection is fixed, the position of the main flow of the spurting current is away from the wall above the window. However, this does not mean that the shape of trajectory of the current moves away in parallel by as many centimeters as are equal to the width of the projection. As a matter of fact, the higher the current goes up, the more similar does its shape become

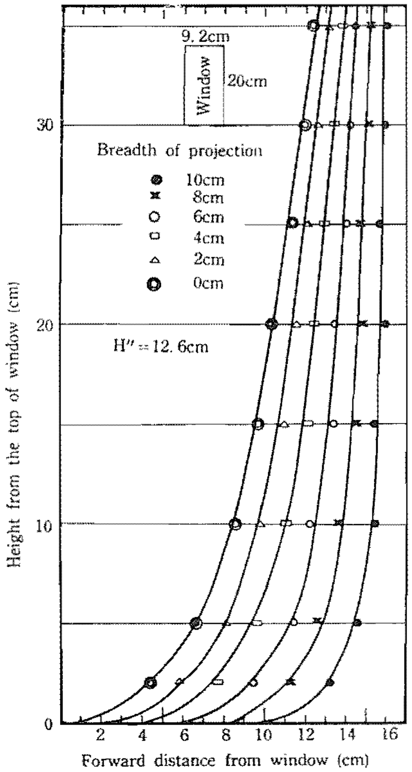

Figure 10.2

Trajectories of ejected currents according to the width of projection (Ⅰ)

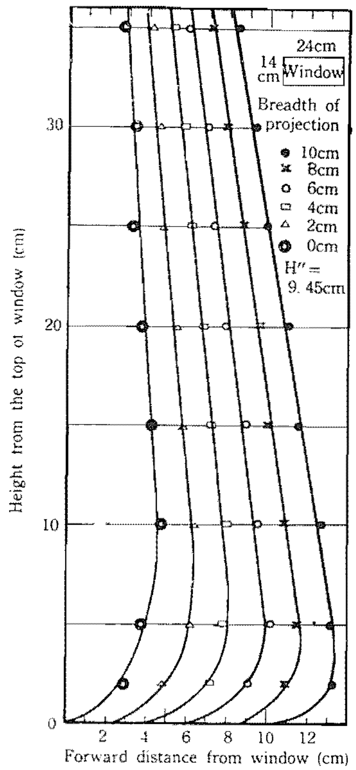

Figure 10.3

Trajectories of ejected currents according to the width of projection (Ⅱ)

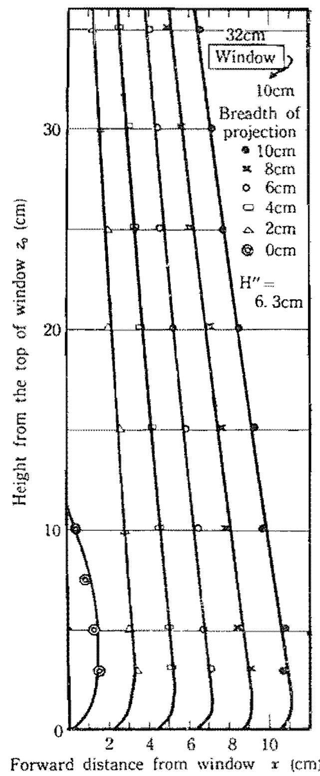

Figure 10.4

Trajectories of ejected currents according to the width of projection (Ⅲ)

to the shape when there is no projection, regardless of the shape of the window. This is seen from the results of observations shown in Figures 10.2~10.4. It is supposed that, in the case of a projection width much, the current which has been forced to move away from the window goes back to the stabilized condition as that of the case without any projection.

According to Section 7.4, Chapter 7, the shape of the spurting current in the case where there is no projection was proportional to the window height if the ratio between the width and height of the window is definite. For the same reason, it was inferred that the shape of trajectory in the case where there is a projection would also be proportional to the window height if the ratio between the width and height of the window be definite.

In the second step experiments, projections were placed at two places, one just above the window and the other 20 cm further up, and it was found that in the case of the window 9.2×20 cm the result was nearly the same as that of the case of only one projection, because the position of the main flow of the spurting current is considerably away from the edge of the upper projection. In the case of the window 24×14 cm, there is some turbulence because the position of the main flow of the spurting current is adjacent to the edge of the upper projection. In this case also, however, the position of trajectory is on an average nearly the same as in the case of only one projection. When the window size is 32×10 cm, the main flow of the spurting current runs directly against the upper projection and goes up by detouring the outside of it. Therefore, the position of trajectory of the part above this area in this case is somewhat different from that in the case of only one projection. However, in the part below the upper projection for which trajectory is needed for the purpose of practical use, the position of the trajectory is practically the same as the case of only one projection (Figure 10.5).

For the sake of simplicity based on the above stated reason and for the sake of being on the safe side in practical use, let us here consider the case of only one projection alone as far as trajectory is concerned.

In order to find the trajectory of a fire current spurting out of a window under the condition that the dimensions of the window and the width of the projection are known, it is necessary first to plot the trajectory on the non-dimensional coordinate system where the law of similarity holds. There, as in the case of Figure 7.5 in Chapter 7, instead of the height, z_0, measured from the upper edge of the window and the horizontal distance, x, measured forwarded from the window face, non-dimensional coordinates obtained by dividing them by H'', which is the height measured from the neutral zone on the window face to the upper edge of the window are used. When the curves in Figures 10.2, 10.3 and 10.4 are re-drawn by use of them, they are as shown in Figures 10.6, 10.7 and 10.8. The results are of practical use in finding (when the distance, z, from the window along the trajectory of the spurting current is known for windows different in horizontal width and vertical length and provided with a projecton which is variant in width), the vertical distance, z_0, of the point corresponding to the said distance, of which an explanation will be given later in Section 10.6. Then, for each of the curves in the three figures obtained above, a table is made to express the relation between the non-dimensional value, z/H'', of the length measured from the window face along the curve and the corresponding value of the non-dimensional value, z_0/H'', of the vertical distance measured from the upper edge of the window. As in these tables there are only three values (1.0, 3.4 and 6.4) for the ratio, n, between the horizontal width of window and one half of the vertical length of window, tables expressing the relation for the respective values of n are prepared according to the interpolation method: they are Tables 10.1.1, 10.1.2 and 10.1.3.

If the distance, z, from the window face along the trajectory of the spurting hot current is given, its vertical distance, z_0, measured from the upper edge of the window is found in the following way: —— First, the ratio, n, between the horizontal width of the window and one half of the vertical length thereof is found, and the proper table is selected. Next, the value of H'' in relation to the fire temperature in the room is found by use of Table 7.1, and, by dividing the width, s, of the projection by H'', s/H'' is calculated. Then, the value of z_0/H'' corresponding thereto in the column of the corresponding value of s/H'' is found, the result is multiplied by H'', and the necessary value of z_0 is obtained.

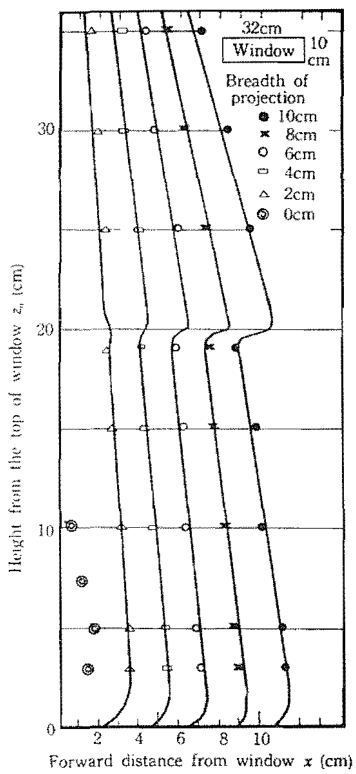

Figure 10.5
Trajectories of ejected currents when projections are attached in two steps

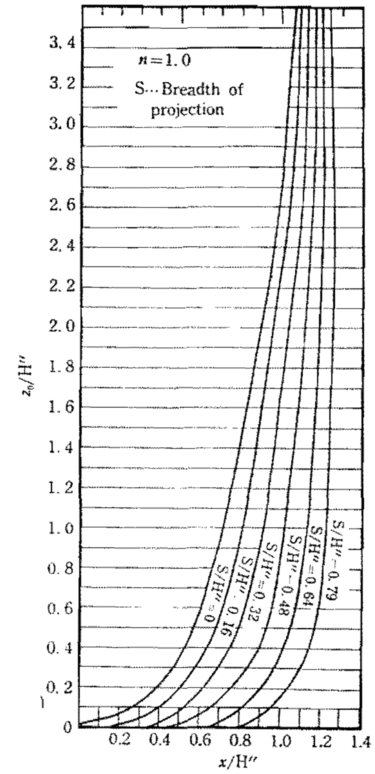

Figure 10.6
Trajectories of spurting hot currents shown on non-dimensional coordinate system (I)

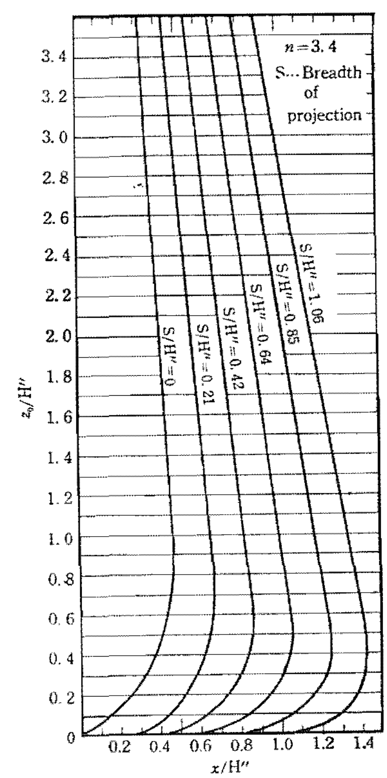

Figure 10.7
Trajectories of spurting hot currents shown on non-dimensional coordinate system (II)

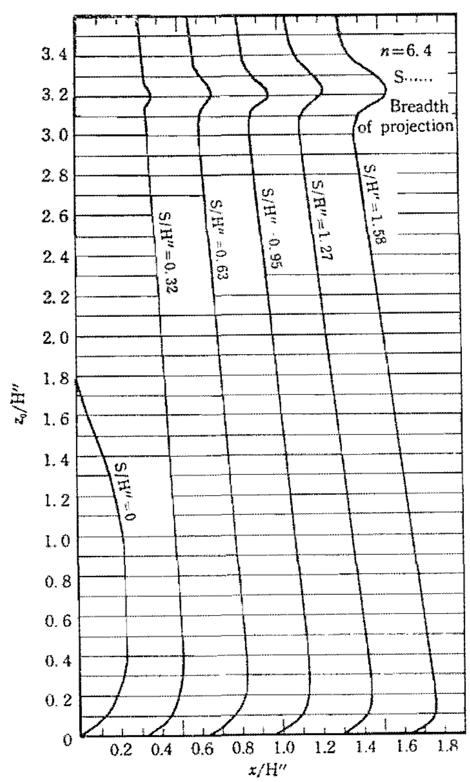

Figure 10.8
Trajectories of spurting hot currents shown on non-dimensional coordinate system (III)

Table 10.1.1 Table to find the vertical distance, z_0/H'', of a point when the distance, z, along the trajectory of the fire current spurting from the window provided with a projection above is given (in cases $n=1$ and $n=2$)

n / z/H'' \ s/H''	$n=1$					$n=2$					
	0.15	0.30	0.45	0.60	0.75	0.15	0.30	0.45	0.60	0.75	0.90
0.1	0	0	0	0	0	0	0	0	0	0	0
0.2	0.01	0	0	0	0	0.02	0	0	0	0	0
0.4	0.08	0.02	0	0	0	0.09	0.02	0	0	0	0
0.6	0.20	0.14	0.06	0	0	0.19	0.13	0.06	0	0	0
0.8	0.38	0.29	0.16	0.07	0	0.37	0.28	0.17	0.07	0	0
1.0	0.56	0.47	0.32	0.21	0.09	0.55	0.46	0.33	0.19	0.11	0.03
1.2	0.75	0.66	0.50	0.39	0.24	0.74	0.65	0.52	0.38	0.26	0.13
1.4	0.94	0.85	0.69	0.58	0.41	0.93	0.84	0.71	0.56	0.40	0.24
1.6	1.13	1.04	0.88	0.77	0.60	1.13	1.04	0.91	0.75	0.59	0.43
1.8	1.32	1.23	1.07	0.96	0.79	1.32	1.23	1.10	0.95	0.78	0.62
2.0	1.52	1.42	1.26	1.16	0.99	1.52	1.42	1.30	1.14	0.98	0.82
2.2	1.71	1.62	1.46	1.35	1.18	1.71	1.62	1.49	1.34	1.17	1.01
2.4	1.90	1.81	1.65	1.55	1.38	1.90	1.81	1.69	1.53	1.37	1.21
2.6	2.10	2.01	1.85	1.74	1.57	2.10	2.01	1.88	1.73	1.57	1.40
2.8	2.30	2.20	2.04	1.93	1.77	2.30	2.20	2.08	1.92	1.76	1.60
3.0	2.49	2.40	2.24	2.12	1.96	2.49	2.40	2.27	2.11	1.95	1.79
3.2	2.69	2.59	2.43	2.32	2.16	2.69	2.59	2.47	2.31	2.15	1.99
3.4	2.88	2.79	2.63	2.52	2.36	2.88	2.79	2.66	2.50	2.34	2.19
3.6	3.07	2.98	2.83	2.71	2.56	3.07	2.98	2.86	2.70	2.54	2.38

Notice : H'' is the height measured from the neutral zone of the window to the upper edge thereof, and its value varies according to the fire temperature in the room. Its ratio to the vertical length, H, of the window is obtained by use of Table 7.1; n is the quotient of the horizontal width of the window divided by one-half of the vertical length thereof; s is the width of the projection.

Table 10.1.2 Cases of $n=3$ and $n=4$

n / z/H'' \ s/H''	$n=3$					$n=4$					
	0.2	0.4	0.6	0.8	1.0	0.2	0.4	0.6	0.8	1.0	1.2
0.1	0	0	0	0	0	0	0	0	0	0	0
0.2	0	0	0	0	0	0	0	0	0	0	0
0.4	0.05	0	0	0	0	0.05	0	0	0	0	0
0.6	0.18	0.06	0	0	0	0.18	0.06	0	0	0	0
0.8	0.35	0.19	0.07	0	0	0.37	0.20	0.09	0	0	0
1.0	0.54	0.35	0.18	0.05	0	0.57	0.38	0.20	0.05	0	0
1.2	0.74	0.54	0.35	0.16	0.04	0.77	0.57	0.38	0.19	0.07	0
1.4	0.93	0.74	0.54	0.32	0.15	0.96	0.77	0.57	0.38	0.21	0.03
1.6	1.13	0.94	0.73	0.50	0.32	1.16	0.97	0.76	0.57	0.39	0.16
1.8	1.33	1.13	0.93	0.70	0.51	1.36	1.16	0.96	0.77	0.58	0.35
2.0	1.52	1.33	1.12	0.89	0.71	1.55	1.36	1.15	0.96	0.78	0.54
2.2	1.72	1.52	1.32	1.09	0.90	1.75	1.55	1.35	1.16	0.97	0.74
2.4	1.91	1.72	1.51	1.28	1.09	1.94	1.75	1.54	1.36	1.17	0.93
2.6	2.11	1.91	1.71	1.48	1.29	2.14	1.94	1.74	1.55	1.36	1.13
2.8	2.31	2.11	1.90	1.67	1.48	2.34	2.14	1.94	1.75	1.55	1.32
3.0	2.50	2.30	2.10	1.87	1.67	2.53	2.33	2.13	1.95	1.75	1.51
3.2	2.70	2.50	2.29	2.06	1.87	2.73	2.53	2.33	2.15	1.94	1.70
3.4	2.90	2.70	2.49	2.26	2.06	2.93	2.73	2.52	2.34	2.14	1.89
3.6	3.09	2.89	2.69	2.45	2.26	3.10	2.92	2.72	2.54	2.33	2.09

Table 10.1.3 Cases of $n=5$ and $n=6$

z/H'' \ s/H''	$n=5$					$n=6$				
	0.3	0.6	0.9	1.2	1.5	0.3	0.6	0.9	1.2	1.5
0.1	0	0	0	0	0	0	0	0	0	0
0.2	0	0	0	0	0	0	0	0	0	0
0.4	0.03	0	0	0	0	0.04	0	0	0	0
0.6	0.16	0	0	0	0	0.19	0	0	0	0
0.8	0.32	0.09	0	0	0	0.36	0.10	0	0	0
1.0	0.51	0.23	0.02	0	0	0.56	0.26	0.02	0	0
1.2	0.71	0.41	0.13	0	0	0.76	0.46	0.14	0	0
1.4	0.90	0.61	0.29	0.04	0	0.95	0.66	0.33	0.05	0
1.6	1.10	0.80	0.48	0.19	0	1.15	0.85	0.53	0.22	0
1.8	1.29	1.00	0.67	0.39	0.10	1.34	1.05	0.72	0.42	0.08
2.0	1.49	1.19	0.87	0.58	0.29	1.54	1.24	0.92	0.61	0.27
2.2	1.69	1.39	1.06	0.77	0.48	1.74	1.44	1.11	0.81	0.47
2.4	1.88	1.58	1.26	0.96	0.67	1.93	1.63	1.31	1.00	0.67
2.6	2.08	1.78	1.45	1.16	0.86	2.13	1.83	1.50	1.20	0.86
2.8	2.27	1.97	1.65	1.35	1.05	2.32	2.02	1.70	1.39	1.06
3.0	2.47	2.17	1.85	1.54	1.24	2.52	2.22	1.89	1.59	1.25
3.2	2.67	2.37	2.04	1.73	1.43	2.72	2.42	2.09	1.78	1.45
3.4	2.87	2.56	2.24	1.93	1.63	2.92	2.61	2.29	1.98	1.64
3.6	3.06	2.76	2.33	2.13	1.83	3.11	2.81	2.48	2.18	1.84

10.4 Temperature Distribution along the Trajectory of the Spurting Fire Current

The results of plotting the value of the first step observations for the three kinds of windows provided with only one projection on the coordinate system of both-logarithmic graduation whose ordinate is the distance, z, measured from the window face along the trajectory of the spurting current and whose abscissa is the temperature, $\Delta\theta$, of the points are shown in Figures 10.9, 10.10 and 10.11.

In the case of a window of a slender shape as shown in Figure 10.9, the temperature distribution along the trajectory is, as is known from the Figure, nearly the same as that in the case where there is no projection, regardless of the width of the projection. In the case of a window of this shape, no great difference in temperature distribution was observed between the case where the space above the window was free and the case where there was a wall above the window, because the main flow of the spurting current was away from the wall even when there was no projection (cf. the figure shown left above in Figure 8.5 in Chapter 8). As the temperature distribution cannot, for this reason, be made lower than that in the case of free space even if the main flow of the spurting current is driven away from the wall by attaching a projection above the window, it is no wonder that there is hardly any difference in temperature distribution. Therefore, in this case, no great advantage for fire prevention can be brought by attaching a projection. When the window is short and wide in shape as in the case of Figures 10.10 and 10.11, the matter is a little different. In this case it is clearly observed that the greater the width of the projection, the

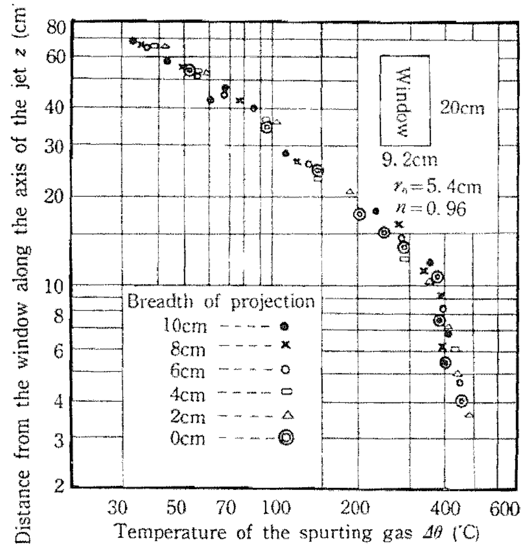

Figure 10.9

Temperature distributions along the trajectories of spurting hot currents (I), (One projection)

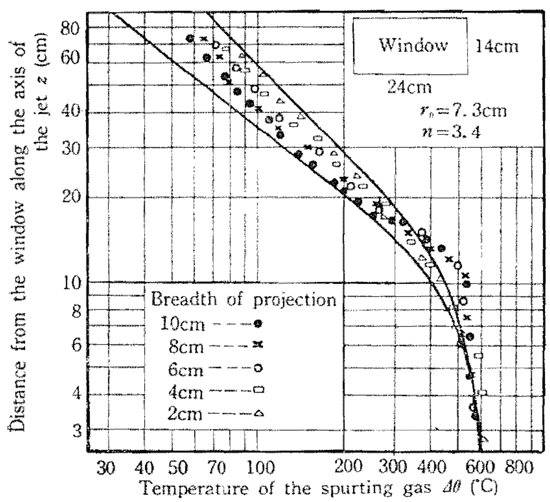

Figure 10.10

Temperature distributions along the trajectories of spurting hot currents (II), (One projection)

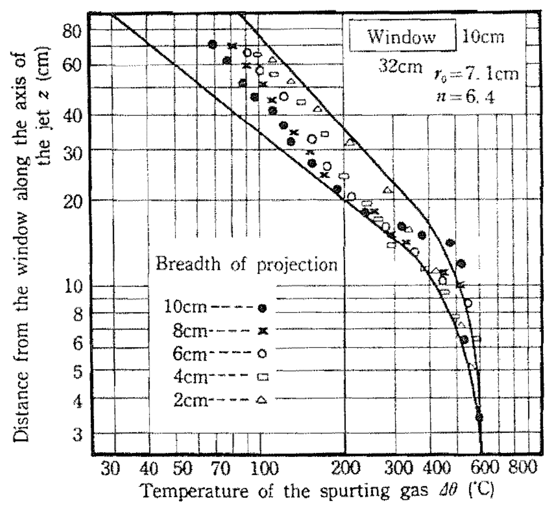

Figure 10.11

Temperature distributions along the trajectories of spurting hot currents (III), (One projection)

more the temperature is lowered. If the width of the projection is great, the main flow of the spurting hot current is driven away from the wall, and resultantly the temperature distribution along the trajectory is, for some distance, a low distribution like temperature distribution in the case where there is no wall above the window (Distribution line shown by marks in Figure 8.5). In Figures 10.10 and 10.11, the lower solid curve expresses the temperature distribution in the case where the space above the window is free on the condition that the same quantity of heat is discharged from the window. However, when the main flow of the spurting current goes up, it gradually comes near the wall as shown in Figures 10.3 and 10.4, and under the effect of the wall, the temperature distribution becomes higher than that in the case of the free space. The upper curve in Figures 10.10 and 10.11 is the temperature distribution curve in the case where there is a wall above the window and there is no projection, as shown by • marks in Figure 8.5. In the case where the window is short and wide in shape, the temperature distribution when there is no projection changes, for the respective windows, from the distribution in the case where there is no projection and the space above the window is free to the distribution where there is a wall above the window. In this case, the wider the projection is, the slower the change is because the spurting current is driven the farther away from the window face, and as a result the temperature is the lower.

The reason why in Figures 10.10 and 10.11 the temperatures in the vicinity of $z=10$ cm are higher in the case there is a wide projection (8 cm or 10 cm) than those in the case where there is no projection, is supposed to be as follows: For instance, in the case where the dimensions of the window are 32×10 cm, the temperature distribution changes from the first domain to the second domain at about $z=7$ cm according to Section 8.4. In this case, however, as the projection is as wide as 8 cm or 10 cm, the type of temperature distribution cannot change to that of the second domain at least to the distance, z, corresponding to the width of the projection. As a result, when the current reaches a point of abont 2 cm beyond the distance corresponding to the width of the projection, the temperature rapidly decreases and the distribution changes to the type in the case where the space above the window is free. The fact that at a certain place the temperature is higher when there is a projection does not lead to the conclusion that the projection is detrimental to fire prevention, because the place is near the edge of the projection or where the vertical distance from the upper edge of the window is nearly zero, and a little above the place the temperature rapidly decreases and so the existence of the projection does not necessitate increase of the spandrel height. To sum up, if a short and wide window is provided with a projection, its fire preventive effects can be expected to some extent because not only it drives the main flow of the hot current away from the wall and increases the horizontal distance corresponding to the width of the projection but also lowers the value of the temperature itself. The results of observation of the relation between the temperature and the distance from the window face, measured along the trajectory of the spurting current, in the case where two projections are attached in the second step experiment are plotted on the same coordinate system of both-logarithmic graduation as was used before, as shown in Figures 10.12, 10.13 and 10.14. Comparison of these with Figures 10.9, 10.10 and 10.11 reveals that the corresponding couples of the two series practically coincide with each other, from which it can be concluded that there is little difference between the temperature distribution in the case of two projections and that in the case of one projection.

In short, the temperature distribution in the case where there is a wall above the window varies according to the ratio, n, of the horizontal width of the window to one half of the vertical length thereof. Concerning the respective values of n, the temperature distribution is between that in the case where the space above the window is free and that in the case where there is a wall above the window. Therefore, in terms of the non-dimensional coordinates as stated in Section 8.5, it is a temperature distribution between those in Figures 8.6 and 8.7.

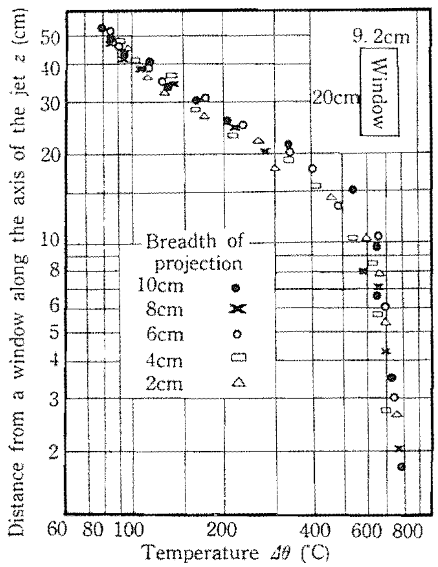

Figure 10.12

Temperature distributions along the trajectories of spurting hot currents when there are two projections (Ⅰ)

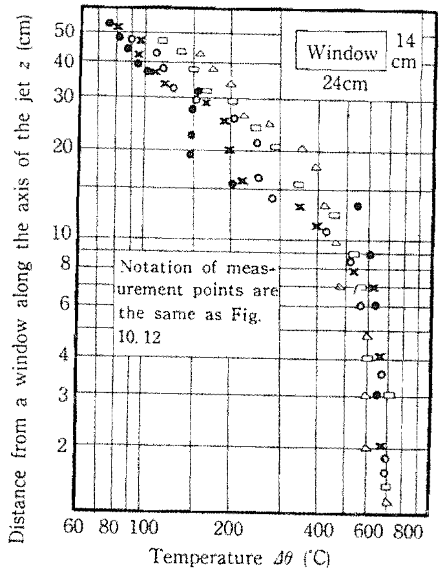

Fiugre 10.13

Temperature distributions along the trajectories of spurting hot currents when there are two projections (Ⅱ)

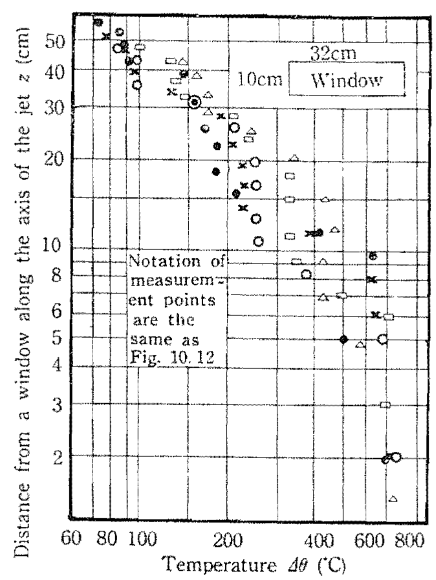

Figure 10.14

Temperature distributions along the trajectories of spurting hot currents when there are two projections (Ⅲ)

Now the temperature distributions relative to the three values of n referred to above are re-plotted on the said non-dimensional coordinate system z/r_0 and Θ are tabulated, and from this the relation between z/r_0 and Θ for the respective values of n is calculated by use of the interpolation method. The results are shown in Table 10.2.1, 10.2.2 and 10.2.3. These tables express the values of the non-dimensional temperature Θ corresponding to z/r_0 according to the respective values of n and s/r_0 (s express the width of the projection and r_0 the equivalent radius of the window).

Table 10.2.1 Values of z/r_0 corresponding to Θ in the temperature distribution along the trajectories when a projection with a width of s is attached above the window (in cases $n=1$, $n=2$)

z/r_0 \ n, s/r_0	$n=1.0$					$n=2.0$				
	0.3	0.6	0.9	1.2	1.5	0.3	0.6	0.9	1.2	1.5
0.20	0.46	0.46	0.46	0.46	0.46	0.46	0.46	0.46	0.46	0.46
0.25	0.45	0.45	0.45	0.45	0.45	0.45	0.45	0.45	0.45	0.45
0.30	0.445	0.445	0.445	0.445	0.445	0.445	0.445	0.445	0.445	0.445
0.40	0.44	0.44	0.44	0.44	0.44	0.44	0.44	0.44	0.44	0.44
0.50	0.43	0.43	0.43	0.43	0.43	0.43	0.43	0.43	0.43	0.43
0.60	0.425	0.425	0.425	0.425	0.425	0.425	0.425	0.425	0.425	0.425
0.70	0.42	0.42	0.42	0.42	0.42	0.42	0.42	0.42	0.42	0.42
0.80	0.41	0.41	0.41	0.41	0.41	0.41	0.41	0.41	0.41	0.41
0.90	0.40	0.40	0.40	0.40	0.40	0.40	0.40	0.40	0.40	0.40
1.0	0.39	0.39	0.39	0.39	0.39	0.39	0.39	0.39	0.39	0.39
1.2	0.37	0.37	0.37	0.37	0.37	0.37	0.37	0.37	0.37	0.37
1.4	0.355	0.355	0.355	0.355	0.355	0.355	0.355	0.355	0.355	0.355
1.6	0.345	0.345	0.345	0.345	0.345	0.345	0.345	0.345	0.345	0.345
1.8	0.335	0.335	0.335	0.335	0.335	0.335	0.335	0.335	0.335	0.335
2.0	0.32	0.32	0.32	0.32	0.32	0.32	0.32	0.32	0.32	0.32
2.2	0.31	0.31	0.31	0.31	0.31	0.31	0.31	0.31	0.31	0.31
2.4	0.30	0.30	0.30	0.30	0.30	0.30	0.30	0.30	0.30	0.30
2.6	0.29	0.29	0.29	0.29	0.29	0.29	0.29	0.29	0.29	0.29
2.8	0.28	0.28	0.28	0.28	0.28	0.28	0.28	0.28	0.28	0.28
3.0	0.265	0.265	0.265	0.265	0.265	0.265	0.265	0.265	0.265	0.265
3.5	0.245	0.245	0.245	0.245	0.245	0.245	0.245	0.245	0.245	0.245
4.0	0.225	0.225	0.225	0.225	0.225	0.225	0.225	0.225	0.225	0.22
4.5	0.205	0.205	0.205	0.205	0.205	0.205	0.203	0.200	0.197	0.195
5.0	0.19	0.19	0.19	0.19	0.19	0.19	0.183	0.180	0.178	0.176

Table 10.2.2 Cases of $n=3$, $n=4$

z/r_0 \ n, s/r_0	$n=3.0$					$n=4.0$				
	0.3	0.6	0.9	1.2	1.5	0.3	0.6	0.9	1.2	1.5
0.20	0.46	0.46	0.46	0.46	0.46	0.46	0.46	0.46	0.46	0.46
0.25	0.45	0.45	0.45	0.45	0.45	0.45	0.45	0.45	0.45	0.45
0.30	0.445	0.445	0.445	0.445	0.445	0.445	0.445	0.445	0.445	0.445
0.40	0.44	0.44	0.44	0.44	0.44	0.44	0.44	0.44	0.44	0.44
0.50	0.43	0.43	0.43	0.43	0.43	0.43	0.43	0.43	0.43	0.43
0.60	0.425	0.425	0.425	0.425	0.425	0.425	0.425	0.425	0.425	0.425
0.70	0.42	0.42	0.42	0.42	0.42	0.42	0.42	0.42	0.42	0.42
0.80	0.41	0.41	0.41	0.41	0.41	0.41	0.41	0.41	0.41	0.41
0.90	0.40	0.40	0.40	0.40	0.44	0.39	0.395	0.40	0.40	0.40
1.00	0.39	0.39	0.39	0.39	0.39	0.38	0.385	0.39	0.39	0.39

z/r_0 \ n, s/r_0	$n=3.0$ 0.3	0.6	0.9	1.2	1.5	$n=4.0$ 0.3	0.6	0.9	1.2	1.5
1.2	0.365	0.365	0.365	0.37	0.37	0.36	0.36	0.365	0.365	0.37
1.4	0.35	0.35	0.35	0.35	0.355	0.34	0.34	0.345	0.345	0.35
1.6	0.33	0.33	0.33	0.335	0.345	0.32	0.325	0.33	0.335	0.34
1.8	0.32	0.32	0.325	0.325	0.33	0.305	0.31	0.31	0.315	0.32
2.0	0.30	0.30	0.305	0.305	0.31	0.29	0.29	0.295	0.30	0.31
2.2	0.29	0.29	0.29	0.29	0.29	0.28	0.28	0.28	0.28	0.28
2.4	0.28	0.28	0.28	0.28	0.28	0.27	0.265	0.265	0.265	0.265
2.6	0.27	0.265	0.265	0.265	0.265	0.26	0.255	0.25	0.25	0.25
2.8	0.26	0.255	0.255	0.25	0.25	0.25	0.245	0.24	0.24	0.24
3.0	0.25	0.245	0.245	0.24	0.235	0.24	0.235	0.23	0.23	0.225
3.5	0.23	0.225	0.22	0.215	0.21	0.23	0.22	0.21	0.20	0.195
4.0	0.21	0.20	0.195	0.19	0.185	0.21	0.20	0.19	0.18	0.175
4.5	0.19	0.18	0.175	0.17	0.165	0.19	0.18	0.17	0.165	0.16
5.0	0.19	0.19	0.19	0.19	0.19	0.18	0.17	0.16	0.15	0.14

Table 10.2.3 Cases of $n=5$, $n=6$

z/r_0 \ n, s/r_0	$n=5.0$ 0.3	0.6	0.9	1.2	1.5	$n=6.0$ 0.3	0.6	0.9	1.2	1.5
0.20	0.46	0.46	0.46	0.46	0.46	0.46	0.46	0.46	0.46	0.46
0.25	0.45	0.45	0.45	0.45	0.45	0.45	0.45	0.45	0.45	0.45
0.30	0.445	0.445	0.445	0.445	0.445	0.445	0.445	0.445	0.445	0.445
0.40	0.44	0.44	0.44	0.44	0.44	0.44	0.44	0.44	0.44	0.44
0.50	0.43	0.43	0.43	0.43	0.43	0.43	0.43	0.43	0.43	0.43
0.60	0.425	0.425	0.425	0.425	0.425	0.425	0.425	0.425	0.425	0.425
0.70	0.42	0.42	0.42	0.42	0.42	0.41	0.41	0.415	0.42	0.425
0.80	0.40	0.405	0.41	0.41	0.41	0.39	0.395	0.40	0.405	0.41
0.90	0.38	0.385	0.39	0.395	0.40	0.375	0.38	0.385	0.39	0.40
1.00	0.37	0.375	0.38	0.385	0.39	0.36	0.365	0.37	0.38	0.39
1.2	0.345	0.35	0.355	0.36	0.37	0.34	0.345	0.35	0.36	0.37
1.4	0.32	0.325	0.33	0.34	0.35	0.315	0.315	0.32	0.33	0.35
1.6	0.31	0.315	0.32	0.33	0.34	0.30	0.30	0.31	0.32	0.34
1.8	0.29	0.295	0.30	0.31	0.32	0.28	0.285	0.29	0.30	0.32
2.0	0.28	0.28	0.285	0.29	0.30	0.26	0.26	0.26	0.27	0.30
2.2	0.27	0.27	0.27	0.27	0.27	0.25	0.25	0.25	0.25	0.25
2.4	0.26	0.255	0.25	0.25	0.25	0.24	0.23	0.22	0.22	0.22
2.6	0.25	0.24	0.23	0.225	0.225	0.23	0.22	0.205	0.205	0.205
2.8	0.23	0.255	0.22	0.215	0.21	0.22	0.21	0.195	0.195	0.19
3.0	0.22	0.215	0.21	0.205	0.20	0.21	0.20	0.185	0.185	0.18
3.5	0.20	0.19	0.18	0.175	0.17	0.20	0.19	0.18	0.17	0.16
4.0	0.19	0.18	0.17	0.16	0.15	0.19	0.177	0.164	0.152	0.14
4.5	0.18	0.17	0.16	0.15	0.135	0.18	0.167	0.154	0.142	0.13
5.0	0.17	0.16	0.15	0.14	0.125	0.17	0.157	0.144	0.132	0.12

10.5 Comparison with Experimental Full Scale Fire

On December 2, 1958, a full scale fire test was conducted in the precincts of the Building Research Institute for examining the condition of the fire currents spurting out the window. The building used was the two-storied building of R. C. rigid frame monolithick construction which had been employed in No. 3 and No. 4 full scale fire tests stated in Chapter 6. Reinforced concrete projection 74 cm wide and about 5 cm thick was attached to the upper edge of the window whose width is 3 m and vertical length is 1 m. Another projection of the same size was attached to the part of the wall 260 cm above it. The building was ignited in the first floor as in the preceding tests and the condition of the fire currents spurting out of the window was observed. The trajectory of the fire current that had spurted and temperature distribution were observed by use of 31 thermocouples attached to poles of steel angles. The temperature observation was conducted according to the same process as in the case of No. 3 test stated in Section 6.3.

According to the results of observation, a temperature-time curve is as shown in Figure 10.15. Roughly speaking, the fire was at its maximum intensity during the period from the 25 th minute to about the 40 th minute after the ignition. During the time, the average room temperature θ was 907°C and the excess temperature $\Delta\theta$, between the indoor and the outdoor temperature was 887°C.

The burning rate v, in the room is calculated to be 18.9 kg/min. according to Section 9.2 as in the case of No. 3 and No. 4 tests. Therefore, from Equation (9.1_1), the quantity of heat, Q, discharged in unit time out of the window during the period of maximum intensity of fire is calculated as follows:

$$Q=434195 \text{ cal/sec.} \quad \cdots\cdots\cdots(10.1)$$

The flame that had spurted out of the window and run along the downside of the projection and after detouring along the farther side of the projection, went up not vertically upward but changing its direction as if it were drawn near by the wall in the similar way as in the case of the model experiments. The average temperatures during the period of maximum intensity at measurement points arranged in front of the wall above the window were as shown in Figure 10.16.

In regard to this experiment, the height, H'', measured along the window face from the neutral zone to the upper edge of the window becomes to $H''=0.65H=65$ cm from Table 7.1, at $n=6.0$ (n is the ratio between the horizontal width of the window and one half of the vertical length of the window) and at the room temperature$=907$°C. As the width of the projection $s=74$ cm $s/H''=1.14$ according to the calculation. The scale of the trajectory curve corresponding to this value of s/H'' in Figure 10.8 is multiplied by H'', and the result plotted on Figure 10.16 is the curve in broken line in the same Figure. From the values of temperature at the measurement points around the broken line, the broken line may be considered to be the trajectory of the spurting hot current. Figures 10.6, 10.7 and 10.8 are the results of the extended application of the law of similarity obtained in Section 7.4.2 for the case where there was no projection to the case where there is a projection. Theoretically, these curves can be applied from model fires to full scale fires. The experiment

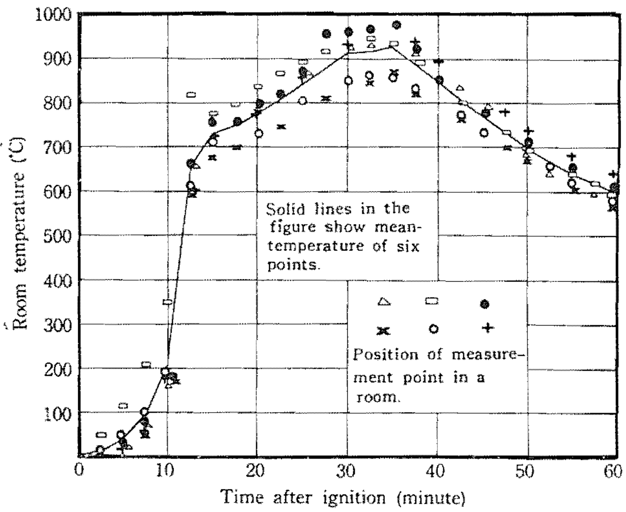

Figure 10.15
Temperature-time curves in an full scale fire test in which a projection is attached above the window

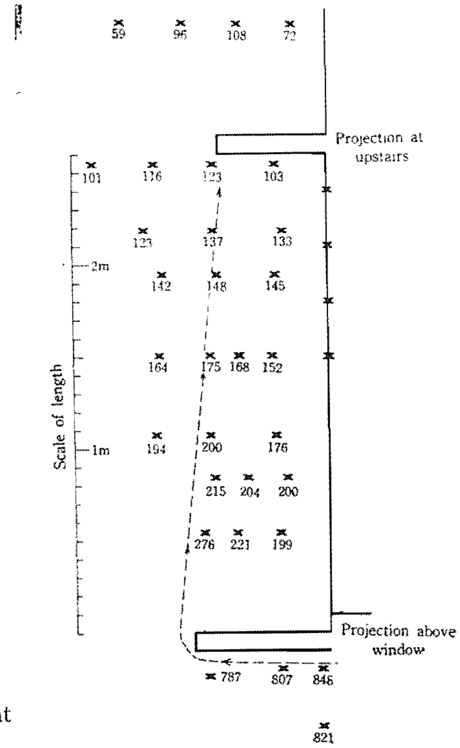

Figure 10.16
Relation between the spurting current and the temperature

× Measurement point
Numbers written under × mean mean-temperature at maximum intensity

was conducted to make sure of it by means of an example.

Next, the equivalent radius of this window is $r_0=69.1$ cm according to Section 8.6. Accordingly, from this and from Equation (10.1), $r_0^{5/3}/Q=0.20293$ and Θ which is the non-dimensional expression of the temperature $\Delta\theta$ is calculated as follows by use of Equation (8.3):

$$\Theta = \frac{0.20293\Delta\theta}{\sqrt[3]{\dfrac{\theta_0}{c_p{}^2\rho^2 g}}} \quad \cdots\cdots(10.2)$$

Then, each of the temperature measurement points near the trajectory of the spurting hot current in Figure 10.16 is plotted on the coordinate system of both-logarithmic graduation whose ordinate axis is the quotient of the distance, z, from the window face measured along the trajectory divided by r_0 and whose abscissa axis is the average temperature at the point during the maximum intensity of fire expressed in non-dimensional quantity by use of Equation (10.2), and the distribution is as shown by × marks in Figure 10.17. In the Figure, the two curves, upper and lower, are the non-dimensional curve of temperature distribution in the cases where the spaces above the windows without projections, a wall exists and a wall does not exist, respectively; they are copies of the distribution curves relative to $n=6.0$ in Figures 8.6 and 8.7. The temperature distribution in this full scale fire test plotted on this coordinate system comes between the said two curves and is similar to the result of the model experiment in the case of $n=6.4$ in Figure 10.11. From these findings, it can be said that the experiment gave a proof that the law of similarity concerning the temperature

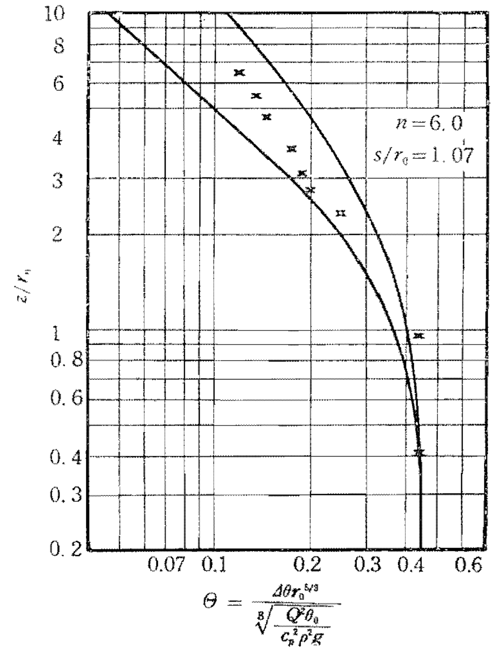

Figure 10.17

Temperature distributions along trajectories of fire currents spurting out of the window provided with a projection (Full scale fire test)

distribution of spurting hot currents in the case where the window is provided with a projection stated in Section 10.4 is applicable to full scale fires. Therefore, the temperature distribution along the trajectory of a spurting current can be expressed by a non-dimensional distribution curve according to n of the window and according to the ratio between the width, s, of the projection and r_0 of the window.

Incidentally, in this experiment a sash with panes of ordinary glass was attached about 30 cm above the floor window. As is shown in Figure 10.16, the temperature in front of the glass was much lower than 500°C, and during the fire no cracks were caused in the glass: nothing happened to the glass.

10.6 Spandrel Height Necessary for Fire Prevention in Case There Is a Projection

It has been found that the existence of a projection just above the window considerably diminishes the danger of the fire's spreading to the upper story because the projection increases the horizontal component of the trajectory by driving away the fire current that has spurted out of the window and so it lowers the temperature at the point for the same value of z compared with the case without projection. Here, by taking up an example, let us make calculation of the extent to which the height of spandrel may be decreased by attaching such a projection.

As an example of calculation, let us take fire resistive room 4 m by 5 m whose celing height is 4 m provided with a window which was used in Section 9.8. Let us consider various combinations in which the horizontal width and vertical length of the window vary from 1 m to 4 m and the quantity of the combustibles in the room from 25 kg/m² to 200 kg/m² and seek the spandrel height necessary for preventing the hot current that has spurted out of the window from breaking the upstair window-glass and from causing spreading of the fire to the upper story on the condition that a projection with a width of 50 cm is attached to the upper edge of the window horizontally.

In this case the following conditions are given as in the calculation of the example in Section 9.8:

1) Fire fighting activities of firemen begin to take effect at the 50 th minute from the outbreak of fire and so the fire temperature in the room does not rise after that. Accordingly, in case the maximum room temperature is reached posterior to the 50 th minute after the fire outbreak according to calculation, the temperature at the 50 th minute is made the maximum temperature, here.

2) The temperature at which the window-panes are broken by the heat of the fire current spurting out of the window and fall, is set at $\Delta\theta=500°C$ on the assumption that the panes are heated at a heating rate of the Outdoor Second Grade Heating Curve.

3) When the temperature of the main flow of the fire current that has spurted out of the window is 500°C, the temperature of the current in touch with the window glass at the same height is little lower. In this case, however, the glass receives the radiation heat from the hot current as well. Therefore, for simplicity's sake, the height at which the temperature of the main flow of the spurting hot current is 500°C is made the limit of danger.

4) When the fire current has just spurted out of the window, the position of the main flow is a little lower than the upper edge of the window. Therefore, the value of the height of spandrel, z_0, calculated here should be theoretically the height measured from the position of the main flow on the window face. However, partly for simplicity's sake and partly from the principle of using the safer value for establishing regulations, the calculation of the height of spandrel is done on the assumption that the position of the main flow is at the upper edge of the window.

Now, as the given conditions of the room size, the window, the quantity of the combustibles, etc. are precisely the same as those given in Section 9.8, the values of the room temperature at the 30 th minute after the outbreak of fire, the burning rate in the room, the ration, n, between the horizontal width of the window and one half of the vertical length thereof, the equivalent radius, r_0, of the window, etc. are equal to the values indicated in Table 9.3; the values of the duration of fire and the maximum room temperature are equal to those in Table 9.4; the values of the quantity of heat, Q, discharged out of the window in unit time are equal to those in Table 9.5; the calculation values of the non-dimensional temperature, Θ_{500}, corresponding to $\Delta\theta=500°C$ are equal to those in Table 9.6; and the values of the height, H'', measured from the neutral zone on the window face to the upper edge of the window are equal to those in Table 9.7.

Next, when the width of the projection is $s=50$ cm, its non-dimensional quantity s/r_0 and s/H'' for the respective windows are calculated as shown in Table 10.3. Then the values of Θ_{500} for the respective windows are obtained from Table 9.6, and, from the corresponding value of s/r_0 and the value of n obtained from Table 9.3 and by use of the proper value in Table 10.2, the value of z/r_0 corresponding to Θ_{500} is obtaind. This is the non-dimensional quantity of the distance, z_0, of the point where the

Table 10.3 Values of the non-dimensional quantities s/r_0 and s/H'' when the projection width $s=50$cm

Dimensions of opening (Horizontal) (Vertical)	s/r_0	s/H''	Dimensions of opening (Horizontal) (Vertical)	s/r_0	s/H''
1m × 1m	1.25	0.82	1 × 3	0.72	0.26
2 × 1	0.89	0.79	2 × 3	0.51	0.26
3 × 1	0.72	0.78	3 × 3	0.41	0.25
4 × 1	0.63	0.78	4 × 3	0.36	0.25
1 × 2	0.89	0.40	1 × 4	0.63	0.192
2 × 2	0.63	0.39	2 × 4	0.44	0.190
3 × 2	0.51	0.38	3 × 4	0.36	0.190
4 × 2	0.44	0.38	4 × 4	0.31	0.191

Table 10.4 Calculated values of z/r_0, z, z/H'' and z_0/H'' (projection width: 50cm)

Dimensions of opening	Quantity of combustibles in the room (kg/m²)					
(Horizontal) (Vertical)	25	50	75	100	150	200
1m × 1m	0.24, 9.60 0.00, 0.16	0.24, 9.60 0.00, 0.16	0.24, 9.60 0.00, 0.16	0.24, 9.60 0.00, 0.16	0.24, 9.60 0.00, 0.16	0.24, 9.60 0.00, 0.16
2 × 1	0.70, 39.5 0.00, 0.63	0.79, 44.6 0.00, 0.71	0.79, 44.6 0.00, 0.71	0.79, 44.6 0.00, 0.71	0.79, 44.6 0.00, 0.71	0.79, 44.6 0.00, 0.71
3 × 1	0.62, 42.8 0.00, 0.68	0.82, 56.7 0.05, 0.89	0.82, 56.7 0.05, 0.89	0.82, 56.7 0.05, 0.89	0.82, 56.7 0.05, 0.89	0.82, 56.7 0.05, 0.89
4 × 1	0.63, 50.3 0.09, 0.79	0.80, 63.8 0.12, 1.00	0.87, 69.4 0.22, 1.08	0.87, 69.4 0.22, 1.08	0.87, 69.4 0.22, 1.08	0.87, 69.4 0.22. 1.08
1 × 2	1.42, 80.1 0.08, 0.64	1.68, 94.8 0.15, 0.75	1.68, 94.8 0.15, 0.75	1.68, 94.8 0.15, 0.75	1.68, 94.8 0.15, 0.75	1.68, 94.8 0.15, 0.75
2 × 2	1.35, 108 0.26, 0.84	1.85, 148 0.53, 1.15	2.00, 160 0.62, 1.24	2.03, 162 0.65, 1.27	2.03, 162 0.65, 1.27	2.03, 162 0.65, 1.27
3 × 3	1.19, 117 0.29, 0.91	1.50, 147 0.48, 1.13	1.66, 163 0.58, 1.24	1.80, 176 0.67, 1.33	1.84, 180 0.70, 1.36	1.84, 180 0.70, 1.36
4 × 4	1.00, 113 0.28, 0.88	1.27, 143 0.48, 1.10	1.43, 161 0.60, 1.23	1.64, 185 1.77, 1.40	1.73, 195 0.84, 1.47	1.74, 196 0.85, 1.48
1 × 3	2.42, 167 0.37, 0.87	2.79, 193 0.48, 1.00	2.91, 201 0.52, 1.04	2.91, 201 0.52, 1.04	2.91, 201 0.52, 1.04	2.91, 201 0.52, 1.04
2 × 3	2.10, 205 0.54, 1.06	2.58, 252 0.76, 1.30	2.78, 272 0.85, 1.39	2.92, 285 0.90, 1.44	3.06, 299 0.95, 1.50	3.06, 299 0.95, 1.50
3 × 3	1.44, 172 0.38, 0.90	2.28, 273 0.85, 1.40	2.52, 302 0.97, 1.52	2.67, 320 1.06, 1.61	2.84, 340 1.14, 1.70	2.96, 354 1.21, 1.77
4 × 3	0.84, 116 0.18, 0.61	1.84, 254 0.83, 1.30	2.20, 304 1.06, 1.53	2.33, 322 1.14, 1.62	2.45, 339 1.19, 1.70	2.57, 354 1.29, 1.77
1 × 4	2.86, 228 0.46, 0.89	3.30, 263 0.56, 1.01	3.55, 283 0.65, 1.08	3.69, 294 0.67, 1.12	3.78, 302 0.69, 1.14	3.78, 302 0.69, 1.14
2 × 6	2.17, 245 0.52, 0.97	2.92, 329 0.79, 1.25	3.17, 358 0.88, 1.35	3.40, 384 0.99, 1.46	3.60, 406 1.05, 1.53	3.78, 426 1.11, 1.59
3 × 4	1.12, 155 0.20, 0.61	2.56, 354 0.88, 1.35	2.82, 390 1.01, 1.48	2.98, 412 1.08, 1.55	3.30, 456 1.24, 1.71	3.40, 470 1.27, 1.75
4 × 4	0.16, 25.5 0.00, 0.10	1.99, 318 0.77, 1.23	2.58, 412 1.09, 1.56	2.77, 442 1.20, 1.67	2.96, 472 1.29, 1.77	3.12, 498 1.38, 1.86

Table 10.5 Height of spandrel necessary for fire prevention in case a projection 50cm wide is attached above the window (The figures in parentheses indicate the difference between this height and the necessary spandrel height in the case where the window is not provided with a projection, obtained in Table 9.9). Unit: cm.

Dimensions of opening		Quantity of combustibles in the room (kg/m²)					
(Horizontal)	(Vertical)	25	50	75	100	150	200
1 m ×	1 m	0.0(− 4)	0.0(− 4)	0.0(− 4)	0.0(− 4)	0.0(− 4)	0.0(− 4)
2 ×	1	0.0(−31)	0.0(−35)	0.0(−35)	0.0(−35)	0.0(−35)	0.0(−35)
3 ×	1	0.0(−41)	3.2(−54)	3.2(−54)	3.2(−54)	3.2(−54)	3.2(−54)
4 ×	1	5.8(−43)	7.7(−62)	14(−62)	14(−62)	14(−62)	14(−62)
1 ×	2	10(−32)	19(−34)	19(−34)	19(−34)	19(−34)	19(−34)
2 ×	2	33(−40)	68(−43)	79(−43)	83(−42)	83(−42)	83(−42)
3 ×	2	37(−58)	62(−73)	75(−86)	88(−82)	92(−84)	92(−84)
4 ×	2	36(−59)	62(−78)	79(−94)	102(−89)	111(−100)	112(−111)
1 ×	3	70(−32)	91(−30)	100(−29)	100(−29)	100(−29)	100(−29)
2 ×	3	104(−34)	147(−37)	166(−36)	178(−36)	189(−36)	189(−36)
3 ×	3	73(−47)	166(−49)	192(−50)	211(−50)	228(−52)	242(−50)
4 ×	3	34(−40)	162(−64)	210(−59)	227(−64)	238(−84)	258(−76)
1 ×	4	118(−10)	146(−18)	170(−13)	176(−19)	182(−19)	182(−19)
2 ×	4	132(−22)	207(−24)	232(−24)	262(−24)	279(−24)	296(−24)
3 ×	4	50(−33)	230(−34)	257(−34)	286(−32)	330(−32)	340(−35)
4 ×	4	0.0(− 7)	199(−44)	288(−45)	318(−45)	343(−45)	370(−45)

temperature of the main flow of the fire current which has spurted from the corresponding one of the windows is 500°C, measured from the window face along its trajectory. By multiplying this with the value of the equivalent radius r_0 of the window in question, we obtain the value of z. By calculating the value of s/H'' and by finding the value of z/H'' relative to the values of n and s/H'' of the window in question, this can be transformed into non-dimensional quantity of the vertical distance, z_0, measured from the upper edge of the window. The results of calculation of the four steps for the respective windows are shown in Table 10.4. The four numerals mentioned in each column of the Table show the calculated values of z/r_0, z, $z/H''$and z_0/H'' respectively according to the order of left above, right above, right down and left down. By multiplying z_0/H'' obtained lastly by H'' we obtain the vertical distance, z_0, of the point where the temperature of the spurting fire current $\Delta\theta$ is 500°C measured from the upper edge of the window or, in other words, the value of the necessary height of spandrel. The results of the calculation are shown in Table 10.5. In the Table, the numerals in parentheses show, as stated in the note, the numerals by which the height of spandrel may be reduced from the height necessary for the same window when no projection is attached. The maximum reduction is possible in the case of the window 4 m in horizontal width and 2 m in vertical length. The reduction value in terms of percentage is about 82% for the window of 4 m×1 m, 50∼55% for the 4 m×3 m window and 11∼14% for the 4 m×4 m window, which shows that, as stated in Section 10.4, the greater the value of n relative to the window —— that is, the shorter and wider in shape the window is —— the more effective the projection is for preventing the fire from spreading, as already stated in Section 10.4.

10.7 Concluding Words

In the above has been examined the projection's effect of preventing the fire from spreading to the upper story caused by the fire current which spurts out of the window of lower story.

1) If the building is provided with a projection above the window, the fire current spurting out of the window is first driven away from the building by the projection, but as it goes up it gradually comes close to the course that would be followed in case there was no projection.

2) The trajectories of fire currents which have spurted out of the window have shapes which are proportionate to H'' if the ratio, n , between the horizontal width of the window and one half of the vertical length thereof and the ratio between the width, s of the projection and the height measured from the neutral zone on the window face to the upper edge of the window are given. This is a kind of similarity law.

3) The temperature distribution along the main flow of the spurting hot current does not greatly vary whether there is a projection or not. But the temperature at a certain height above the window is lower when there is a projection by the quantity of temperature-decrease for the distance corresponding to the width of the projection.

4) The above-mentioned temperature distribution in the case where there is a projection falls between that in the case where the space above the window is free and that in the case where there is a wall above the window. Therefore, the temperatures itself is lower in the case where there is a projection.

5) Thus, the effect of the projection for preventing fire from spreading is the combination of items 3 and 4. In case the window is slender in shape, the effect mentioned in item 3 is the only effect that can be expected because there is little difference in temperature whether the space above the window is free or there is a wall there (Figure 8.5 in Chapter 8); but in case the window is short and wide, both 3 and 4 take effect. Therefore the projection is more effective if the window is short and wide.

6) With regard to the temperatere distribution along the trajectory of the spurting hot current, a non-dimensional temperature distribution curve without any relation to the scale can be drawn according to the ratio, n, of the horizontal width of the window to the one half oi the vertical length thereof and according to the ratio of the projection width to the equivalent radius of the window, s/r_0.

7) If the quantity of the combustibles in a room of fire-proof construction, the dimensions of the room and the window, and the width of the projection are given, the position of the main flow of flames spurting out of the window and the temperature distribution can be estimated by use of the law of similarity mentioned in item 2 and that mentioned in item 6, and accordingly the height of the spandrel necessary for

preventing the fire from spreading to the upper story, can be calculated.

In the above have been stated the effects of the projection for prevention of the spread of fire. This is concerned with the case where fire spreads from the window of the lower floor to the upper floor of the same building. In case there is a wooden building adjacent to this building and a fire breaks out in the wooden building, this protection acts as if it were eaves and increases the danger of fire spread. Attention must be paid to this point. Such being the case, to attach a projection or not should be decided accroding to the condition of the surroundings of the building.

References

1 Shigeo Uchida : Report. Inst. Sci. and Tech. Univ. Tokyo 3, 11–12, 1949.
2 Kunio Kawage : Report Build. Res. Inst. 27. 1958.
3 Prandtl L : Zeits. f. angew. Math. u. Mech. 5. 137, 138, 1925.
4 Taylor, G. I. : Proc. Roy. Soc. A. 135, 685, 1932.
5 V. Tollmien : Zeits. f. angew. Math. u. Mech. 6, 1925.
6 A. M. Kuethe : Jour. Appl. Mech, 2. 1935.
7 Insurance Company : "Study of Fire" p. 49, Vol. 1. 1951.
8 Shōkoku-sha : "Outline of Architecture" vol. 21. p. 134, 1956.
9 Shōkoku-sha : "Outline of Architecture" vol. 21. p. 129, 1956.
10 Shōkoku-sha : "Outline of Architecture" vol. 21. p. 136, 1956.
11 Shōkoku-sha : "Outline of Architecture" vol. 21. p. 129, 1956.
12 Kin-ichirō Fujita : Tans. Archi. Inst. Jap. 4, 1941.
13 Kin-ichirō Fujita : Report Build. Res. Inst, 1, 1954.
14 Kin-ichirō Fujita : Report Archi. Inst. Jap. 20, 1952.
15 Gurney, H. P. & Lurie : Ind. Eng. Chem. 15, 1923.
16 Fire Prev. Soc. Jap. : Hand-book of Fire p. 857, 1955.
17 Kin-ichirō Fujita : Report Build. Res. Inst. 1, 1954.
18 Kunio Kawagoe : Bul. Fire Prev. Soc. Jap. 4, 1. 1954.
19 Kunio Kawagoe : Bul. Fire Prev. Soc. Jap. 2, 1, 1952.
20 Kunio Kawagoe : Bul. Fire Prev. Soc. Jap. 3, 1, 1953.
21 Shōkoku-sha : "Outline of Architecture" vol. 21, p. 157, 1956.
22 Kunio Kawagoe : Report Build. Res. Inst. 27, p. 6, 1958.
23 Kin-ichirō Fujita : Report Build. Res. Inst. 1, 1954.
24 Takeshi Sekine : Bul. Fire Prev. Soc. Jap. 8, 2, 1959.
25 Matake Kurokawa : "Combustion Engineering" p. 48.
26 Minoru Hamada & Shōji Ikeda : Bul. Fire Prev. Soc. Jap. 7, 2, 1959.
27 Kin-ichirō Fujita : Trans. Arch. Inst. Jap. 1936.